

February 2022

# **MultiWell Program Suite User Manual**

**(MultiWell-2022)**

**John R. Barker, T. Lam Nguyen, John F. Stanton,  
Chiara Aieta, Michele Ceotto, Fabio Gabas, T. J. Dhillip Kumar,  
Collin G. L. Li, Lawrence L. Lohr, Andrea Maranzana,  
Nicholas F. Ortiz, Jack M. Preses, John M. Simmie,  
Jason A. Sonk, and Philip J. Stimac**

University of Michigan  
Ann Arbor, MI 48109-2143

Contact:  
[jrbarker@umich.edu](mailto:jrbarker@umich.edu)

MultiWell Web site:  
[clasp-research.engin.umich.edu/multiwell](http://clasp-research.engin.umich.edu/multiwell)

(Copyright 2022, John R. Barker)

# CONTENTS

<b>0. Preliminaries</b>	<b>1</b>
About the Authors	1
MultiWell Literature Citations	2
Help! Comments! Bug Reports!	3
Acknowledgements	3
<b>1. Getting Started</b>	<b>5</b>
1.1 Software Tools in the MultiWell Suite	5
1.2 How the Tools Work Together	9
1.3 Examples and Models	13
1.4 Installing and Executing the Codes	16
1.5 Some Technical Issues on Input/Output Files	19
References	20
<b>2. MultiWell Master Equation Code</b>	<b>22</b>
2.1 Brief Description	22
2.2 Terminology	22
2.3 Default Array Dimensions	24
2.4 Notes on FORTRAN source code and compilation	24
2.5 MultiWell Input Files and Program Execution	25
2.6 MultiWell Output Files	26
2.7 MultiWell Input Data File (FileName.dat)	27
2.8 Collision Models	36
2.9 Format of External Data Files	39
2.10 Fatal Input Errors and Warnings	43
References	45
<b>3. Separable Molecular Degrees of Freedom</b>	<b>47</b>
3.1 Types of Degrees of Freedom	47
3.2 Format for Input Files	52
References	55
<b>4. DenSum: <i>Separable Sums and Densities of States</i></b>	<b>56</b>
4.1 DenSum Data File Format	56
4.2 DenSum in Batch Mode	58
References	60

<b>5. MomInert: Moments of Inertia</b>	<b>61</b>
5.1 Data File Format	61
5.2 Computational Approach	63
References	63
<b>6. thermo: Thermodynamics</b>	<b>64</b>
6.1 Introduction	64
6.2 Data File Format	70
6.3 MultiWell Thermodynamics Database	74
References	74
<b>7. gauss2multi: A Tool for Creating Data Files</b>	<b>75</b>
References	77
<b>8. bdens, paradensum, parsctst, and sctst: <i>non-Separable Vibrations</i></b>	<b>79</b>
8.1 Program bdens	80
8.2 Program paradensum	86
8.3 Program sctst	91
8.4 Program parsctst	95
References	101
<b>9. lamm: Effective Mass for Internal Rotation</b>	<b>103</b>
9.1 Introduction	103
9.2 Compiling and Running lamm	103
9.3 Notes and Limits	104
9.4 Data File Format	104
9.5 Example Data File	105
9.6 Example Output:	105
9.7 gauss2lamm: A script for generating lamm.dat	106
References	108
<b>10. ktools: <i>J</i>-Resolved Variational Transition State Theory</b>	<b>110</b>
10.1 Introduction	110
10.2 Theory	111
10.3 ktools Input File	118
10.4 Running ktools	121
10.5 ktools Output Files	122
10.6 ktools Examples	123
References	132
<b>11. TS and pTS: <i>J</i>-Resolved Steady-State Master Equation Solver</b>	<b>133</b>
<b>Appendix A. Theoretical Basis</b>	<b>134</b>
A.1. Introduction	134

A.2. The Active Energy Master Equation	134
A.3. Stochastic Method	149
A.4. Processes	152
A.5. Initial Conditions	178
A.6. Input	181
A.7. Output	182
A.8. Concluding Remarks	183
References	185
<b>Appendix B. Technical Notes</b>	<b>187</b>
B.1 Conversion Factors (Rotational Data)	187
B.2 Anharmonic Vibrations	187
B.3 Vibrational Degeneracies	191
B.4 External molecular rotations	191
B.5 Symmetry numbers, internal rotation, and optical isomers (mirror images)	194
B.6 A Handy List of Lennard-Jones Parameters	200
B.7 Elements and Isotopes in MomInert and Thermo	201
B.8 Eigenstates for large amplitude motions	202
B.9 Semi-Classical Transition State Theory (SCTST)	206
B.10 Legacy and Current Versions of $k_0$ and $k_\infty$ in MultiWell	213
<b>Appendix C. How to ...</b>	<b>218</b>
C.1 How to set up the double arrays in MultiWell	218
C.2 How to test the double-array parameters in MultiWell	219
C.3 How estimate Lennard-Jones and energy transfer parameters	219
C.4 How to obtain rate constants from MultiWell simulations	220
C.5 How to tell if the simulated time is long enough	231
C.6 How to deal with Barrierless Reactions	234
C.7 Some Questions and Answers	235
<b>Index</b>	<b>239</b>

## 0. Preliminaries

### About the Authors

JOHN BARKER wrote or contributed to most of the codes. The original set of codes was based on his 1983 paper and subsequent developments.<sup>3-7,9</sup>

LAM NGUYEN installed a method for using quantum eigenvalues for hindered internal rotations, wrote a code for computing the effective mass of large amplitude motions, and helped in developing codes for non-separable vibrations,<sup>7</sup> and semi-classical transition state theory (SCTST).<sup>8</sup> In addition, he and John Stanton are responsible for the code TS.

JOHN STANTON was a key participant in implementing semi-classical transition state theory<sup>8</sup> and vibrational anharmonicities in his quantum chemistry code CFOUR.<sup>10</sup> He and Lam Nguyen also are responsible for the code TS.

CHIARA AIETA, FABIO GABAS, and MICHELE CEOTTO (Università degli Studi di Milano) developed `paradensum`, a parallelized code<sup>1</sup> for computing sums and densities of states for fully coupled vibrational models, and `parsctst` a parallelized code<sup>2</sup> for computing cumulative reaction probabilities from Semi-Classical Transition State Theory (SCTST).

DHILIP KUMAR wrote several scripts for automatically using output files from electronic structure programs to build input/output files.

COLLIN LI wrote much of the code for program `bdens`.

LARRY LOHR contributed to the development of hindered rotor subroutines.

ANDREA MARANZANA (University of Turin) contributed codes for automatically generating input files for the MultiWell Suite from output files produced in quantum chemical calculations.

NICK ORTIZ (as an undergraduate student) wrote most of the code for `MOMINERT`.

JACK PRESES (Brookhaven Nat'l Lab.) added several helpful features.

JOHN SIMMIE (Galway, Ireland) is helping to maintain and extend the MultiWell Thermodynamics Database.

JASON SONK wrote most of the code for `ktools` and has contributed to other codes as well.

PHIL STIMAC implemented 1-dimensional quantum tunneling *via* an unsymmetrical Eckart barrier in the `multiwell` master equation code.

## MultiWell Literature Citations

Please cite the following papers to acknowledge results obtained using this version of the MultiWell Program Suite:

### *For citing the MultiWell Program Suite*

In the following, **<version>** refers to the version number (e.g. 2022) and **<year>** refers to the year of publication (e.g. 2022):

- (a) J. R. Barker, T. L. Nguyen, J. F. Stanton, C. Aieta, M. Ceotto, F. Gabas, T. J. D. Kumar, C. G. L. Li, L. L. Lohr, A. Maranzana, N. F. Ortiz, J. M. Preses, J. M. Simmie, J. A. Sonk, and P. J. Stimac; MultiWell-**<version>** Software Suite; J. R. Barker, University of Michigan, Ann Arbor, Michigan, USA, **<year>**; <http://clasp-research.engin.umich.edu/multiwell/>.
- (b) John R. Barker, *Int. J. Chem. Kinetics*, **33**, 232-45 (2001).
- (c) John R. Barker, *Int. J. Chem. Kinetics*, **41**, 748-763 (2009).

### *References for program **bdens***

**References (a) through (c), above, plus ...**

- (d) M. Basire, P. Parneix, and F. Calvo, *J. Chem. Phys.* **129**, 081101 (2008).
- (e) F. Wang and D. P. Landau, *Phys. Rev. Letters* **86**, 2050 (2001).
- (f) Thanh Lam Nguyen and John R. Barker, *J. Phys. Chem. A.*, **114**, 3718–3730 (2010).

### *References for program **paradensum***

**References (a) through (f), above, plus ...**

- (g) C. Aieta, F. Gabas, and M. Ceotto, *J. Phys. Chem. A*, DOI: 10.1021/acs.jpca.5b12364 (2016).

### *References for program **sctst***

**References (a) through (c), above, plus ...**

- (h) W. H. Miller, *J. Chem. Phys.* **62**, 1899 (1975).
- (i) W. H. Miller, *Faraday Discuss. Chem. Soc.* **62**, 40 (1977).
- (j) W. H. Miller, R. Hernandez, N. C. Handy, D. Jayatilaka, and A. Willets, *Chem. Phys. Letters* **172**, 62 (1990).
- (k) R. Hernandez and W. H. Miller, *Chem. Phys. Lett.* **214** (2), 129 (1993).
- (l) T. L. Nguyen, J. F. Stanton, and J. R. Barker, *Chem. Phys. Letters* **499**, 9 (2010).
- (m) T. L. Nguyen, J. F. Stanton, and J. R. Barker, *J. Phys. Chem. A* **115**, 5118 (2011).

### *References for program **parsctst***

**References (a) through (c), above, plus References (h) through (m), above, plus**

- (n) Aieta C.; Gabas, F.; Ceotto, M. Parallel Implementation of Semiclassical Transition State Theory *J. Chem. Theory Comput.* **2019**, DOI: 10.1021/acs.jctc.8b01286.

### *References for program **TS***

**Reference (a), above, plus ...**

- (o) "TS is a chemical kinetic program that solves a two-dimensional master-equation for gas-phase reactions in parallel using the Steady-State approach. It is developed, implemented, and maintained by **T. L. Nguyen** and **J. F. Stanton**, **version 01-03-2017**."
- (p) T. L. Nguyen and J. F. Stanton, A Steady-State Approximation to the Two-Dimensional Master Equation for Chemical Kinetics Calculations, *J. Phys. Chem. A* **119**, 7627-7636 (2015).
- (q) T. L. Nguyen, H. Lee, D. A. Matthews, M. C. McCarthy and J. F. Stanton, Stabilization of the Simplest Criegee Intermediate from the Reaction between Ozone and Ethylene: A High-Level Quantum Chemical and Kinetic Analysis of Ozonolysis, *J. Phys. Chem. A* **119**, 5524-5533 (2015).

## Help! Comments! Bug Reports!

Please send pleas for help, comments, and bug reports to the "**Multiwell and Chemical Kinetics**" **question and answer forum**: all users are invited to join the forum, where questions can be asked and answered, and future upgrades will be announced. This forum is set up as a Google Group, which you can join at <https://groups.google.com/>. If for any reason it is difficult for you to use Google, please contact John R. Barker ([jrbarker@umich.edu](mailto:jrbarker@umich.edu)) and he will answer your question or pass it along to the appropriate person.

## Acknowledgements

Thanks go to the following people for particularly helpful suggestions, discussions, debugging, or other assistance:

Amity Andersen  
A. Bencsura  
Hans-Heinrich Carstensen  
David M. Matheu  
Gabriel R. Da Silva  
Theodore S. Dibble  
David Edwards  
Benj FitzPatrick  
Michael Frenklach  
David M. Golden  
Erin Greenwald  
John Herbon  
Keith D. King

Keith Kuwata  
George Lendvay  
Robert G. ('Glen') MacDonald  
Milad Marinami  
Connor Martin  
Nigel W. Moriarty  
William F. Schneider  
Colleen Shovelin  
Robert M. Shroll  
Gregory P. Smith  
Al Wagner  
Ralph E. Weston, Jr.

Some sections of the computer codes were developed as part of research funded by NSF (Atmospheric Chemistry Division), NASA (Upper Atmosphere Research Program), and NASA (Planetary Atmospheres). JMS thanks the Irish Centre for High-End Computing, ICHEC, for the provision of computational resources, ngche041c.

***Disclaimer:** This material is based in part upon work supported by the U.S. National Science Foundation. Any opinions, findings, and conclusions or recommendations expressed in this material are those of the author(s) and do not necessarily reflect the views of the National Science Foundation.*

## References

- (1) Aieta, C.; Gabas, F.; Ceotto, M. An Efficient Computational Approach for the Calculation of the Vibrational Density of States. *J. Phys. Chem. A* **2016**, DOI: 10.1021/acs.jpca.1025b12364; DOI: 10.1021/acs.jpca.5b12364.
- (2) Aieta, C.; Gabas, F.; Ceotto, M. Parallel Implementation of Semiclassical Transition State Theory. *J. Chem. Theory Comput.* **2019**, *15*, 2143-2153; DOI: 10.1021/acs.jctc.8b01286.
- (3) Barker, J. R. Monte-Carlo Calculations on Unimolecular Reactions, Energy-Transfer, and IR-Multiphoton Decomposition. *Chem. Phys.* **1983**, *77*, 301-318.
- (4) Barker, J. R. Radiative Recombination in the Electronic Ground State. *J. Phys. Chem.* **1992**, *96*, 7361-7367; DOI: 10.1021/j100197a042.
- (5) Barker, J. R. Energy Transfer in Master Equation Simulations: A New Approach. *Int. J. Chem. Kinet.* **2009**, *41*, 748-763.
- (6) Barker, J. R.; King, K. D. Vibrational Energy Transfer in Shock-Heated Norbornene. *J. Chem. Phys.* **1995**, *103*, 4953-4966.
- (7) Nguyen, T. L.; Barker, J. R. Sums and Densities of Fully-Coupled Anharmonic Vibrational States: A Comparison of Three Practical Methods. *J. Phys. Chem. A* **2010**, *114*, 3718-3730.
- (8) Nguyen, T. L.; Stanton, J. F.; Barker, J. R. A Practical Implementation of Semi-Classical Transition State Theory for Polyatomics. *Chem. Phys. Letters* **2010**, *499*, 9-15.
- (9) Shi, J.; Barker, J. R. Incubation in Cyclohexene Decomposition at High Temperatures. *Int. J. Chem. Kinet.* **1990**, *22*, 187-206.
- (10) Stanton, J. F.; Gauss, J.; Harding, M. E.; Szalay, P. G.; Auer, A. A.; Bartlett, R. J.; Benedikt, U.; Berger, C.; Bernholdt, D. E.; Bomble, Y. J.; Cheng, L.; Christiansen, O.; Heckert, M.; Heun, O.; Huber, C.; Jagau, T.-C.; Jonsson, D.; Jusélius, J.; Klein, K.; Lauderdale, W. J.; Lipparini, F.; Matthews, D. A.; Metzroth, T.; Mück, L. A.; O'Neill, D. P.; Price, D. R.; Prochnow, E.; Puzzarini, C.; Ruud, F. S.; Schwalbach, W.; Simmons, C.; Stopkowitz, S.; Tajti, A.; Vázquez, J.; Wang, F.; Watts, J. D.; Almlöf, J.; Taylor, P. R.; Helgaker, T.; Jensen, H. J. A.; Jørgensen, P.; Olsen, J.; Mitin, A. V.; Wüllen., C. v. CFOUR, a quantum chemical program package, 2016.



# 1. Getting Started

## 1.1 Software Tools in the MultiWell Suite

### *multiwell (master equation code)*

Calculates time-dependent concentrations, yields, vibrational distributions, and rate constants as functions of temperature and pressure for unimolecular reaction systems that consist of multiple stable species, multiple reaction channels interconnecting them, and multiple dissociation channels from each stable species. Reactions can be reversible or irreversible. Can include tunneling and/or the effects of slow intramolecular vibrational energy redistribution (IVR).<sup>16,18</sup> NOTE:  $k(E)$ 's can be calculated by other programs and read in (see Input file description below).

### Is the multiwell master equation right for your problem?

Like any other tool, this code has strengths and weaknesses. Therefore, it is more suitable for some problems than for others. The code is based on Gillespie's stochastic simulation algorithm (SSA),<sup>9-11</sup> which uses Monte Carlo sampling ("stochastic trials"). This enables a very flexible approach to simulations, but the precision of a simulation depends on the number of stochastic trials (more trials, more precise results), as does the dynamic range, which is limited by the number of trials. Moreover, stochastic simulations are accompanied by stochastic sampling "noise", which is tolerable for most applications, but perhaps not for all. In multiwell, collisions are treated very accurately and computer execution times are roughly proportional to the number of collisions in a simulated time period. Thus, simulations can become very tedious and time-consuming if high precision is needed in simulations that require very long simulated time periods.

Multiwell is an extremely useful tool for simulating experiments, since no assumptions are made beyond assuming the validity of statistical rate theory (e.g. RRKM theory). In some cases, even the statistical assumption is not necessary, since a model<sup>13,15-18</sup> for intramolecular vibrational relaxation (IVR) has also been implemented.<sup>3</sup> Multiwell is particularly useful for simulating rapidly evolving systems that are simultaneously undergoing vibrational relaxation and chemical reaction (e.g. photoactivation, shock excitation, chemical activation). It is not as suitable for slowly reacting systems that are gradually approaching equilibrium or at steady state. Note that experiments can be simulated accurately even under conditions when phenomenological rate constants are not well-defined.

One of the principal uses in recent years of master equations has been the prediction of reaction rate constants as functions of temperature and pressure, especially in multi-well, multi-channel unimolecular reaction systems. For any experiment from which rate constants can be obtained, the corresponding rate constants can be extracted from an appropriate master equation simulation of the experiment. The data from the simulation can be analyzed by using least squares fitting and other techniques, just as is done in analyzing experiments.<sup>1,2,6,8,19,21,26</sup> This approach is useful and accurate for relatively simple reaction systems, but not convenient for more complicated ones. The most convenient method for extracting rate constants for the reversible isomerization reactions in linked multi-well systems is currently the Barts-Widom approach,<sup>4</sup> which has been implemented in several eigenvalue codes.<sup>7,12,20</sup> Because the Barts-Widom method relies on linear algebra techniques, it is not available for stochastic simulations,

which are accompanied by stochastic sampling noise. However, least squares analysis of stochastic simulations can be used to obtain similar results.<sup>21</sup> When the details of complicated linked isomerization reactions are not needed, both the eigenvalue and the stochastic methods produce satisfactory results, but if the details of the linked isomerizations are important, then the Bartis-Widom approach is more convenient.

The stochastic method is particularly suited to systems that require high energy resolution, such as photo-activation and chemical activation at moderate and low temperatures, because execution time is only weakly dependent on the energy resolution, while the eigenvalue methods are much slower when the energy grain size is reduced.<sup>2</sup>

Some information on how to extract rate constants from MultiWell master equation simulations is provided in Sec. C.4.

In summary, the MultiWell master equation code is well suited to addressing many, but not all, demanding problems. Users should consider the various options that are available. **Multiwell** is intended to be relatively easy to use and hands-on trial runs using **multiwell** are a good way to assess its utility when it is not clear which method to choose. If you would like to discuss the various options, or have questions that are not addressed in this Manual, please contact John Barker ([jrbarker@umich.edu](mailto:jrbarker@umich.edu)).

### ***densum***

Performs exact counts for sums and densities of states via the Stein-Rabinovitch extension<sup>27</sup> of the Beyer-Swinehart algorithm.<sup>5</sup> This code is the best choice for separable degrees of freedom; for coupled degrees of freedom, use **bdens** or **paradensum**. The following types of separable modes are accepted:

- a) vibrations (harmonic and anharmonic; quantized)
- b) free rotations (classical or quantized)
- c) hindered rotations, symmetrical and unsymmetrical (quantized eigenvalues)
- d) particle in a box (quantized)
- e) translation (classical)

### ***thermo***

Calculates entropy, heat capacity, and  $H(T)-H(0)$  for individual species, based on vibrational frequencies, moments of inertia, internal rotation barriers, and electronic state properties. It includes all of the types of modes listed for **densum**. It calculates equilibrium constants, which are useful for obtaining recombination rate constants from the corresponding unimolecular decomposition rate constants. When provided with parameters for reactants and the transition state, it uses canonical transition state theory (CTST) to calculate rate constants (including tunneling corrections based on the 1-D unsymmetrical Eckart barrier). By using input files generated by Programs **bdens**, **paradensum**, **parsctst**, or **sctst** (see below), **thermo** can include the effects of fully coupled anharmonic vibrations and/or compute thermal rate constants using the fully-coupled anharmonic semi-classical transition state theory (SCTST) formulated by W. H. Miller and coworkers.

The text file named **multiwell-thermo-database** has been formatted for use by program **THERMO**. Data for more than 100 chemical species are included in the file. See Section 6.2 of this User Manual for more information about the database.

### ***mominert***

Calculates principal moments of inertia for chemical species and approximate reduced moments of inertia for internal rotors. Requires the Cartesian coordinates for the atoms in the molecule, as obtained from many software packages in common use (e.g., HyperChem, Chem3D, MOPAC, GAUSSIAN, C-FOUR, etc.).

### ***gauss2multi***

Reads output files from the Gaussian electronic structure program and generates data files for the other four programs in the MultiWell Suite. (Parameters not calculated using Gaussian must be added by hand.)

### ***lamm***

Uses Cartesian coordinates along a path (obtained from electronic structure calculations) to compute the effective mass for hindered internal rotations. For this purpose, **lamm** is more accurate than **mominert**. A script, **gauss2lamm**, is provided to read Gaussian output files and construct most of the data file needed for **lamm**.

### ***bdens***

This code is available for computing sums and densities of states for non-separable anharmonic vibrations, based on the perturbation theory expansion. It is appropriate for use with species that contain up to perhaps 20 coupled vibrations. For larger molecules, **paradensum** is a better choice. **bdens** computes *exact counts* at low energies and uses the Wang-Landau algorithm to compute approximate counts at high energies. **bdens** is the best choice for highest accuracy, but execution is very slow for very large molecules at high energies, and **paradensum** is a better choice if errors of a few percent are tolerable. **bdens**, like **densum**, produces output files that can be used directly as input files for **multiwell**. In addition, it produces a file containing partition functions for the fully coupled anharmonic vibrations; these partition functions can then be used by **thermo** to compute rate constants and thermodynamic data.

### ***paradensum***

This parallelized code replaces the serial code **adensum**, which is no longer being maintained (last release was **multiwell-2014.1b**). **paradensum** computes sums and densities of states for fully coupled vibrational models that can include >150 degrees of freedom. **paradensum**, like **densum**, produces output files that can be used directly as input files for **multiwell**. In addition, it produces a file containing partition functions for the fully coupled anharmonic vibrations; these partition functions can then be used by **thermo** to compute rate constants and thermodynamic data.

### ***sctst***

This code is for using Semi-Classical Transition State Theory (SCTST), which was formulated by W. H. Miller and coworkers<sup>14,22,24,25</sup> to compute cumulative reaction probabilities (CRPs), which are analogous to the sums of states for the transition state. This enables computation for microcanonical rate constants (k(E)s), which are needed for master equation simulations (using **multiwell**). Miller's theory is founded on second order vibrational perturbation theory (VPT2). An additional feature of the code is the implementation of J. F. Stanton's

additional correction term, which is based on fourth-order perturbation vibrational theory (VPT4). The code also computes the partition function corresponding to the CRP at a set of temperatures from 50 K to 3400 K and generates a data file that can be used by program thermo to conveniently compute thermal rate constants using SCTST.

### *parsctst*

This code is the parallel version of `sctst`. It can also be run as a serial code and will replace `sctst` in a future release. It is for using Semi-Classical Transition State Theory (SCTST), which was formulated by W. H. Miller and coworkers<sup>14,22,24,25</sup> to compute cumulative reaction probabilities (CRPs), which are analogous to the sums of states for the transition state. This enables computation for microcanonical rate constants ( $k(E)$ s), which are needed for master equation simulations (using `multiwell`). Miller's theory is founded on second order vibrational perturbation theory (VPT2). An additional feature of the code is the implementation of J. F. Stanton's additional correction term, which is based on fourth-order perturbation vibrational theory (VPT4). The code also computes the partition function corresponding to the CRP at a set of temperatures from 50 K to 3400 K and generates a data file that can be used by program thermo to conveniently compute thermal rate constants using SCTST.

### *ktools*

This code implements two varieties of Variational Transition State Theory (VTST): Canonical (i.e. thermal) and J-resolved Microcanonical (i.e. for fixed internal energies and angular momentum). From molecular vibration frequencies, moments of inertia, and potential energy provided at points along a reaction path to compute variationally optimized sums of states and J-resolved microcanonical rate constants (i.e.  $k(E,J)$ ) for the reaction. These quantities can be used in 2-dimensional (i.e. depending on both E and J) master equations. By summing over J, it also gives microcanonical VTST rate constants (i.e.  $k(E)$  that can be used in 1-D (i.e. depending on E, alone) master equations. An important feature of the code is that it automatically identifies cases where two or more bottlenecks occur along the same reaction path and then uses W. H. Miller's unified statistical theory<sup>23</sup> to compute the over-all effective rate constant.

### *TS*

This code features a J-resolved steady-state master equation code that is solved by eigenvalue methods on large parallel computers. It utilizes the frozen-J approximation.

## 1.2 How the Tools Work Together

In this section, we describe the input and output of codes in the MultiWell Program Suite and indicate how some codes generate output files that are used as input by other codes. In the following table, **<species>** denotes the name of a chemical species (i.e. a Well or a Transition State).

**Table 1. Software Tools Input/Output Information**

<b>Tool</b>	<b>Input Quantities</b>	<b>Output</b>	
<b>thermo</b> (Chap. 6)	Separable D.O.F. (Chap. 3) Vibrations Rotations Hindered rotors etc. Electronic energies Symmetries	Heat Capacity Entropy Enthalpy function Equilibrium Const. Canonical (Thermal) Rate Constants	
	<b>Input Files</b>	<b>Description</b>	<b>Generated by...</b>
	<b>thermo.dat</b> <b>&lt;species&gt;.qvib</b> <b>&lt;species&gt;.crp</b>	data file (required) Partition functions Partition functions Cumulative React. Probability	User <b>bdens</b> <b>paradensum</b> <b>sctst</b> <b>parsctst</b>
	<b>Output Files</b>	<b>Description</b>	<b>used by program...</b>
	<b>thermo.out</b> <b>thermo.partfxns</b> <b>thermo.details</b>	General output Partition functions Details	(none)

<b>Tool</b>	<b>Input Quantities</b>	<b>Output</b>	
<b>densum</b> (Chap. 4)	Separable D.O.F. (Chap. 3) Vibrations Rotations Hindered rotors etc.	G(E), sum of states $\rho(E)$ , density of states	
	<b>Input Files</b>	<b>Description</b>	<b>Generated by...</b>
	<b>densum.dat</b>	data file (required)	User
	<b>Output Files</b>	<b>Description</b>	<b>used by program...</b>
	<b>densum.out</b> <b>&lt;species&gt;.dens</b>	General output G(E) and $\rho(E)$	User <b>multiwell</b>

<b>Tool</b>	<b>Input Quantities</b>	<b>Output</b>	
<b>multiwell</b> (Chap. 2) Master equation simulations.	Cartesian coordinates	Fractional concentrations vs. time. Branching fractions, internal energies, etc.	
	<b>Input Files</b>	<b>Description</b>	<b>Generated by...</b>
	<b>multiwell.dat</b> <species name>.dens  <TS name>.crp (other optional input files)	data file (required) Sums and densities of states  Cumulative Reaction probabilities k(E), initial energy distributions, etc.	User <b>densum, ktools, paradensum, bdens sctst</b>  User
	<b>Output Files</b>	<b>Description</b>	<b>used by program...</b>
<b>multiwell.out</b> <b>multiwell.sum</b> <b>multiwell.array</b> <b>multiwell.rates</b> <b>multiwell.flux</b> <b>multiwell.dist</b>	General output Output summary Input and meta data Reaction flux coefficients Reactive fluxes Energy distributions		

<b>Tool</b>	<b>Input Quantities</b>	<b>Output</b>	
<b>mominert</b> (Chap. 5)	Cartesian coordinates	External moments of inertia and rotational constants Reduced moment of inertia and rotational constants for internal rotors	
	<b>Input Files</b>	<b>Description</b>	<b>Generated by...</b>
	<b>mominert.dat</b>	data file (required)	User
	<b>Output Files</b>	<b>Description</b>	<b>used by program...</b>
<b>mominert.out</b>	General output	input data used by many of the other codes	

<b>Tool</b>	<b>Input Quantities</b>	<b>Output</b>	
<b>lamm</b> (Chap. 9)	Cartesian coordinates as a function of dihedral angle for an internal rotation.	Reduced moment of inertia and rotational constant as a function of dihedral angle	
	<b>Input Files</b>	<b>Description</b>	<b>Generated by...</b>
	<b>lamm.dat</b>	data file (required)	User
	<b>Output Files</b>	<b>Description</b>	<b>used by program...</b>
<b>lamm.out</b>	General output	thermo densum bdens paradensum sctst parsctst ktools	

<b>Tool</b>	<b>Input Quantities</b>	<b>Output</b>	
<b>ktools</b> (Chap. 10) J-Resolved VTST code	For a Transition State Separable D.O.F. (Chap. 3) Vibrations Rotations Hindered rotors etc. Electronic energies Symmetries	Canonical $k(T)$ and J-resolved microcanonical $k(E,J)$ VTST rate constants; also J-resolved sums $G(E,J)$ and densities $\rho(E,J)$ of states; also J-summed quantities.	
	<b>Input Files</b>	<b>Description</b>	<b>Generated by...</b>
	<b>ktools.dat</b>	data file (required)	User
	<b>Output Files</b>	<b>Description</b>	<b>used by ...</b>

<b>Tool</b>	<b>Input Quantities</b>	<b>Output</b>	
<b>bdens</b> (Chap. 8) Fully coupled vibrational models for small species.	Coupled vibrations (Chap. 8) Harmonic frequencies Anharmonicities ( $X_{ij}$ ) Separable D.O.F. (Chap. 3) Vibrations Rotations Hindered rotors etc.	$G(E)$ , sum of states $\rho(E)$ , density of states partition functions	
	<b>Input Files</b>	<b>Description</b>	<b>Generated by...</b>
	<b>bdens.dat</b>	data file (required)	User
	<b>Output Files</b>	<b>Description</b>	<b>used by program...</b>
	<b>bdens.out</b> <b>&lt;species&gt;.dens</b> <b>&lt;species&gt;.qvib</b>	General output $G(E)$ and $\rho(E)$ s Partition functions	User <b>multiwell</b> <b>thermo</b>

<b>Tool</b>	<b>Input Quantities</b>	<b>Output</b>	
<b>paradensum</b> (Chap. 8) Fully coupled vibrational models for large species.	Coupled vibrations (Chap. 8) Harmonic frequencies Anharmonicities ( $X_{ij}$ ) Separable D.O.F. (Chap. 3) Vibrations Rotations Hindered rotors, etc.	$G(E)$ , sum of states $\rho(E)$ , density of states partition functions	
	<b>Input Files</b>	<b>Description</b>	<b>Generated by...</b>
	<b>paradensum.dat</b>	data file (required)	User
	<b>Output Files</b>	<b>Description</b>	<b>used by ...</b>
	<b>paradensum.out</b> <b>&lt;species&gt;.dens</b> <b>&lt;species&gt;.qvib</b>	General output $G(E)$ and $\rho(E)$ Partition functions	User <b>multiwell</b> <b>thermo</b>

Tool	Input Quantities	Output	
<b>sctst</b> (Chap. 8)	<b>For a Transition State</b> Coupled vibrations (Chap. 8) Harmonic frequencies Anharmonicities ( $X_{ij}$ ) Separable D.O.F. (Chap. 3) Vibrations Rotations Hindered rotors, etc.	CRP(E), cumulative reaction probability CRP partition function	
	<b>Input Files</b>	<b>Description</b>	<b>Generated by...</b>
	<b>sctst.dat</b>	data file (required)	User
	<b>Output Files</b>	<b>Description</b>	<b>used by ...</b>
	<b>sctst.out</b> <b>&lt;species&gt;.crp</b> <b>&lt;species&gt;.qcrp</b>	General output CRP CRP Partition function	User <b>multiwell</b> <b>thermo</b>

### Preparing Input Data Files

All of the input files are text files and can be easily prepared using a text editor (a word processor can be used, but tends to be cumbersome, since the input files do not require formatting). Data from quantum chemistry programs can be copied and pasted into the input files. If GAUSSIAN was used to generate molecular data, then the program **gauss2multi** can be used to automatically extract data from the GAUSSIAN log files and generate major portions of the input files, but manual entry of much information is still required.

*However, we recommend that new users start by preparing the data files manually, so that they can become familiar with the input files and the input data that cannot be obtained from quantum chemistry programs.* After learning more about the input files, experienced users will find that **gauss2multi** can save them some work.

**Hindered internal rotations** are very important in determining thermodynamics quantities and molecular energy state densities. The data for hindered internal rotations can be prepared for input by first using programs **mominert** (for simple symmetric internal rotors) and **lamm** (for any hindered internal rotor. From these data, the MultiWell codes compute the eigenvalues of the appropriate Schrödinger equation.

### Equilibrium Constants and Canonical (Thermal) Rate Constants

Equilibrium constants thermal rate constants are calculated by **thermo**, which normally employs partition functions for the set of separable degrees of freedom recognized by the MultiWell Program Suite (see Chapter 3). Rate constants for reactions with intrinsic energy barriers are computed by **thermo** using tunneling corrections for the unsymmetrical Eckart barrier.

In applications that require very accurate results for reactants and products, harmonic frequencies and all of the  $X_{ij}$  anharmonicity coefficients for fully coupled anharmonic vibrations models must be computed. For these applications, programs **bdens** (typically  $\leq 5$  atoms) and **paradensum** (typically  $>5$  atoms) are used to compute the partition functions for the set of



coupled vibrations; these two programs generate output files that can be read as input to **thermo**.

For tight transition states (i.e. with intrinsic energy barriers) with fully-coupled vibrations (including the reaction coordinate), program **parsctst** (or **sctst**) calculates the cumulative reaction probability (CRP) and appropriate partition functions, which are placed in an output file that can be read as input to **thermo**.

For loose transition states (i.e. with little or no intrinsic energy barriers), program **ktools** is appropriate. This code utilizes separable degrees of freedom and information at points along the reaction path. It automatically identifies situations with multiple transition states along the reaction path and computes the net rate constant.

### ***RRKM Master Equation Calculations***

These calculations are performed using **multiwell**, the master equation code. **multiwell** has a standard input file for many of the required parameters, but it also requires densities of states for Wells and sums of states for Transition States. For standard calculations that adopt separable degrees of freedom, the densities of states for the Wells are computed using **densum**. For tight Transition States, **densum** is appropriate, but for loose Transition States, **ktools** is the proper choice.

For applications that use fully coupled vibrations, **bdens** and **paradensum** can be used to calculate the densities of states for the Wells and **parsctst** (or **sctst**) can be used for the Transition States; these programs generate output files that can be read by **multiwell**.

## **1.3 Examples and Models**

### ***Examples***

Several examples are provided for each of the codes: **multiwell**, **densum**, **mominert**, **thermo**, **gauss2multi**, **ktools**, **bdens**, **paradensum**, **sctst**, and **parsctst**. The **densum** examples include a set of cases discussed in the literature: useful for testing the accuracy of **densum**. The **multiwell** examples include various reaction Models.

The input files found in the Examples can be used as templates to construct new input files. Example input files can also be found in the "test" directories, which are located in each source (**src**) directory (see section 1.4 for the directory structure).

The MultiWell Software Suite directory is organized as follows:

<b>/multiwell-&lt;version&gt;</b>		Main MultiWell Directory
<b>/bin</b>		binary executables
<b>/doc</b>		version history, license, etc.
<b>/scripts</b>		admin scripts for running tests and examples
<b>/src</b>		
<b>/bdens</b>		source code for bdens
<b>/test</b>	test files	
<b>/gauss2multi</b>		source code for gauss2multi
<b>/test</b>	test files	
<b>/densum</b>		source code for densum
<b>/test</b>	test files	

<b>/mominert</b>		source code for mominert
<b>/test</b>	test files	
<b>/multiwell</b>		source code for multiwell
<b>/test</b>	test files	
<b>/sctst</b>		source code for sctst
<b>/test</b>	test files	
<b>/thermo</b>		source code for thermo
<b>/test</b>	test files	
<b>etc.</b>		

Each "**test**" directory associated with the source code (see above) contains an example data file and output. In each **test** directory, files with the suffix ".test" are example output files used in the testing.

In addition to the **test** directories, we provide a directory of examples. In each example, files with the suffix ".test" are example output files generated from the data files in the example. The data files can be used as templates when constructing new models. The **examples** directory is organized as follows:

```

/examples
  /bdens-examples
    /anthracene
    /CH4
    /H2O2
  /densum-examples
  /mominert-examples
  /multiwell-examples [Example multiwell Models]
    /multiwell-chemact
    /multiwell-sctst
    /multiwell-thermal
    /multiwell-recombination
    /multiwell-shock
    /multiwell-tunneling
  /thermo-examples
  /gauss2multi-examples
  etc.

```

## ***Recommended Directory Structure for Models***

Because there are multiple input and output files associated with any reaction model, we have found that it is most convenient to organize them in the following way. Each model should have its own individual directory named for the specific model. By not cluttering the `multiwell-<version>` directory with input and output files for models, it is easy to install updates without disturbing the files associated with models.

Recommended Model directory structure:

<b>/model</b>	[name of model; e.g. "c2h6", "clo+clo", etc.]
multiwell.dat	[MultiWell input data file]
multiwell.out	[MultiWell output file]
multiwell.sum	[MultiWell output file]
multiwell.rate	[MultiWell output file]
multiwell.flux	[MultiWell output file]
multiwell.array	[MultiWell output file]
readme.model	[read-me file for description, literature citation, etc.]
<b>/DensData</b>	[REQUIRED for sums and densities of states used by MultiWell]
<b>/multidata</b>	[for stored multiwell data files]
<b>/vibs</b>	[densum data files (suggested file suffix: ".vibs")]
<b>/thermodata</b>	[thermo data files (suggested file suffix: ".therm")]
<b>/momidata</b>	[mominert data files (suggested file suffix: ".mom")]
<b>/results</b>	[stored output]

## 1.4 Installing and Executing the Codes

### *Linux/Unix (and Mac OS X) Versions*

#### Installation of GNU Fortran and Openmpi

Before starting, check that you have installed on your computer a C compiler (e.g. gcc), a C++ (e.g. g++) compiler, and the **make** command. In addition you need a Fortran compiler (e.g. gfortran) as well.

Download from the official OpenMPI website (<https://www.open-mpi.org/software/ompi/v4.0/>) the preferred compressed folder (e.g. openmpi-4.0.0.tar.gz). Then open up a terminal window, move to the directory in which you saved the compressed folder, and type the following instructions (a lot of output is produced, be patient!):

- 1) `sudo -i`
- 3) `tar -xvf openmpi-4.0.0.tar.gz`
- 4) `cd openmpi-4.0.0`
- 5) `mkdir build`
- 6) `cd build`
- 7) `../configure --prefix=/usr/local`
- 8) `make all install`
- 9) `ldconfig`
- 10) `exit`

For more information on how to build OpenMPI and troubleshooting we refer the user to the FAQ section of OpenMPI website (<https://www.open-mpi.org/faq/?category=building>)

<https://gcc.gnu.org/fortran/>

[https://www.open-mpi.org/faq/?category=building - easy-build](https://www.open-mpi.org/faq/?category=building-easy-build)

[https://en.wikipedia.org/wiki/Synaptic\\_\(software\)](https://en.wikipedia.org/wiki/Synaptic_(software))

#### Compiling (executing "make") and Testing

A Makefile script located in the main MultiWell directory sequentially calls makefiles in each source directory. To execute the Makefile and compile the binary executables, type the command "**make**" (omit the quotation marks and use all lower case characters) followed by a carriage return: <return>. After compiling, the binary executables are stored in directory **bin**.

To test that the compiled codes are operating correctly, run the script **runtest\_all** by going to the **scripts** directory and typing the command "**./runtest\_all**". This script will run the newly compiled codes and allow you to compare the output files to "test" outputs stored in the **test** directories associated with the source code. The new outputs will differ from the test outputs with regard to date and computation time. If compiled with FORTRAN compilers other

than GNU Fortran, there may be minor numerical differences. If significant differences appear, then it is possible that the compiled codes are not working properly.

It is highly recommended that users do *not* place user data files, etc., in directory **/multiwell-<version>** (see Section 1.3) Instead, users should create individual directories for user models (see Section 1.5) and execute MultiWell from within those directories. This approach makes it very easy to replace the entire directory **/multiwell-<version>** with a newer version. Programs in the MultiWell Suite are executed as described in Section 2.5.

### Running Serial (NOT parallel) Programs on Linux

Change directories until the present working directory (PWD) is the directory for a model, i.e. the directory where the input data file resides. This Model directory (see Section 1.3) may also contain required sub-directories, such as **DensData**, which is required by the multiwell master equation code.

To run a program named "codename", type the following in the PWD:

```
<PATH>/multiwell-<version>/bin/codename <RETURN>
```

where <PATH> designates the PATH to the MultiWell directory: **/multiwell-<version>**. If directory **/multiwell-<version>** resides in the user's home directory, type:

```
~/multiwell-<version>/bin/multiwell <RETURN>
```

*For example:*

```
~/multiwell-2017/bin/thermo
```

### Running Parallel (NOT serial) Programs **paradensum** and **parsctst** on Linux

*paradensum* and *parsctst* are parallel codes. To compile and run these codes on LINUX it is necessary to have a previously installed version of the free **Open-MPI compiler** as described in the installation Appendix Above. <https://www.open-mpi.org/>

If the Open-MPI compiler has been previously installed, **paradensum** and **parsctst** are compiled along with all of the other codes (the proper commands already reside in the Makefile that is included in the src directory).

The executable (binary) program resides in (or should be placed in) the directory **multiwell-<version>/bin**, where <version> is the version number. To execute the compiled parallel program **paradensum**, for example, enter the directory that contains the input data file "paradensum.dat" and then type:

```
mpirun -np <nwind> paradensum
```

where <nwind> is the number of windows. See Section 8.2 for definitions and more details.

## **Windows Versions**

In the Windows version, binary executables (application, or .EXE files) have already been compiled and are found in the sub-directory "multiwell-<version>/bin".

## **Running Serial (NOT Parallel) Programs on Windows**

To run any of the programs in the MultiWell Suite, **except for parallel codes like paradensum and parsctst** (for parallel codes, see below), the steps are as follows:

1. Prepare a data file (for instructions, see the User Manual and the Examples directory) and place it in a directory devoted to your Model (see Section 1.3). This "Model" directory may also contain required sub-directories, such as **DensData**, which is required by the **multiwell** master equation code.
2. Change directories until the present working directory (PWD) is the directory for a model, i.e. the directory where the input data file resides. For **densum** calculations, for example, the data file (**densum.dat**) may reside in the directory **Model/vibs**.
3. Create an alias of the executable of interest (e.g. **densum.exe**) and place the alias in the Model directory (folder) as the data file. For **densum** calculations, for example, if the data file **densum.dat** resides in the directory **Model/vibs**, the alias should also be placed in directory **Model/vibs**.
4. Double-click the alias. The output files (e.g. **densum.out**, etc.) will be written to the same directory.

## **Expert Users**

Expert Users can set the PATH in Windows and run all of the programs, **except for paradensum and parsctst**, in a DOS window.

From the Model directory where the input data file resides, type:

```
<PATH>/multiwell-<version>/bin/densum.exe <RETURN>
```

*For example:*

```
~/multiwell-2017/bin/densum.exe
```

## **Running Parallel Programs *paradensum* and *parsctst* on Windows**

### **Installation**

1. The **paradensum** and **parsctst** versions for Windows can be downloaded as a precompiled executable files **paradensum.exe** and **parsctst.exe**.
2. These are parallel codes. *To properly run parallel codes it is necessary to have a previously*

*installed version of Microsoft MPI implementation.* To download the Microsoft MPI, the reader is referred to the website:

<https://www.microsoft.com/en-us/download/details.aspx?id=56727>

Download both mspisdsk.msi and MSMpiSetup.exe and execute them.

### **Execution**

1. Put the paradensum.exe or the parsctst.exe executable and parameters.dat input data file in the Model directory.
2. Open the Windows Command Prompt and change directory to the folder that contains paradensum.exe or the parsctst.exe. To run the code with the selected number of windows <nwind>, type:

```
mpiexec -n <nwind> paradensum.exe
```

or

```
mpiexec -n <nwind> parsctst.exe
```

3. All of the output files are automatically generated in the same folder.

## **1.5 Some Technical Issues on Input/Output Files**

All input and output files are text. Input files can be created using almost any text editor that generates unformatted text files. For ease of reading the output files, do not use word-wrapping.

When compiled using GNU and Open-MPI compilers, the following constructs are allowed in the text datafiles (they may, or may not, be permitted when the codes are compiled using other compilers):

- Numerical entries can be separated by commas, blanks, tabs, and line returns.
- Blank lines are ignored.
- In most cases, end of line comments can be entered following a "!" symbol.
- Character variables may be enclosed in a matched pair of 'single quotation marks', or "double-quotation marks". Often, character variables that are single words do not require any quotes if separated from other entries by tabs, blanks, or line returns. When in doubt, enclose them in a matched pair of quotes.
- Title lines are separated from other entries by line returns.

## References

- (1) Andraos, J. A Streamlined Approach to Solving Simple and Complex Kinetic Systems Analytically. *J. Chem. Educ.* **1999**, *76*, 1578-1583; DOI: 10.1021/ed076p1578.
- (2) Barker, J. R.; Frenklach, M.; Golden, D. M. Reply to “Comment on ‘When Rate Constants Are Not Enough’”. *J. Phys. Chem. A* **2016**, *120*, 313–317; DOI: 10.1021/acs.jpca.5b06652.
- (3) Barker, J. R.; Stimac, P. J.; King, K. D.; Leitner, D. M.  $\text{CF}_3\text{CH}_3 \rightarrow \text{HF} + \text{CF}_2\text{CH}_2$ : A non-RRKM Reaction? *J. Phys. Chem. A* **2006**, *110*, 2944-2954; 10.1021/jp054510x.
- (4) Bartis, J. T.; Widom, B. Stochastic models of the interconversion of three or more chemical species. *J. Chem. Phys.* **1974**, *60*, 3474-3482; doi: 10.1063/1.1681562.
- (5) Beyer, T.; Swinehart, D. F. Number of multiply-restricted partitions. *Comm. Assoc. Comput. Machines* **1973**, *16*, 379.
- (6) Boyd, S.; Vandenberghe, L. *Convex Optimization*; Cambridge University Press: Cambridge, UK, 2004.
- (7) Duong, M. V.; Nguyen, H. T.; Truong, N.; Le, T. N. M.; Huynh, L. K. Multi-Species Multi-Channel (MSMC): An Ab Initio-based Parallel Thermodynamic and Kinetic Code for Complex Chemical Systems. *International Journal of Chemical Kinetics* **2015**, *47*, 564-575; doi: 10.1002/kin.20930.
- (8) Frenklach, M.; Packard, A.; Feeley, R. Optimization of Reaction Models with Solution Mapping. In *Modeling of Chemical Reactions*; Carr, R. W., Ed.; Elsevier: Amsterdam, 2007; Vol. 42; pp 243–291.
- (9) Gillespie, D. T. A general method for numerically simulating the stochastic time evolution of coupled chemical reactions. *J. Comp. Phys.* **1976**, *22*, 403-434.
- (10) Gillespie, D. T. Exact stochastic simulation of coupled chemical reactions. *J. Phys. Chem.* **1977**, *81*, 2340-2361.
- (11) Gillespie, D. T. A rigorous derivation of the chemical master equation. *Physica A: Statistical and Theoretical Physics (Amsterdam)* **1992**, *188*, 404-425.
- (12) Glowacki, D. R.; Liang, C. H.; Morley, C.; Pilling, M. J.; Robertson, S. H. MESMER: An Open-Source Master Equation Solver for Multi-Energy Well Reactions. *J. Phys. Chem. A* **2012**, *116*, 9545-9560; 10.1021/jp3051033.
- (13) Gruebele, M.; Wolynes, P. G. Vibrational energy flow and chemical reactions. *Accounts of Chemical Research* **2004**, *37*, 261-267.
- (14) Hernandez, R.; Miller, W. H. Semiclassical transition state theory. *Chem. Phys. Lett.* **1993**, *214*, 129-136.
- (15) Leitner, D. M. Heat Transport in Molecules and Chemical Kinetics: The Role of Quantum Energy Flow and Localization. In *Geometric Structures of Phase Space in Multi-Dimensional Chaos: Applications to Chemical Reaction Dynamics in Complex Systems, Adv. Chem. Phys., vol. 130 (Part B)*; Toda, M., Komatsuzaki, T., Konishi, T., Rice, S. A., Berry, R. S., Eds.; Wiley, 2005; Vol. 130 (Part B); pp 205-256.
- (16) Leitner, D. M.; Levine, B.; Quenneville, J.; Martinez, T. J.; Wolynes, P. G. Quantum energy flow and trans-stilbene photoisomerization: an example of a non-RRKM reaction. *Journal of Physical Chemistry A* **2003**, *107*, 10706-10716.



- (17) Leitner, D. M.; Wolynes, P. G. Many-dimensional quantum energy flow at low energy. *Phys. Rev. Lett.* **1996**, *76*, 216-219.
- (18) Leitner, D. M.; Wolynes, P. G. Quantum energy flow during molecular isomerization. *Chemical Physics Letters* **1997**, *280*, 411-418.
- (19) Lewis, E. S.; Johnson, M. D. The Reactions of p-Phenylene-bis-diazonium Ion with Water. *J. Am. Chem. Soc.* **1960**, *82*, 5399–5407; DOI: 10.1021/ja01505a027.
- (20) Miller, J. A.; Klippenstein, S. J. Master Equation Methods in Gas Phase Chemical Kinetics. *J. Phys. Chem. A* **2006**, *110*, 10528-10544.
- (21) Miller, J. A.; Klippenstein, S. J.; Robertson, S. H.; Pilling, M. J.; Shannon, R.; Zádor, J.; Jasper, A. W.; Goldsmith, C. F.; Burke, M. P. Comment on “When Rate Constants Are Not Enough”. *J. Phys. Chem. A* **2016**, *120*, 306–312; DOI: 10.1021/acs.jpca.5b06025.
- (22) Miller, W. H. Semiclassical limit of quantum mechanical transition state theory for nonseparable systems. *J. Chem. Phys.* **1975**, *62*, 1899-1906.
- (23) Miller, W. H. Unified statistical model for "complex" and "direct" reaction mechanisms. *J. Chem. Phys.* **1976**, *65*, 2216-2223; <https://doi.org/10.1063/1.433379>.
- (24) Miller, W. H. Semi-Classical Theory for Non-separable Systems: Construction of "Good" Action-Angle Variables for Reaction Rate Constants. *Faraday Discuss. Chem. Soc.* **1977**, *62*, 40-46.
- (25) Miller, W. H.; Hernandez, R.; Handy, N. C.; Jayatilaka, D.; Willetts, A. Ab initio Calculation of Anharmonic Constants for a Transition-State, with Application to Semiclassical Transition-State Tunneling Probabilities. *Chemical Physics Letters* **1990**, *172*, 62-68; Doi 10.1016/0009-2614(90)87217-F.
- (26) Mucientes, A. E.; Peña, M. A. d. I. Kinetic Analysis of Parallel-Consecutive First-Order Reactions with a Reversible Step: Concentration–Time Integrals Method. *J. Chem. Educ.* **2009**, *86*, 390-392; DOI: 10.1021/ed086p390.
- (27) Stein, S. E.; Rabinovitch, B. S. Accurate evaluation of internal energy level sums and densities including anharmonic oscillators and hindered rotors. *J. Chem. Phys.* **1973**, *58*, 2438-2445.

## 2. MultiWell Master Equation Code

Codes, examples, and this manual are available from the MultiWell Program Suite web site: [clasp-research.engin.umich.edu/multiwell](http://clasp-research.engin.umich.edu/multiwell)

### 2.1 Brief Description

MultiWell calculates time-dependent concentrations, yields, vibrational distributions, and rate constants as functions of temperature and pressure for unimolecular reaction systems which consist of multiple stable species, multiple reaction channels interconnecting them, and multiple dissociation channels from each stable species. The stochastic method is used to solve the resulting Master Equation. Users may supply unimolecular reaction rates, sums of states and densities of states, or optionally use Forst's Inverse Laplace Transform method<sup>10-12</sup> to calculate  $k(E)$ . For weak collisions, users can select from among many collision models, or provide user-defined functions.

The code is intended to be relatively easy to use. It is designed so that very complicated and very simple unimolecular reaction systems can be handled via the data file. Restructuring of the code and recompiling are NOT necessary to handle even the most complex systems.

MultiWell is most suitable for time-dependent non-equilibrium systems. The real time needed for a calculation depends mostly upon the number of collisions during a simulated time period and on the number of stochastic trials needed to achieve the desired precision. For slow reaction rates and precise yields of minor reaction products, the code will require a long run time, but it will produce results. For long calculation runs, we often just let it run overnight.

MultiWell is based on the Gillespie Exact Stochastic algorithm,<sup>13-15</sup> as modified and implemented in our laboratory.<sup>1,2,5,22</sup> It has been described in considerable detail in a recent publication.<sup>3</sup> An example calculation has also been published.<sup>6</sup>

In the example,<sup>6</sup> chemical activation and shock wave simulations were carried out for a system consisting of six isomers and 49 energy-dependent unimolecular reactions. The isomers were interconnected by reversible isomerization reactions, and each isomer could also decompose, resulting in 14 sets of products. Many of the capabilities of MultiWell are illustrated in that paper.<sup>6</sup>

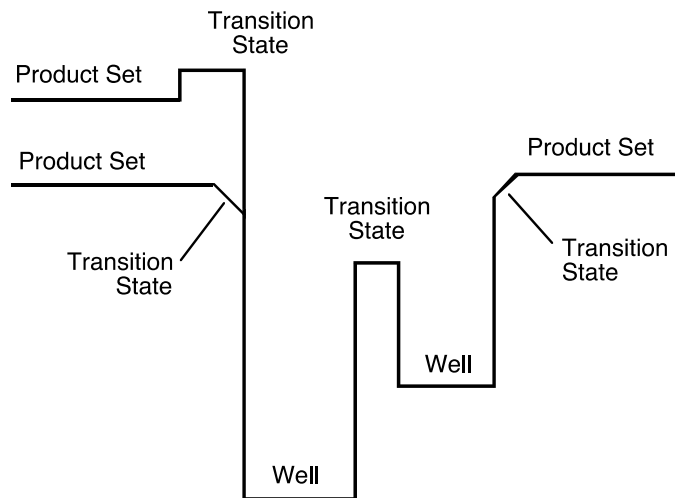
### 2.2 Terminology

The following sketch shows the potential energy as a function of reaction coordinate for a typical unimolecular system with multiple wells.

- **Wells** are chemical species corresponding to local minima on the potential energy surface (PES). They must have at least one bound vibrational state (i.e., at least the zero point,  $v=0$  state). This definition is precise, sufficient, and economical; we do not find it useful to attach any other conditions.
- **Transition states** for reaction are defined in the usual way. They may be fixed (i.e. associated with a local maximum on the PES), or variational.
- **Product sets** are the fragmentation products corresponding to irreversible reaction *via* a given transition state. In this user Manual, **Product Sets** and **Reactant Sets** are synonymous, since they refer to the same reaction channel.

In MultiWell, each Well, each Transition State, and each Product Set is given a name and is designated by an index number, as described below. The names and index numbers are arbitrary, but they provide unique identification.

Collisional activation and deactivation can take place within each well and therefore energy transfer parameters are designated for each. In most cases, energy transfer parameters are poorly known, if known at all, and thus it is usually convenient to assign the same energy transfer parameters to all of the wells.



The energy scheme assumed by MultiWell is shown schematically by the following diagram:

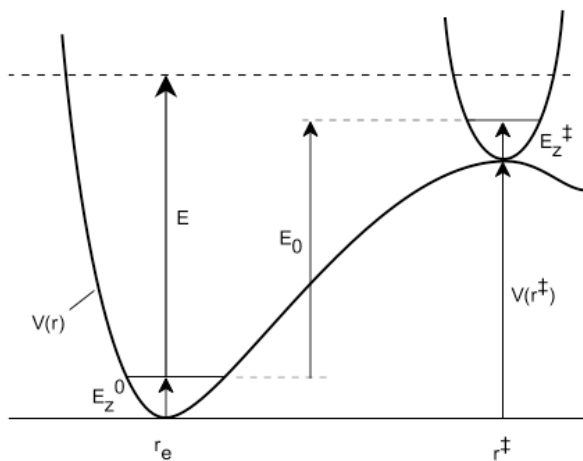


**Figure 0.** Energy schematic. The active energy  $E$  is measured from the zero point energy of the reactant well. The critical energy  $E_0$  is the zero point energy difference between the transition state and the reactant well.

## 2.3 Default Array Dimensions

Currently, the array dimensions are set for use with up to the following defaults, but the true limits are much larger, depending on computer memory available for running the code. (See the Appendix Above on "Terminology".)

- Up to 200 Wells.
- Up to 200 Reaction channels per well.
- Up to 200 Product Sets.
- Double Arrays with user-selected sizes up to 100,000 energy bins.
- 101 time steps (including  $t = 0$ ).
- 1001 energy bins x 101 time steps for reporting vibrational distributions.

Array dimensions can be changed by revising the following file:

```
multiwell/src/multiwell/ declare_mod.f
```

After changing the file, the multiwell master equation code must be completely re-compiled (To re-compile on the LINUX platform, change directories to multiwell- $\langle$ version $\rangle$ ; type "make clean  $\langle$ return $\rangle$ " and then type "make  $\langle$ return $\rangle$ "; the entire multiwell package will be re-compiled.)

## 2.4 Notes on FORTRAN source code and compilation

- There are many explanatory comments embedded in the source code.
- The source code is written for the GNU FORTRAN compiler for LINUX; a makefile (with suitable options) is distributed with the code. The code can also be compiled with almost any other FORTRAN compiler.
- A few sections of the source code are platform-dependent (e.g., OPEN statements, date & time calls, and file & path names). These can be found in the following source code segments:

```
MultiWell.f [main program]  
DateTime.f  
DensArray.f  
Estart.f  
RateArray.f
```

- The following compiler options are required, or recommended:
  - variables and constants initialized to zero (RECOMMENDED).
  - double precision transcendentals (RECOMMENDED).
  - promote REAL and COMPLEX to double precision (RECOMMENDED).
  - basic optimizations (RECOMMENDED).

## 2.5 MultiWell Input Files and Program Execution

The default input data filename is **multiwell.dat** (all lower case). Starting with version 2008.1, it is possible to change the input data file name and run multiple sessions in the same directory at the same time, each with a user-selected **FileName**.

### To run MultiWell using the default data filename (multiwell.dat):

LINUX/UNIX: in the directory where the input data file and the auxiliary directory DensData reside, type:

```
<PATH>/multiwell-<version>/bin/multiwell <RETURN>
```

where <PATH> designates the PATH to /multiwell-<version>. If directory /multiwell-<version> resides in the user home directory, type:

```
~/multiwell-<version>/bin/multiwell <RETURN>
```

WINDOWS in a DOS window: in the directory where the input data file and the auxiliary directory DensData reside, type:

```
<PATH>/multiwell-<version>/bin/multiwell <RETURN>
```

#### *For example:*

```
~/multiwell-2013/bin/multiwell
```

### To run MultiWell using a user-defined filename (FileName.dat):

Follow the same procedures described above, but type:

```
<PATH>/multiwell-<version>/bin/multiwell <FileName> <RETURN>
```

#### *For example:*

```
~/multiwell-2017/bin/multiwell final.dat
```

All of the resulting output files will take names with the same prefix:

```
final.out  
final.sum  
final.rate  
final.dist  
final.flux  
final.array
```

## 2.6 MultiWell Output Files

Output files with an identical FileName (including the default: 'multiwell') are erased and written-over for every calculation (for optionally naming of files at run time, see Section 2.5). To be saved, they must be re-named. Use a word processor/editor capable of wide-open (no truncation of lines) output, because the output can be hundreds of characters in width, depending on the number of species and products. In Linux, Xemacs, Emacs, Nedit and other editors are available for this purpose. For Macintosh OS X, "Tex-Edit Plus" (share-ware available at <http://www.nearside.com/trans-tex/>) and "TextWrangler" (free-ware available at <http://www.barebones.com/>) are very convenient word processors for text files, although full-featured word processors can be used as well.

### *FileName.out*

Time-dependent output of concentrations and average energies. Also includes summaries of input parameters. The time-dependent quantities are the instantaneous values at the time indicated: they are not averaged over the time interval. Hence, the averages are only over the number of trials.

### *FileName.sum*

Summary output file intended for convenient calculations of fall-off curves and other pressure-dependent quantities. This file gives all of the header material in the full output file, but instead of the time-dependent results, only the final results of each simulation are given in the form of a summary table.

### *FileName.rate*

Time-dependent output of average reaction flux coefficients, which vary with time in non-steady-state systems. (When the energy distributions are independent of time and for the reactions are irreversible, the flux coefficients can be identified with rate constants.) Many trials are needed to accumulate good statistics. To improve statistics, the binned results correspond to the number of visits to the bin (which can be many times larger than the number of trials) and are averaged over the time-bin.

### *FileName.dist*

Time-dependent vibrational distributions in Wells (not initial or final products). Only the non-zero array elements are listed. Many trials are needed to accumulate good statistics. Note that the distributions are normalized according to the number of stochastic trials. Therefore, the sum of the array elements for a chemical species (Well) at a given time is equal to the fractional population of that species at that time. Thus the distributions report not only the relative populations as functions of energy and time, but also the growth and decay of species concentrations.

### *FileName.array*

Tabulations of all energy-dependent input data. Includes tables of densities of states, specific rate constants, collision probabilities and normalization factors, and initial energy distributions.

### ***FileName.flux***

Tabulates the reactive flux via each of the unimolecular channels. The reactive flux is useful for identifying quasi-equilibrium situations and for tracing chemical pathways.

## **2.7 MultiWell Input Data File (FileName.dat)**

(See Section 2.5 for optional naming of data files at run time.)

The datafile uses free input format.

NOTES ON FREE INPUT FORMAT: Fields separated by delimiters.

- Standard delimiters on most platforms: commas and spaces.
- Additional delimiters acceptable on some platforms: tabs.
- CHARACTER constants enclosed in apostrophes (') are accepted on most platforms. Some platforms will accept CHARACTER constants without their being enclosed in apostrophes, but then they cannot contain any of the delimiter characters.

### MULTIWELL MAJOR INPUT OPTIONS

1. Densities of states are read from an external file created by DenSum, or other code.
2. Specific Rate constants:  $k(E)$ 
  - a) RRKM theory via sums of states read from an external file (created by DenSum, or other code).
  - b)  $k(E)$  values read from external file.
  - c) Reversible and/or irreversible reactions.
3. Initial energy distributions:
  - a) thermal (with an optional energy offset), calculated internally.
  - b) chemical activation, calculated internally.
  - c) delta function
  - d) distribution can be read from an external file.
4. Separate initial vibrational temperature and translational temperature.
5. Can incorporate the effects of slow intramolecular vibrational energy redistribution (IVR).
6. Can include tunneling via an unsymmetrical Eckart barrier.

## MULTIWELL INPUT DATA FILE FORMAT

**Note: Starting with version 2.0, the data file format is no longer compatible with previous versions.**

### PART A: PHYSICAL PARAMETERS

#### Line 1 (line count ignores blank lines following TITLE)

**TITLE** (up to 100 characters)

#### Line 2

**Egrain1, imax1, lsize , Emax2, IDUM**

Egrain1	energy grain size of first segment in "double arrays", see Note (units: $\text{cm}^{-1}$ )
imax1	size of first segment of double array; selected so that sums or densities of states is a smooth function of energy (less than $\sim 1\%$ relative fluctuations). Note that imax1 must be less than lsize.
lsize	user-selected size of double array. The Default array size starting in version 2.08 is set for a maximum of 14000 elements in the INCLUDE file " <b>declare1.inc</b> ". (The array size is defined by <b>lmax=14000</b> in declare1.inc.) This large maximum array size allows users to select any value of <b>lsize</b> $\leq$ 14000 elements without having to recompile the code. If array sizes greater than 14000 elements are needed, the lmax can be changed in the Linux/Unix version by deleting old object files (by typing 'make clean' in /multiwell/src/multiwell) and then recompiling (by typing 'make').
Emax2	maximum energy of 2nd segment of double arrays (units: $\text{cm}^{-1}$ )
IDUM	random number seed (integer); EXAMPLE: "2113989025"

\*\*\*\*\* **NOTE: "Double arrays"** have two sections: segment 1 consists of imax1 equally spaced (Egrain1) data ranging from  $E=0$ ; segment 2 consists of equally spaced values from  $E=0$  to Emax2; the size of the second segment is (lsize - imax1); the energy grain of the second segment is  $\text{Emax2}/(\text{lsize} - \text{imax1} - 1)$ .

(Appendix A, continued...)



### Line 3

#### **Punits, Eunits, Rotatunits**

*[It is required that the three keywords be entered in this exact order!]*

**Punits** one of the following pressure units keywords:  
'BAR', 'ATM', or 'MCC'[for molecules/cc] (Note that 'TOR' is no longer accepted.)

**Eunits** one of the following energy units keywords:  
'CM-1', 'KCAL', or 'KJOU' for  $\text{cm}^{-1}$ , kcal/mole or kJ/mole

**Rotatunits** one of the following keywords for rotational information (upper or lower case):  
'AMUA', 'GMCM', 'CM-1', 'MHZ', 'GHZ'(for moments of inertia in units of  $\text{amu}\cdot\text{\AA}^2$  or  $\text{g}\cdot\text{cm}^2$ , and rotational constants in units of  $\text{cm}^{-1}$ , MHz, or GHz)

### Line 4

#### **Temp , Tvib**

**Temp** translational temperature (units: Kelvin)  
**Tvib** initial vibrational temperature (units: Kelvin)

For shock-tube simulations, **Temp** is set equal to the shock (translational) temperature and **Tvib** is set equal to the vibrational temperature prior to the shock (usually room temperature).

### Line 5

**Np** number of pressures

### Line 6

**PP(1), PP(2), ..., PP(Np)**

List of Np pressures

## **PART B: PARAMETERS FOR WELLS AND FOR PRODUCT SETS**

### **Line 7**

#### **NWells , NProds**

NWells      number of "wells" (includes irreversible product sets)  
NProds      number of entrance/exit channels; each channel has a product set associated with it.

### **Line 8**

#### **IMol , MolName , HMol , MolMom , Molsym , Molele , Molopt**

(REPEAT NWells times: once for each well.)

IMol          index number for well (1 ... NWells)  
MolName      name of well ( $\leq 10$  characters)  
HMol          enthalpy of formation at 0 K (units defined by keyword)  
MolMom      rotational parameter for 2-dimensional external rotation (moment of inertia or rotational constant; units defined by keyword on Line 3)  
Molsym      external symmetry number for well (see Appendices B4 and B.5)  
Molele      electronic partition function for well (REAL number); depends on temperature; can be obtained from THERMO output.  
Molopt      number of chiral stereoisomers (or "optical isomers", or mirror images) for well (see Appendix B.5)

**See Appendices B.4 and B.5 for a discussion of proper input for External Molecular Rotations and number of "optical isomers" (i.e. mirror images).**

### **Line 9**

#### **IMol , MolName , Hmol**

(REPEAT NProds times: once for each entrance/exit channel, i.e. for each product set.)

IMol          index for channel (NWells+1...NWells+NProds)  
MolName      name of Product set (max 10 characters)  
Hmol          enthalpy of formation at 0 K (units defined by keyword on Line 3) [ignored unless tunneling is used]

\*\*\*\*\* NOTE: the numbering of entrance/exit channels starts with NWells+1.

### **Line 10**

#### **SigM, EpsM, AmuM, Amu**

SigM	Lennard-Jones $\sigma$ (Å) for collider
EpsM	Lennard-Jones $\epsilon/k_B$ (Kelvins) for collider
AmuM	Molecular weight (g/mole) of collider
Amu	Molecular weight (g/mole) of reactant

### **Optional Line 10a**

**OLDET** To change the default treatment of collisional energy transfer from Barker's "New Approach" (see Ref. <sup>4</sup>) to the traditional approach, insert the keyword **OLDET** (upper or lower case) on a new line. The "New Approach" (the default) attenuates the inelastic collision frequency (and hence the rate of inelastic energy transfer) at low energies, where the densities of states are very sparse. The traditional method was based on the convenient assumption that the inelastic collision frequency is independent of internal energy. This feature facilitates intercomparisons between multiwell and other master equation codes.

### **Line 11**

**Mol, Sig, Eps, ITYPE, DC(1), DC(2), ... , DC(8)**

(REPEAT Lines 11 and 12 NWells times: once for each well.)

Mol	index number of Well
Sig	Lennard-Jones $\sigma$ (Å) for this well
Eps	Lennard-Jones $\epsilon/k_B$ (Kelvins) for this well
ITYPE	selects model type in Subroutine PDOWN (see below for description of collision models). Model types and explanations are given below.
DC(8)	eight (8) coefficients for energy transfer model

### **Line 12**

**LJQM** keyword for type of collision rate constant:  
'LJ' for Lennard-Jones collision rate constant. This rate constant is computed using the empirical expression of Neufeld et al. for the collision integral.<sup>20</sup>  
'QM' for quantum mechanical total collision rate constant<sup>9</sup>

(REPEAT Lines 11 and 12 NWells times: once for each well.)

## PART C: PARAMETERS FOR TRANSITION STATES AND REACTIONS

### Line 13

**NForward** number of forward unimolecular (not recombination) reactions to be input.

### Line 14

**Mol, ito, TS, RR, j, k, l, AA, EE, KEYWORD, KEYWORD, KEYWORD, KEYWORD, KEYWORD**

(REPEAT NForward times: once for each forward reaction.)

**Mol** index of reactant well  
**ito** index of entrance/exit channel or well  
**TS** Name of transition state (up to 10 characters)  
**RR** 2-D external rotational parameter (moment of inertia or rotational constant; units defined by keyword on Line 3) ; **See Appendix B.4 for a discussion of proper input for External Molecular Rotations.**  
**j** external symmetry number for TS (see Appendix B.5 for a discussion)  
**Qel** electronic partition function for TS (REAL number)  
**l** number of optical isomers for TS (see Appendix B.5 for a discussion)  
**AA** A-factor for reaction (units:  $s^{-1}$ ); only used for ILT method, but ALWAYS read in  
**EE** reaction critical energy ( $E_0$ ), relative to ZPE of reactant (Mol) (i.e. the barrier height with zpe corrections). When using CRP files generated by program SCTST,  $E_0$  is set to the larger of zero, or the enthalpy difference (at 0 K) between product and reactant; i.e.  $E_0 = \text{MAX}[0.0, (\Delta H(\text{ito}) - \Delta H(\text{Mol}))]$ .  
**KEYWORDS** ALWAYS SPECIFY FIVE KEYWORDS, IN ANY ORDER. Select one from each of the Five Groups below. **See Section 2.10 (FATAL INPUT ERRORS) for a list of incompatible choices.**

#### Group 1

'NOREV' for neglecting the reverse reaction  
'REV' for calculating reverse reaction rate (automatically treated as NOREV for dissociation reactions).

#### Group 2

'FAST' for neglecting limitations due to IVR  
'SLOW' for including IVR limitations; line 14b contains parameters (see below).

#### Group 3

'NOTUN' for neglecting tunneling

'TUN' for including tunneling *via* unsymmetrical Eckart barrier; line 14a contains parameters (see below). **This option cannot be selected if SCTST was used to generate the cumulative reaction probability (~sum of states).**

#### Group 4

'NOCENT' for no centrifugal correction

'CENT1' for quasi-diatomic centrifugal correction with 1 adiabatic external rotation (**for special cases**)

'CENT2' for quasi-diatomic centrifugal correction with 2 adiabatic external rotations

'CENTX' for **legacy centrifugal correction** with 2 adiabatic external rotations (**not recommended**)

[**Note:** the calculated  $k_{\infty}$  is numerically the same for all options in Group 4.]

#### Group 5

'ILT' Inverse Laplace transform method for  $k(E)$ .

'SUM' External file containing sums of states (i.e. generated by densum, or bdens)

'CRP' External file containing cumulative reaction probability (i.e. generated by program sctst).

'RKE' External file containing  $k(E)$ : <TS filename>'.rke' (e.g. 'TS-1.rke'). NOTE:  $k(E)$ 's can be calculated by other programs and read in as an external file (see Section 2.9).

### **Line 14: Supplementary Lines**

The following supplementary lines provide additional information corresponding to some of the Keywords in Line 14. *The supplementary line immediately follows the line invoking the Keyword.* (On the rare occasion when more than one supplementary line is required, they must be entered in the order given here.)

#### **Supplementary Line 14a**

**'TUN', vimag(Mol,i)**

This line appears only if KEYWORD 'TUN' was used in Line 14. It gives the imaginary frequency ( $\text{cm}^{-1}$ ) for the specified reaction. It can only be used when 'NOCENT' is invoked. Cannot be used simultaneously with 'ILT' or 'RKE'.

#### **Supplementary Line 14b**

**'SLOW', vivr(Mol,i), vave(Mol,i), kcivr(Mol,i), tivr(Mol,i), civr(Mol,i,1), civr(Mol,i,2), civr(Mol,i,3)**

This line appears only if KEYWORD 'SLOW' was used in Line 14. It gives parameters for the IVR transmission coefficient for this reaction:

$$\text{Transmission Coefficient} = \frac{k_{IVR}(E) + k_{IVR}^c [M]}{k_{IVR}(E) + k_{IVR}^c [M] + \nu_{IVR}}$$

where  $\nu_{IVR}$  is the characteristic reaction frequency (as in RRK unimolecular reaction rate theory). At energies above the IVR threshold energy (i.e.  $E \geq E_{IVR}^0$ ), the IVR rate constant  $k_{IVR}(E)$  is:

$$k_{IVR}(E - E_{Or}) = civr(Mol, i, 1) + civr(Mol, i, 2) \times (E - E_{Or}) + civr(Mol, i, 3) \times (E - E_{Or})^2$$

where  $E$  (expressed in  $\text{cm}^{-1}$ ) is the energy relative to the reactant zero point energy and  $E_{Or}$  is the reaction critical energy (which may include the centrifugal correction).

vivr(Mol,i)	Characteristic frequency ( $\text{cm}^{-1}$ ) for the reaction; $\nu_{IVR}/\text{s}^{-1} = \text{vivr} * 2.9979 \times 10^{10}$ .
vave(Mol,i)	Average frequency ( $\text{cm}^{-1}$ ) of the reactant; used to define an upper limit to $k_{IVR}$ , the IVR rate constant: $k_{IVR} \leq 2 * \text{vave} * 2.9979 \times 10^{10}$ .
kcivr	Bimolecular rate constant $k_{IVR}^c$ [ $\text{cm}^3 \text{ molecule}^{-1} \text{ sec}^{-1}$ ] for collision-induced IVR. In the absence of other information, $k_{IVR}^c$ may be estimated as approximately equal to the quantum mechanical total collision frequency bimolecular rate constant, as obtained from the MultiWell output (see Line #12, above).
tivr(Mol,i)	IVR threshold energy ( $\text{cm}^{-1}$ ), measured from the reaction critical energy (i.e. $E_{IVR}^0 - E_{Or}$ ).
civr(Mol,i,..)	Three (3) coefficients for second order polynomial fit of $k_{ivR}$ ( $\text{s}^{-1}$ ) as a function of $E - E_{Or}$ ( $\text{cm}^{-1}$ ; energy measured from the reaction critical energy).

### Optional Line 14opt

' **MORERXN** ' This option can be invoked for including supplementary canonical (i.e. thermal) unimolecular reactions and bimolecular reactions of Mol (a Well) with the bath gas. Each line following the keyword line supplies the needed information for the canonical rate constant, which is assumed to be expressed with Arrhenius parameters:  $k_{\text{sup}}(T) = \text{Afc} \times \exp(-\text{Bbm}/T)$ , where T is the translational temperature.

**Mol, bto(Mol,n), SupName(Mol,n), norder(Mol,n) , Afc(Mol,n), Bsr(Mol,n),  
dde(Mol,n)**

(integer, integer, character(len=10), real, real, real)

This feature is useful for reaction rate constants that do not have significant dependence on the internal energy of Mol (i.e.  $k_{\text{sup}}(E)$  for the supplementary reaction is approximately constant, as in the work of Matthias Oltzmann<sup>21</sup>). Rate constant  $k_{\text{sup}}(E)$  is approximately constant when canonical rate constant  $k_{\text{sup}}(T)$  has little or no dependence on temperature. When the energy dependence *cannot* be neglected, this **MORERXN** option should not be used. Instead, the microcanonical  $k_{\text{sup}}(E)$  can be entered as an external RKE type file (see above). For bimolecular reactions, the microcanonical rate constants can be obtained from bimolecular microcanonical transition state theory, as described by Maranzana and Barker.<sup>18</sup>

Mol	Index number for a Well that reacts with the bath gas.
bto(Mol,n)	Index number of the reaction product(s): either a Well, or a terminal product set.
SupName(Mol,n)	Name of the supplementary reaction.
norder(Mol,n)	Order of reaction (=1 for unimolecular, =2 for bimolecular)
Afc(Mol,n)	A-factor (units: $\text{s}^{-1}$ for unimolecular and $\text{cm}^3 \text{ molecule}^{-1} \text{ s}^{-1}$ for bimolecular). <b>Note that when the bath gas is a mixture</b> (e.g. air) and only one component is reactive (e.g. O <sub>2</sub> ), parameter Afc for the bimolecular reaction must be adjusted accordingly, e.g. for 21% O <sub>2</sub> , the adjusted $\text{Afc}(\text{adjusted}) = 0.21 \times \text{Afc}$ .
Bsr(Mol,n)	$E_{\text{activation}}/R$ (units: dimensionless)
dde(Mol,n)	When the product is a Well, dde is the energy lost to the bath. Usually set equal to 0; this is for modeling electronic quenching (units: $\text{cm}^{-1}$ ).

## PART D: CALCULATION SPECIFICATIONS

### Line 15

#### **Ntrials, Tspec, Tread, KEYTEMP, Molinit, IR, Einit**

Ntrials	number of trials
Tspec	a KEYWORD that specifies meaning of Tread (CHARACTER*4) 'TIME' indicates Tread = max time simulated (Tlim) 'LOGT' indicates Tread = max time simulated (Tlim). Keyword 'LOGT' calls for a log(t) time scale, so that so that a simulation can be displayed for many orders of magnitude, starting from t = 100 attosecond and ending at the time designated by Tread. 'COLL' indicates Tread = max time simulated is calculated from the specified maximum number of collisions experienced by initial well number (Molinit).
Tread	maximum simulated <b>time</b> or maximum number of <b>collisions</b> (see Tspec, above).
KEYTEMP	a KEYWORD that specifies the type of initial energy distribution 'DELTA': Monoenergetic at energy Einit 'THERMAL': Thermal (Tvib) with energy offset Einit 'CHEMACT': Chemical activation (Tvib) from "product" #IR 'EXTERNAL': Read cumulative energy distribution from external file "multiwell.pstart" placed in directory " DensData "
Molinit	index of initial well
IR	index number of the "product set" which reacts to produce Molinit via chemical activation; neglected if 'CHEMACT' is not specified.
Einit	initial energy (relative to ZPE of Molinit); neglected if 'CHEMACT' is specified; same units as Eunits.

### Line 16

BLANK LINE TO INSURE THAT THE LAST LINE IS FOLLOWED BY A CARRIAGE RETURN (needed for all READ statements). THE CARRIAGE RETURN IS EASILY OVERLOOKED!

## 2.8 Collision Models

(see Line 11 in multiwell data file described above)

This selection of collision models includes most of the empirical models discussed in the literature. Function subroutine "Pdown.f" can be revised to include additional models.

For general guidance in selecting models and parameters, see Barker et al.<sup>8</sup> and King and Barker.<sup>16</sup> For the **EXPONENTIAL MODEL**, use IYPE=1 with coefficient C(4) set equal to zero so that the second exponential term is equal to zero; Model Types 12 or 13 can also be used



with appropriate parameter choices. Note that by default, the MultiWell master equation code uses Barker's "New Approach" (see Ref. <sup>4</sup>), but this can be turned off by entering the key word "**OLDET**" on Optional Line 10a of the multiwell input file (see above).

#### ITYPE

- 1 Biexponential Model
- 2 Density-weighted Biexponential Model
- 3 Off-set Gaussian with constant offset and E-dependent width
- 4 Biexponential Model with energy-dependent fraction
- 5 Generalized Gaussian with energy-dependent exponent
- 6 Generalized Gaussian plus Exponential term
- 7 Weibull Model
- 8 Lorentzian Step-Ladder Model
- 9 Exponential+Elastic Model
- 10 Klaus Luther's empirical function
- 11 Radiationless transition empirical function
- 12 Exponential Model with  $\alpha(E)=\text{linear} + \text{exponential}$
- 13 Exponential Model with  $\alpha(E)$  switching function
- 14 Boltzmann-weighted exponential

#### FUNCTION AND COEFFICIENT DESCRIPTIONS:

##### ITYPE = 1 for Biexponential Model

$$P_{\text{down}} = (1-C(4))*\text{EXP}(-(E-EE)/\text{Alpha1}) + C(4)*\text{EXP}(-(E-EE)/\text{Alpha2})$$

$$\text{Alpha1} = [C(1) + E*C(2) + E*E*C(3)]*(T/300)**C(8)$$

$$\text{Alpha2} = [C(5) + E*C(6) + E*E*C(7)]*(T/300)**C(8)$$

##### ITYPE = 2 for Density-of-States-weighted Biexponential Model

$$P_{\text{down}} = \rho(E)*((1-C(4))*\text{EXP}(-(E-EE)/\text{Alpha1}) + C(4)*\text{EXP}(-(E-EE)/\text{Alpha2}))$$

$$\text{Alpha1} = [C(1) + E*C(2) + E*E*C(3)]*(T/300)**C(8)$$

$$\text{Alpha2} = [C(5) + E*C(6) + E*E*C(7)]*(T/300)**C(8)$$

##### ITYPE = 3 for Off-set Gaussian with constant offset and E-dependent width

$$P_{\text{down}} = \text{EXP}(-(0.5*(E-EE-C(4))/\text{Alpha1})**2)$$

C(4) = constant off-set, Alpha1 is the std. dev.

$$\text{Alpha1} = [C(1) + E*C(2) + E*E*C(3)]*(T/300)**C(8)$$

##### ITYPE = 5 for Generalized Gaussian with energy-dependent exponent

$$P_{\text{down}} = \text{EXP}(-[(E-EE)/\text{Alpha}]^{**}\text{Exponent})$$

$$\begin{aligned}\text{Alpha} &= C(1) + [E*C(2) + E*E*C(3)] \\ \text{exponent} &= C(5) + [E*C(6) + E*E*C(7)]\end{aligned}$$

**ITYPE = 6 for Generalized Gaussian plus Exponential term**

$$P_{\text{down}} = (1-C(6))*\text{EXP}(-[(E-EE)/\text{Alpha1}]^{**}\text{Exponent}) + C(6)*\text{EXP}(-(E-EE)/\text{Alpha2})$$

$$\begin{aligned}\text{Alpha1} &= C(1) + [E*C(2) + E*E*C(3)] \\ \text{Alpha2} &= C(7) + E*C(8) \\ \text{Exponent} &= C(4) + E*C(5)\end{aligned}$$

**ITYPE = 7 for Exponential Model with Switching function**

$$P_{\text{down}} = \text{EXP}(-(E-EE)/\text{Alp})$$

$$\begin{aligned}\text{Alpha1} &= C(1) + E*C(2) \\ \text{Alpha2} &= C(3) + E*C(4) \\ \text{Alp} &= \text{Alpha1} + 0.5*(\text{Alpha2} - \text{Alpha1})*(1. - \text{TANH}((C(5) - E)/C(6) ) )\end{aligned}$$

**ITYPE = 8 for Lorentzian Step-Ladder Model**

$$P_{\text{down}} = 1 / [(E-EE-\text{Alpha})^2 + \text{Width}^2]$$

$$\begin{aligned}\text{Alpha} &= C(1) + [E*C(2) + E*E*C(3)] \\ \text{Width} &= C(5) + [E*C(6) + E*E*C(7)]\end{aligned}$$

**ITYPE = 9 for Exponential+Elastic Model**

$$P_{\text{down}} = [F/(F+C(4))]*\text{EXP}(-(E-EE)/\text{Alpha}) + \text{elastic}$$

$$\begin{aligned}\text{Alpha} &= [C(1) + E*C(2) + E*E*C(3)]*(T/300)^{**}C(8) \\ F &= [C(5) + (E/C(6))^{**}C(7)]*(T/300)^{**}C(8); \text{ when } E=EE\end{aligned}$$

**ITYPE = 10 for Klaus Luther's empirical function**

$$\begin{aligned}P_{\text{down}} &= \text{EXP}[-[(E-EE)/\text{Alpha}]^{\text{Beta}}] \\ \text{Alpha} &= C(1) + E*C(2) \\ \text{Beta} &= C(3)\end{aligned}$$

**ITYPE = 11 for radiationless transition empirical Function**

$$P_{\text{down}} = \text{EXP}[-(E-EE)/\text{Alpha}]'$$

$$\text{Alpha} = C(1)*[1-\text{exp}[-(E/C(2))^{\text{C}(3)}] + C(4)]$$

### **ITYPE = 12 for Exponential Model with $\alpha(E)$ = Linear+exponential**

$$P_{\text{down}} = \text{EXP}(-(E-EE)/\text{Alpha1})$$

$$\text{Alpha1} = C(1) + E*C(2) + C(3)*\text{exp}(-E/C(4))$$

### **ITYPE = 13 for Exponential Model with $\text{Alpha}(E)$ Switching function**

$$P_{\text{down}} = \text{EXP}(-(E-EE)/\text{Alp})$$

$$\text{Alp} = \text{Alpha1} + 0.5*(\text{Alpha2} - \text{Alpha1})*(1. - \text{TANH}((C(5) - E)/C(6)))$$

$$\text{Alpha1} = C(1) + E*C(2)$$

$$\text{Alpha2} = C(3) + E*C(4)$$

### **ITYPE = 14 for Boltzmann-Weighted Exponential** (motivated by recent trajectory calculations<sup>7</sup>)

$$P_{\text{down}} = B(T;EE,E)*\text{EXP}(-(E-EE)/\text{Alp})$$

$$B(T;EE,E) = \text{SQRT}(\text{rho}(EE)*\text{exp}(-(EE-E)/RT))$$

where  $\text{rho}(EE)$  = density of states

$$\text{Alp} = C(1)$$

## **2.9 Format of External Data Files**

Location: EXTERNAL DATA FILES MUST BE STORED IN FOLDER (DIRECTORY) "DensData", which is in the folder (directory) from which the MultiWell application is executed.

### ***Densities, Sums and $k(E)$ 's***

Creation: Typically, the external files for densities of states and sums of states are generated using the program DenSum, which calculates sums and densities via exact counts. A similar format is used for specific rate constants, as described here.

#### **FILE NAMES**

For sums and densities of states: CHARACTER\*10 + '.dens'

Example: 'Ethyl-Cl .dens'

For specific rate constants [ $k(E)$ 's]: CHARACTER\*10 + '.rke'

Example: 'HCl+C2H4.rke'

#### **FILE FORMAT**

Note: Starting with version 2008.1, " \_\_\_\_ .dens" files, which contain sums and densities of states, may have a block of comment lines preceding Line 1 (below). The first and last comment lines in the block must have *exactly* the following 46 characters:

\*\*\*\*\*INPUT DATA SUMMARY\*\*\*\*\*

### **Line 1 (LINE COUNT IGNORES BLANK LINES FOLLOWING TITLE)**

Name of species or transition state [CHARACTER\*10]: up to 10 characters (skipped when read by MultiWell, and therefore can be left blank)

### **Line 2**

Title/Comment line [CHARACTER\*100]: up to 100 characters (skipped when read by MultiWell, and therefore can be left blank)

### **Line 3**

**Egrain1 , imax1 , Emax2 , Isize , Viblo**  
[REAL, INTEGER, REAL, INTEGER, REAL]

Note that this ordering of parameters is *not* the same as in multiwell.dat. If Egrain1, imax1, & Emax2 do not match those for the MultiWell run (see line #2 of the MultiWell data file), then execution terminates with a message. In density and sums of states files, Viblo is the lowest vibrational frequency for a given species; it is used in the collision step routines. In rate constant input files, A real number must be input for Viblo, but it is ignored by MultiWell.

### **Line 4**

Column labels (skipped when read by MultiWell, and therefore can be left blank)

For sums of states, this line might read:

" **No. (cm-1) Density Sum**"

For a rate constant input file, this line might read:

" **No. Energy Dummy RateConst**"

### **Line 5**

(Repeated Isize times)

**j, A, B, C**  
[INTEGER,REAL,REAL,REAL]

FOR FILES CONTAINING SUMS & DENSITIES (these are double arrays)

j = array element index (a total of Isize elements)

A = energy starting with E = 0.0 (units: cm-1), which corresponds to the zero point energy of the species or transition state.

B = density of states (units: states/cm-1)

C = sum of states (dimensionless)

FOR FILES CONTAINING SPECIFIC RATE CONSTANTS [k(E)'s] (these are double arrays)

j = array element index (a total of lsize elements)

A = energy starting with E = 0.0 (units: cm<sup>-1</sup>). For reactions without tunneling, E=0 corresponds to the zero point energy of the transition state (i.e. barrier height with zero point energy corrections), relative to the reactant energy (with zero point energy corrections). For reactions with tunneling, E = 0.0 corresponds to the lowest energy considered, which is usually significantly lower than the barrier height with zero point energy corrections (this same energy is entered in the MultiWell data file).

B = dummy real number (ignored by MultiWell)

C = k(E) (units: s<sup>-1</sup>)

### **Line 6**

BLANK LINE TO INSURE THAT THE LAST LINE IS FOLLOWED BY A CARRIAGE RETURN (needed for all READ statements). THE CARRIAGE RETURN IS EASILY OVERLOOKED.

## ***Initial Energy Distribution Function***

File name: "multiwell.pstart"

Location: EXTERNAL DATA FILES MUST BE STORED IN FOLDER (DIRECTORY) "DensData", which is in the folder (directory) from which the MultiWell application is executed.

### **Line 1 (BLANK LINES ARE NOT ALLOWED)**

#### **Jsize, Hstart, Edel**

**Jsize** user-selected array length ( $\leq 14000$  elements). **Jsize** must be chosen to be large enough (for a given **Hstart**) so that the entire initial energy distribution is represented.

**Hstart** energy grain (express in  $\text{cm}^{-1}$ ) for initial energy distribution: "Pstart". **Hstart** should be  $\geq E_{\text{grain1}}$  used to generate sums and densities of states.

**Edel** energy origin of array, relative to zero point energy of initial excited well (express in  $\text{cm}^{-1}$ )

### **Line 2**

(REPEAT **Jsize** times)

#### **DUMMY, Pstart**

**DUMMY** Must be input, but ignored by MultiWell (may be equal to E, for example)

**Pstart** NORMALIZED cumulative initial energy distribution function. Thus, **Pstart(i)** ranges monotonically from **Pstart(1)=0** (approximately), up to **Pstart(Jsize) = 1.0**.

(Note that other columns may be present in the data file, but they will be ignored.)

### **Line 3**

BLANK TO INSURE THAT THE LAST LINE IS FOLLOWED BY A CARRIAGE RETURN (needed for all READ statements). THE CARRIAGE RETURN IS EASILY OVERLOOKED.

## 2.10 Fatal Input Errors and Warnings

A FATAL INPUT ERROR is reported and execution is stopped if any of the following parameters for a well or transition state does not match the corresponding value from Line 2 of multiwell.dat:

**Egrain1, imax1, lsize , Emax2**

### Incompatible Keywords or other Options, resulting in a Fatal Error:

**ILT and CENT1, CENT2, or CENTX**

**ILT and TUN**

**RKE and TUN**

**CRP and TUN**

**CENT and TUN**

**CENT1, CENT2, or CENTX with TSmom(Mol,nchann)  $\leq 0$**   
(moment of inertia or rotational constant of the transition state)

### Non-Fatal Warnings:

**"WARNING: number of energy grains where Reactant Well has states, but Product Well has none to match [set k(E) = 0]"**

This warning can arise when the density of states is sparse and some energy grains (“empty grains”) do not contain any ro-vibrational states. This can cause a problem when Well-to-Well reactions (especially tunneling reactions) are important. When reactions occur in MultiWell, population in an energy grain of the reactant Well passes to an energy grain of the product Well, but this process becomes undefined if the product energy grain does not contain any ro-vibrational states. This problem is most common when quantum mechanical tunneling is important, but it may also occur at energies above a reaction critical energy if the density of states in the product Well is particularly sparse.

MultiWell handles this problem pragmatically by allowing the reaction to take place as long as the corresponding energy grain in the second Well not empty, and it forbids the reaction and issues the Warning if the energy grain in the second Well is empty. This procedure is followed because states must be present in order to support population in any given energy grain, while standard barrier-tunneling models (like the Eckart model) implicitly assume that a continuum of (translational) states exists on both sides of the barrier.

When the warning is issued, the user must decide whether the simulation is valid, since the “tunneling correction” is affected quantitatively when reactive flux is forbidden to pass into an empty grain. If tunneling is a very important component of the reaction model, then measures can be taken to minimize this problem (although the various measures may introduce other issues).

Here are two ways to minimize this problem:

1. Larger energy grain sizes might be adopted, since with larger grain size there will be fewer empty energy grains. However, this measure will reduce the energy resolution, which is often (but not always) an important consideration.

2. When centrifugal corrections are being applied to a reaction (i.e. with keyword **CENT2**), densities of states are often sparse, because they are based only on the vibrations and the external K-rotor. Instead of using centrifugal corrections, one might instead use the Smith and Gilbert method of treating angular momentum<sup>17,19,23,24</sup> (see Section A.2.3 in this User Manual). In this method, densities of states are computed based on the vibrations and ALL of the external rotational degrees of freedom, which significantly increases the density of states and greatly reduces the number of empty energy grains. This is a good approach when the Smith-Gilbert method is acceptable.



## References

- (1) Barker, J. R. Monte-Carlo Calculations on Unimolecular Reactions, Energy-Transfer, and IR-Multiphoton Decomposition. *Chem. Phys.* **1983**, *77*, 301-318.
- (2) Barker, J. R. Radiative Recombination in the Electronic Ground State. *J. Phys. Chem.* **1992**, *96*, 7361-7367; DOI: 10.1021/j100197a042.
- (3) Barker, J. R. Multiple-well, multiple-path unimolecular reaction systems. I. MultiWell computer program suite. *Int. J. Chem. Kinet.* **2001**, *33*, 232-245; <https://doi.org/10.1002/kin.1017>.
- (4) Barker, J. R. Energy Transfer in Master Equation Simulations: A New Approach. *Int. J. Chem. Kinet.* **2009**, *41*, 748-763.
- (5) Barker, J. R.; King, K. D. Vibrational Energy Transfer in Shock-Heated Norbornene. *J. Chem. Phys.* **1995**, *103*, 4953-4966.
- (6) Barker, J. R.; Ortiz, N. F. Multiple-Well, multiple-path unimolecular reaction systems. II. 2-methylhexyl free radicals. *Int. J. Chem. Kinet.* **2001**, *33*, 246-261; DOI: 10.1002/kin.1018.
- (7) Barker, J. R.; Weston, R. E., Jr. Collisional Energy Transfer Probability Densities P(E,J;E',J') for Monatomic Colliding with Large Molecules. *J. Phys. Chem. A* **2010**, *114*, 10619-10633; 10.1021/jp106443d.
- (8) Barker, J. R.; Yoder, L. M.; King, K. D. Feature Article: Vibrational Energy Transfer Modeling of Non-Equilibrium Polyatomic Reaction Systems. *J. Phys. Chem. A* **2001**, *105*, 796-809.
- (9) Durant, J. L.; Kaufman, F. Calculation and use of total collision rates in thermal systems. *CPL* **1987**, *142*, 246-251.
- (10) Forst, W. Unimolecular rate theory test in thermal reactions. *J. Phys. Chem.* **1972**, *76*, 342-348; <https://doi.org/10.1021/j100647a012>.
- (11) Forst, W. *Theory of Unimolecular Reactions*; Academic Press: New York, 1973.
- (12) Forst, W. *Unimolecular Reactions. A Concise Introduction*; Cambridge University Press: Cambridge, 2003.
- (13) Gillespie, D. T. A general method for numerically simulating the stochastic time evolution of coupled chemical reactions. *J. Comp. Phys.* **1976**, *22*, 403-434.
- (14) Gillespie, D. T. Exact stochastic simulation of coupled chemical reactions. *J. Phys. Chem.* **1977**, *81*, 2340-2361.
- (15) Gillespie, D. T. Monte Carlo simulation of random walks with residence time dependent transition probability rates. *J. Comp. Phys.* **1978**, *28*, 395-407.
- (16) King, K. D.; Barker, J. R. Experiments on collisional energy transfer. In *Unimolecular Kinetics. Parts 2 and 3: Collisional Energy Transfer and The Master Equation*; Robertson, S. H., Ed.; Elsevier, 2019; Vol. 43; pp 3-62.
- (17) Klippenstein, S. J.; Harding, L. B. A direct transition state theory based study of methyl radical recombination kinetics. *Journal of Physical Chemistry A* **1999**, *103*, 9388-9398.
- (18) Maranzana, A.; Barker, J. R.; Tonachini, G. Master Equation Simulations of Competing Unimolecular and Bimolecular Reactions: Application to OH Production in the Reaction

- of Acetyl Radical with O<sub>2</sub>. *Phys. Chem. Chem. Phys.* **2007**, *9*, 4129 - 4141; DOI:10.1039/b705116f.
- (19) Miller, J. A.; Klippenstein, S. J. Master Equation Methods in Gas Phase Chemical Kinetics. *J. Phys. Chem. A* **2006**, *110*, 10528-10544.
- (20) Neufeld, P. D.; Janzen, A. R.; Aziz, R. A. Empirical Equations to Calculate 16 of the Transport Collision Integrals  $\Omega(l, s)^*$  for the Lennard - Jones (12-6) Potential. *J. Chem. Phys.* **1972**, *57*, 1100.
- (21) Olzmann, M. On the role of bimolecular reactions in chemical activation systems. *Phys. Chem. Chem. Phys.* **2002**, *4*, 3614–3618; <https://doi.org/10.1039/B203244A>.
- (22) Shi, J.; Barker, J. R. Incubation in Cyclohexene Decomposition at High Temperatures. *Int. J. Chem. Kinet.* **1990**, *22*, 187-206.
- (23) Smith, S. C.; Gilbert, R. G. Angular momentum conservation in multichannel unimolecular reactions. *International Journal of Chemical Kinetics* **1988**, *20*, 979-990.
- (24) Smith, S. C.; Gilbert, R. G. Angular momentum conservation in unimolecular and recombination reactions. *International Journal of Chemical Kinetics* **1988**, *20*, 307-329.

### 3. Separable Molecular Degrees of Freedom

In this chapter, the various types of separable molecular degrees of freedom recognized by the codes in the MultiWell Program Suite are defined (Section 3.1) and the formats for the input data are described (Section 3.2). These types of molecular degrees of freedom are used by the following codes, which are described in the designated chapters:

densum (Chapter 4)  
thermo (Chapter 6)  
bdens (Chapter 8)  
sctst (Chapter 8)  
paradensum (Chapter 8)  
parasctst (Chapter 8)  
ktools (Chapter 10)

#### 3.1 Types of Degrees of Freedom

##### *(An)Harmonic Vibration (vib)*

The energy of an anharmonic oscillator is

$$E = \omega_e \left( v + \frac{1}{2} \right) + \omega_e x_e \left( v + \frac{1}{2} \right)^2 - ZPE$$

where  $\omega_e$  is the harmonic frequency and the zero point energy ( $v = 0$ ) is

$$ZPE = \omega_e \left( \frac{1}{2} \right) + \omega_e x_e \left( \frac{1}{2} \right)^2.$$

For a Morse oscillator, the anharmonicity is

$$\omega_e x_e = -\frac{\omega_e^2}{4D_e}$$

where  $D_e$  is the Morse oscillator well depth (from the bottom of the potential well). *Note that the sign convention for anharmonicity used here is not the usual convention for diatomic molecules, but it conforms to the convention for polyatomics.*

By the "fundamental frequency" (key word 'FUN'; **obsolete** key word "OBS") for a vibrational mode, we mean, the 0-1 transition frequency for the specific mode when all other vibrational quantum numbers are set to zero. When  $\omega_{e,x_e} \neq 0$  for a separable mode, the fundamental frequency  $\omega^f$  is related to the harmonic frequency according to the following expression:

$$\omega_e = \omega^f - 2\omega_e x_e$$

For the fundamental frequency, the codes compute  $\omega_e$  from this expression and use it and the anharmonicity to calculate the vibrational energy levels.

### **Classical Rotation (rot)**

DenSum uses the method of Astholz et al.<sup>1</sup> For expressions, see Appendix 5 of Robinson and Holbrook,<sup>8</sup> or Section 4.5 of Holbrook et al.<sup>5</sup> Also see Appendix (Theoretical Basis), Appendix A.2.2 Note that starting with version 2.04, classical rotations are treated purely classically; previously, a semi-classical approximation was imposed (which amounted to requiring that the sum of states is equal to unity at  $E = 0$ ). Classical expressions are implemented for simple 1D (i.e.  $d = 1$ ) and 2D (i.e.  $d = 2$ ) rotors with rotational constants  $B_1$  and  $B_2$ , respectively. Symmetric tops ( $B_1 \neq B_2$ ) and spherical tops ( $B_1 = B_2$ ) must be entered as pairs of separable rotors: a 1D rotor with rotational constant  $B_1$  and a 2D rotor with rotational constant  $B_2$ . **See Appendix B.4 for a discussion of proper input for External Molecular Rotations.**

### **Quantized Rotation (qro)**

When  $J = 0$ ,  $E = 0$  and degeneracy ( $g$ ) is unity. When  $J > 0$ , the degeneracy ( $g$ ) and the energy depend on the dimensionality ( $d$ ) of the rotor<sup>6</sup>:

$d = 1$	$g = 2$	$E = BJ^2$	$J = 0, 1, 2, 3, \dots$
$d = 2$	$g = (2J + 1)$	$E = BJ(J+1)$	$J = 0, 1, 2, 3, \dots$
$d = 3$	$g = (2J + 1)(2J + 1)$	$E = BJ(J+1)$	$J = 0, 1, 2, 3, \dots$

Prior to version 2.04, the sum of states at  $E=0$  was set equal to unity, regardless of rotational symmetry number ( $\sigma$ ). The current version gives the sum of states equal to  $1/\sigma$  at  $E=0$ .

This type is appropriate for treating the **external rotations of a linear molecule** ( $d = 2$ ) and **external rotations of a spherical top molecule** ( $d = 3$ ), such as methane.

See Appendix B.4 for a discussion of input for External Molecular Rotations.

### **Symmetric Top (top)**

This type is for treating the **external rotations of a non-linear molecule.**

For a symmetric top, two of the external rotational constants are equal to each other and one is unique:  $A \neq B = C$  (prolate top), or  $A = B \neq C$  (oblate top). To account for both prolate and oblate symmetric tops, it is convenient to denote  $B_1$  for the unique 1D rotational constant and  $B_2$  for the 2D rotational constant that is twinned. Using these definitions, the rotational energy of the symmetric top is given by

$$E_{top} = B_2 J(J+1) + (B_1 - B_2) K^2$$

where  $J$  is the quantum number of total angular momentum (the "J-rotor") and  $K$  is the quantum number for the projection of the total angular momentum vector  $\mathbf{J}$  on the molecular symmetry axis. Quantum number  $J$  can take integer values starting with  $J=0$  and  $K$  is restricted to the range  $-J \leq K \leq +J$ ; in addition, the rotational energy of the top must be  $E_{top} \geq 0$ . The densities of states are evaluated by direct calculation using the above equation and including the restrictions on  $E_{top}$  and  $K$ .

The input for the symmetric top consists of  $B_2$ ,  $B_1$ , and the rotational symmetry number. Users optionally may (a) set the external symmetry number to unity while specifying the rotational symmetry number when invoking the **top** degree of freedom, or (b) specify the external symmetry number and set the rotational symmetry number to unity; either approach is acceptable, but **the symmetry number should not be different from unity in both entries**.

This type can be used for **spherical tops** (when  $B_1 = B_2$ ), but the **qro** type is more computationally efficient and produces exactly the same results.

**See Appendix B.4 for a discussion of proper input for External Molecular Rotations.**

### ***K-rotor Rotation (kro)***

This degree of freedom type should **NOT** be selected for normal calculations using MultiWell. It is provided in DenSum only for special purposes. **See Appendix B.4 for a discussion of the proper input for External Molecular Rotations.**

### ***Particle in a Box (box)***

1-D box of length  $L$  with particle of mass  $m$ :

$$E = \frac{h^2 n^2}{8mL^2} - \frac{h^2}{8mL^2} \quad \text{for } n = 1, 2, 3, \dots$$

where  $E$  is the energy in excess of the "zero" point energy (ZPE), which is identified with  $n=1$ .

The codes in the MultiWell Program Suite can handle boxes of  $\geq 1$  dimensions as long as they are "hyper-cubical", with  $L_x = L_y = \dots = L$ . For an  $N_{dim}$  dimensional hyper-cubical box, the eigenenergies (relative to the ZPE) and the ZPE are given by:

$$E = \frac{h^2}{8mL^2} \sum_{i=1}^{N_{dim}} \{n_i^2 - 1\} \quad \text{for } n_i = 1, 2, 3, \dots$$

$$ZPE = \frac{h^2 N_{dim}}{8mL^2}$$

The "frequency parameter" that is needed by the MultiWell codes is  $h^2/(8mL^2)$ .

### ***1-D Hindered Rotation, Symmetrical (hra, hrb, hrc)***

These types are intended for use with symmetrical internal rotors, i.e. those with symmetrical mass distribution and potential energy that can be described with acceptable

accuracy using a single sine or cosine term as a function of dihedral angle  $\chi$  (e.g. the CH<sub>3</sub>–CH<sub>3</sub> torsion). Relationships among parameters for a symmetrical hindered rotor:

$$B / \text{cm}^{-1} = \frac{16.85763}{I_r / \text{amu } \text{Å}^2}$$

$$V = \frac{1}{B} \left[ \frac{\omega}{n} \right]^2$$

where,  $n$  is the symmetry number,  $B$  is the rotational constant,  $I_r$  is the reduced moment of inertia,  $V$  is the barrier to internal rotation, and  $\omega$  is the small amplitude harmonic frequency (cm<sup>-1</sup>) evaluated at the minimum energy (e.g. the harmonic torsion frequency from a quantum chemistry calculation). Because of the relationship connecting  $n$ ,  $V$ ,  $\omega$ , and  $I_r$ , only three parameters are independent. Given the parameter  $n$ , there are three ways of choosing two independent parameters from the set  $V$ ,  $\omega$ ,  $I_r$ . For convenience, these three combinations are implemented as types **hra**, **hrb** and **hrc**.

### **1-D Hindered Rotation, General (hrd)**

This type is general, and is particularly useful for unsymmetrical rotors, i.e. those that lack a symmetrical mass distribution and/or have potential energy that can only be described accurately by using multiple sine or cosine terms (e.g. the CHF<sub>2</sub>-CH<sub>2</sub>Cl torsion). For this type, one must provide the torsional potential energy and reduced moment of inertia (or rotational constant) as functions of the dihedral angle  $\chi$  (radians).

For convenience, three forms of the torsional potential energy are accepted (all coefficients in units of cm<sup>-1</sup>):

Type **Vhrd1** 
$$V(\chi) = \sum_{n=1}^N \frac{V_n}{2} \left[ 1 - \cos(n\sigma_v(\chi + \phi_v)) \right]$$

Type **Vhrd2** 
$$V(\chi) = V_0 + \sum_{n=1}^N V_n \cos(n\sigma_v(\chi + \phi_v))$$

Type **Vhrd3** 
$$V(\chi) = V_0 + \sum_{n=1}^N V_n^c \cos(n\sigma_v(\chi + \phi_v)) + \sum_{n=1}^N V_n^s \sin(n\sigma_v(\chi + \phi_v))$$

where  $\chi$  is the dihedral angle (radians),  $\sigma_v$  is the symmetry number for the potential energy,  $\phi_v$  is a phase angle for the potential (radians).

Also for convenience, either the rotational constant or the moment of inertia, which are functions of the dihedral angle, can be entered (all coefficients in units of cm<sup>-1</sup>). **It is VERY IMPORTANT that the angles are defined in the same way both for the potential and for the mass factor.**

Type **Bhrd1** (all coefficients in units of cm<sup>-1</sup>)

$$B(\chi) = B_0 + \sum_{n=1}^N B_n \cos(n\sigma_B(\chi + \varphi_B))$$

Type **lhrd1** (all coefficients in units of amu.Å<sup>2</sup>)

$$I(\chi) = I_0 + \sum_{n=1}^N I_n \cos(n\sigma_I(\chi + \varphi_I))$$

where  $\chi$  is the dihedral angle (radians),  $\sigma_B$  and  $\sigma_I$  are symmetry numbers and  $\varphi_B$  and  $\varphi_I$  are phase angles. **Repeat: It is VERY IMPORTANT that the same phase angle be used both for the potential and for the mass factor:  $\varphi_V = \varphi_B$  or  $\varphi_I$ .**

If the reduced moment of inertia or rotational constant is assumed to be independent of dihedral angle, just the one  $B_0$  or  $I_0$  term is needed.

### **Translation (trn)**

DenSum uses an adaptation of the method of Astholz et al.,<sup>1</sup> but applies it to relative translations (standard state corresponding to 1 molecule/cc). According to this method, the number of translational states ( $G(E)$ ) in a single energy grain ( $\delta E$ ) is given by

$$G(E) = F \left[ E^{3/2} - (E - \delta E)^{3/2} \right]$$

where  $F$  is a constant that depends on  $\mu$ , the reduced mass (gram atomic mass units). When classical rotors are convolved with the 3-D translation, the following expression is used:

$$G(E) = F_r \left[ E^{(r+3)/2} - (E - \delta E)^{(r+3)/2} \right]$$

where  $F_r$  depends on  $\mu$ , the number of rotor degrees of freedom ( $r$ ), and the moments of inertia. For more details, see the Appendix (Theoretical Basis). Note that  $G(0) = 0$ , since the nominal energy corresponds to the top energy in each bin.

### **Rotation + Spin-Orbit (rso)**

This type can be used only in program Thermo to obtain better accuracy at low temperatures.<sup>7</sup> It accounts for the coupling between electronic and rotational degrees of freedom for chemical species in degenerate electronic states. Currently, it is implemented ONLY for diatomic species in <sup>2</sup>Π states, such as OH(X<sup>2</sup>Π). It is based on the Hill and Van Vleck formalism,<sup>4</sup> as described by Herzberg in his Eq. (V,28).<sup>3</sup>

## 3.2 Format for Input Files

The following format is used for lines describing the separable molecular degrees of freedom. The same format is used in all of the codes listed above. Not all of the codes recognize all of the formats. For example, THERMO does not recognize the type `trns` (translation), since it automatically calculates the translational partition function without it being specified as a degree of freedom.

Each of the separable degrees of freedom, except for type **rso**, is specified on a standardized line of the input file. The Standard Line is formatted and the parameters have the definitions and units as described below. The input for type **rso** is at the end of the list.

### Standard Line for separable degrees of freedom:

#### MODE(I), IDOF(I), AAA(I), BBB(I), CCC(I)

MODE index number for degree of freedom  
IDOF KEY WORD for type of degree of freedom

- 'vib' (vibration)
  - AAA = vibration frequency ( $\text{cm}^{-1}$ ) [see VHAR, line 3]
  - BBB = vibration anharmonicity ( $\text{cm}^{-1}$ )
  - CCC = vibration degeneracy
- 'box' (particle-in-a-box vibration)
  - AAA = vibration frequency parameter ( $\text{cm}^{-1}$ )
  - BBB = (not used; but a dummy placeholder value must be included)
  - CCC = vibration degeneracy
- 'rot' (classical rotation)
  - AAA = rotation moment of inertia [units specified by Vrot, Line 3]
  - BBB = rotation symmetry number
  - CCC = rotation dimension
- 'qro' (quantized rotation)
  - AAA = rotation moment of inertia [units specified by Vrot, Line 3]
  - BBB = rotation symmetry number
  - CCC = rotation dimension
- 'top' (symmetric top); quantized rotations
  - AAA =  $B_2$  (2D) rotational constant [units specified by Vrot, Line 3]
  - BBB =  $B_1$  (1D, unique) rotational constant [units specified by Vrot, Line 3]
  - CCC = rotational symmetry number
- 'kro' (K-rotor (1-dimensional); quantized rotation; **NOT FOR GENERAL USE!!**)
  - AAA = (2D) moment of inertia [units specified by Vrot, Line 3]
  - BBB = (1D) moment of inertia [units specified by Vrot, Line 3]
  - CCC = J (specified quantum number for total angular momentum)
- 'hra' (1-D *symmetrical* hindered rotor)
  - AAA = vibration frequency ( $\text{cm}^{-1}$ )
  - BBB = reduced moment of inertia [units specified by Vrot, Line 3]



CCC = symmetry of Potential Energy (number of minima per  $2\pi$ )

[For an unsymmetrical hindered rotor, type 'hrd' is preferred. However, for a symmetrical potential energy and unsymmetrical mass distribution, the present type can be used for approximate results by giving the potential energy symmetry number CCC as a negative value (i.e. -CCC) and a new line inserted containing NSIG = symmetry number for the mass distribution]

'hrb' (1-D *symmetrical* hindered rotor)

AAA = vibration frequency ( $\text{cm}^{-1}$ )

BBB = barrier ( $\text{cm}^{-1}$ )

CCC = symmetry of Pot. Energy (number of minima per  $2\pi$ )

[For an unsymmetrical hindered rotor, type 'hrd' is preferred. However, for a symmetrical potential energy and unsymmetrical mass distribution, the present type can be used for approximate results by giving the potential energy symmetry number CCC as a negative value (i.e. -CCC) and a new line inserted containing NSIG = symmetry number for the mass distribution]

'hrc' (1-D *symmetrical* hindered rotor)

AAA = reduced moment of inertia [units specified by Vrot, Line 3]

BBB = barrier ( $\text{cm}^{-1}$ )

CCC = symmetry of Pot. Energy (number of minima per  $2\pi$ )

[For an unsymmetrical hindered rotor, type 'hrd' is preferred. However, for a symmetrical potential energy and unsymmetrical mass distribution, the present type can be used for approximate results by giving the potential energy symmetry number CCC as a negative value (i.e. -CCC) and a new line inserted containing NSIG = symmetry number for the mass distribution]

'hrd' (1-D *General* hindered rotor)

**Note: care must be taken to treat optical isomers and unsymmetrical hindered internal rotors in a mutually consistent fashion (see Appendix B.5).**

AAA = total number of coefficients for potential energy function (including  $V_0$  term, if present).

BBB = total number of coefficients for rotational constant or moment of inertia function (including  $I_0$  or  $B_0$ ).

CCC = symmetry number of internal hindered rotor (symmetry number of a symmetric rotor; unity for a non-symmetric rotor)

INSERT 2 ADDITIONAL LINES:

LINE1: VTYPE, SYMMV, PHASEV, COEFF1, COEFF2, ...(in order)

VTYPE = "Vhrd1", "Vhrd2", or "Vhrd3"

SYMMV = symmetry number for the potential

PHASEV = phase angle (radians) for potential

COEFF1 = coefficients (including  $V_0$ ) for potential, **in proper order**, on the same line (units of  $\text{cm}^{-1}$ )

LINE2: MTYPE, SYMMM, PHASEV, COEFF1, COEFF2, ...(in order)

MTYPE = "Bhrd1" for rotational constant or "lhrd1" for moment of inertia

SYMMM = symmetry number for Bhrd1 or lhrd1

PHASEM = phase angle (radians) for Bhrd1 or lhrd1

COEFF1 = coefficients (including  $B_0$  or  $I_0$ ) for Bhrd1 (units of  $\text{cm}^{-1}$ ) or  
lhrd1 ( $\text{amu}\cdot\text{\AA}^2$  units), **in proper order**, on the same line  
'trn' (3-dimensional relative translation)  
AAA = mass of A (amu)  
BBB = mass of B (amu)  
CCC = ignored, but convenient to set it equal to "3"

### Format for type **RSO**:

**MODE(i),IDOF(i),MULT(i),LAMBDA(i),ASO(i),BSO(i),D(i),NRSO(i)**

MODE index number for degree of freedom  
IDOF Must be "**RSO**" for this type of degree of freedom  
MULT Spin multiplicity of electronic state, =**2 in the current implementation**  
LAMBDA Magnetic quantum number, =**1 (for a  $\Pi$ -state) in the current implementation**  
ASO Spin-orbit parameter (units of  $\text{cm}^{-1}$ )  
BSO Rotational constant (units of  $\text{cm}^{-1}$ )  
D Rotation distortion coefficient (units of  $\text{cm}^{-1}$ )  
NRSO Rotation symmetry number

**IMPORTANT:** RSO includes the electronic degeneracies and all external rotational states.  
Therefore, to avoid double-counting of states when invoking RSO for species  $i$ , the  
number of electronic states ( $\text{Nele}(i)$ ) **must be set to  $\text{Nele}(i) = 0$**  and types **ROT** and  
**QRO** **must NOT be invoked again** for the external rotations of that species.

*Example Data Line for  $\text{OH}(X^2\Pi)$*  (data from Brooke et al.<sup>2</sup>)

2, RSO, 2, 1, -139.051, 18.535, 1.91E-03, 1

## References

- (1) Astholz, D. C.; Troe, J.; Wieters, W. Unimolecular processes in vibrationally highly excited cycloheptatrienes. I. Thermal isomerization in shock waves. *J. Chem. Phys.* **1979**, *70*, 5107-5116.
- (2) Brooke, J. S. A.; Bernath, P. F.; Western, C. M.; Sneden, C.; Afşar, M.; Li, G.; Gordon, I. E. Line strengths of rovibrational and rotational transitions in the X<sup>2</sup>Π ground state of OH. *J. Quant. Spectrosc. Radiat. Transf.* **2016**, *168*, 142–157; <http://dx.doi.org/10.1016/j.jqsrt.2015.07.021>.
- (3) Herzberg, G. *Molecular Spectra and Molecular Structure. I. Spectra of Diatomic Molecules*, 2 ed.; Van Nostrand Reinhold Co.: Cincinnati, 1950.
- (4) Hill, E.; Van Vleck, J. H. On the Quantum Mechanics of the Rotational Distortion of Multiplets in Molecular Spectra. *Phys. Rev.* **1929**, *32*, 250-272.
- (5) Holbrook, K. A.; Pilling, M. J.; Robertson, S. H. *Unimolecular Reactions*, 2 ed.; Wiley: Chichester, 1996.
- (6) McHale, J. L. *Molecular Spectroscopy*; Prentice Hall: Upper Saddle River, 1999.
- (7) Nguyen, T. L.; Ruscic, B.; Stanton, J. F. A master equation simulation for the  $\dot{\text{O}}\text{H} + \text{CH}_3\text{OH}$  reaction. *J. Chem. Phys.* **2019**, *150*, 084105; doi: 10.1063/1.5081827.
- (8) Robinson, P. J.; Holbrook, K. A. *Unimolecular Reactions*; Wiley-Interscience: London; New York, 1972.

## 4. DenSum: *Separable Sums and Densities of States*

This computer code carries out exact counts for sums and densities of states for *separable* degrees of freedom via the Stein-Rabinovitch<sup>2</sup> extension of the Beyer-Swinehart algorithm.<sup>1</sup> Optionally, the Whitten-Rabinovitch approximation<sup>3,4</sup> can be used.

**Default array dimensions** are easily changed in file src/densum/declare.inc

150 degrees of freedom (enough for a 50 atom molecule)

50000 energy grains (enough for 100000 cm<sup>-1</sup> energy maximum, with 2 cm<sup>-1</sup> grains)

### Output Files

densum.out	File containing complete output.
densum.lev	Energy levels of quantized degrees of freedom.
<FNAME>.dens	File formatted for input into MultiWell.

Example data and output files are given in the examples directory:  
multiwell/examples/densum-examples.

### 4.1 DenSum Data File Format

**Note: Starting with version 2009.0, the data file format is no longer compatible with previous versions.**

#### Line 1

**TITLE (CHARACTER\*180): up to 180 characters**

#### Line 2

#### **FNAME**

FNAME (CHARACTER\*10): Filename to be created with ".dens" appended (up to 10 characters). Example: "hexadiene" produces file named "hexadiene.dens".

#### Line 3

#### **N, IWR, VHAR, VROT**

N no. of DoF's, IWR (flag)

IWR 0: Uses exact state counts (energy grain = Egrain1)

1: Uses Whitten-Rabinovitch state densities

VHAR KEYWORD for vibrations

'HAR': for vibrational frequencies input as harmonic frequencies.

'FUN': for vibrational frequencies input as 0-1 fundamental frequencies.

VROT KEYWORD for molecular internal and external rotations, except for hindered rotors of type **hrd** (see special instructions below for type hrd). Entries in upper or lower case:  
'AMUA': for moments of inertia input with units of amu Å<sup>2</sup>.  
'GMCM': for moments of inertia input with units of g cm<sup>2</sup>.  
'CM-1': for rotational constant input with units of cm<sup>-1</sup>.  
'MHZ': for rotational constant input with MHz.  
'GHZ': for rotational constant input with GHz.

Notes: (a) All of the rotational information in a DenSum data file must be given in the form specified by VROT; (b) VHAR and VROT can be stated in either order on Line 3.

#### **Line 4**

##### **Egrain1, Imax1, Isize, Emax2**

Egrain1 energy grain in units of cm<sup>-1</sup>  
Imax1 number of array elements in first segment of double array\*  
Isize total size of double array (number of elements)  
Emax2 maximum energy (cm<sup>-1</sup>) for calculation

\* Starting with MultiWell Version 2.08, densum.out provides information about the number of elements (Imax1) needed to achieve fluctuations of less than 5% in the density of states. If Egrain1 and Imax1 are chosen so that fluctuations in the density of states is greater than 5%, a warning is printed to the screen with a suggestion as to what Imax1 should be increased to. Note that a user can choose to disregard this warning and proceed to run MultiWell.

#### **Line 5..N+3**

##### **MODE(I), IDOF(I), AAA(I), BBB(I), CCC(I)**

MODE index number for degree of freedom  
IDOF KEY WORD for type of degree of freedom

See Chapter 3 and for descriptions of the types of molecular degrees of freedom recognized by DENSUM.

#### **Line N+4**

BLANK LINE TO INSURE THAT THE LAST LINE IS FOLLOWED BY A CARRIAGE RETURN (needed for all READ statements). THE CARRIAGE RETURN IS EASILY OVERLOOKED.

## 4.2 DenSum in Batch Mode

In order to run densum with the 'batch' option, one must first prepare a file: densum.batch. This file lists the names of the DenSum data files (".vibs files") to be processed and the energy grain and double array boundaries. The batch file format is given below.

To use this option, the DenSum data files must all reside in one directory (e.g. directory /vibs) and each must be named "<name>.vibs", where <name> does not contain any blank spaces. When listed in densum.batch, each file name must be listed on a separate line, including the extension ".vibs".

### ***densum.batch Batch File Format***

Line 1 Egrain1, lmax1, lsize, Emax2

Line 2 <name1>.vibs

Line 3 <name2>.vibs

Line 4 <name3>.vibs

.... etc.

<end of file>

-----  
**Sample densum.batch for three .vibs files**

10. , 400 , 500 , 50000.

B1.vibs

B2.vibs

CH3CO.vibs

-----

## ***Execution***

### **a) On linux:**

From within the directory in which `densum.batch` and the `.vibs` data files reside, type '`<PATH>densum -batch`' in a terminal shell, where `PATH` is the full path to the `densum` executable.

or

type '`densum -batch`' in a terminal shell, if the `PATH` variable has been set to include the `/bin` directory that holds the `densum` executable.

or

type '`./densum -batch`' in a terminal shell, if a copy of the `densum` executable resides in the same directory with `densum.batch` and the `.vibs` files.

### **b) On windows**

There are two possibilities:

1) type "`densum -batch`" in a DOS shell

or

2) double-click on "`densum-batch.bat`". Note that `densum.exe` and `densum-batch.bat` must be in the same directory as `densum.batch` and the `.vibs` files.

## References

- (1) Beyer, T.; Swinehart, D. F. Number of multiply-restricted partitions. *Comm. Assoc. Comput. Machines* **1973**, *16*, 379.
- (2) Stein, S. E.; Rabinovitch, B. S. Accurate evaluation of internal energy level sums and densities including anharmonic oscillators and hindered rotors. *J. Chem. Phys.* **1973**, *58*, 2438-2445.
- (3) Whitten, G. Z.; Rabinovitch, B. S. Accurate and Facile Approximation for Vibrational Energy - Level Sums. *J. Chem. Phys.* **1963**, *38*, 2466.
- (4) Whitten, G. Z.; Rabinovitch, B. S. Approximation for Rotation—Vibration Energy Level Sums. *J. Chem. Phys.* **1964**, *41*, 1883.



## 5. MomInert: Moments of Inertia

This code was written mostly by Nicholas F. Ortiz under the direction of John R. Barker. From Cartesian coordinates, it calculates the principal moments of inertia and approximate reduced moment of inertia for an internal rotation.

Example data and output files can be down-loaded from the MultiWell web site: <http://aoss.engin.umich.edu/multiwell/>.

*Note that computer program lamm, described in Chapter 8 is designed to assist in computing moments of inertia as a function of dihedral angle. Thus lamm is more appropriate than MomInert for flexible internal rotations.*

### 5.1 Data File Format

**Note: Starting with version 2.0, the data file format is no longer compatible with previous versions.**

**To run Mominert using the default filename (mominert.dat):**

LINUX/UNIX: in the directory where the input data file resides, type:

```
<PATH>/multiwell-<version>/bin/mominert <RETURN>
```

where <PATH> designates the PATH to /multiwell-<version>. If directory /multiwell-<version> resides in the user home directory, type:

```
~/multiwell-<version>/bin/mominert <RETURN>
```

WINDOWS in a DOS window: in the directory where the input data file resides, type:

```
<PATH>/multiwell-<version>/bin/mominert <RETURN>
```

*For example:*

```
~/multiwell-2013/bin/mominert
```

**To run Mominert using a user-defined filename (FileName.dat):**

Follow the same procedures described above, but type:

```
<PATH>/multiwell-<version>/bin/mominert <FileName> <RETURN>
```

*For example:*

```
~/multiwell-2013/bin/mominert final.dat
```

The resulting output file will take the same prefix: **final.out**.

### **Line 1**

**TITLE** A line, up to 100 characters, describing the data. This title is reproduced in the output file.

### **Line 2**

**UNITS** Keyword designating units of coordinate values.

ANGS Angstrom units.

BOHR Atomic (Bohr) units (1 Bohr  $\approx$  0.529 Å)

### **Line 3**

**NATOMS** Total number of atoms in the molecule (up to 100 atoms).

### **Line 4**

(Repeat for every atom type [see Appendix B.7])

### **ATYPE, IA, X, Y, Z**

ATYPE case sensitive atomic symbol, e.g. "C", "H", "Br79" (see Sec. 9.7)

IA Index number of the atom (1 to NATOMS).

X,Y,Z Cartesian coordinates (Å or Bohr; see Line 2) of the atom.

### **To assign an arbitrary mass to an atom:**

1. Designate "XX" for ATYPE (instead of e.g. "H" or "C") in Line 3.
2. On the line following the atom type designation, insert a line giving the mass to be assigned to this particular atom.

This must be done each time a special mass is to be assigned. It is not necessary for the mass to always be the same. In other words, atom type "XX" may be designated multiple times in the same molecule, and a different mass may be specified each time.

### **Line 5**

### **IAI, IAJ**

Atom indices for the two atoms defining the axis of internal rotation. If the atom indices are set equal to zero, then internal rotor is not calculated and **Line 6** and **Line 7** can be omitted.

### **Line 6**

## NR

Number of atoms in one of the two rotating moieties.

### Line 7

List of the atom indices that comprise the rotating moiety containing NR atoms.

### Line 8

For additional internal rotors, REPEAT lines 5-7. TO TERMINATE, enter two zeros: "0 , 0".

### Line 9

BLANK LINE TO INSURE THAT THE LAST LINE IS FOLLOWED BY A CARRIAGE RETURN (needed for all READ statements). THE CARRIAGE RETURN IS EASILY OVERLOOKED.

## 5.2 Computational Approach

This code uses the two axis-defining atoms and one other atom to define two perpendicular planes which intersect at the rotation axis. The distance from all atoms in the molecule to each plane is calculated. The Pythagorean Theorem is then used to define the distance of each atom to the axis. The mass is defined for each atom type, and then the mass and distance are used to calculate the moment of inertia for the internal rotations in  $\text{amu \AA}^2$ .

The center-of-mass is then defined. This is used to calculate all external products and moments of inertia. These values are put into the proper matrix, and eigenvalues are found. The eigenvalues are the principle moments of inertia.

For the reduced moment of inertia for internal rotation, MomInert uses the approximation that the reduced moment is calculated for the axis that contains the twisting bond. This approximation is reasonably accurate (errors of less than 5-10%) for many species.<sup>1</sup>

## References

- (1) East, A. L. L.; Radom, L. Ab initio statistical thermodynamical models for the computation of third-law entropies. *J. Chem. Phys.* **1997**, *106*, 6655-6673.

## 6. thermo: Thermodynamics

### 6.1 Introduction

thermo calculates **equilibrium constants**, **thermodynamic parameters**, and **canonical transition state theory (CTST) rate constants** (including **Eckart tunneling** through an unsymmetrical barrier) *via* standard statistical mechanics formulae. It can also compute canonical rate constants using W. H. Miller's **Semiclassical Transition State Theory (SCTST)** when used in conjunction with programs `sctst` and `bdens`, or `paradensum`.

Example data and output files are given in the `examples` directory

**Note that the data file for Thermo (thermo.dat) is intentionally very similar in format to the data file for DenSum (densum.dat). Thus major parts of the data files can be copied and pasted.**

#### 6.1.1 Thermodynamic Output

When given a collection of molecular properties, thermo uses statistical mechanics formulae to calculate the corresponding thermodynamics parameters. Thermo can also calculate canonical transition state theory rate constants. The input and output are intended to be easily understood, but some items are explained below.

Three output files are generated by THERMO. "**thermo.out**" is the general output file, which contains all of the information needed by most users. The following two output files are useful, but of less general interest. "**thermo.details**" displays contributions from every degree of freedom to the heat capacity, entropy, and enthalpy function for each chemical species at 298.15 K and groupings of degrees of freedom at each temperature. "**thermo.partfxns**" displays the partition functions for grouped degrees of freedom for each chemical species at each temperature. (The grouped degrees of freedom include electronic, translational, vibrational, free rotational, and hindered rotational.)

**Standard State:** the standard state must be selected. The conventional standard state for most data tabulations is 1 bar, ideal gas. For analysis involving reaction rate constants, it is usually appropriate to choose the standard state of 1 molecule  $\text{cm}^{-3}$ . The units and numerical values of entropies, equilibrium constants and other thermodynamic quantities are determined by the selection of the standard state.

Standard States recognized by THERMO:

- 1 bar, ideal gas (keyword `BAR`)
- 1 atm, ideal gas (keyword `ATM`)
- 1 molecule  $\text{cm}^{-3}$ , ideal gas (keyword `MCC`)
- free translations ignored (keyword `NOT`)

**Molar Enthalpy:** The enthalpy for formation at 0 K is required input. THERMO output echoes the input and also reports the enthalpy of formation at 298.15 K and the standard free energy of formation (DelG(298)).

For convenience, THERMO recognizes several energy units for enthalpy, which can be selected by the user:

- kJ/mol (keyword KJOU)
- kcal/mol (keyword KCAL)
- $\text{cm}^{-1}$  (wavenumbers) (keyword CM-1)

**Equilibrium constant:** Note that the numerical value of the equilibrium constant depends on the standard state. **Kequil** is reported for each temperature listed in the input file. The values of **Kequil** generally fall on a curved line when plotted on an Arrhenius plot ( $\log(\text{Kequil})$  vs.  $1/T$ ):  $\text{Kequil} = A(T) \cdot \exp(B(T)/T)$ . The parameters  $A(T)$  and  $B(T)$  are based on the local slope:  $d(\ln \text{Keq})/d(1/T)$ . This slope is evaluated by finite differences centered on each  $T$  and the results are usually accurate to within 1%, or better, at the specified  $T$ . The error is mostly due to round-off error in the value of Arrhenius parameter  $B$ . For best accuracy, one should use THERMO to evaluate **Kequil** at each and every temperature of interest.

**Canonical Transition State Theory Rate Constant (CTST):** Note that the user must select the standard state of 1 molecule  $\text{cm}^{-3}$  (i.e. "MCC") when calculating rate constants. Rate constant " $k(T)$ " is reported for each temperature listed in the input file. In addition, it is reported as the Arrhenius function of temperature:  $k(T) = A(T) \cdot \exp(B(T)/T)$ . The parameters  $A(T)$  and  $B(T)$  are based on the local slope:  $d(\ln(k(T)))/d(1/T)$ . This slope is evaluated by finite differences centered on each  $T$  and the results are usually accurate to within 1%, or better, at the specified  $T$ . The error is mostly due to round-off error in the value of Arrhenius parameter  $B$ . For best accuracy, one should use THERMO to evaluate  $k(T)$  at each and every temperature of interest.

**Molar Entropy:** the numerical value for the entropy depends on the standard state that is selected, as well as on the enthalpy units that are selected.

**Molar Heat Capacity:**  $C_p$  depends on enthalpy units that are selected.

**Enthalpy Function:**  $[H(T)-H(0)]$  depends on the enthalpy units that are selected.

**Accuracy:**

All accuracies depend on the accuracy of the input data. For a given set of input data, the accuracies achieved by THERMO are relative to a benchmark based on the same input data. The benchmarks most commonly used are taken from the NIST-JANAF Thermochemical Tables.<sup>1</sup> Note that when rotations are treated classically, the entropy, heat capacity, free energy, and equilibrium constant are less accurate at low temperatures.

- molecular weights are accurate to  $0.002 \text{ g mol}^{-1}$ , or better.
- enthalpies and Gibbs free energy for individual species generally agree with the JANAF tables to within  $0.05 \text{ kJ mol}^{-1}$ , or better.

- entropies computed for individual species are generally accurate to 0.1 J K<sup>-1</sup> mol<sup>-1</sup> or better.
- electronic partition function is accurate to 0.1% or better.
- enthalpy, entropy, heat capacity, and Gibbs free energy differences for reaction (DelS(rxn), DelH(rxn), DelCp(rxn) and DelG(rxn), respectively) are generally more accurate than the corresponding quantities for the individual species, due to cancellation of errors.

### 6.1.2 Types of Degrees of Freedom

The following types used by THERMO are described in Chapter 3:

Harmonic or Anharmonic Vibration (vib)  
 Classical Rotation (rot)  
 Quantized Rotation (qro)  
 Symmetric Top (top):  
 Particle in a Box (box)  
 1-D Hindered Rotation, Symmetrical (hra, hrb, hrc)  
 1-D Hindered Rotation, General (hrd)

The following types are unique to THERMO:

#### Hindered Gorin Model (gor) and Fitting (fit)

Thermo includes the capability to automatically find the hindrance parameters for the Hindered Gorin transition state.<sup>2-7,10,11</sup> One can choose one or both of the following types (IDOF) of degrees of freedom.

1) IDOF = gor selected for one vibrational stretching mode. For a selected potential energy function, Thermo finds the center of mass distance  $r_{\max}$  corresponding to maximum of  $V_{\text{effective}}$  at temperature T, where the rotational energy in the 2-D pseudo-diatomic rotation is assumed to be RT. From the value of  $r_{\max}$ , Thermo computes the 2-D moment of inertia.

2) IDOF = fit selected for two (linear molecule) or three (non-linear) rotational dimensions. Thermo finds the hindrance parameters  $\gamma$  (gamma) and  $\eta$  (eta) that produce a good fit at each temperature to experimental rate constants (one for each temperature) that are entered.

$$\gamma = (1 - \eta)^{1/2}$$

If both IDOF = gor and IDOF = fit are selected, Thermo finds the maximum of  $V_{\text{effective}}$  and uses it to find the hindrance parameters (gamma and eta) that produce a good fit to experimental rate constants (one for each of the Nt temperatures) that are entered.

The selectable potential energy functions are:

MORSE (*Morse Oscillator*)

$$V_{Morse}(r) = D_e \left\{ 1 - \exp\left[-\beta_{Morse}(r - r_e)\right] \right\}^2 - D_e$$

$$\beta_{Morse} = 2\pi\nu_e \sqrt{\frac{\mu}{2D_e}}$$

VARSHNI (*Varshni Oscillator*<sup>12</sup>)

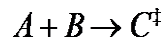
$$V_{Varshni}(r) = D_e \left\{ 1 - \left(\frac{r_e}{r}\right) \exp\left[-\beta_{Varshni}(r^2 - r_e^2)\right] \right\}^2 - D_e$$

$$\beta_{Varshni} = \frac{1}{2r_e} \left[ 2\pi\nu_e \sqrt{\frac{\mu}{2D_e}} - \frac{1}{r_e} \right] = \frac{1}{2r_e} \left[ \beta_{Morse} - \frac{1}{r_e} \right]$$

sMORSE ("*Stiff Morse*" *Oscillator*)

This is a Morse oscillator, but replaces  $\beta_{Morse}$  with  $\beta_{Stiff} = \beta_{Morse} \left[ 1 + c_s (r - r_e)^2 \right]$ ;  $c_s$  is an empirical parameter and must be  $\geq 0$ .

The input is assumed to correspond to the following generic recombination reaction:



In the thermo input, A and B are labeled as reactants ("**reac**") and  $C^\ddagger$  is labeled as a transition state ("**ctst**"). For a barrier-less recombination reaction, the enthalpy of formation at 0 K ( $\Delta_f H$ ) for  $C^\ddagger$  must be set equal to the sum of the enthalpies of formation for the two reactants. All of the internal and rotational degrees of freedom for A and B are entered as usual. The *internal* degrees of freedom for  $C^\ddagger$  consist of the *combined* degrees of freedom (*internal* and *external*) of A and B, *plus* the external rotations for  $C^\ddagger$ . Thus the number of degrees of freedom (including degeneracies and multiple dimensions) of  $C^\ddagger$  is

$$n_C = n_A + n_B + n_C^{rots}$$

where  $n_A$  and  $n_B$  are the total number of degrees of freedom for A and B, and  $n_C^{rots}$  is the number of external rotations of  $C^\ddagger$ .

In order to find the center of mass distance  $r_{max}$  corresponding to maximum of  $V_{effective}$  at temperature T, the external 2-D rotation for  $C^\ddagger$  is labeled "**gor**" (see below). This signals that this particular entry is a dummy and will be adjusted in the process of finding the maximum  $V_{effective}$ . The potential energy function is specified later in the data file (see below).

In order to adjust the "hindrance" to fit specified rate constants, some of the rotations in  $C^\ddagger$  that were originally associated with A and B must be multiplied by  $\gamma$  (see above). These are labeled "fit" (see below). These rotations do *not* include internal rotation about the new bond in  $C^\ddagger$ , but only the rotations about internal axes perpendicular to the new bond. Later in the data file, the (experimental) rate constants to be fitted are entered... one for each temperature.

### Fully Coupled Anharmonic Vibrations (qvb)

This type specifies that program Thermo must read a supplementary data file named <name>.qvib, generated by programs `bdens` (Section 8.1), or `paradensum` (Section 8.2). This supplementary file must be present in the same directory as data file `thermo.dat`.

By using this supplementary data file, Thermo can utilize full intermode vibrational anharmonic coupling when computing thermodynamic data. This coupling is most important at high temperatures. This option is used when computing thermal rate constants with semi-classical transition state theory (SCTST; see Sections 8.3 and B.9 for more details).

IMPORTANT NOTE: Programs `bdens` and `paradensum` can optionally include separable degrees of freedom of the types listed in Chapter 3. In this case, the supplementary file <name>.qvib includes these degrees of freedom as well. To avoid double-counting, any separable degrees of freedom included in the `bdens` or `paradensum` calculations should not be listed again in the thermo data file.

### Thermal Rate Constants from SCTST (crp)

This type specifies that program Thermo reads a supplementary data file named <name>.qcrp, which must be generated previously by program `sctst` (Section 8.3) or `parsctst` (Section 8.4). File <name>.qcrp must be present in the same directory as data file `thermo.dat`. See Sections 8.3, 8.4, and B.9 for more details. By using this supplementary data file, Thermo can utilize the semi-classical transition state theory (SCTST) of W. H. Miller and coworkers. SCTST accounts for fully coupled degrees of freedom, including the reaction coordinate. **As a result, the theory incorporates multidimensional quantum tunneling along the curved reaction path**, which is very important at low temperatures. To prevent applying a second tunneling correction, **the imaginary frequency, `vimag`, (entered on Line 5, see below) must be given a value of `vimag` = 0.0** (actually  $<20\text{ cm}^{-1}$ ), or execution of THERMO will be terminated.

Note that in order to obtain the best possible accuracy at both low and high temperatures, a fully coupled vibrational model for a unimolecular reactant is usually used in addition to the `crp` degree of freedom when computing SCTST rate constants. The fully coupled vibrational model is specified with degree of freedom type "qvb" (see above) and it requires a supplementary data file from program `bdens`, or `paradensum` (see Chapter 8).

IMPORTANT NOTE: Programs `parsctst` and `sctst` can optionally include separable degrees of freedom of the types listed in Chapter 3. In this case, the supplementary file <name>.qcrp includes these degrees of freedom as well. To avoid double-counting, any separable degrees of freedom included in the `parsctst` and `sctst` calculations should not be listed again in the thermo data file.

### Rotation Coupled to Spin-Orbit Splitting (rso)



This type accounts for the coupling between electronic and rotational degrees of freedom for chemical species in degenerate electronic states. Currently, it is implemented ONLY for diatomic species in  $^2\Pi$  states, such as OH( $X^2\Pi$ ). It is based on the Hill and Van Vleck formalism,<sup>9</sup> as described by Herzberg in his Eq. (V,28).<sup>8</sup> It is invoked in order to obtain better accuracy at low temperatures.

## 6.2 Data File Format

**Note:** Starting with version 2009.0, the data file format is no longer compatible with previous versions.

### To run Thermo using the default filename (thermo.dat):

LINUX/UNIX: in the directory where the input data file resides, type:

```
<PATH>/multiwell-<version>/bin/thermo <RETURN>
```

where <PATH> designates the PATH to /multiwell-<version>. If directory /multiwell-<version> resides in the user home directory, type:

```
~/multiwell-<version>/bin/thermo <RETURN>
```

WINDOWS in a DOS window: in the directory where the input data file resides, type:

```
<PATH>/multiwell-<version>/bin/thermo <RETURN>
```

*For example:*

```
~/multiwell-2013/bin/thermo
```

### To run Thermo using a user-defined filename (FileName.dat):

Follow the same procedures described above, but type:

```
<PATH>/multiwell-<version>/bin/thermo <FileName> <RETURN>
```

*For example:*

```
~/multiwell-2013/bin/thermo final.dat
```

The resulting output file will take the same prefix: final.out.

## Line 1

### EKEY , SSKEY

- EKEY Key Word for Enthalpy units: "KCAL" or "KJOU" (upper or lower case). Note that "CM-1" is a reserved keyword to be fully implemented later.
- SSKEY Key Word for Standard State: "BAR", "ATM", "MCC" (molecule/cc), or "NOT" (free translations ignored)

## Line 2

**Nt** number of temperatures

## Line 3

**T1, T2, T3,...** List of Nt temperatures

## Line 4

**Ns** number of chemical species

Line 5 for reactants, products, or "none"; *see below for transition states*

### REPROD, MOLNAME, DeIH

REPROD key word:

"**reac**" = reactant

"**prod**" = product

"**none**" = not included in equilibrium constant

MOLNAME Name of chemical species (up to **32** characters)

DeIH enthalpy of formation at 0 K (Note that absolute enthalpies are not necessary, as long as the enthalpy differences between reactants and products are correct.)

## Line 5' for *transition states*

### REPROD, MOLNAME, DeIH, vimag, VVR

REPROD = "ctst"

For transition states, only. This choice calculates the canonical transition state theory rate constant based on reactant and transition state parameters. It assumes the reaction consists of reactants (each labeled "**reac**") and a transition state (labeled "ctst"). Note that for bimolecular and termolecular reactions, the standard state should be set to "MCC" for concentration units.

For 1-D quantum mechanical tunneling via an unsymmetrical Eckart energy barrier, enter **vimag** >0 and **VVR** >0. *Eckart tunneling is neglected when **vimag** <20 cm<sup>-1</sup> and/or **VVR** and/or the forward barrier are <0.01 cm<sup>-1</sup>.*

For use with SCTST rate constants, **vimag** = 0.0 and/or **VVR** must be set equal to 0.0 in order to prevent including tunneling twice (i.e. once via the SCTST rate constants and again via 1-D Eckart tunneling).

MOLNAME Name of transition state (up to **32** characters)

DeIH enthalpy of formation at 0 K. (Note that absolute enthalpies are not necessary, as long as the enthalpy differences between reactants and transition state are correct.)

**vimag** magnitude of imaginary frequency (units of  $\text{cm}^{-1}$ ). When using "crp" files from program **sctst** (see section 8.3), **vimag** must set to  $0.0 \text{ cm}^{-1}$ .

**VVR** Height of barrier for the reverse reaction (energy units specified in Line 1). When using **crp** files from program **sctst** (see section 8.3), **VVR** must be set to 0.0, but must be entered. *Eckart tunneling is neglected when  $VVR = 0.0$ .*

### Line 6

**FORMULA** Empirical chemical formula written in the usual way with atomic symbols. These symbols include "D" for deuterium and "T" for tritium. Special atomic symbols used for other isotopic species (e.g. "Cl35") are summarized in Section 10.7. Whenever an atomic symbol includes numeric characters (e.g. "Cl35"), it must be enclosed in square brackets, e.g. "[Cl35]". Examples of empirical formulas: C2H6O, CH3CH2OH, (CH3)2OH, (CH3)2(N)O2H, CH[Br79]2(CH3)3, CH3OD, C([C13]H3)4.

### Line 7

Up to 20 comment lines. The first non-blank character on each comment line must be "!" (omit the quotation marks).

### Line 8

#### **Sym, Sopt, Nele**

**Sym** external symmetry number (INTEGER); see Appendices B.4 and B.5  
**Sopt** number of optical isomers (INTEGER); see Appendix B.5  
**Nele** number of electronic energy levels (INTEGER)  
**NOTE:**  $Nele \geq 1$ , except  $Nele = 0$  (required!) when invoking  $IDOF(i) = \text{'RSO'}$  type for the coupled electronic-rotation degrees of freedom in  $^2\Pi$  diatomics (like OH radical).

### Line 9

**Elev, gele** (Repeat line for **Nele** electronic states)

**Elev** electronic level energies (REAL), always expressed as wavenumbers ( $\text{cm}^{-1}$ ).  
**NOTE:** lowest energy level should be at energy **Elev** = 0.0.  
**gele** electronic level degeneracies (INTEGER)

### Line 10

**N, VHAR, VROT** number of vibrations and rotations to be read in

**VHAR** KEYWORD for vibrations

'HAR': for vibrational frequencies input as harmonic frequencies.  
 'FUN': for vibrational frequencies input as 0-1 fundamental frequencies.  
**VROT** KEYWORD for molecular internal and external rotations, except for hindered rotors of type **hrd** (see special instructions below for type **hrd**). Entries in upper or lower case:  
 'AMUA': for moments of inertia input with units of amu Å<sup>2</sup>.  
 'GMCM': for moments of inertia input with units of g cm<sup>2</sup>.  
 'CM-1': for rotational constant input with units of cm<sup>-1</sup>.  
 'MHZ': for rotational constant input with MHz.  
 'GHZ': for rotational constant input with GHz.

Note: All of the rotational information for a given molecular species must be given in the form specified by **VROT** for that species.

**Line 11**

(repeat N times for the N molecular degrees of freedom)

**MODE(I), IDOF(I), AAA(I), BBB(I), CCC(I)**

**MODE** index number for degree of freedom  
**IDOF** KEY WORD for type of degree of freedom

**See Section 6.1.2 and Chapter 3 for descriptions of the types of separable molecular degrees of freedom recognized by THERMO.**

RETURN TO **LINE #5** and REPEAT FOR THE NEXT CHEMICAL SPECIES

AFTER ALL CHEMICAL SPECIES HAVE BEEN ENTERED, RESUME HERE:

**Line 12** (when 'fit' is used)

kexp(1), kexp(2), .... list of Nt experimental recombination rate constants (units of cm<sup>3</sup> molecule<sup>-1</sup> s<sup>-1</sup>): one for each of the Nt temperatures.

**Line 13-17** (required if 'gor' is used)

**Line 13** readpot Keyword 'MORSE', 'VARSHNI', or 'sMORSE' (Stiff-Morse). This is the type of bonding potential energy function.  
**Line 14** freq Harmonic frequency (cm<sup>-1</sup>) of the normal mode associated with the forming bond.  
**Line 15** De Dissociation Energy De (units of Eunit) of the forming bond.  
**Line 16** re EQUILIBRIUM center-of-mass distance (Å) between the of the two fragments that are forming the new bond.  
**Line 17** c Stiff-Morse parameter (needed only for 'sMORSE' type of potential).

**Line 18** (BLANK LINE)

### 6.3 MultiWell Thermodynamics Database

A database of molecular constants (for use by program thermo) is provided on the MultiWell website. The chemical species in this database are of interest to us in our research. We add entries from time to time, depending on current research interests.

The following are some excellent sources of molecular constants and enthalpies, which can be used with program thermo to generate thermodynamics data:

- NIST WebBook [<http://webbook.nist.gov/chemistry/>]
- Active Thermochemical Tables [<http://atct.anl.gov/>]
- NIST Computational Chemistry Comparison and Benchmark Database (NIST Standard Reference Database Number 101 Release 18, October 2016, Editor: Russell D. Johnson III) [<http://cccbdb.nist.gov/>]
- NIST-JANAF Thermochemical Tables.<sup>1</sup>

### References

- (1) Chase, M. W., Jr. NIST-JANAF Thermochemical Tables. Fourth Edition. *J. Phys. Chem. Ref. Data* **1998**, *Monograph No. 9*, 1-1951.
- (2) Golden, D. M. Reaction  $\text{ClO}+\text{ClO} \rightarrow$  Products: Modeling and Parameterization for Use in Atmospheric Models. *International Journal of Chemical Kinetics* **2003**, *35*, 206-211.
- (3) Golden, D. M. Evaluating data for atmospheric models, an example:  $\text{CH}_3\text{O}_2+\text{NO}_2=\text{CH}_3\text{O}_2\text{NO}_2$ . *International Journal of Chemical Kinetics* **2005**, *37*, 625-632.
- (4) Golden, D. M. Evaluating data for atmospheric models, an example:  $\text{IO}+\text{NO}_2=\text{IONO}_2$ . *Journal of Physical Chemistry A* **2006**, *110*, 2940-2943.
- (5) Golden, D. M. The reaction  $\text{Cl}+\text{NO}_2 \rightarrow \text{ClONO}$  and  $\text{ClNO}_2$ . *Journal of Physical Chemistry A* **2007**, *111*, 6772-6780.
- (6) Golden, D. M.; Barker, J. R.; Lohr, L. L. Master Equation Models for the Pressure- and Temperature-Dependent Reactions  $\text{HO} + \text{NO}_2 \rightarrow \text{HONO}_2$  and  $\text{HO} + \text{NO}_2 \rightarrow \text{HOONO}$ . *JPCA* **2003**, *107*, 11057-11071.
- (7) Golden, D. M.; Smith, G. P. Reaction of  $\text{OH} + \text{NO}_2 + \text{M}$ : A new view. *JPCA* **2000**, *104*, 3991-3997.
- (8) Herzberg, G. *Molecular Spectra and Molecular Structure. I. Spectra of Diatomic Molecules*, 2 ed.; Van Nostrand Reinhold Co.: Cincinnati, 1950.
- (9) Hill, E.; Van Vleck, J. H. On the Quantum Mechanics of the Rotational Distortion of Multiplets in Molecular Spectra. *Phys. Rev.* **1929**, *32*, 250-272.
- (10) Patrick, R.; Golden, D. M. *Int. J. Chem. Kinet.* **1983**, *15*, 1189-1227.
- (11) Smith, G. P.; Golden, D. M. Application of RRKM Theory to Reactions  $\text{OH}+\text{NO}_2+\text{N}_2 = \text{HONO}_2+\text{N}_2$  (1) and  $\text{ClO}+\text{NO}_2+\text{N}_2 = \text{ClONO}_2+\text{N}_2$  (2) - Modified Gorin Model Transition-State. *IJCK* **1978**, *10*, 489.
- (12) Varshni, Y. P. Comparative Study of Potential Energy Functions for Diatomic Molecules. *Rev. Mod. Phys.* **1957**, *29*, 664-682.

## 7. gauss2multi: A Tool for Creating Data Files

In many cases, one wants to create data files from calculated properties of molecules and transition states. The program `gauss2multi` is a tool designed to assist in this process. The source code is located in the `multiwell/src` directory and the executable is located in the `multiwell/bin` directory. The tool reads vibrational frequencies, coordinates, and energies from the standard `.log` or `.out` output files produced by GAUSSIAN 98<sup>2</sup> and GAUSSIAN 03.<sup>1</sup>

This tool does not create complete data files: it inserts only the data produced by quantum chemistry codes. It inserts some additional information as placeholders: the user must review the files created by `gauss2multi` and insert missing data and replace the placeholder data.

**We recommend that new users create input files manually, so that they will become familiar with the required input data. Experienced users will gain more benefit when using `gauss2multi`.**

In order to convert GAUSSIAN output files into multiwell input files you need:

- GAUSSIAN output files with frequency calculation (file extension: `.log` or `.out`)
- `gauss2multi.cfg` configuration file, which must reside in the same directory as the gaussian output files. An example is found in the `examples` directory

The following files will be created for each GAUSSIAN file that is read:

FILE NAME DESCRIPTION (see MultiWell User Manual)

<code>name.coords</code>		mominert input file
<code>name.coords.out</code>		mominert output file
<code>name.vibs</code>		densum input file
<code>name.dens</code>		densum output file
<code>name.therm </code>		thermo input file
<code>name.therm.out</code>		thermo output file
<code>multiwell.dat</code>		rough drat fof multiwell input file

("name" refers to the GAUSSIAN file name, which cannot exceed 10 characters in length)

### **gauss2multi.cfg Configuration File**

You can create and edit the configuration file by yourself or use the step-by-step script to create it.

The `gauss2multi.cfg` configuration file contains the following items (an example file is given below):

#### **Line:**

1. Energy units: `KCAL` , `KJOU`, or `CM-1` (upper or lower case)
2. number of temperatures
3. list of temperatures separated by one or more blank spaces

4. Pressure units: TOR, BAR, ATM, or MCC (upper or lower case). [Note: the TOR pressure unit is not one of the allowed standard states, which are required for setting up data file thermo.dat; therefore, BAR is used as default in creating thermo.dat.]
5. number of pressures
6. list of pressures separated by one or more blank spaces
7. Egrain, imax1, lsize, Emax2
8. index number (ascending order), name of gaussian output file (.log or .out), type of structure: WELL, PROD, or TS (upper or lower case)
9. Repeat Line-8 for additional species.

## TO RUN **gauss2multi**

There are two modes of operation:

### (a) To set up files for an entire multi-species model.

In this case, the energies (i.e.  $\Delta H_f^0(0\text{ K})$ ) for all of the species will be calculated with respect to the energy of the first well (index number = 1) listed in gauss2multi.cfg.

In the same directory as the GAUSSIAN files, type 'gauss2multi'

or

### (b) To generate data files for a single species.

In the same directory as the GAUSSIAN files, type 'gauss2multi <GAUSSIAN \_Name\_File>'

## IMPORTANT:

**The conversion to MultiWell data files cannot be completely automated:  
Many of these files will require manual changes! Be careful!**

## EXAMPLE CONFIGURATION FILE (gauss2multi.cfg)

```
KCAL
3
298.15 398 498
TOR
5
0.1 1.0 10. 100. 1000.
10. 400 900 50000.
1 A.log WELL
2 B.log WELL
3 TS-A-B.log TS
4 C.log PROD
```



## References

- (1) Frisch, M. J.; Trucks, G. W.; Schlegel, H. B.; Scuseria, G. E.; Robb, M. A.; Cheeseman, J. R.; Montgomery, J. A., Jr.; Vreven, T.; Kudin, K. N.; Burant, J. C.; Millam, J. M.; Iyengar, S. S.; Tomasi, J.; Barone, V.; Mennucci, B.; Cossi, M.; Scalmani, G.; Rega, N.; Petersson, G. A.; Nakatsuji, H.; Hada, M.; Ehara, M.; Toyota, K.; Fukuda, R.; Hasegawa, J.; Ishida, M.; Nakajima, T.; Honda, Y.; Kitao, O.; Nakai, H.; Klene, M.; Li, X.; Knox, J. E.; Hratchian, H. P.; Cross, J. B.; Bakken, V.; Adamo, C.; Jaramillo, J.; Gomperts, R.; Stratmann, R. E.; Yazyev, O.; Austin, A. J.; Cammi, R.; Pomelli, C.; Ochterski, J. W.; Ayala, P. Y.; Morokuma, K.; Voth, G. A.; Salvador, P.; Dannenberg, J. J.; Zakrzewski, V. G.; Dapprich, S.; Daniels, A. D.; Strain, M. C.; Farkas, O.; Malick, D. K.; Rabuck, A. D.; Raghavachari, K.; Foresman, J. B.; Ortiz, J. V.; Cui, Q.; Baboul, A. G.; Clifford, S.; Cioslowski, J.; Stefanov, B. B.; Liu, G.; Liashenko, A.; Piskorz, P.; Komaromi, I.; Martin, R. L.; Fox, D. J.; Keith, T.; Al-Laham, M. A.; Peng, C. Y.; Nanayakkara, A.; Challacombe, M.; Gill, P. M. W.; Johnson, B.; Chen, W.; Wong, M. W.; Gonzalez, C.; Pople, J. A. Gaussian 03, Revision C.02; Gaussian, Inc.: Wallingford CT, 2004.
- (2) Frisch, M. J.; Trucks, G. W.; Schlegel, H. B.; Scuseria, G. E.; Robb, M. A.; Cheeseman, J. R.; Zakrzewski, V. G.; Montgomery, J.; Stratmann, R. E.; Burant, J. C.; Dapprich, S.; Millam, J. M.; Daniels, A. D.; Kudin, K. N.; Strain, M. C.; Farkas, O.; Tomasi, J.; Barone, V.; Cossi, M.; Cammi, R.; Mennucci, B.; Pomelli, C.; Adamo, C.; Clifford, S.; Ochterski, J.; Petersson, G. A.; Ayala, P. Y.; Cui, Q.; Morokuma, K.; Malick, D. K.; Rabuck, A. D.; Raghavachari, K.; Foresman, J. B.; Cioslowski, J.; Ortiz, J. V.; Baboul, A. G.; Stefanov, B. B.; Liu, G.; Liashenko, A.; Piskorz, P.; Komaromi, I.; Gomperts, R.; Martin, R. L.; Fox, D. J.; Keith, T.; Al-Laham, M. A.; Peng, C. Y.; Nanayakkara, A.; Challacombe, M.; Gill, P. M. W.; Johnson, B.; Chen, W.; Wong, M. W.; Andres, J. L.; González, C.; Head-Gordon, M.; Replogle, E. S.; Pople, J. A. Gaussian 98, Revision A.7 Pittsburgh, 1998.



## 8. *bdens*, *paradensum*, *parsctst*, and *sctst*: *non-Separable Vibrations*

Program *bdens* computes sums and densities of states for non-separable vibrations. In addition to fully-coupled non-separable vibrations, the code can also include separable degrees of freedom, such as free rotations and hindered internal rotations. The code combines two fundamentally different algorithms:

a) Brute force direct counting (via a recursive algorithm), which is suitable for both small and large molecules at energies low enough so that the total sum of states is not too large. For some small molecules, direct brute force counting can be carried out even at energies above the dissociation energy.

b) The Wang-Landau algorithm, which is most suitable for large molecules at high energies.<sup>4,14,21</sup>

Direct counting produces *exact* sums and densities of states, but it is very slow when the total sum of states is large. The Wang-Landau algorithm is computationally quite efficient, but suffers from stochastic fluctuations unless a very large number of stochastic samples is used. In addition, its sampling is impeded when the density of states is very sparse. In program *bdens*, the two algorithms are combined in one "smart" code that produces exact (directly counted) results at low energies, where the density of states is sparse, and rapidly computed results of sufficient accuracy at high energies, where the densities and sums of states are very large.

Program *paradensum* is a parallelized, improved version replacing *adensum*, which is no longer supported (its last release was in *multiwell-2014.1b*). *paradensum* computes sums and densities of states for fully-coupled vibrational models. It utilizes the Wang-Landau algorithm with a flatness criterion and is suitable for fully-coupled vibrational models that consist of from 3 to >100 degrees of freedom.

The third program, *parsctst*, is for computing rate constants by using semi-classical transition state theory (SCTST) of W. H. Miller and coworkers, as described below. It is a parallelized, improved that will replace the serial code *sctst* in a future release. At the user's option, *parsctst* can be executed either as a serial code, or as a parallel code, thus effectively replacing the older code *sctst*.

### *Anharmonic vibrations*

For a brief introduction to non-separable anharmonic vibrations and definitions of technical terms, see Technical Note #2 (Appendix B.2 of this User Manual). Note that "exact" refers to exact at the level of second order vibrational perturbation theory (VPT2).

**NOTE.** In VPT2, the zero point energy includes contributions from the harmonic frequencies, the anharmonicities, and an additional term denoted  $G_0$  (see Eq. 9 in Appendix B.9).<sup>13,19</sup> This term, which cancels-out in spectroscopy applications but must be included for thermochemistry and kinetics, is computed by electronic structure programs that employ VPT2 (e.g. GAUSSIAN and CFOUR), but it is not computed by MultiWell. For *ab initio* kinetics calculations involving small molecules the term may be significant, but it is very small for molecules with small rotational constants. For high accuracy *ab initio* kinetics calculations (e.g. <sup>16</sup>,  $G_0$  can be included manually by modifying the reaction critical energy ( $E_0$ ).

## Acceptable Vibrational States

The vibrational energy  $E_v$  in principle can be computed when all acceptable values of  $v$  are known. Acceptable values of  $v$  correspond to bound vibrational states. Therefore, the problem reduces to finding all acceptable values of  $v$  up to a given total internal energy. For a separable harmonic oscillator, all quantum numbers from  $v=0$  to  $v=\infty$  are acceptable. A Morse oscillator, however, can dissociate and thus has a finite number of acceptable vibrational states ranging from  $v=0$  to  $v=v_{max}$ . For a *coupled* set of anharmonic vibrations, the maximum quantum number allowed for the  $k^{\text{th}}$  vibration,  $v_{D,k}$ , depends on the quantum numbers assigned for all other vibrations; the dissociation energy of the  $k^{\text{th}}$  vibration corresponds to the energy at which  $E_v$  reaches a maximum as  $v_k$  is increased, i.e.  $(\partial E_v / \partial v_k) = 0$  at  $v_k = v_{D,k}$ .<sup>3,14,16</sup> For a state to be "bound" with respect to the  $k^{\text{th}}$  degree of freedom, the derivative must be greater than zero for the trial value of quantum number  $v_k$ :  $(\partial E_v / \partial v_k) > 0$ . In the codes `bdens`, `paradensum`, and `parstst`, this criterion must be satisfied for a quantum number to be deemed "acceptable". In addition, quantum numbers in `parstst` must also satisfy the condition that the amplitude of the effective imaginary frequency (which is affected by coupling to all of the other vibrations) must be greater than zero.

## $G_0$ Term in the ZPE from VPT2

In second order vibrational perturbation theory (VPT2), the zero point energy includes contributions from the harmonic frequencies, the anharmonicities, and an additional term denoted  $G_0$  (see Eq. 9 in Appendix B.9).<sup>13,19</sup> This term, which cancels-out in spectroscopy applications but must be included for thermochemistry and kinetics, is computed by electronic structure programs that employ VPT2 (e.g. GUSSIAN and CFOUR), but it is not computed by MultiWell. For *ab initio* kinetics calculations involving small molecules the term may be significant, but it is very small for molecules with small rotational constants. For high accuracy *ab initio* kinetics calculations (e.g. <sup>16</sup>,  $G_0$  can be included manually by modifying the reaction critical energy.

## 8.1 Program `bdens`

Program `bdens` replaces previous programs `adensum`, `doloops`, and `ansum`, which were last released in version 2014.1b. For definitions of the terms used in the following, see Technical Note #2 (Appendix B.2 of this User Manual).

Program `bdens` computes sums and densities of acceptable bound and quasi-bound states as a function of vibrational energy  $E_v$  up to a high energy (measured from the zero point energy). The state energies are binned in energy grains specified by user (typically  $10 \text{ cm}^{-1}$ ). Total sums and densities of states can then be computed by convoluting the results for the fully coupled vibrational model with separable degrees of freedom, such as rotations, hindered rotors, etc. (using the combined Beyer-Swinhart<sup>5</sup> and Stein-Rabinovitch<sup>18</sup> algorithms (the BSSR algorithm)).

Program `bdens` combines two algorithms: direct count and the Wang-Landau algorithm. The resulting sums and densities of states are exact at low energies (where direct counting is used) and of very high accuracy at high energies (where the Wang-Landau method is used). For

larger species, the combination gives both faster execution times and better accuracy at low energies.

### ***Direct count Algorithm***

The direct count (DC) algorithm is a recursive version of a set of nested do-loops. Because it is recursive, it (ideally) can be used for any number of coupled vibrational modes; practically speaking, the default array size limits the number of vibrations to 150, which is large enough for most applications.

### ***Wang-Landau Algorithm***

Wang and Landau<sup>20,21</sup> pioneered an efficient random walk algorithm in energy space to compute densities of states for use in classical statistical models. Their approach is based on the idea that a density-weighted Monte Carlo sampling of the energy states of the system will produce a flat histogram of samples in equally-spaced energy bins if the density of states function is exact, in the limit of an infinite number of trials. The algorithm is initiated with a trial density of states in every energy bin and the density-weighted Monte Carlo sampling begins. A histogram records every visit to an energy bin. The algorithm is designed to modify the relative density of states  $G(E_i)$  on every visit to an energy bin (at energy  $E_i$ ) in such a way so that  $G(E_i)$  approaches exact proportionality with the true density of states after a large number of samples.<sup>20,21</sup> The algorithm can be halted by monitoring the "flatness" of the histogram, or by limiting the number of Monte Carlo samples. Basire et al.<sup>4</sup> adapted the Wang-Landau algorithm for computing quantum densities of states for fully coupled anharmonic systems using the perturbation theory expansion for vibrational energy. It is a powerful method. For a full description of the algorithm and notation, see the paper by Basire et al.<sup>4</sup> As one of their demonstrations, they computed the density of states for naphthalene, based on the fully-coupled  $\mathbf{X}$  matrix reported by Cané et al.<sup>6</sup>

We have modified the Basire et al. version<sup>4</sup> of the Wang-Landau algorithm in several minor ways to meet the needs for the density of states in chemical kinetics and master equation applications. In our approach, we compute statistics for the histogram based only on energy bins that contain states. We do not use the "flatness" criterion for halting the algorithm, but instead use the number of Monte Carlo trials per energy bin, since that is the principal factor that controls the relative error (see below). We also apply the tests described above to ensure that selected states are bound or quasi-bound.

We have automated the algorithm by choosing the probability of accepting a move (parameter  $p$ ; see Basire et al. for notation) according to  $N$ , the number of DOF. As discussed by Basire et al., if  $p$  is too large, the Monte Carlo selection can sample the entire energy range rapidly, but there may be many wasted samples that fall out of range. On the other hand if  $p$  is too small, the entire energy range may not be sampled efficiently, and more trials will be needed. In this work, we adopt  $p = \text{MIN}(1/N, 0.25)$ . This protocol is consistent with the values for  $p$  used by Basire et al.<sup>4</sup> As discussed in a later section, our results show little sensitivity to the selection of  $p$ .

An important new modification we have made to the Basire et al. version<sup>4</sup> of the Wang-Landau algorithm is to introduce automatic normalization of the density of states. Recall that the Wang-Landau algorithm produces results that are *proportional* to the exact density of states. The un-normalized  $G(E_i)$  may be sufficient for many applications, but the absolute density of states  $\rho(E_i)$  is needed for calculating rate constants from statistical rate theories, for example. In our

approach, the size of the energy bins (i.e. the energy grain size  $\Delta E$ ) is chosen small enough so that only one state, the lowest energy state (i.e. the zero point energy state), falls in the lowest energy bin. Since we know that only one state resides in the lowest energy bin, the density of states in lowest energy bin must be  $(\Delta E)^{-1}$ , we then obtain the absolute density of states:

$$\rho(E_i) = \frac{G(E_i)}{G(E_i = 0)} \frac{1}{\Delta E}$$

For vibrational states, it is easy to choose  $\Delta E$  small enough so that only the zero point energy state falls within the lowest energy bin.

In the `bdens` code, this normalization method has been improved by taking advantage of the exact state count obtained from the Direct Count algorithm. The DC algorithm is used to calculate exact densities of states in an energy range that overlaps the energy range in which the WL algorithm is used. The overlapped energy range is approximately from `Eswitch` to `1.1*Eswitch`. Over that overlapped energy range, the ratio of the exact density of states divided by the relative density of states is evaluated in each occupied energy grain and the average is identified with the scale factor that normalizes the WL relative densities. Since this scale factor depends on not just one, but on multiple energy grains, it is not as susceptible to stochastic noise as our original normalization method.

Note that our modified version<sup>14</sup> of the Wang-Landau algorithm<sup>20,21</sup> draws heavily on that of Basire et al.,<sup>4</sup> which should also be cited.

### ***Switching from Direct Count to Wang-Landau***

At energy `Eswitch`, the `bdens` code switches execution from the direct count (DC) algorithm to the Wang-Landau (WL) algorithm (see next section). `Eswitch` can be optionally declared manually (by choosing keyword "MAN " and giving the energy `Eswitch` ( $\text{cm}^{-1}$  units)) or automatically (keyword "AUTO"). By carrying out tests, we have determined how the execution time using each algorithm depends on the sum of states as a function of energy. At low energies, DC is faster than the WL, while the reverse is true at high energies. When `Eswitch` is determined automatically, it is selected in order to minimize total execution time. In other words, the "AUTO" option results nearly optimum over-all execution times.

### ***Running bdens***

The executable (binary) program resides in the directory `multiwell<version>/bin`, where `<version>` is the version number (e.g. "2010.0") To execute the compiled program, enter the directory that contains the `bdens` data file ("`bdens.dat`") and then type `~/multiwell<version>/bin/ bdens`. Directory `multiwell<version>` is assumed to reside in your Home directory. The output file `bdens.out` is automatically placed in the directory that contains `bdens.dat`. A second output file `<name>.dens`, which is designed to be an input file for the MultiWell master equation code, is also generated, where `<name>` is the name of the chemical species (specified in `bdens.dat`).

`bdens` has been designed to run using a "checkpoint file" (`<name>.chk`), which is generated after the density of states of the fully coupled vibrations have been calculated; this is the most time-consuming section. The following section convolutes the separable degrees of freedom, if any are specified. The separable degrees of freedom may include free or hindered rotors, harmonic vibrations, etc. In particular, the K-rotor and possibly other external rotational

degrees of freedom may be specified. If desired, the densities of states may be recalculated using various combinations of separable degrees of freedom, but retaining the same set of fully coupled vibrations. Repetitive calculations like these can be restarted using the checkpoint file, which saves considerable computer time.

In addition to the checkpoint file (<name>.chk), three output files are generated by bdens: bdens.out, <name>.dens, and <name>.qvib. The first file (bdens.out) is a standard output file, which summarizes all input and output. The second file (<name>.dens), which takes a chemical species name (<name>) as part of the file name, gives sums and densities of states, formatted as double arrays; it can be used as input for the MultiWell master equation code. By using this input file, master equation calculations can be carried out with densities of states computed by including the fully-coupled vibrations. The third file (<name>.qvib) is formatted as a supplementary input file for program Thermo; it tabulates the partition function and other thermodynamic properties of the coupled vibrational modes at a set of fixed temperatures from 50 K to >3000 K. Thermo can utilize these partition functions to compute and thermodynamics data and canonical rate constants. See Section 6.3 of this User Manual for a description of how the <name>.qvib file is used by Thermo.

### ***bdens.dat Data File Format***

**For definitions of terms, see Technical Note #9.** (Appendix B.2 of this User Manual)

**Line 1:** Name (species name;  $\leq 10$  characters)

**Line 2:** Title 1 ( $\leq 100$  characters)

**Line 3:** Title 2 ( $\leq 100$  characters)

**Line 4:** ns (number of vibrational modes), NY (number of Y matrix elements), NZ (number of Z matrix elements), WW (a keyword to designate frequencies as  $\omega_e$  or  $\omega^0$ )

WW = We for  $\omega$

WW = Wf for fundamental vibrations (0-1 transitions)

WW = W0 for  $\omega^0$  [note: "0" is a zero]

(The distinction between  $\omega$  and  $\omega^0$  is explained by eqs. (II,267) through (II,269) of Herzberg<sup>8</sup>.  
The computer code carries out the conversion between them.)

**Lines 5+ (5 to 4+ns):** wa(i) [ $i = 1, \dots, ns$ ] vibrational frequencies ( $\text{cm}^{-1}$ )

**Line 6 (5+ns):** KEYWORD for reading the X anharmonicity matrix:  
= lower (for reading lower half of matrix, plus the diagonal)  
= upper (for reading upper half of matrix, plus the diagonal)

**Lines 7+ (6+ns to 5+2ns):** xa(k,j) anharmonicities ( $\text{cm}^{-1}$ ) in upper or lower halves (plus the diagonal) of the  $ns \times ns$  anharmonicity matrix.

**Line 8: Nsep , Vrot**

Nsep = number of separable modes to be convoluted with the ns non-separable modes)  
Vrot = KEYWORD for specifying units for internal and external rotations, except for hindered rotors of type **hrd** (see special instructions in the chapter on DenSum for type hrd). Entries in upper or lower case.

'AMUA': for moments of inertia input with units of amu Å<sup>2</sup>.

'GMCM': for moments of inertia input with units of g cm<sup>2</sup>.

'CM-1': for rotational constant input with units of cm<sup>-1</sup>.

'MHZ': for rotational constant input with MHz.

'GHZ': for rotational constant input with GHz.

(upper or lower case)

**Line 9:** input data for the separable modes (classical or quantum free rotors, hindered rotors of several types, and Morse oscillators). The various types are defined and appropriate input format are described in Chapter 3.

**Line 10:** Egrain1, imax1, lsize, Emax2, KEYWORD1, KEYWORD2, Eswitch

Egrain1 = energy grain (cm<sup>-1</sup>)

imax1 = number of array elements in lower part of the Double Array (see MultiWell User Manual)

lsize = total number elements in the Double Array.

Emax2 = upper energy limit

KEYWORD1 = controls number of stochastic trials:

Fair: low statistical accuracy (10<sup>2</sup> trials per energy grain)

Good: good statistical accuracy (10<sup>3</sup> trials per energy grain).

Better: better statistical accuracy (10<sup>4</sup> trials per energy grain)

Best: best statistical accuracy (10<sup>5</sup> trials per energy grain)

Extra: best statistical accuracy (10<sup>6</sup> trials per energy grain, but no more than 2×10<sup>9</sup> total trials for all energy grains)

KEYWORD2 = controls how Eswitch is chosen

AUTO: an optimum Eswitch is chosen automatically by bdens.

MAN: Eswitch is defined manually by the User

Eswitch = defined by the User (units: cm<sup>-1</sup>) (a place-holder value must be present even when KEYWORD2 = AUTO).

**Line 11:** checkpoint

If checkpoint = "chekstart" (**Note the spelling!**), then the new calculation starts by reading the pre-existing checkpoint file (<name>.chk). Otherwise, the full calculation is carried out. Line 10 must be identical to the data file used to create the pre-existing checkpoint file.



## *Notes*

1. Energies are relative to the zero point energy.
2. Be careful when using Gaussian! The Gaussian log file has two sections related to vibrations. The first section is for the usual vibrational analysis to obtain harmonic frequencies. These frequencies are listed from lowest to highest. The second section is for anharmonicities. In the second section, the harmonic frequencies are listed again (along with the fundamental frequencies), but the ordering may not be the same as in the first section. The input for the codes distributed in MultiWell will accept the frequencies in any order, but the ordering of the harmonic frequencies must be consistent with the ordering used for the anharmonicities. For consistency, the Gaussian user must be sure to use the ordering of the harmonic frequencies as listed in association with the anharmonicities in the Gaussian log file.

## 8.2 Program paradensum

paradensum:<sup>1</sup> parallel and improved version of adensum (adensum was last released in multiwell-2014.1b)

Program Authors:

paradensum: **C. Aieta, F. Gabas, and M. Ceotto**

adensum: **T. L. Nguyen and J. R. Barker**

Contact: **Michele Ceotto**: michele.ceotto@unimi.it

(For definitions, see Technical Note #2. (Appendix B.2 of this User Manual))

Wang and Landau<sup>20,21</sup> pioneered an efficient random walk algorithm in energy space to compute densities of states for use in classical statistical models. Their approach is based on the idea that a density-weighted Monte Carlo sampling of the energy states of the system will produce a flat histogram of samples in equally-spaced energy bins if the density of states function is exact, in the limit of an infinite number of trials. The algorithm is initiated with a trial density of states in every energy bin and the density-weighted Monte Carlo sampling begins. A histogram records every visit to an energy bin. The algorithm is designed to modify the relative density of states  $G(E_i)$  on every visit to an energy bin (at energy  $E_i$ ) in such a way so that  $G(E_i)$  approaches exact proportionality with the true density of states after a large number of samples.<sup>20,21</sup> The algorithm can be halted by monitoring the "flatness" of the histogram, or by limiting the number of Monte Carlo samples. Basire et al.<sup>4</sup> adapted the Wang-Landau algorithm for computing quantum densities of states for fully coupled anharmonic systems using the perturbation theory expansion for vibrational energy. It is a powerful method. For a full description of the algorithm and notation, see the paper by Basire et al.<sup>4</sup> As one of their demonstrations, they computed the density of states for naphthalene, based on the fully-coupled **X** matrix reported by Cané et al.<sup>6</sup>

We have modified the Basire et al. version<sup>4</sup> of the Wang-Landau algorithm in several minor ways to meet the needs for the density of states in chemical kinetics and master equation applications.<sup>14</sup> In our approach, we compute statistics for the histogram based only on energy bins that contain states. In **paradensum** we use the "flatness" criterion for halting the algorithm (this is in contrast to **adensum**, which used specified numbers of stochastic trials). We also apply the tests described elsewhere<sup>3</sup> to ensure that selected states are bound or quasi-bound.

We have automated the algorithm by choosing the probability of accepting a move (parameter  $p$ ; see Basire et al. for notation) according to  $N$ , the number of coupled DOF.<sup>14</sup> As discussed by Basire et al., if  $p$  is too large, the Monte Carlo selection can sample the entire energy range rapidly, but there may be many wasted samples that fall out of range. On the other hand if  $p$  is too small, the entire energy range may not be sampled efficiently, and more trials will be needed. In this work, we adopt  $p = \text{MIN}(1/N, 0.25)$ . This protocol is consistent with the values for  $p$  used by Basire et al.<sup>4</sup> Our results show little sensitivity to the selection of  $p$ .

The most important new modification we have made to the Basire et al. version<sup>4</sup> of the Wang-landau algorithm is to introduce automatic normalization of the density of states.<sup>1,14</sup> Recall that the Wang-Landau algorithm produces results that are *proportional* to the exact density of states. The un-normalized  $G(E_i)$  may be sufficient for many applications, but the absolute density of states  $\rho(E_i)$  is needed for calculating partition functions and rate constants from statistical rate

theories, for example. In our approach, the size of the energy bins (i.e. the energy grain size  $\Delta E$ ) is chosen small enough so that only one state, the lowest energy state (i.e. the zero point energy state), falls in the lowest energy bin. Since we know that only one state resides in the lowest energy bin, the density of states in lowest energy bin must be  $\rho(0) = 1/\Delta E$ , we then obtain the absolute density of states:

For vibrational states, it is easy to choose  $\Delta E$  small enough so that only the zero point energy state falls within the lowest energy bin. For master equation and chemical kinetics applications, the typical energy grain is  $\Delta E \leq 10 \text{ cm}^{-1}$  and vibrational frequencies are typically much larger. If rotations were to be included with the vibrations, normalization can still be achieved easily by using one of the other methods described above to count the number of rotational states in the lowest energy grain and normalizing accordingly.

Our modified version of the Wang-Landau algorithm<sup>20,21</sup> draws heavily on that of Basire et al.,<sup>4</sup> and is summarized elsewhere.<sup>1,14</sup> Also see Section 8.1 of this User Manual for a description of program `bdens`, which also uses the Wang-Landau algorithm.

`paradensum` is a parallel code that can exploit not only single but also multiple core architectures. In this way the computation of the density of states is significantly accelerated when considering high dimensionality systems. The parallelization strategy is to divide the energy range into energy “windows” and set the calculations of  $G(E_i)$  for each window on a single processor. This strategy is dictated by the observation that less random sampling events and reduced computational effort is needed for Monte Carlo to converge in a restricted energy range.

The number of processors is given by the windowing choice and, by default, all windows have the same width. This setting can be changed modifying the appropriate keyword in the input file. If the computational time spent by each window to reach the flatness criterion is unbalanced, the code prints a warning in the `Windows_info.txt` output file. Then, the user can decide to halve the width of the first two or the last two windows.

Since the Wang-Landau density of states is notoriously biased at the edges of small energy windows, we always keep a percentage of overlap between neighbor windows. This is also necessary for the normalization of the  $G(E_i)$  obtained in each window to give the complete function on the whole energy domain.<sup>1</sup> The code supports the possibility to run serially multiple walkers in each energy window. This feature improves the statistics of sampling in each window but does not have any impact on the speedup. To run the code the user has to supply the number of processors that is equal to the number of windows and a percentage of overlap between them as input parameters. When the number of processors (windows) is set to unity, then `paradensum` will run in serial mode (i.e. it can run on a single cpu or core). The set up of the input file for these parameters is described below. For a full description of the `paradensum` implementation, see the paper by Aieta et al.<sup>1</sup>

## **Running `paradensum`**

*`paradensum` is a parallel code. To compile and run the code, it is necessary to have previously installed supplementary software. Details are given in Section 1.4).*

`paradensum` has been designed to run using a "checkpoint file" (`<name>.chk`), which is generated after the density of states of the fully coupled vibrations have been calculated, which is the most time-consuming section. The next section in the code convolutes the separable

degrees of freedom, if any are specified. The separable degrees of freedom may optionally include free or hindered rotors, harmonic vibrations, etc. In particular, the K-rotor and possibly other external rotational degrees of freedom may be specified. If desired, the densities of states may be recalculated using various combinations of separable degrees of freedom, but retaining the same set of fully coupled vibrations, available from the checkpoint file. Repetitive calculations like these can be restarted using the checkpoint file, which saves considerable computer time. Note that when using checkpoint file, it is not necessary to run the code in parallel mode.

The input data file `paradensum.dat` includes molecular parameters for computing the densities of states, as well as parallel execution parameters. Directory `multiwell-<version>` is assumed to reside in your Home directory. Execution of `paradensum` is carried out within the directory that contains the input data file `paradensum.dat`. All of the output files are automatically placed in the directory that contains `paradensum.dat`.

Four output files are generated by `paradensum`: `paradensum.out`, `<name>.dens`, `<name>.qvib.`, and `Windows_info.txt`. The file `paradensum.out` is a standard output file, which summarizes all input and output. The file `<name>.dens`, which takes a chemical species name as part of the file name, gives sums and densities of states, formatted as double arrays; it can be used as input for the MultiWell master equation code. By using this input file, master equation calculations can be carried out with densities of states computed by including the fully-coupled vibrations. The file `<name>.qvib` is formatted as a supplementary input file for program `Thermo`; it tabulates the partition function and other thermodynamic properties of the coupled vibrational modes at a set of fixed temperatures from 1 K to >3000 K. `Thermo` can utilize these partition functions to compute thermodynamics data (from statistical mechanics formulae) and canonical rate constants (from statistical rate theory). See Section 6.1.2 of this User Manual for a description of how the `<name>.qvib` file is used by `Thermo`. The file `Windows_info.txt` contains details about windows division, i.e. the total number of energy grains, the number of energy grains in each window after the overlap has been added, and the low and high energy boundaries of each window.

Users may also select a supplementary writing option, which generates a file called `Rank<N>.txt` for each parallel process (here, `<N>` is an integer number that identifies the process). These files report all details about the Wang-Landau algorithm executed by each parallel process. Users may freely enable or disable writing the `Rank<N>.txt` files, which are intended as a user check on parallel execution.

## ***Format for paradensum.dat Input File***

(For definitions of terms, see **Technical Note #9**. (Appendix B.2 of this User Manual))

**Line 1:** Name (species name;  $\leq 10$  characters)

**Line 2:** Title 1 ( $\leq 100$  characters)

**Line 3:** Title 2 ( $\leq 100$  characters)

**Line 4:** ns (number of vibrational modes), NY (number of **Y** matrix elements), NZ (number of **Z** matrix elements), WW (a keyword to designate frequencies as  $\omega_e$  or  $\omega^0$ )  
WW = We for  $\omega$   
WW = Wf for fundamental vibrations (0-1 transitions)  
WW = W0 for  $\omega^0$  [note: 0 is a zero]  
(The distinction between  $\omega$  and  $\omega^0$  is explained by eqs. (II,267) through (II,269) of Herzberg<sup>8</sup>. The computer code carries out the conversion between them.)

**Lines 5+ (5 to 4+ns):** wa(i) [ $i = 1, ns$ ] vibrational frequencies ( $\text{cm}^{-1}$ )

**Line 6 (5+ns):** KEYWORD for reading the **X** anharmonicity matrix:  
= lower (for reading lower half of matrix, plus the diagonal)  
= upper (for reading upper half of matrix, plus the diagonal)

**Lines 7+ (6+ns to 5+2ns):** xa(k,j) anharmonicities ( $\text{cm}^{-1}$ ) in upper or lower halves (plus the diagonal) of the ns $\times$ ns anharmonicity matrix.

**Line 8: Nsep, Vrot**

Nsep = number of separable modes to be convoluted with the ns non-separable modes)  
Vrot = KEYWORD for specifying units for internal and external rotations, except for hindered rotors of type **hrd** (see special instructions in the chapter on DenSum for type **hrd**). Entries in upper or lower case:  
'AMUA': for moments of inertia input with units of amu  $\text{\AA}^2$ .  
'GMCM': for moments of inertia input with units of g  $\text{cm}^2$ .  
'CM-1': for rotational constant input with units of  $\text{cm}^{-1}$ .  
'MHZ': for rotational constant input with MHz.  
'GHZ': for rotational constant input with GHz.

**Line 9:** input data for the separable modes (classical or quantum free rotors, hindered rotors of several types, and Morse oscillators). The various types are defined and appropriate input format are described in Chapter 3.

**Line 10:** Egrain1, imax1, lsize, Emax2

Egrain1 = energy grain ( $\text{cm}^{-1}$ )

imax1 = number of array elements in lower part of the Double Array (see MultiWell User Manual)

lsize = total number elements in the Double Array.

Emax2 = upper energy limit

**Line 11:** checkpoint, <chekname>

If checkpoint = "chekstart" (**Note the spelling!**), then the new calculation starts by reading the pre-existing checkpoint file (<name>.chk). Otherwise, the full calculation is carried out. Line 10 must be identical to the data file used to create the pre-existing checkpoint file.

<chekname> = filename ( $\leq 15$  characters) for the checkpoint file to be generated, or read as input. The filename must contain the suffix, ".chk" and may be different from the name entered on Line 1.

**Line 12:** (Blank line)

**Line 13:** nwalkers = number of independent random walks in each window; integer.

**Line 14:** perc\_wind\_overlap = percentage of overlap between neighboring windows; real.

**Line 15:** flatness = flatness criterion for halting the Wang-Landau algorithm: a real number between 0 and 1. The closer to unity, the more accurate is the density of states.

**Line 16:** writing (writing out Rank<N>.txt files)

= 1 (Writing enabled.)

= 0 (Writing disabled.)

**Line 17:** seed\_modifier = an integer number which is added to the default random number generator seed in order to get a new random number chain. For usual applications of the code it is set to 0.

**Line 18:** windbal\_key = this keyword sets the windows width.

= "const" (default) windows width is equal for all windows.

= "low" the first two windows are smaller than the others.

= "high" the last two windows are smaller than the others.

## Notes

1. Energies are relative to the zero point energy.
2. Be careful when using Gaussian! The Gaussian log file has two sections related to vibrations. The first section is for the usual vibrational analysis to obtain harmonic frequencies. These frequencies are listed from lowest to highest. The second section is for anharmonicities. In the second section, the harmonic frequencies are listed again (along

with the fundamental frequencies), but the ordering may not be the same as in the first section. The input for the codes distributed in MultiWell will accept the frequencies in any order, but the ordering of the harmonic frequencies must be consistent with the ordering used for the anharmonicities. For consistency, the Gaussian user must be sure to use the ordering of the harmonic frequencies as listed in association with the anharmonicities in the Gaussian log file.

3. See Sections 1.3 and 1.4 for special instructions for executing `paradensum`.

### 8.3 Program `sctst`

(In a future release, `sctst` will no longer be supported, since it is being replaced by `parsctst`, an improved, parallelized version. See Section 8.4.)

This program is an implementation<sup>16</sup> of the semi-classical transition state theory (SCTST) formulated by W. H. Miller and coworkers.<sup>7,9-11</sup> Our implementation is based on the Wang and Landau algorithm<sup>21</sup> and the density of states algorithm of Basire et al.,<sup>4</sup> as refined by Nguyen and Barker.<sup>14</sup> The literature references should be consulted for further details about the theory, its usefulness, and applications. The literature should be cited as described at the Preface of this User Manual.

The SCTST is a powerful method, since it can be used for computing both thermal (i.e. canonical  $k(T)$ ) and microcanonical (i.e.  $k(E)$ ) rate constants, which are essential for master equation calculations. Unlike ordinary transition state theory, the SCTST is fully non-separable: all of the degrees of freedom may be coupled and it is not necessary to assume that the reaction coordinate is separable from the others. It also accounts naturally for zero point energy and for quantum mechanical tunneling along the curved reaction path in hyperdimensional space. In test cases, it is highly accurate.<sup>15</sup>

The input is similar to that for program `bdens` (Section 8.1), but it also includes the imaginary frequency and the anharmonicity coefficients associated with the reaction coordinate. The imaginary frequency and the off-diagonal anharmonicity coefficients associated with the reaction coordinate are pure imaginary numbers; the diagonal anharmonicity for the reaction coordinate is a pure real number. These facts affect how the parameters are specified in the input data file `sctst.dat`. In addition, SCTST as formulated by Miller and coworkers is based on second order vibrational perturbation theory (VPT2).<sup>12</sup> Recently, Stanton investigated SCTST based on VPT4 (fourth order perturbation theory) and arrived as a simple correction that is appropriate for symmetrical Eckart barriers.<sup>17</sup> To the extent that the actual energy barrier resembles an Eckart barrier, this VPT4 correction improves the performance of SCTST/VPT2. Stanton suggested two slightly different versions of this correction, but the difference between them is small. In program `sctst`, either of the two corrections (or neither) can be selected by selecting the appropriate key word.

The output files are analogous to the output files from programs `bdens` and `densum`. The general output file `sctst.out` summarizes the input and gives "sums" and "densities" of states for the full energy range specified. These "sums" and "densities" actually correspond to the cumulative reaction probability<sup>7,9-11</sup> (CRP) and the corresponding energy derivative, which are equal to the sums and densities in the absence of quantum tunneling. The second output files takes the name of the transition state with ".dens" added: `<name>.dens`, just as in programs `densum` and `bdens`. These files are formatted for use by the MultiWell master equation code. An output file is also generated that gives the thermal partition function (excluding the

translations) for the transition state at a set of 100 fixed temperatures (25 K to 3383 K). This file, named `<name>.qcrp`, is used by program `Thermo` to calculate canonical rate constants (see Section 6.3 of this User Manual for a description of how the file is used by `Thermo`).

### **Running `sctst`**

The executable (binary) program resides in the directory `multiwell<version>/bin`, where `<version>` is the version number (e.g. "2014.1b"). To execute the compiled program, enter the directory that contains the `sctst` data file ("`sctst.dat`") and then type `~/multiwell-<version>/bin/sctst`. Directory `multiwell<version>` is assumed to reside in your Home directory. The output file `sctst.out` is automatically placed in the directory that contains `sctst.dat`. A second output file `<name>.crp`, which is designed to be an input file for the MultiWell master equation code, is also generated, where `<name>` is the name of the transition state specified in `sctst.dat`.

`sctst` has been designed to run using a "checkpoint file" (named `<chekname>`), which is generated after the density of states of the fully coupled vibrations have been calculated (the most time-consuming part of the calculation). The next part of the calculation convolutes the separable degrees of freedom, if any are specified. The separable degrees of freedom may include free or hindered rotors, harmonic vibrations, etc. In particular, the 1-D external rotation (the K-rotor) and possibly also the 2-D external rotational degrees of freedom may be specified, depending on the application. If desired, the densities of states may be recalculated using various combinations of separable degrees of freedom, but retaining the same set of fully coupled vibrations. Repetitive calculations like these can be restarted using the checkpoint file, which saves considerable computer time.

Another reason for running repetitive calculations by starting with the checkpoint file is because whenever the reaction threshold energy is changed, the SCTST requires that the density of states of the transition state and the cumulative reaction probability be recalculated.<sup>16</sup> Adjusting reaction barriers to fit experimental data may require multiple repetitive calculations, and restarting by using the checkpoint file will reduce the computer time by an order of magnitude or more.

In summary, four output files are generated by `sctst`: `sctst.out`, `<name>.crp`, `<chekname>` (which must include the `.chk` suffix), and `<name>.qcrp`. The first file (`sctst.out`) is a standard output file, which summarizes all input and output. The second file (`<name>.chk`), which takes a chemical species name as part of the file name, is the checkpoint file, which is an important time-saving measure for subsequent runs using the same vibrational parameters, as described in the preceding paragraph. The third file (`<name>.crp`), tabulates the cumulative reaction probability (CRP) and its energy derivative (analogous to sums and densities of states), formatted as double arrays; it is formatted for use as input for the MultiWell master equation code. By using this input file, master equation calculations can be carried out with microcanonical rate constants (i.e.  $k(E)$ ) computed by including the fully-coupled vibrations. The fourth file (`<name>.qcrp`) is formatted as a supplementary input file for program `Thermo`; it tabulates the partition function for the CRP and other thermodynamic properties of the coupled vibrational modes at a set of fixed temperatures from 50 K to >3000 K. `Thermo` can utilize these partition functions to compute thermal rate constants using the SCTST. See Section 6.3 of this User Manual for a description.



## Data File Format

(For definitions of terms, see Technical Note B.9 and Nguyen et al.<sup>16</sup>)

**Line 1:** Name (transition state name;  $\leq 10$  characters)

**Line 2:** Title 1 ( $\leq 100$  characters)

**Line 3:** Title 2 ( $\leq 100$  characters)

**Line 4:** ns (number of orthogonal vibrational modes, not including the reaction coordinate), NY (number of Y matrix elements), NZ (number of Z matrix elements), WW (a keyword to designate frequencies as  $\omega_e$  or  $\omega^0$ )

WW = We for  $\omega$

WW = Wf for fundamental vibrations (0-1 transitions)

WW = W0 for  $\omega^0$  [note: 0 is a zero]

(The distinction between  $\omega$  and  $\omega^0$  is explained by eqs. (II,267) through (II,269) of Herzberg<sup>8</sup>. The computer code carries out the conversion between them.)

**Lines 5+ (5 to 4+ns):** wa(i) [i = 1 , ns] vibrational frequencies ( $\text{cm}^{-1}$ )

**Line 6 (5+ns):** KEYWORD for reading the X anharmonicity matrix:

= lower (for reading lower half of matrix, plus the diagonal)

= upper (for reading upper half of matrix, plus the diagonal)

**Lines 7+ (6+ns to 5+2ns):** xa(k,j) anharmonicities ( $\text{cm}^{-1}$ ) in upper or lower halves (plus the diagonal) of the ns $\times$ ns anharmonicity matrix.

**Line 8: Nsep , Vrot**

Nsep = number of active separable modes (as in Line 5 of Densum) to be convoluted with the ns non-separable modes entered above)

Vrot = KEYWORD for specifying units for internal and external rotations, except for hindered rotors of type **hrd** (see special instructions in the chapter on DenSum for type hrd). Entries in upper or lower case:

Vrot Keywords:

'AMUA': for moments of inertia input with units of amu  $\text{\AA}^2$ .

'GMCM': for moments of inertia input with units of g  $\text{cm}^2$ .

'CM-1': for rotational constant input with units of  $\text{cm}^{-1}$ .

'MHZ': for rotational constant input with MHz.

'GHZ': for rotational constant input with GHz.

**Line 9:** input data for the separable modes (classical or quantum free rotors, hindered rotors of several types, and Morse oscillators). The various types are defined and appropriate input format are described in Chapter 3.

**Line 10:** Egrain1, imax1, lsize, Emax2, KEYWORD1

Egrain1 = energy grain ( $\text{cm}^{-1}$ )  
imax1 = number of array elements in lower part of the Double Array (see MultiWell User Manual)  
lsize = total number elements in the Double Array.  
Emax2 = upper energy limit  
KEYWORD1 = controls number of stochastic trials (note that execution time is proportional to the number of trials):  
Fair: low statistical accuracy ( $10^2$  trials per energy grain)  
Good: good statistical accuracy ( $10^3$  trials per energy grain).  
Better: better statistical accuracy ( $10^4$  trials per energy grain)  
Best: best statistical accuracy ( $10^5$  trials per energy grain)  
Extra: best statistical accuracy ( $10^6$  trials per energy grain, but no more than  $2 \times 10^9$  total trials for all energy grains)

**Line 11:** KEYWORD "checkpoint", <chekname>

If "chekpoint" = "chekstart" (**Note the spelling!**), then the new calculation starts by reading a pre-existing checkpoint file. Otherwise, the full calculation is carried out, including generation of a new checkpoint file. All data from Line 2 through Line 10, inclusive, must be identical to the data file used to create the pre-existing checkpoint file in the first place.

<chekname> = filename ( $\leq 15$  characters) for the checkpoint file to be generated, or read as input. The filename must contain the suffix, ".chk" and may be different from the name entered on Line 1.

**Line 12:** KEYWORD3

KEYWORD3 = controls number of samples for the semi-classical calculation (typically the same as KEYWORD1). The samples are used to compute average quantities employed by the theory.

Fair: low accuracy ( $10^2$  samples per energy grain)  
Good: good accuracy ( $10^3$  samples per energy grain).  
Better: better accuracy ( $10^4$  samples per energy grain)  
Best: best accuracy ( $10^5$  samples per energy grain)  
Extra: best accuracy ( $10^6$  samples per energy grain, but no more than  $2 \times 10^9$  total samples for all energy grains)

**Line 13:** KEYWORD "VPTx"

**New Feature in 2017; this line must be added to older files that are run using 2017 version, or newer.**

VPTx = controls corrections to the basic SCTST/VP2.

VPT2: no correction.

VPT4A: **Recommended.** VPT4 correction (Eq. 42 in the paper by Stanton.<sup>17</sup>)

VPT4B: VPT4 correction (Eq. 37 in the paper by Stanton.<sup>17</sup>)

**Line 14:** Vf, Vr, Eunits

Barrier heights (including zero point energy corrections) in forward (Vf) and reverse (Vr) directions, and their energy units (Eunits: kcal, kJou, or  $\text{cm}^{-1}$ )

**Line 15:** vimag, Xff

Imaginary frequency and the diagonal anharmonicity coefficient for the reaction coordinate (units of  $\text{cm}^{-1}$ )

**Line 16:** Xkf

Off-diagonal anharmonicity coefficients (units of  $\text{cm}^{-1}$ ) multiplied by  $i = (-1)^{1/2}$ : ns of them, in order. Since the  $X_{k,F}$  coefficients are pure imaginary, they can be written  $X_{k,F} = i\tilde{X}_{k,F}$ , where  $\tilde{X}_{k,F}$  is a real number. The quantities to be input are  $i \cdot X_{k,F} = i \cdot i\tilde{X}_{k,F} = -\tilde{X}_{k,F}$ , which is in the same format as GAUSSIAN output. In contrast, CFOUR output gives  $X_{k,F}$  expressed as  $\tilde{X}_{k,F}$  followed by the symbol "i", i.e. " $\tilde{X}_{k,F}$ .i". These conventions are equivalent, but it is easy to make a sign error. Be careful!

**Notes**

1. Energies are relative to the zero point energy.
2. In second order vibrational perturbation theory (VPT2), the zero point energy (ZPE) includes contributions from the harmonic frequencies, the anharmonicities, but it does NOT include the harmonic imaginary frequency or any of the anharmonicity coefficients involving the imaginary frequency. The ZPE also includes an additional term denoted  $G_0$  (see Eq. 9 in Appendix B.9),<sup>13,19</sup> which cancels-out in spectroscopy applications but must be included for every species in high-accuracy thermochemistry and kinetics calculations. The value of  $G_0$  must be computed by electronic structure programs employing VPT2 (e.g. GAUSSIAN and CFOUR), and is not computed by MultiWell itself. For *ab initio* kinetics calculations involving chemical species and transition states with large rotational constants,  $G_0$  may be significant, but it is very small for molecules with small rotational constants. For high accuracy *ab initio* kinetics calculations (e.g. Ref. <sup>16</sup>,  $G_0$  can be included manually by modifying the reaction critical energy (which already includes zero point energy corrections).
3. Be careful when using Gaussian! The Gaussian log file has two sections related to vibrations. The first section is for the usual vibrational analysis to obtain harmonic frequencies. These frequencies are listed from lowest to highest. The second section is for anharmonicities. In the second section, the harmonic frequencies are listed again (along with the fundamental frequencies), but the ordering may not be the same as in the first section. The input for the codes distributed in MultiWell will accept the frequencies in any order, but the ordering of the harmonic frequencies must be consistent with the ordering used for the anharmonicities. For consistency, the Gaussian user must be sure to use the ordering of the harmonic frequencies as listed in association with the anharmonicities in the Gaussian log file.

**8.4 Program parsctst**

parsctst: parallel and improved version of sctst (in a future release, sctst will no longer be supported.)

Program Authors:

parsctst: C. Aieta, F. Gabas, and M. Ceotto

sctst: **T. L. Nguyen and J. R. Barker**  
Contact: **Michele Ceotto**: michele.ceotto@unimi.it

This program is an implementation<sup>19</sup> of the semi-classical transition state theory (SCTST) formulated by W. H. Miller and coworkers.<sup>10,12-14</sup> Our implementation is based on the Wang and Landau algorithm<sup>25</sup> and the density of states algorithm of Basire et al.,<sup>3</sup> as refined by Nguyen and Barker.<sup>17</sup> The literature references should be consulted for further details about the theory, its usefulness, and applications. The literature should be cited as described at the Preface of this User Manual.

The SCTST is a powerful method, since it can be used for computing both thermal (i.e. canonical  $k(T)$ ) and microcanonical (i.e.  $k(E)$ ) rate constants, which are essential for master equation calculations. Unlike ordinary transition state theory, the SCTST is fully non-separable: all of the degrees of freedom may be coupled and it is not necessary to assume that the reaction coordinate is separable from the others. It also accounts naturally for zero point energy and for quantum mechanical tunneling along the curved reaction path in hyperdimensional space. In test cases, it is highly accurate.<sup>18</sup>

`paradensum` is a parallel code<sup>2</sup> that can exploit not only single but also multiple core architectures. In this way the computation of the density of states is significantly accelerated when considering high dimensionality systems. The parallelization strategy is to divide the energy range into energy “windows” and set the calculations of  $G(E_i)$  for each window on a single processor. This strategy is dictated by the observation that less random sampling events and reduced computational effort is needed for Monte Carlo to converge in a restricted energy range.

The number of processors is given by the windowing choice and, by default, all windows have the same width. This setting can be changed by modifying the appropriate keyword in the input file. If the computational time spent by each window to reach the flatness criterion is unbalanced, the code prints a warning in the `Windows_info.txt` output file. Then, the user can decide to halve the width of the first two or the last two windows.

Since the Wang-Landau density of states is notoriously biased at the edges of small energy windows, we always keep a percentage of overlap between neighbor windows. This is also necessary for the normalization of the  $G(E_i)$  obtained in each window to give the complete function on the whole energy domain. The code supports the possibility to run serially multiple walkers in each energy window. This feature improves the statistics of sampling in each window but does not have any impact on the speedup. To run the code the user has to supply the number of processors that is equal to the number of windows and a percentage of overlap between them as input parameters. When the number of processors (windows) is set to unity, then `paradensum` will run in serial mode (i.e. it can run on a single cpu or core). The set up of the input file for these parameters is described below. For a full description of the `parstst` implementation, see the paper by Aieta, Gabas and Ceotto.<sup>2</sup>

The input is similar to that for programs `bdens` (Section 8.1), and `paradensum` (Section 8.2) but it also includes the imaginary frequency and the anharmonicity coefficients associated with the reaction coordinate. The imaginary frequency and the off-diagonal anharmonicity coefficients associated with the reaction coordinate are pure imaginary numbers; the diagonal anharmonicity for the reaction coordinate is a pure real number. These facts affect how the parameters are specified in the input data file `parctst.dat`. In addition, SCTST as formulated by Miller and coworkers is based on second order vibrational perturbation theory (VPT2).<sup>15</sup>

Recently, Stanton investigated SCTST based on VPT4 (fourth order perturbation theory) and arrived as a simple correction that is appropriate for symmetrical Eckart barriers.<sup>20</sup> To the extent that the actual energy barrier resembles an Eckart barrier, this VPT4 correction improves the performance of SCTST/VPT2. Stanton suggested two slightly different versions of this correction, but the difference between them is small. In program `parctst`, either of the two corrections (or neither) can be selected by selecting the appropriate key word.

The output files are analogous to the output files from programs `paradensum`, `bdens` and `densum`. The general output file `parctst.out` summarizes the input and gives "sums" and "densities" of states for the full energy range specified. These "sums" and "densities" actually correspond to the cumulative reaction probability<sup>10,12-14</sup> (CRP) and the corresponding energy derivative, which are identified with the sums and densities in the absence of quantum tunneling. The second output file takes the name of the transition state with ".crp" added: `<name>.crp`, just as in programs `densum`, `bdens` and `paradensum`. These files are formatted for use by the MultiWell master equation code. An output file is also generated that gives the thermal partition function (excluding the translations) for the transition state at a set of 100 fixed temperatures (1 K to 3383 K). This file, named `<name>.qcrp`, is used by program `Thermo` to calculate canonical rate constants (see Section 6.3 of this User Manual for a description of how the file is used by `Thermo`).

### **Running `parctst`**

`Parctst` is a parallel code. To compile and run the code, it is necessary to have previously installed supplementary software. Details are given in Section 1.4.

`sctst` has been designed to run using a "checkpoint file" (named `<chekname>`), which is generated after the density of states of the fully coupled vibrations have been calculated (the most time-consuming part of the calculation). The next part of the calculation convolutes the separable degrees of freedom, if any are specified. The separable degrees of freedom may include free or hindered rotors, harmonic vibrations, etc. In particular, the 1-D external rotation (the K-rotor) and possibly also the 2-D external rotational degrees of freedom may be specified, depending on the application. If desired, the densities of states may be recalculated using various combinations of separable degrees of freedom, but retaining the same set of fully coupled vibrations. Repetitive calculations like these can be restarted using the checkpoint file, which saves considerable computer time. Note that when using the checkpoint file, it is not necessary to run the code in parallel mode.

Another reason for running repetitive calculations by starting with the checkpoint file is because whenever the reaction threshold energy is changed, the SCTST requires that the cumulative reaction probability be recalculated.<sup>19</sup> Adjusting reaction barriers to fit experimental data may require multiple repetitive calculations, and restarting by using the checkpoint file will reduce the computer time by an order of magnitude or more.

The input data file `parctst.dat` includes molecular parameters for computing the cumulative reaction probability, as well as parallel execution parameters. Directory `multiwell-<version>` is assumed to reside in your Home directory. Execution of `parctst` is carried out within the directory that contains the input data file `parctst.dat`. All of the output files are automatically placed in the directory that contains `parctst.dat`.

In summary, five output files are generated by `parctst`: `parctst.out`, `<name>.crp`, `<chekname>` (which must include the `.chk` suffix), and `<name>.qcrp`, and `Windows_info.txt`. The first file (`parctst.out`) is a standard output file, which summarizes all

input and output. The second file (<chlname>), which takes a chemical species name as part of the file name, is the checkpoint file, which is an important time-saving measure for subsequent runs using the same vibrational parameters, as described in the preceding paragraph. The third file (<name>.crp), tabulates the cumulative reaction probability (CRP) and its energy derivative (analogous to sums and densities of states), formatted as double arrays for use as input for the MultiWell master equation code. By using this input file, master equation calculations can be carried out with microcanonical rate constants (i.e.  $k(E)$ ) computed by including the fully-coupled vibrations. The fourth file (<name>.qcrp) is formatted as a supplementary input file for program Thermo; it tabulates the partition function for the CRP and other thermodynamic properties of the coupled vibrational modes at a set of fixed temperatures from 50 K to >3000 K. Thermo can utilize these partition functions to compute thermal rate constants using the SCTST. See Section 6.3 of this User Manual for a description.

The file Windows\_info.txt contains details about windows division, i.e. the total number of energy grains, the number of energy grains in each window after the overlap has been added, and the low and high energy boundaries of each window.

Users may also select a supplementary writing option, which generates a file called Rank<N>.txt for each parallel process (here, <N> is an integer number that identifies the process). These files report all details about the Wang-Landau algorithm executed by each parallel process. Users may freely enable or disable writing the Rank<N>.txt files, which are intended as a user check on parallel execution.

### ***Format for parsctst.dat Input File***

(For definitions of terms, see Technical Note B.9 and Nguyen et al.[19](#))

**Line 1:** Name (transition state name;  $\leq 10$  characters)

**Line 2:** Title 1 ( $\leq 100$  characters)

**Line 3:** Title 2 ( $\leq 100$  characters)

**Line 4:** ns (number of orthogonal vibrational modes, not including the reaction coordinate), NY (number of **Y** matrix elements), NZ (number of **Z** matrix elements), WW (a keyword to designate frequencies as  $\omega_e$  or  $\omega^0$ )

WW = We for  $\omega$

WW = Wf for fundamental vibrations (0-1 transitions)

WW = W0 for  $\omega^0$  [note: 0 is a zero]

(The distinction between  $\omega$  and  $\omega^0$  is explained by eqs. (II,267) through (II,269) of Herzberg [11](#).)

The computer code carries out the conversion between them.)

**Lines 5+ (5 to 4+ns):** wa(i) [i = 1 , ns] vibrational frequencies ( $\text{cm}^{-1}$ )

**Line 6 (5+ns):** KEYWORD for reading the **X** anharmonicity matrix:

= lower (for reading lower half of matrix, plus the diagonal)

= upper (for reading upper half of matrix, plus the diagonal)

**Lines 7+ (6+ns to 5+2ns):** xa(k,j) anharmonicities ( $\text{cm}^{-1}$ ) in upper or lower halves (plus the diagonal) of the ns×ns anharmonicity matrix.

**Line 8: Nsep , Vrot**

Nsep = number of active separable modes (as in Line 5 of Densum) to be convoluted with the ns non-separable modes entered above)

Vrot = KEYWORD for specifying units for internal and external rotations, except for hindered rotors of type **hrd** (see special instructions in the chapter on DenSum for type hrd). Entries in upper or lower case:

Vrot Keywords:

'AMUA': for moments of inertia input with units of  $\text{amu \AA}^2$ .

'GMCM': for moments of inertia input with units of  $\text{g cm}^2$ .

'CM-1': for rotational constant input with units of  $\text{cm}^{-1}$ .

'MHZ': for rotational constant input with MHz.

'GHZ': for rotational constant input with GHz.

**Line 9:** input data for the separable modes (classical or quantum free rotors, hindered rotors of several types, and Morse oscillators). The various types are defined and appropriate input format are described in Chapter 3.

**Line 10: Egrain1, imax1, lsize, Emax2**

Egrain1 = energy grain ( $\text{cm}^{-1}$ )

imax1 = number of array elements in lower part of the Double Array (see MultiWell User Manual)

lsize = total number elements in the Double Array.

Emax2 = upper energy limit

**Line 11: KEYWORD "checkpoint", <chekname>**

If "checkpoint" = "chekstart" (**Note the spelling!**), then the new calculation starts by reading a pre-existing checkpoint file. Otherwise, the full calculation is carried out, including generation of a new checkpoint file. All data from Line 2 through Line 10, inclusive, must be identical to the data file used to create the pre-existing checkpoint file in the first place.

<chekname> = filename ( $\leq 15$  characters) for the checkpoint file to be generated, or read as input. The filename must contain the suffix, ".chk" and may be different from the name entered on Line 1.

**Line 12: KEYWORD "VPTx"**

**New Feature in 2017; this line must be added to older files that are run using 2017 version, or newer.**

VPTx = controls corrections to the basic SCTST/VP2.

VPT2: no correction.

VPT4A: **Recommended.** VPT4 correction (Eq. 42 in the paper by Stanton.<sup>20</sup>)

VPT4B: VPT4 correction (Eq. 37 in the paper by Stanton.<sup>20</sup>)

**Line 14: Vf , Vr , Eunits**

Barrier heights (including zero point energy corrections) in forward (Vf) and reverse (Vr) directions, and their energy units (Eunits: kcal, kjou, or cm-1)

**Line 15:** vimag, Xff

Imaginary frequency and the diagonal anharmonicity coefficient for the reaction coordinate (units of cm<sup>-1</sup>)

**Line 16:** Xkf

Off-diagonal anharmonicity coefficients (units of cm<sup>-1</sup>) multiplied by  $i = (-1)^{1/2}$ : ns of them, in order. Since the  $X_{k,F}$  coefficients are pure imaginary, they can be written

$X_{k,F} = i\tilde{X}_{k,F}$ , where  $\tilde{X}_{k,F}$  is a real number. The quantities to be input are  $i \cdot X_{k,F} = i \cdot i\tilde{X}_{k,F} = -\tilde{X}_{k,F}$ , which is in the same format as GAUSSIAN output. In contrast, CFOUR output gives  $X_{k,F}$  expressed as  $\tilde{X}_{k,F}$  followed by the symbol "i", i.e. " $\tilde{X}_{k,F}i$ ". These conventions are equivalent, but it is easy to make a sign error. Be careful!

**Line 17:** (Blank line)

**Line 18:** nwalkers = number of independent random walks in each window; integer.

**Line 19:** perc\_wind\_overlap = percentage of overlap between neighboring windows; real.

**Line 20:** flatness = flatness criterion for halting the Wang-Landau algorithm: a real number between 0 and 1. The closer to unity, the more accurate is the density of states.

**Line 21:** writing (writing out Rank<N>.txt files)

= 1 (Writing enabled.)

= 0 (Writing disabled.)

**Line 22:** seed\_modifier = an integer number which is added to the default random number generator seed in order to get a new random number chain. For usual applications of the code it is set to 0.

**Line 23:** windbal\_key = this keyword sets the windows width.

= "const" (default) windows width is equal for all windows.

= "low" the first two windows are smaller than the others.

= "high" the last two windows are smaller than the others.

## Notes

1. Energies are relative to the zero point energy.



2. In second order vibrational perturbation theory (VPT2), the zero point energy (ZPE) includes contributions from the harmonic frequencies, the anharmonicities, but it does NOT include the harmonic imaginary frequency or any of the anharmonicity coefficients involving the imaginary frequency. The ZPE also includes an additional term denoted  $G_0$  (see Eq. 9 in Appendix B.9),<sup>16,23</sup> which cancels-out in spectroscopy applications but must be included for every species in high-accuracy thermochemistry and kinetics calculations. The value of  $G_0$  must be computed by electronic structure programs employing VPT2 (e.g. GAUSSIAN and CFOUR), and is not computed by MultiWell itself. For *ab initio* kinetics calculations involving chemical species and transition states with large rotational constants,  $G_0$  may be significant, but it is very small for molecules with small rotational constants. For high accuracy *ab initio* kinetics calculations (e.g. Ref. [19](#),  $G_0$  can be included manually by modifying the reaction critical energy (which already includes zero point energy corrections).

3. Be careful when using Gaussian! The Gaussian log file has two sections related to vibrations. The first section is for the usual vibrational analysis to obtain harmonic frequencies. These frequencies are listed from lowest to highest. The second section is for anharmonicities. In the second section, the harmonic frequencies are listed again (along with the fundamental frequencies), but the ordering may not be the same as in the first section. The input for the codes distributed in MultiWell will accept the frequencies in any order, but the ordering of the harmonic frequencies must be consistent with the ordering used for the anharmonicities. For consistency, the Gaussian user must be sure to use the ordering of the harmonic frequencies as listed in association with the anharmonicities in the Gaussian log file.

## References

- (1) Aieta, C.; Gabas, F.; Ceotto, M. An Efficient Computational Approach for the Calculation of the Vibrational Density of States. *J. Phys. Chem. A*. **2016**, DOI: 10.1021/acs.jpca.1025b12364; DOI: 10.1021/acs.jpca.5b12364.
- (2) Aieta, C.; Gabas, F.; Ceotto, M. Parallel Implementation of Semiclassical Transition State Theory. *J. Chem. Theory Comput.* **2019**, *15*, 2143-2153; DOI: 10.1021/acs.jctc.8b01286.
- (3) Barker, J. R. Sums of Quantum States for Non-Separable Degrees of Freedom: Multidimensional Monte Carlo Integration. *J. Phys. Chem.* **1987**, *91*, 3849-3854.
- (4) Basire, M.; Parneix, P.; Calvo, F. Quantum anharmonic densities of states using the Wang-Landau method. *J. Chem. Phys.* **2008**, *129*, 081101.
- (5) Beyer, T.; Swinehart, D. F. Number of multiply-restricted partitions. *Comm. Assoc. Comput. Machines* **1973**, *16*, 379.
- (6) Cané, E.; Miani, A.; Trombetti, A. Anharmonic Force Fields of Naphthalene-h8 and Naphthalene-d8. *J. Phys. Chem. A*. **2007**, *111*, 8218-8222.
- (7) Hernandez, R.; Miller, W. H. Semiclassical transition state theory. *Chem. Phys. Lett.* **1993**, *214*, 129-136.
- (8) Herzberg, G. *Molecular Spectra and Molecular Structure. II. Infrared and Raman Spectra*, 2 ed.; Van Nostrand Reinhold Co.: Cincinnati, 1945.
- (9) Miller, J. H. The kinetics of polynuclear aromatic hydrocarbon agglomeration in flames. *Proc. Combust. Inst.* **1990**, *23*.

- (10) Miller, W. H. Semiclassical limit of quantum mechanical transition state theory for nonseparable systems. *J. Chem. Phys.* **1975**, *62*, 1899-1906.
- (11) Miller, W. H. Semi-Classical Theory for Non-separable Systems: Construction of "Good" Action-Angle Variables for Reaction Rate Constants. *Faraday Discuss. Chem. Soc.* **1977**, *62*, 40-46.
- (12) Mills, I. M. *Modern Spectroscopy; Modern Research*; Academic Press: New York, NY, 1972.
- (13) Mills, I. M. Vibration-Rotation Structure in Asymmetric- and Symmetric-Top Molecules. In *Molecular Spectroscopy: Modern Research*; Rao, K. N., Mathews, C. W., Eds.; Academic Press: New York, 1972; Vol. 1; pp 115-140.
- (14) Nguyen, T. L.; Barker, J. R. Sums and Densities of Fully-Coupled Anharmonic Vibrational States: A Comparison of Three Practical Methods. *J. Phys. Chem. A* **2010**, *114*, 3718–3730.
- (15) Nguyen, T. L.; Barker, J. R.; Stanton, J. F. Atmospheric Reaction Rate Constants and Kinetic Isotope Effects Computed Using the HEAT Protocol and Semi-Classical Transition State Theory. In *Advances in Atmospheric Chemistry*; Barker, J. R., Steiner, A. L., Wallington, T. J., Eds.; World Scientific: Singapore, 2017; Vol. 1; pp 403-492.
- (16) Nguyen, T. L.; Stanton, J. F.; Barker, J. R. A Practical Implementation of Semi-Classical Transition State Theory for Polyatomics. *Chem. Phys. Letters* **2010**, *499*, 9-15.
- (17) Stanton, J. F. Semiclassical Transition-State Theory Based on Fourth-Order Vibrational Perturbation Theory: The Symmetrical Eckart Barrier. *J. Phys. Chem. Lett.* **2016**, *7*, 2708-2713.
- (18) Stein, S. E.; Rabinovitch, B. S. Accurate evaluation of internal energy level sums and densities including anharmonic oscillators and hindered rotors. *J. Chem. Phys.* **1973**, *58*, 2438-2445.
- (19) Truhlar, D. G.; Isaacson, A. D. Simple perturbation theory estimates of equilibrium constants from force fields. *J. Chem. Phys.* **1990**, *94*, 357-359.
- (20) Wang, F.; Landau, D. P. Determining the density of states for classical statistical models: A random walk algorithm to produce a fat histogram. *Phys. Rev. E* **2001**, *64*, 056101-056101.
- (21) Wang, F.; Landau, D. P. Efficient, Multiple-Range Random Walk Algorithm to Calculate the Density of States. *Phys. Rev. Letters* **2001**, *86*, 2050-2053.

## 9. lamm: Effective Mass for Internal Rotation

lamm: Large Amplitude Motion Mass  
Program Author: **Thanh Lam Nguyen**  
Contact: LNGUYEN@cm.utexas.edu

### 9.1 Introduction

This program is a tool for obtaining the effective mass (as a function of angle or distance) for large amplitude motions, such as internal rotation. The output is used as part of the input data file needed for computing sums and densities of states (using program DenSum) and partition functions (program Thermo).

Program lamm uses the ro-vibrational G matrix-based algorithm described in the papers of Harthcock et al.<sup>3,4</sup> and others to compute the effective reduced mass for one-dimensional torsions and other large amplitude motions, which are assumed to be separable from the other molecular degrees of freedom.

Molecular geometries can be computed at discrete values of  $\chi$  by using any of the many available quantum chemistry codes, such as Gaussian,<sup>2</sup> Molpro,<sup>6</sup> CFour,<sup>5</sup> etc. Program lamm is intended to help users compute the torsion rotational constant  $B_{hr}(\chi)$  and the potential energy  $V(\chi)$ , based on the output from the quantum chemistry program.

For hindered internal rotation, lamm employs Cartesian coordinates obtained from quantum chemical calculations carried out as a function of the dihedral angle  $\chi$  ( $0 \leq \chi < 2\pi$ ). The output of lamm consists of the torsion rotational constant function  $B_{hr}(\chi)$  (or the corresponding moment of inertia function  $I(\chi)$ ) tabulated as a function of  $\chi$ . The potential energy can also be obtained from the quantum chemistry calculations and expressed as a function of  $\chi$ . These functions must then be fitted by the user to any one of the several truncated Fourier series that are recognized by DenSum and Thermo (see the MultiWell User Manual). The Fourier coefficients are used by programs DenSum and Thermo to solve the Schrödinger equation for the energy eigenstates (see Appendix B.8), which are needed to compute densities of states and partition functions, respectively.

A script is provided to assist users in extracting the required information from Gaussian output files (see Section 9.7).

### 9.2 Compiling and Running lamm

The source directory for lamm resides in the MultiWell src directory. The program is compiled on *Linux* by entering the MultiWell directory and typing “make” (omit the quotation marks), followed by a carriage return. The executable file is stored in the MultiWell bin directory. The default compiler is gfortran. The compiler can be changed by revising lines in file src/lamm/Makefile. To remove old object files and executables, enter directory src/lamm and type “make clean”, followed by a carriage return.

To execute the compiled program, enter the directory that contains the lamm data file (“lamm.dat”) and then type ~/multiwell-<version>/bin/lamm, where <version> refers to the multiwell version number (e.g. “2010.0”). This command executes the binary executable file. The output file (“lamm.out”) is automatically placed in the directory that contains lamm.dat.

### 9.3 Notes and Limits

For the current version of the `lamm` program, Cartesian coordinates of optimized geometries must be obtained by constrained optimizations. When using Gaussian, the keyword “NOSYM” and/or OPT=“Z-Matrix”, or the equivalent must be specified.

The `lamm` program does not automatically identify the molecular symmetry; it always assumes that the molecule has no symmetry ( $C_1$  symmetry). Therefore the effective reduced moment of inertia will be computed only for the number of optimized geometries that are input.

Since the derivatives of the nuclear positions with respect to the torsional coordinate are computed by central finite differences, a fairly small torsional angle step-size must be used in order to achieve numerical accuracy. In our experience, a step-size of  $\leq 10^\circ$  is a good choice for most purposes.

In addition to torsional motions, the `lamm` program can be used for computing the effective mass for other separable large-amplitude vibrational motions. Specific implementations will be added in the future.

Users may be interested in program `I_Eckart`, which was coded in MATLAB by Wong, Thom and Field<sup>7</sup>. We would like to thank Dr. Wong and Prof. Field for useful discussions and for providing a copy of their program, which we used for benchmarks.

### 9.4 Data File Format

**Line 1:** Name of molecule ( $\leq 100$  characters)

**Line 2:** Title ( $\leq 100$  characters)

**Line 3:**  $N_{\text{atom}}$  (number of atoms in molecule)

**Line 4:**  $A_{\text{min}}$  (lower limit of torsion angle in degrees),  $M$  (number of optimized geometries),  $\text{DELA}$  (step-size of torsion angle in degrees).

**Line 5+ (lines 5 to 4 + N):** list of atomic masses (in amu)

**Line 6+ (lines 5 + N to 4 + N + N\*M):** list of Cartesian coordinates (in Angstroms) for  $M$  optimized geometries as a function of the torsion dihedral angle.

**Line 7 (lines 5 + N + N\*M):** comment line ( $\leq 100$  characters)

**Line 8+ (lines 6 + N + N\*M to 5 + N + N\*M + M):** list of torsional angle (in degrees) and relative energies (in  $\text{cm}^{-1}$ ).

## 9.5 Example Data File

H2O2

Calculated at 6-311G\*\* level of theory

4 ! Number of atoms in the molecule

0, 36, 10 ! Minimum angle, No. of optimized geometries and Step-size (in degrees)

1. ! list of atomic mass (in amu)

16.

16.

1.

0.000000 0.000000 0.000000 !list of X, Y, Z cartesian coordinate

0.000000 0.000000 0.966404

1.412522 0.000000 1.340839

1.891238 0.000000 0.501335

0.000000 0.000000 0.000000

0.000000 0.000000 0.966493

1.412776 0.000000 1.339296

1.886024 0.162275 0.512367

And so on ....

## 9.6 Example Output:

H2O2

Calculated at 6-311G\*\* level of theory

WARNING: The zero of the relative energy is arbitrary minimum

INDEX	ANG(DEG)	ANG(RAD)	E(cm-1)	I(amu.A**2)	B(cm-1)
-------	----------	----------	---------	-------------	---------

10.0	0.000000	2980.5	0.387	43.6	
2	10.0	0.174533	2913.6	0.390	43.3
3	20.0	0.349066	2720.4	0.393	42.9
4	30.0	0.523599	2421.2	0.396	42.5
5	40.0	0.698132	2047.2	0.400	42.2
6	50.0	0.872665	1635.9	0.403	41.9
7	60.0	1.047198	1224.6	0.405	41.6
8	70.0	1.221730	846.6	0.407	41.4
9	80.0	1.396263	527.1	0.410	41.2
10	90.0	1.570796	282.2	0.412	40.9
11	100.0	1.745329	116.9	0.415	40.6
12	110.0	1.919862	27.0	0.418	40.4
13	120.0	2.0943950.0	0.420	40.2	
14	130.0	2.268928	19.3	0.421	40.0
15	140.0	2.443461	65.6	0.423	39.9
16	150.0	2.617994	122.1	0.423	39.8
17	160.0	2.792527	173.9	0.423	39.8
18	170.0	2.967060	209.5	0.423	39.8
19	180.0	3.141593	222.3	0.424	39.8
20	190.0	3.316126	209.5	0.423	39.8
21	200.0	3.490659	173.9	0.423	39.8
22	210.0	3.665191	122.1	0.423	39.8
23	220.0	3.839724	65.6	0.423	39.9

24	230.0	4.014257	19.3	0.421	40.0
25	240.0	4.1887900.0	0.420	40.2	
26	250.0	4.363323	27.0	0.418	40.4
27	260.0	4.537856	116.9	0.415	40.6
28	270.0	4.712389	282.2	0.412	40.9
29	280.0	4.886922	527.1	0.410	41.2
30	290.0	5.061455	846.6	0.407	41.4
31	300.0	5.235988	1224.6	0.405	41.6
32	310.0	5.410521	1635.9	0.403	41.9
33	320.0	5.585054	2047.2	0.400	42.2
34	330.0	5.759587	2421.2	0.396	42.5
35	340.0	5.934119	2720.4	0.393	42.9
36	350.0	6.108652	2913.6	0.390	43.3
37	360.0	6.283185	2980.5	0.387	43.6

## 9.7 gauss2lamm: A script for generating lamm.dat

The shell script **gauss2lamm.sh** is designed to create data files for program **lamm** (see Chapter 8), which computes effective mass for large amplitude motions, such as hindered internal rotation. The script is located in directory `multiwell-<version>/bin`, where `<version>` refers to the version number (e.g. "2010.0"). This script reads the input orientations or Z-matrix of optimized geometries and corresponding energies as a function of the appropriate coordinate (i.e. the torsion dihedral angle) from "`____.log`" or "`____.out`" output files produced by GAUSSIAN-03<sup>1</sup> or GAUSSIAN-09<sup>2</sup> software.

To execute the script, enter the directory that contains the Gaussian output file and then type `~/multiwell-<version>/bin/gauss2lamm.sh`. This command goes to the directory `multiwell-<version>/bin` (which is assumed to reside in your Home directory) and executes the script file `gauss2lamm.sh`, which stored there.

The script generates `lamm.dat` in the Gaussian output file directory.

The script prompts the user to input the Gaussian output file name, number of atoms in the molecule and minimum angle, no. of points and stepsize (in degrees) used in the calculation. First it verifies whether the user has used the keyword "NOSYM and/or Z-Matrix" in Gaussian output. If the keyword is found the script writes `lamm.dat` containing geometry and energy (in  $\text{cm}^{-1}$ ) information. The energy is tabulated as a function of angle (in degrees). The zero of relative energy is arbitrary minimum. If the keyword is not found in the Gaussian output, the script prompts the user to redo the Gaussian calculation using the keyword "NOSYM and/or Z-Matrix".

It is important to note that the `lamm.dat` file created automatically from Gaussian output needs manual changes. Line 5+ (lines 5 to 4+N) in the `lamm.dat` created using the script is atomic number, where N is number of atoms in the molecule. This has to be replaced with corresponding atomic masses (amu units) for subsequent use by program **lamm**.

An example Gaussian output file `lamm.log` is available in the examples directory and procedure to execute `gauss2lamm` is shown below.

```
$ ../../bin/gauss2lamm.sh

Enter Gaussian Output Filename
lamm.log
```

Keyword NOSYM found in the output

Enter total number of atoms in the molecule

5

Enter MIN angle, No. of Points and Stepsize in degrees used  
in the calculation

0 36 10

Proceeding to collect data from lamm.log

Lowest energy in the surface scan: -740.457504043 hartrees

## References

- (1) Frisch, M. J.; Trucks, G. W.; Schlegel, H. B.; Scuseria, G. E.; Robb, M. A.; Cheeseman, J. R.; Montgomery, J. A., Jr.; Vreven, T.; Kudin, K. N.; Burant, J. C.; Millam, J. M.; Iyengar, S. S.; Tomasi, J.; Barone, V.; Mennucci, B.; Cossi, M.; Scalmani, G.; Rega, N.; Petersson, G. A.; Nakatsuji, H.; Hada, M.; Ehara, M.; Toyota, K.; Fukuda, R.; Hasegawa, J.; Ishida, M.; Nakajima, T.; Honda, Y.; Kitao, O.; Nakai, H.; Klene, M.; Li, X.; Knox, J. E.; Hratchian, H. P.; Cross, J. B.; Bakken, V.; Adamo, C.; Jaramillo, J.; Gomperts, R.; Stratmann, R. E.; Yazyev, O.; Austin, A. J.; Cammi, R.; Pomelli, C.; Ochterski, J. W.; Ayala, P. Y.; Morokuma, K.; Voth, G. A.; Salvador, P.; Dannenberg, J. J.; Zakrzewski, V. G.; Dapprich, S.; Daniels, A. D.; Strain, M. C.; Farkas, O.; Malick, D. K.; Rabuck, A. D.; Raghavachari, K.; Foresman, J. B.; Ortiz, J. V.; Cui, Q.; Baboul, A. G.; Clifford, S.; Cioslowski, J.; Stefanov, B. B.; Liu, G.; Liashenko, A.; Piskorz, P.; Komaromi, I.; Martin, R. L.; Fox, D. J.; Keith, T.; Al-Laham, M. A.; Peng, C. Y.; Nanayakkara, A.; Challacombe, M.; Gill, P. M. W.; Johnson, B.; Chen, W.; Wong, M. W.; Gonzalez, C.; Pople, J. A. Gaussian 03, Revision C.02; Gaussian, Inc.: Wallingford CT, 2004.
- (2) Frisch, M. J.; Trucks, G. W.; Schlegel, H. B.; Scuseria, G. E.; Robb, M. A.; Cheeseman, J. R.; Scalmani, G.; Barone, V.; Mennucci, B.; Petersson, G. A.; Nakatsuji, H.; Caricato, M.; Li, X.; Hratchian, H. P.; Izmaylov, A. F.; Bloino, J.; Zheng, G.; Sonnenberg, J. L.; Hada, M.; Ehara, M.; Toyota, K.; Fukuda, R.; Hasegawa, J.; Ishida, M.; Nakajima, T.; Honda, Y.; Kitao, O.; Nakai, H.; Vreven, T.; J. A. Montgomery, J.; Peralta, J. E.; Ogliaro, F.; Bearpark, M.; Heyd, J. J.; Brothers, E.; Kudin, K. N.; Staroverov, V. N.; Kobayashi, R.; Normand, J.; Raghavachari, K.; Rendell, A.; Burant, J. C.; Iyengar, S. S.; Tomasi, J.; Cossi, M.; Rega, N.; Millam, J. M.; Klene, M.; Knox, J. E.; Cross, J. B.; Bakken, V.; Adamo, C.; Jaramillo, J.; Gomperts, R.; Stratmann, R. E.; Yazyev, O.; Austin, A. J.; Cammi, R.; Pomelli, C.; Ochterski, J. W.; Martin, R. L.; Morokuma, K.; Zakrzewski, V. G.; Voth, G. A.; Salvador, P.; Dannenberg, J. J.; Dapprich, S.; Daniels, A. D.; Farkas, O.; Foresman, J. B.; Ortiz, J. V.; Cioslowski, J.; Fox, D. J. Gaussian 09, Revision A.1; Revision A.1 ed.; Gaussian, Inc.: Wallingford CT, 2009.
- (3) Harthcock, M. A.; Laane, J. Calculation of kinetic energy terms for the vibrational Hamiltonian: Application to large-amplitude vibrations using one-, two-, and three-dimensional models. *J. Mol. Spectros.* **1982**, *91*, 300-324.
- (4) Harthcock, M. A.; Laane, J. Calculation of two-dimensional vibrational potential energy surfaces utilizing prediagonalized basis sets and Van Vleck perturbation methods. *J. Phys. Chem.* **1985**, *89*, 4231-4240.
- (5) Stanton, J. F.; Gauss, J.; Harding, M. E.; Szalay, P. G.; Auer, w. c. f. A. A.; Bartlett, R. J.; Benedikt, U.; Berger, C.; Bernholdt, D. E.; Bomble, Y. J.; Christiansen, O.; Heckert, M.; Heun, O.; Huber, C.; Jagan, T.-C.; Jonsson, D.; Jusélius, J.; Klein, K.; Lauderdale, W. J.; Matthews, D. A.; Metzroth, T.; O'Neill, D. P.; Price, D. R.; Prochnow, E.; Ruud, K.; Schiffmann, F.; Stopkiewicz, S.; Vázquez, J.; Wang, F.; Watts, J. D. and the integral packages MOLECULE (J. Almlöf and P.R. Taylor); PROPS (P.R. Taylor); ABACUS (T. Helgaker, H.J. Aa. Jensen, P. Jørgensen, and J. Olsen); and ECP routines by A. V. Mitin



- and C. van Wüllen. CFOUR, a quantum chemical program package ([www.cfour.de/](http://www.cfour.de/)), 2009.
- (6) Werner, H.-J.; Knowles, P. J.; Lindh, R.; Manby, F. R.; Schütz, M.; Celani, P.; Korona, T.; Rauhut, G.; Amos, R. D.; Bernhardsson, A.; Berning, A.; Cooper, D. L.; Deegan, M. J. O.; Dobbyn, A. J.; Eckert, F.; Hampel, C.; Hetzer, G.; Lloyd, A. W.; McNicholas, S. J.; W. Meyer, W.; Mura, M. E.; Nicklass, A.; Palmieri, P.; Pitzer, R.; Schumann, U.; Stoll, H.; Stone, A. J.; Tarroni, R.; Thorsteinsson, T. MOLPRO version 2006.1 (a package of *ab initio* programs); version 2006.1 ed.; see <http://www.molpro.net>, 2006.
- (7) Wong, B. M.; Thom, R. L.; Field, R. W. Accurate Inertias for Large-Amplitude Motions: Improvements on Prevailing Approximations. *J. Phys. Chem. A* **2006**, *110*, 7406-7413.

## 10. ktools: *J*-Resolved Variational Transition State Theory

This Chapter was written mostly by Jason A. Sonk.

**For assistance:** Users should submit questions to the "**Multiwell and Chemical Kinetics**" **question and answer forum**, which is described in Chapter 0 of this User Manual.

### 10.1 Introduction

ktools calculates **canonical and angular momentum-resolved (i.e. *J*-resolved) microcanonical variational transition state theory rate constants** from an input supplying reactant and trial transition state parameters from a collection of points along a reaction coordinate representing a unimolecular dissociation, such as shown in Fig. 1.

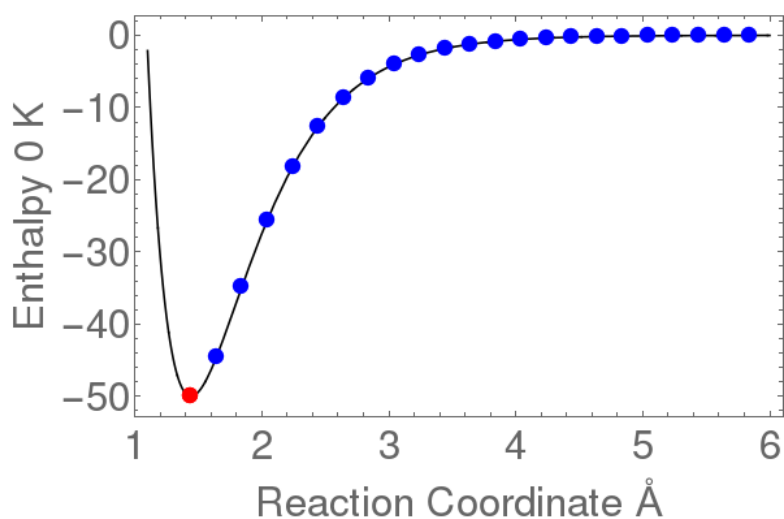


**Figure 1.** Points along a unimolecular dissociation reaction path. The point in red corresponds to the reactant structure while the points in blue are "trial transition states". Units of energy and zero of energy can be designated by the user

Alternatively, if the user supplies parameters only for the reactant(s) and for a single tight transition state (Fig. 2), ktools will calculate rate constants using **both canonical and *J*-resolved microcanonical transition state theories**. If the user supplies the parameters only for a single species then ktools will calculate the **2D sum of states,  $G(E,J)$ , and 2D density of states,  $\rho(E,J)$**  for that species.

When a user intends to use the output from ktools for 1D applications (i.e. for input to an energy-dependent master equation, like multiwell, which is not *J*-resolved), ktools will sum the *J*-resolved quantities over *J* to obtain the total 1D sum of states,  $G(E)$ , 1D density of states,  $\rho(E)$ , and 1D microcanonical rate constant,  $k(E)$ , saved as double-arrays.

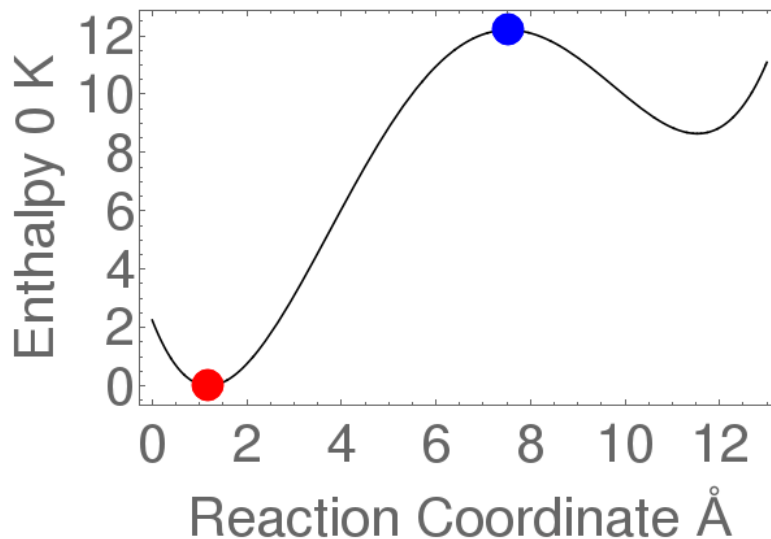


**Figure 2.** Points used in calculating canonical and microcanonical rate constants for a tight transition state. The point in red corresponds to the reactant structure while the point in blue is the transition state. Units of energy and zero of energy can be designated by the user.

## 10.2 Theory

### 10.2.1 Canonical Variational Transition State Theory (CVTST)

Rate constants in canonical variational transition state theory are calculated via RRKM theory.<sup>1-4</sup>

$$k(T) = \frac{k_B T}{h} \frac{\sigma^\ddagger}{\sigma} \frac{m}{m^\ddagger} \frac{Q^\ddagger}{Q} \exp\left(-\frac{E_0}{k_B T}\right) \quad (1)$$

Here  $Q$  and  $Q^\ddagger$  are the total molecular partition functions of the reactant and transition state respectively;  $\sigma$  and  $\sigma^\ddagger$  are the external symmetry numbers, and  $m$  and  $m^\ddagger$  are the number of optical isomers (chiral stereoisomers, or mirror images) of the reactant and transition state, respectively;  $k_B$  is the Boltzmann constant,  $h$  is Planck's constant,  $E_0$  is the reaction critical energy, and  $T$  is a temperature of interest. Each of the partition functions is a product of the partition functions for the individual degrees of freedom of each species. The current code is designed to handle both unimolecular and bimolecular reactions; therefore `ktools` uses the translational, vibrational, rotational, hindered rotor and electronic degrees of freedom when calculating the molecular partition function. The total molecular partition function calculated is then.

$$Q = q_{trans} \times q_{vib} \times q_{rot} \times q_{hindered} \times q_{elec} \quad (2)$$

Reactions can be viewed as a reactive flux on a hyperdimensional potential energy surface and the rate of reaction can be identified with the reactive flux through a dividing surface placed between reactant(s) and product(s). The key assumption in transition state theory is that a

dividing surface (the transition state) can be found where the flux passing through the transition state never returns (i.e. never re-crosses) to the reactant side.<sup>11</sup> This idealization is never actually achieved, but the amount of re-crossing can be minimized by placing the dividing surface where the flux (in both directions) is a minimum. This optimal location for the transition state yields the variationally optimal rate constant, which, for a canonical system, is proportional to  $Q^\ddagger$  (see Eq. 1).

In order to find the optimal dividing surface, the reactive flux must first be evaluated at many "trial" locations. In a canonical system, the reaction flux at a trial location is proportional to  $Q_{\text{trial}}^\ddagger$ , the partition function at the trial dividing surface, and the corresponding trial canonical rate constant,  $k_{\text{trial}}(T)$ . The minimum trial canonical rate constant is optimal and corresponds to the canonical variational transition state theory (CVTST) rate constant.

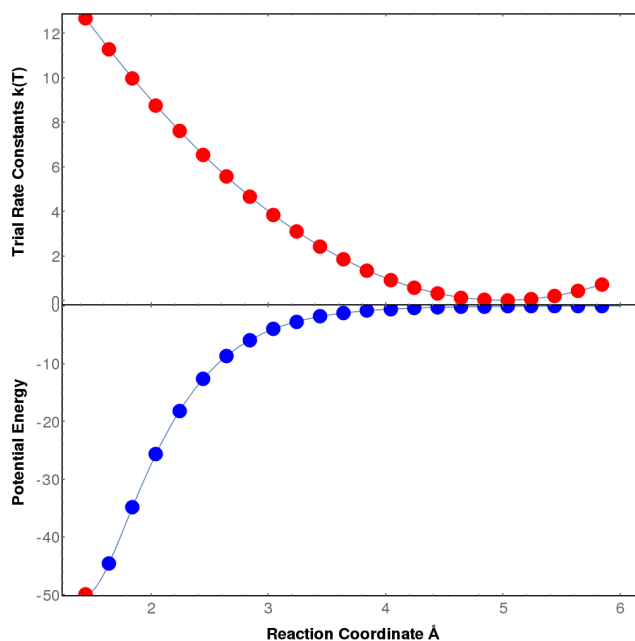


**Figure 3.** Points along a unimolecular dissociation reaction coordinate (bottom) and the corresponding trial canonical rate constants (top). The position of the minimum trial rate constant corresponds to the variational canonical transition state, which is the optional choice for a given temperature.

For a simple reaction that contains only a single bottleneck, the trial rate constants pass through a single minimum, as shown in Figure 3. In many cases, however, the trial rate constants exhibit more than one minimum, as shown in

**Figure 4** for the reaction  $\text{HO} + \text{OCIO}$ .<sup>12</sup> These cases can arise when there is a dramatic change along the reaction path in a) the potential energy, b) the vibrational frequencies, or c) the rotational constants.

Figure 3 shows plots of the potential energy, the zero-point energy, and each of the 1D- and 2D-rotor rotational constants (upper-left, upper-right, lower-left, lower-right respectively) for the system used to generate

**Figure 4.** The system does not exhibit a dramatic change in potential energy, however near 3.0 in the reaction coordinate the potential flattens out slightly and there is a change in both

the ZPE and K-rotor, indicating that there is a significant change in geometry (and possibly symmetry) in the system along this reaction coordinate.

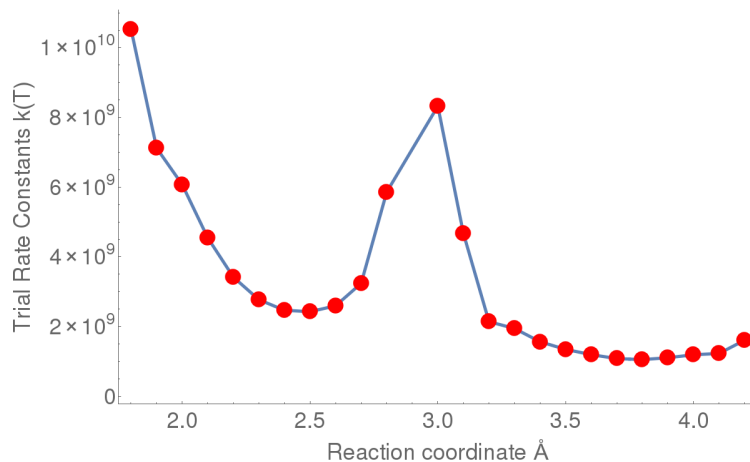


**Figure 4.** Points along a unimolecular dissociation reaction coordinate and the corresponding trial canonical rate constants for HO + OCIO.<sup>12</sup> This system exhibits multiple minima in  $k(T)$ , one on either side of the maximum near 3.0.

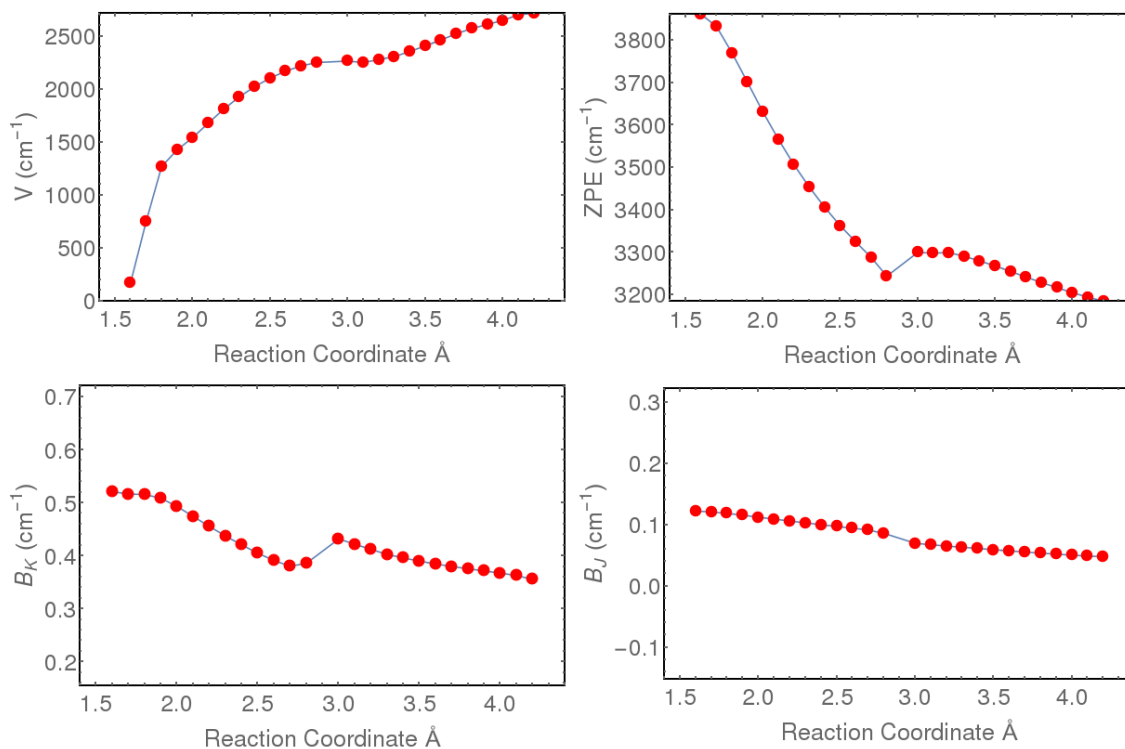


**Figure 3.** Points along a unimolecular dissociation reaction coordinate (HO--OCIO) and the corresponding potential energy (top left), zero point energy (top right), and

rotational constants  $B_K$  (bottom left) and  $B_I$  (bottom right) all in units of  $\text{cm}^{-1}$ .<sup>12</sup> Note the change in ZPE and K-rotor rotational constant near the 3.0 reaction coordinate.

`ktools` automatically searches for multiple minima in the trial rate constant computed at points along the reaction path by comparing the magnitudes of neighboring minima and maxima. This search is not trivial, because there are several sources of numerical "noise" in the calculations. Numerical noise can arise from incomplete convergence when optimizing geometries and when carrying out the SCF calculations. During bond-fission reactions, multireference contributions can erode the accuracy of quantum chemistry calculations that use single-determinant wave functions, resulting in fluctuations. Although the errors and fluctuations may not be very large, they contribute to the numerical noise, which interferes with searching for the minimum trial rate constant.

To distinguish valid minima in the trial rate constants from false minima produced by numerical noise, `ktools` utilizes the following algorithm. Consider two minima separated by a maximum. If the maximum is not at least twice as large as the difference between the two minima, the smaller of the two is kept as the local minima and the other is considered noise (i.e. insignificant). The search then continues to the next pair of minima and repeats the test to see if they satisfy the search condition. If they do then the minima are deemed "significant", i.e. not noise, and are used to find a "unified rate constant", which is the net result of two or more significant minima, according to the theory developed by W. H. Miller.<sup>8</sup> For a series of  $N$  significant minima the unified canonical variational rate constant is given by Eq. 3:<sup>8</sup>

$$k_{\text{unified}}(T) = \left( \sum_{i=1}^N \frac{1}{k_i(T)} \right)^{-1} \quad (3)$$

This unified rate constant thus accounts for two or more bottlenecks and can be described as a "multiple-transition state model".

Miller's unified statistical theory is actually formulated in terms of microcanonical rate constants and thus Eq. 3 is only an approximation. In the next section, the microcanonical VTST implemented in `ktools` is described.

### 10.2.2 *J-Resolved Microcanonical VTST (mVTST)*

This level of VTST is based on sums and densities of states that depend on both total energy ( $E$ ) and angular momentum (quantum number  $J$ ). The two-dimensional (2D)  $J$ -resolved microcanonical reaction rate constant is given by<sup>1-4</sup>:

$$k(E, J) = \frac{1}{h} \frac{G^\ddagger(E - E_{0,J}, J)}{\rho(E, J)} \quad (4)$$

where  $G^\ddagger(E - E_{0,J}, J)$  is the sum of states of the transition state and  $\rho(E, J)$  is the density of states of the reactant for a given  $E, J$ . `ktools` calculates microcanonical rates by parametrically setting  $J$  and calculating the density of states for the reactant and the sum of states for all the trial transition states as functions of total energy  $E$ . Trial rate constants,  $k_{\text{trial}}(E, J)$ , are computed at points along the reaction path, just as in the CVTST calculations described above. The  $J$ -resolved variational microcanonical variational TST (2DVTST) rate constant  $k(E, J)$  must meet two

criteria: (a) The total energy must be greater than the centrifugal barrier and (b)  $k(E,J)$  is identified with the minimum  $k_{\text{trial}}(E,J)$  at each  $E,J$ .

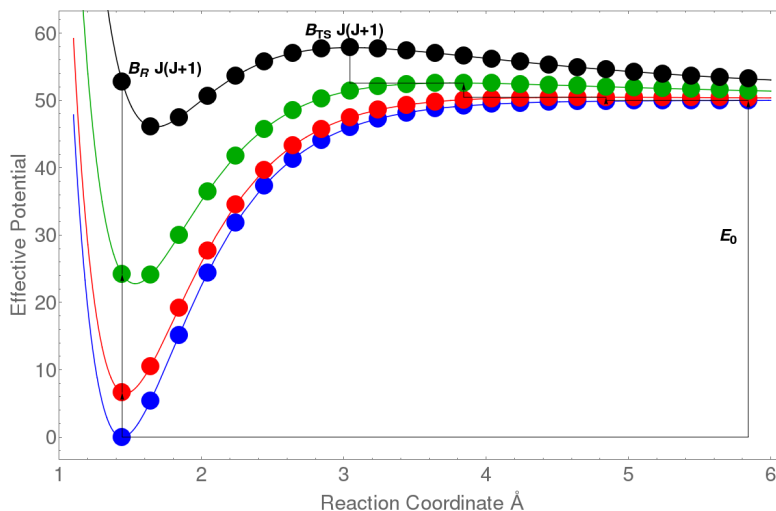


**Figure 6.** Unimolecular dissociation effective potential energy as a function of increasing  $J$  quantum number, (Blue)  $J=0$ , (Red)  $J=5$ , (Green)  $J=10$ , (Black)  $J=15$ . The arrows follow the reactant (left) and centrifugal maximum (right most).  $E_0$  is the reaction critical energy.

For a given  $J$  the effective potential is calculated at each trial location along the reaction path, and the maximum in the effective potential is taken as the centrifugal maximum. Sums and densities of states are calculated at each trial location at energies from the centrifugal maximum to a user-selected maximum energy.

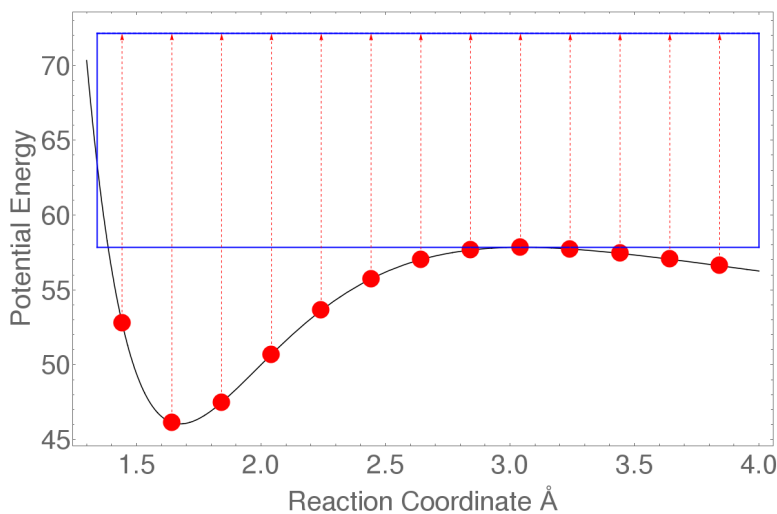


**Figure 7.** Effective potential for  $J=15$ . Blue box represents a window of  $20,000 \text{ cm}^{-1}$ . Red dotted lines represent the vector of sums/densities-of-states calculated for each structure. Blue line is

5000  $\text{cm}^{-1}$  above the centrifugal maximum. The minimum sum of states is evaluated at the same energy level above the centrifugal maximum (i.e. along the blue dotted line for each energy grain).

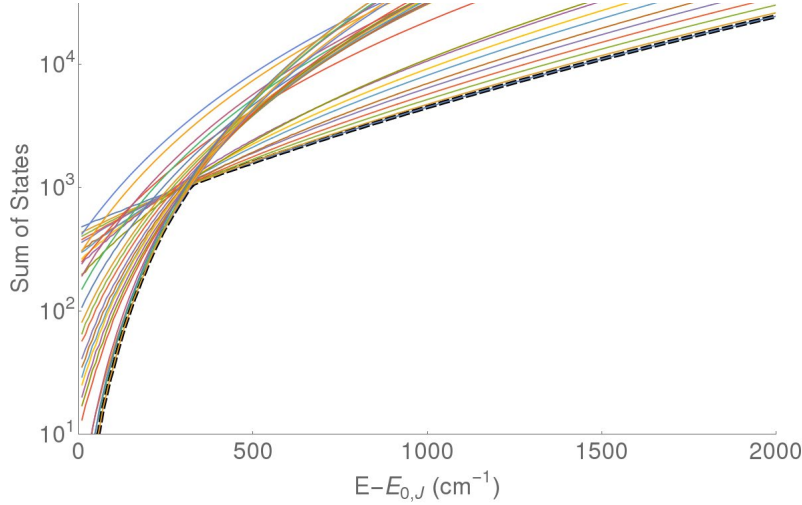


**Figure 8.** Sum of states as a function of energy for trial transition state structures along the **HO--OCIO reaction** path for  $J = 15$ . Each line follows the growth of the sum of states for a particular structure on a reaction path as energy increases. The minimum sum of states at each  $E$  is denoted with the dashed black line, which is identified with the variationally minimized sum of states.

For each  $J$  and each energy grain ( $E$ ) above the centrifugal maximum, the minimum sum of states along the reaction path (i.e. across all trial transition state structures) is identified as the variationally minimized sum of states at  $E, J$ . Each solid line in **Figure 8** is the sum of states as a function of energy ( $J = 15$ ) measured from the centrifugal maximum for a trial transition state structure along the reaction path. The dotted black line is the minimum sum-of-states at each energy.

The 2DVTST rate constants,  $k(E, J)$ , can be averaged over  $E$  and  $J$  at a given temperature to obtain a canonical (thermal) rate constant,  $k_{\infty, \mu}^{uni}(T)$ , which is also identified with the high pressure limit rate constant in a unimolecular (or recombination) reaction.

$$k_{\infty, \mu}^{uni}(T) = \frac{\sum_{J=0}^{J_{\max}} \int_{x=0}^{\infty} G^{\ddagger}(x, J) \exp\left[-(x + V_{TS} + B_{TS}J(J+1)) / k_B T\right] dx}{h \sum_{J=0}^{J_{\max}} \int_{x=0}^{\infty} \rho(x, J) \exp\left[-(x + V_0 + B_R J(J+1)) / k_B T\right] dx} \quad (5)$$

where  $V_{TS}$  and  $V_0$  are the potential energies (including the vibrational zero point energy (VZPE) corrections) of the variational transition state and the reactant, respectively. The VZPE correction for the transition state includes only the vibrations orthogonal to the reaction coordinate, while that for the reactant includes all of the vibrations. In Eq. 5, the integrals are over energy,  $x$ , and the summations are over the quantum number,  $J$ , for total angular



momentum. In the numerator of Eq. 5, the argument contains  $B_{TS}J(J+1)$ , the rotational energy respectively of the transition state; the denominator contains  $B_RJ(J+1)$ , the rotational energy of the reactant the reactant.

ktools also reports J-summed densities of states for the reactant, sums of states for the transition state, and microcanonical rate constants. Starting from the 2D microcanonical quantities, the J-summed<sup>5,9</sup> microcanonical quantities are given by

$$\rho(E) = \sum_{J=0}^{J_{\max}} \rho(E, J) \quad (6)$$

$$G_i^\ddagger(E) = \sum_{J=0}^{J_{\max}} G_i^\ddagger(E, J) \quad (7)$$

Using these quantities and the "E-Model" of Miller et al.,<sup>6,7</sup> one obtains the 1D microcanonical rate constants:

$$k_i(E) = \frac{1}{h} \frac{G_i^\ddagger(E - E_{0,J=0})}{\rho(E)} \quad (8)$$

where  $E_{0,J=0}$  is the critical energy for reaction. For the reactant and for *fixed* transition states, the 1D quantities are the same as would be obtained using program `densum` to calculate the total sums and densities of states (using *all* degrees of freedom) with the "top" rotational degree of freedom type (see Chap. 3). For both fixed and variational transition states, these quantities can be used in 1D master equation calculations that adopt the Smith and Gilbert method for reducing a 2D master equation to 1D. They are appropriate for use in a 1D master equation treatment that makes no centrifugal corrections and treats all degrees of freedom as active.<sup>5,6,9,10</sup>

### 10.3 ktools Input File

The input file for a **ktools** calculation is similar to the input file used by program **thermo**, but with several minor additions/changes. The character-based keywords do not depend on case. The code is based on the assumption that the molecular system of interest can be described with sufficient accuracy as a symmetric top (the quasi-symmetric top approximation; see Appendix B.4 of this User Manual). For that reason, the parameters for the external rotations must be specified as a “J-rotor” and “K-rotor” (corresponding respectively to the B<sub>2</sub> and B<sub>1</sub> rotational constants discussed in Appendix B.4).

**Line 1 Title (BLANK LINES FOLLOWING TITLE ARE IGNORED)**

Title: 180 Character limit title to be used in output files.

**Line 2 Up to 20 Comment lines**, each preceded by "!" (180 character limit, each line)

**Line 3 Ekey, Sskey**

Ekey: keyword for energy units, valid options:

**kcal, kJ, cm-1**

Sskey: keyword for standard state, not currently used (assumed to be **MCC**)

**Line 4 WhatDo**

WhatDo: Flag that controls writing of the large output files containing sums and densities of states, and microcanonical rate constants ( other output files are allways generated). Valid options: **savefiles** generates the large output files, while any other word (e.g. **nosavefiles**) suppresses their output. [Note that the meaning of **WhatDo** was changed starting with the 2020 version of **ktools**.]

**Line 5 Emax, Egrain**

Emax: Max energy to calculate sums and densities of states, in units of cm<sup>-1</sup>

Egrain: energy grain used in microcanonical TST, in units of cm<sup>-1</sup>; corresponds to Egrain1 in a double array.

**Line 6 Jmax, Jgrain**

Jmax: Max J value to calculate sums and densities of state.

Jgrain: step size in J used in microcanonical TST, currently step size of 1 is recommended.

**Line 7 lmax1, lsize, Emax2**

These parameters describe the double arrays (generated by J-summing) for use in the multiwell master equation code (note that Egrain1 is specified on Line 4).

lmax1: Number of array elements in lower part of double array.

lsize: Total number of elements in double array.

Emax2: Maximum energy of double array.

**Line 8 Nt**

Nt: number of temperatures to be read in

**Line 9 T<sub>1</sub>, T<sub>2</sub>, T<sub>3</sub> ... T<sub>nt</sub>**

T<sub>1</sub>, T<sub>2</sub>,...,T<sub>nt</sub>: list of Nt temperatures in kelvin

**Line 10 RCNT, NTTS, PCNT**

RCNT: number of reactant molecules to read in (reactant count). Max=2

NTTS: number of trial transition states to read in

PCNT: number of products to read in

Default Max of RCNT+NTTS+PCNT is set to 100

**Structure blocks: repeated RCNT+NTTS+PCNT times**

*This structure of the data block for each species is slightly different than the structure used in program thermo!*

**Line 11.1 Reprod, molname, delh, dist**

reprod: species identification. Options: **ctst, reac, prod**

molname: name of species. Used for naming relevant output files

delh: enthalpy of formation at 0 K.

dist: corresponding distance along reaction path, defined by the user but typically a bond distance. This allows the canonical variational transition state theory code to report the variationally optimal transition state.

**Line 11.2 Formula**

formula: empirical formula; used only for recombination reactions

**Line 11.3 Comment line A**

1<sup>st</sup> comment: 150-character limit

**Line 11.4 Comment line B**

2<sup>nd</sup> comment: 150-character limit

**Line 11.5 Comment line C**

3<sup>rd</sup> comment: 150-character limit

**Line 11.6 Sym, Sopt, Nele**

Sym: external symmetry number; see Appendices B.4 and B.5

Sopt: number of optical isomers; see Appendix B.5

Nele: number of electronic energy levels

**Line 11.7 Elev, gele (Repeated Nele times)**

Elev: electronic energy level (lowest should be designated as Elev=0.0)

Gele: electronic energy level degeneracies

**Line 11.8 N, Vhar, Vrot**

N: number of degrees of freedom to read in  
Vhar: keyword for vibrations. Options:  
      **har**  
Vrot: keyword for molecular internal (hra, hrb, hrc) and external rotations (kro,  
      jro). Options:  
      **amua** for moments of inertia in units of amu Å<sup>2</sup>  
**gmcm** for moments of inertia in units of g cm<sup>2</sup>  
**cm-1** for rotational constants in wavenumbers  
**mhz** for rotational constants in MHz  
**ghz** for rotational constants in GHz

**Repeat Line 10.9 N times, once for each degree of freedom**

**Line 11.9 Mode(i), Idof(i), AAA(i), BBB(i), CCC(i)**

mode: index number for degree of freedom  
idof: keyword for type of degree of freedom. The separable degrees of freedom  
(except for the J-rotor and K-rotor) that are recognized by **ktools** are defined and  
the data input formats are described in Chapter 3 of this User Manual. The J-  
rotor and K-rotor parameters used by **ktools** are described here:

**kro:** K-rotor 1-dimensional external rotation

AAA = rotational moment of inertia/constant in units of Vrot

BBB = rotational symmetry number

CCC = rotation dimension (should always be set to 1)

**jro:** J-rotor 2-dimensional external rotation

AAA = rotational moment of inertia/constant in units of Vrot

BBB = rotational symmetry number

CCC = rotation dimension (usually should be set to 2)

**Line 12** (Blank Line)

## 10.4 Running ktools

By default the program looks for the input file named “**ktools.dat**” and **ktools** can be executed from the command line by simply typing “**ktools**”, followed by a carriage return. Optionally, the user can use custom names for input files. **ktools** is then executed by typing “**ktools filename.dat**”. Where **filename.dat** is the filename as defined by the user. The program expects a 3-letter extension to be used in the naming of the input file name.

### *Comments on program execution:*

A backup file (**filename.bck**) for the input is saved every time the code is run.

The maximum number of energy grains is limited only by the size of available computer memory (although execution speed will become very slow for extremely large calculations). For accurate canonical rate constants, Users should select **emax**  $\geq 15 \times k_B T \approx 10 * T \text{ cm}^{-1}$  (line 5) and **jmax**  $\geq 500$  (Line 6). Typically, **Egrain** should be set to  $\sim 10 \text{ cm}^{-1}$  and **Jgrain** = 1. For very low temperatures, **Egrain** can be reduced, but the code has not been tested below  $1 \text{ cm}^{-1}$ .

If the maximum number of rotational states selected by the user is not large enough, execution will be terminated and an error message will suggest a larger value.

If the maximum number of rotational states selected by the user exceeds the intrinsic upper limit where  $V_{\text{eff}}$  for the reactant is  $\geq V_{\text{eff}}$  for all of the trial transition states, the output is automatically limited to the intrinsic limit.

The numbers of energy grains, rotational states, and the intrinsic upper limit are now reported along with the canonical rate constants (**filename.canonical**).

## 10.5 ktools Output Files

ktools creates a number of output files. Below is a description of their contents.

File Name	Description
*.log	Contains information on data being generated at each step of the code execution. Final output is the thermally averaged microcanonical rate constant, $\langle k(E, J) \rangle_T$ .
*-efile.txt	Lists $\Delta H(0K)$ , ZPE, $\Delta E_{\text{electronic}}$ , k-rotor and j-rotor rotational constants for the reactant and each TS all in units of $\text{cm}^{-1}$ .
*.canonical	Contains canonical rate constant data. Lists all trial rate constants as a function of temperature, followed by local minimum rate constants and final rate constants as a function of temperature. If more than one rate is determined to be “significant” then all rates contributing to the unified rate are listed as well
*.veff	Lists effective potential for all J from 0 to $J_{\text{max}}$
*.2dens *.2sums *.u2sums *.kej *.ukej	Lists the rotational energies and associated 2D density of states, sum of states, unified sum of states, microcanonical rates, unified microcanonical rates. Sums and rates using a unified transition state <sup>8</sup> are designated by a “u” prefix. Writing of these files is suppressed unless key word <b>WhatDo</b> (Line 4) is set to <b>savefiles</b> .
*-j-000.gmat *-j-jmax.gmat	Lists effective potential followed by the sum of states for all trial TS for $J=0$ and $J=J_{\text{max}}$
*-r.dens *-ts.dens	J-summed <sup>5,9</sup> sum- and densities-of-states for the reactant, transition state, and unified transition state. For use in 1D Multiwell calculations. Writing of these files is suppressed unless key word <b>WhatDo</b> (Line 4) is set to <b>savefiles</b> .
*-nmins.txt	List of all found local minima in the sums-of-state for all energies and J values
*.bck	Backup inputfile

(\* : represents a species name)

## 10.6 ktools Examples

(Example input and output files can be found in the examples/ktools directory.)

### Example Input

```
microrun X+OH ! 1 Title
KCAL MCC ! 3 Ekey, Sskey
savefiles ! 4 Whatdo
30000 10.0 ! 5 Emax Egrain
70000 1 ! 6 Jmax Jgrain
3 ! 7 Nt number of temperatures
100. 500. 1000. ! 8 Nt temperatures
1 1 1 ! 9 RCNT: # of reactants , NTTTS: # of trial TS, PCNT: # of products

! RCNT+NTTS+PCNT # of Structures
! RCNT #1
react 'X-OH-PRE' 0.000 0.0 ! 10.1 reprod, molname, delh, dist
CX3O2 ! 10.2 formula
1. formaldehyde + oh reaction ! 10.3 comment line A
2. (blank comment line) ! 10.4 comment line B
3. (blank comment line) ! 10.5 comment line C
1 1 1 ! 10.6 sys, sopt, nele
0.0 2 ! 10.7 elev, gele (repeated nele times)
15 HAR ghz ! 10.8 N, Vhar, Vrot
1 vib 52.35 0 1 ! 10.9 mode, idof, AAA, BBB, CCC
2 vib 161.26 0 1 ! (repeated N times. 1 for each DOF)
3 vib 195.37 0 1
4 vib 450.63 0 1
5 vib 582.98 0 1
6 vib 1271.09 0 1
7 vib 1317.15 0 1
8 hrd 5 5 1
Vhrd2 1 33.4945 66.1601 90.72679 44.53344 1.72326 0.28367
lhrrd1 1 3.50661 0.78172 0.01627 -0.00487 -0.00111 0.00304
9 vib 1583.82 0 1
10 vib 1889.35 0 1
11 vib 3031.11 0 1
12 vib 3112.55 0 1
13 vib 3717.63 0 1
14 kro 50.63523 1 1
15 jro 4.535349039 1 2 ! Nth DOF of RCNT #1.

! NTTTS #1
ctst 'TS-250' 0.88924 2.5 ! 10.1 reprod, molname, delh, dist
CH3O2 ! 10.2 formula
1. VTST ! 10.3 comment line A
2. (blank comment line) ! 10.4 comment line B
3. (blank comment line) ! 10.5 comment line C
1 1 1 ! 10.6 sys, sopt, nele
0.0 2 ! 10.7 elev, gele (repeated nele times)
14 HAR ghz ! 10.8 N, Vhar, Vrot
1 vib 33.55 0 1 ! 10.9 mode, idof, AAA, BBB, CCC
2 vib 87.6 0 1 ! (repeated N times. 1 for each DOF)
3 vib 250.22 0 1
4 vib 334.82 0 1
5 vib 1265.15 0 1
6 vib 1313.51 0 1
7 vib 1586.22 0 1
8 hrd 5 5 1
Vhrd2 1 33.49326 63.79801 90.66085 38.05053 1.04218 0.15534
lhrrd1 1 3.47908 0.78116 0.01656 -0.00431 -0.00106 0.00225
9 vib 1899.27 0 1
10 vib 3016.85 0 1
11 vib 3090.77 0 1
12 vib 3836.64 0 1
13 kro 74.85529 1 1
14 jro 3.008627473 1 2 ! Nth DOF of NTTTS #1
! Blank Line
```





## Example Logfile

%%%

John R. Barker  
Ktools-2015 University of Michigan  
Ann Arbor, MI 48109-2143  
Jan 2015 jrbarker@umich.edu  
(734) 763 6239

<http://aoss.engin.umich.edu/multiwell/>

%%%

variational tst: ch2o+oh-micro run started. ! Time stamp on initial run  
mar. 2nd 2015 10:50:41:495 am

# of r # of ts ndof r 1 ndof for ts ! Summary of (r)eachants,  
1 31 14 13 ! (t)ransition (s)tates, and  
! the number of degrees of  
! freedom for each to be read in

reactant # 1 14 ! Structure Type, #, # of DOF  
# dof freq anh degen !  $\Delta H$  and reaction coordinate values

-----  
1 vib 52.3500 0.0000 1 ! Reprint of degrees of freedom

2 vib 161.2600 0.0000 1

...

13 kro 50.6352 1.0000 1

14 jro 4.5353 1.0000 2 ! End of structure 1

! Repeated RCNT+NTTS times

...

! End of RCNT+NTTS structures

end of read\_inp.f ! Exit subroutine and time stamp

mar. 2nd 2015 10:50:41:499 am

start bsort ! Bsort converts the rotational

mar. 2nd 2015 10:50:41:499 am ! constants

converting j-rotational constant into cm-1 ! Converting data for the 2D

! external "J-rotor"

# dof# ghz cm-1 cm-1 ! Structure number, # of dofs in

1 14 4.5353 0.1513 0.1513 ! that structure, rotational

2 13 3.0086 0.1004 0.1004 ! converted value, stored value ! info given by the user,

...

converting k-rotational constant into cm-1 ! Converting data for the 1D

# dof# ghz cm-1 cm-1 ! external "K-rotor"

1 13 50.6352 1.6890 1.6890

2 12 74.8553 2.4969 2.4969

...

(a-b) rotational constant ! Rotational energy of a symmetric

! top is Erot = BJ(J+1)+(A-B)K\*\*2

# a b a-b check ! Structure number, K-rotor (A),

! J-rotor (B), a-b, stored a-b

-----  
1 1.6890 0.1513 1.5377 1.5377

2 2.4969 0.1004 2.3965 2.3965

...

end bsort ! Exit subroutine and time stamp

mar. 2nd 2015 10:50:41:500 am

```

start of hsort                                ! Enter subroutine and time stamp
mar. 2nd 2015 10:50:41:500 am

converting pe from kcal to cm-1                ! Hsort converts the enthalpy units
! into cm-1 & sets the 0 of energy.

#      kcal      cm-1  rescale cm-1
-----
1      0.00      0.00    0.00
2      0.89      311.02  311.02
...
exit hsort                                    ! Exit subroutine and time stamp
mar. 2nd 2015 10:50:41:500 am

start zpe_calc                                ! Enter subroutine and time stamp
# of structures:      32

reporting v, zpe, and electronic (cm-1)      ! zpe_calc calculates zero point
! energy and reports enthalpy at
! OK, zpe, and electronic energy

#      v      zpe  electronic
-----
1      0.0000  8682.6450  0.0000
2      311.0162  8357.3000  636.3612
...

end of zpe_calc                                ! Exit subroutine and time stamp
mar. 2nd 2015 10:50:41:501 am

start canonrates                               ! Enter subroutine and time stamp
mar. 2nd 2015 10:50:41:501 am                ! canonrates calculates canonical
! partition functions and canonical
! rates for each structure for each
! temperature.

! listed are the vibrational, rotational, hindered rotation, electronic, and total
! partition functions followed by the canonical rate for going from structure #1 to the
! current structure

structure # t(k)  qvib  qrot  qhin  qele  qtot  k(t)
-----
1  100.00  2.233E+00  5.478E+03  1.000E+00  2.000E+00  2.447E+04  2.083E+12
...
canonical rate constant data can be found in: Ktools.canonical ! name of canonical output

end canonrates                               ! Exit subroutine and time stamp
mar. 2nd 2015 12:03:23:742 pm

start find_jmax                               ! Enter subroutine and time stamp
mar. 2nd 2015 12:03:23:742 pm                ! find_jmax runs through several
! tests to find a maximum j value
! for the system.
! List of kb*Tmax multiples and
! the corresponding Jmax
! E=n*kb*Tmax~Bmin*J**2 =>
! J=SQRT(n*kb*Tmax/Bmin)

kb*Tmax  Jmax
1  161.
2  227.
3  278.
4  321.
5  359.
6  394.
7  425.
8  454.
9  482.

```

10 508.

User requested J value is higher than totally repulsive J value

looking for jmax

10kbt method: 508. ! 10kb\*T Value of Jmax  
pt1 > pt 2 method 79. ! Value of J where E(pt1)> E(pt2)  
pt1 > everything: 102. ! Value of J where E(pt1)>E(pts2-N)  
tot.repul.method: 791. ! Value of J where Veff is entirely repulsive  
setting maxj to: 102. ! Jmax set by the program  
end of find\_jmax ! Exit subroutine and time stamp  
mar. 2nd 2015 12:03:23:742 pm  
! Start looping over every J value to Jmax and calculate all Sums and Densities of States  
for j: 0 vmax@ 1245.12 6.0 ! Jvalue, Veff max, and Veffmax location  
centrifugal max@ 523036243.49 29908648.83 ! Extrapolated centrifugal max and R  
energy difference 523034998.36542666 !  $\Delta E = \text{Centrifugal Max} - \text{Veffmax}$   
start veff

j: 0 ! Current J value  
!#, enthalpy, rotational constant,  $j^*(j+1)$ , veff, emax-veff  
i delh b  $j^*(j+1)$  veff epsilon  
1 0.000000E+00 1.512830E-01 0 0.000000E+00 3.124513E+04  
2 3.110162E+02 1.003570E-01 0 3.110162E+02 3.093411E+04  
...  
veff max is at point # 32 1245.12 ! Veff max struct. number and energy value

end veff  
mar. 2nd 2015 12:03:23:764 pm ! Repeat MaxJ times

for j: 1 vmax@ 1245.18 6.0 ! Jvalue, Veff max, and Veffmax location  
...  
end veff ! Exit subroutine and time stamp

mar. 2nd 2015 12:05:16:702 pm

convergence for reactant ! Integration of reactant

! Temp #, Temp, J used, Energy grains used, Current Norm, Next term, Max Term

#	Temps	J	E	Norm	Term	Maxterm
1	100.00	72	200	9.004825E+03	3.199051E-02	3.769884E+02
2	500.00	103	1383	4.041294E+06	3.932402E+03	7.633520E+04
3	1000.00	103	3127	2.282009E+08	1.206322E+06	3.364758E+06

convergence for transition state ! Integration of TS

#	Temps	J	E	Norm	Term	Maxterm
1	100.00	103	440	1.261268E+18	6.185970E+13	2.473813E+16
2	500.00	103	2662	9.669243E+20	1.494753E+18	1.682981E+19
3	1000.00	103	3002	2.711101E+22	1.516654E+20	3.983837E+20

convergence for unified transition state ! Integration of unified TS (if present)

#	Temps	J	E	Norm	Term	Maxterm
1	100.00	103	440	7.284531E+17	4.966310E+13	1.327708E+16
2	500.00	103	2662	8.431412E+20	1.447493E+18	1.450470E+19
3	1000.00	103	3002	2.653338E+22	1.508069E+20	3.898675E+20

thermally averaged microcanonical partition functions

temp	q(r)	q(ts)	q(uts)	! temperature, $Q_{\text{reactant}}$ , $Q_{\text{TS}}$ , $Q_{\text{unified TS}}$
100.00	9.00482E+03	6.05313E+05	3.49602E+05	
500.00	4.04129E+06	9.28101E+07	8.09288E+07	
1000.00	2.28201E+08	1.30112E+09	1.27340E+09	

thermal averaged microcanonical rate constants

#	temp	<kv(e)>t	<ukv(e)>t	! T, T. Ave. k(e), unified T ave. k(e)
1	100.00	2.32334E+06	1.34186E+06	
2	500.00	6.65010E+12	5.79877E+12	
3	1000.00	1.98064E+13	1.93844E+13	

mar. 6th 2015 10:10:51:889 am ! Time stamp  
elapsed time: 3.16 minutes. ! Run time

### Example Efile

Efile contains summary information about the system suitable for plotting.

It lists the structure number, the distance, enthalpies at 0K, zero point energies, electronic energies, k-rotor rotational constants and the j-rotor rotational constants. All energies reported are in units of  $\text{cm}^{-1}$ .

struct#	distance(a)	dh(cm-1)	zpe(cm-1)	delect(cm-1)	k-rot(cm-1)	j-rot(cm-1)
1	0.0	0.0000	8682.645	0.0000	1.6890	0.1513
2	2.5	311.0162	8357.300	636.3612	2.4969	0.1004
3	2.6	400.3227	8331.595	751.3727	2.5490	0.0954
4	2.7	485.2817	8308.340	859.5867	2.6261	0.0907
5	2.8	564.4243	8287.650	959.4193	2.7420	0.0861

### Example Canonical File

The \*.canonical file lists all canonical rate constants for each temperature. The user can use these values to plot the rate constant as a function of reaction coordinate.

#### Single minimum found

canonical rates for all temperatures and ts

r	100.00	500.00	1000.00
2.50	4.97660E+010	1.07022E+013	2.55589E+013
...			
3.00	4.27324E+008	1.48108E+013	7.05745E+013
3.10	2.12009E+008	1.61207E+013	8.53028E+013
3.20	1.20912E+008	1.81371E+013	1.05068E+014
3.30	6.53084E+007	1.77684E+013	1.11445E+014
3.50	4.19373E+007	3.23287E+013	2.32646E+014
3.60	5.12595E+007	6.10474E+013	4.65332E+014
3.70	3.30816E+007	5.79128E+013	4.64405E+014
3.80	2.03015E+007	5.01871E+013	4.21175E+014
...			
4.60	4.07335E+006	6.26450E+013	6.69339E+014
4.70	3.71415E+006	6.64867E+013	7.24783E+014
4.80	3.51374E+006	7.23704E+013	8.03692E+014
4.90	3.51914E+006	7.89177E+013	8.86627E+014
5.00	3.12963E+006	8.48905E+013	9.77537E+014
5.50	2.85286E+006	1.29030E+014	1.58947E+015
5.60	2.93227E+006	1.40983E+014	1.75106E+015
5.70	3.02479E+006	1.54509E+014	1.93469E+015

reporting all local minima ! List all local minima & position for each  
! temperature along the reaction coordinate

#	temp	# min	r(min)	min k(t)
1	100.00	3	3.50 4.80 5.50	4.193E+07 3.514E+06 2.853E+06
2	500.00	4	2.50 3.30 3.90 4.10	1.070E+13 1.777E+13 4.790E+13 4.7447E+13
3	1000.00	2	2.50 3.90	2.556E+13 4.188E+14

unified canonical rates and contributing minima ! List minima which are not "noise" and  
! list min k(t).

#	temp	# min	r(min)	min k(t)
1	100.00	1	5.50	2.8529E+06
2	500.00	1	2.50	1.0702E+13
3	1000.00	1	2.50	2.5559E+13

## Multiple minima found

canonical rates for all temperatures and ts

r	180.00	242.00	253.00	293.00	298.00
1.60	7.40485E+011	1.33249E+012	1.44307E+012	1.85159E+012	1.90305E+012
...					
2.30	3.06708E+006	2.71097E+008	4.82410E+008	2.77278E+009	3.34400E+009
2.40	1.89269E+006	2.13060E+008	3.91209E+008	2.47375E+009	3.01410E+009
2.50	1.36220E+006	1.88313E+008	3.55112E+008	2.43536E+009	2.99328E+009
2.60	1.11650E+006	1.83896E+008	3.54750E+008	2.60695E+009	3.22802E+009
2.70	1.12259E+006	2.12999E+008	4.18510E+008	3.25234E+009	4.05140E+009
...					
3.60	1.97966E+005	5.92058E+007	1.23097E+008	1.13248E+009	1.43610E+009
3.70	1.44968E+005	4.98038E+007	1.05406E+008	1.02333E+009	1.30516E+009
3.80	1.17920E+005	4.55527E+007	9.78714E+007	9.94479E+008	1.27455E+009
3.90	1.06807E+005	4.54229E+007	9.88071E+007	1.04232E+009	1.34123E+009
4.00	9.93543E+004	4.65172E+007	1.02445E+008	1.12185E+009	1.44934E+009
4.10	8.46946E+004	4.49036E+007	1.00474E+008	1.15432E+009	1.49893E+009
4.20	1.03423E+005	5.73970E+007	1.29193E+008	1.51130E+009	1.96629E+009

reporting all local minima ! List all local minima & position for each  
! temperature along the reaction coordinate

#	temp	# min	r(min)	min k(t)
1	180.00	2	2.60 4.10	1.1165E+06 8.4695E+04
2	242.00	3	2.60 3.90 4.10	1.8390E+08 4.5423E+07 4.4904E+07
3	253.00	3	2.60 3.80 4.10	3.5475E+08 9.7871E+07 1.0047E+08
4	293.00	2	2.50 3.80	2.4354E+09 9.9448E+08
5	298.00	2	2.50 3.80	2.9933E+09 1.2746E+09

unified canonical rates and contributing minima ! List minima which are not "noise" and  
! list min k(t) and unified k(t)

#	temp	uk(t)	# min	r(min)	min k(t)
1	180.00	7.8723E+04	2	2.60 4.10	1.1165E+06 8.4695E+04
2	242.00	3.6091E+07	2	2.60 4.10	1.8390E+08 4.4904E+07
3	253.00	7.6708E+07	2	2.60 3.80	3.5475E+08 9.7871E+07
4	293.00	7.0613E+08	2	2.50 3.80	2.4354E+09 9.9448E+08
5	298.00	8.9392E+08	2	2.50 3.80	2.9933E+09 1.2746E+09

## Example Veff file

\*.veff lists the effective potential for each value of J. Points along the potential read from left to right and J increases along each new line.

	Pt. #1	Pt. #2	Pt. #3	Pt. #4	Pt. #5
J=0	0.00E+00	3.11E+02	4.00E+02	4.85E+02	5.64E+02
J=1	3.03E-01	3.11E+02	4.01E+02	4.85E+02	5.65E+02
J=2	9.08E-01	3.12E+02	4.01E+02	4.86E+02	5.65E+02

### Example 2dens/2sums file

Ktools generates a \*.2dens file for the 2D density of states for the reactant, a \*.2sums for the 2D sum of states for the transition state, and a \*.kej for the 2D microcanonical rate constants. If multiple minima are found among the sum of states arrays then Ktools also generates \*.u2sums and \*.ukej files where the “u” designates the contents represent a unified statistical model<sup>8</sup> has been used. The general structure for all of these files is the same.

66.9755	! lowest vibrational frequency				
	0	1	2	3	! J values
Erot-TS	4.92E+02	4.92E+02	4.92E+02	4.92E+02	! Veff of R/TS
0.0	1.00E+00	3.00E+00	5.00E+00	7.00E+00	! Bin energy and data
10.0	1.00E+00	3.00E+00	5.00E+00	7.00E+00	
20.0	3.00E+00	9.00E+00	1.50E+01	2.10E+01	

## References

- (1) Baer, T.; Hase, W. L. *Unimolecular Reaction Dynamics. Theory and Experiments*; Oxford University Press: New York, 1996.
- (2) Forst, W. *Unimolecular Reactions. A Concise Introduction*; Cambridge University Press: Cambridge, 2003.
- (3) Gilbert, R. G.; Smith, S. C. *Theory of Unimolecular and Recombination Reactions*; Blackwell Scientific Publications: Oxford, 1990.
- (4) Holbrook, K. A.; Pilling, M. J.; Robertson, S. H. *Unimolecular Reactions*, 2 ed.; Wiley: Chichester, 1996.
- (5) Klippenstein, S. J.; Harding, L. B. A direct transition state theory based study of methyl radical recombination kinetics. *Journal of Physical Chemistry A* **1999**, *103*, 9388-9398.
- (6) Miller, J. A.; Klippenstein, S. J. Master Equation Methods in Gas Phase Chemical Kinetics. *J. Phys. Chem. A* **2006**, *110*, 10528-10544.
- (7) Miller, J. A.; Klippenstein, S. J.; Raffy, C. Solution of some one- and two-dimensional master equation models for thermal dissociation: The dissociation of methane in the low pressure limit. *JPCA* **2002**, *106*, 4904-4913.
- (8) Miller, W. H. Unified statistical model for "complex" and "direct" reaction mechanisms. *J. Chem. Phys.* **1976**, *65*, 2216-2223; <https://doi.org/10.1063/1.433379>.
- (9) Smith, S. C.; Gilbert, R. G. Angular momentum conservation in multichannel unimolecular reactions. *International Journal of Chemical Kinetics* **1988**, *20*, 979-990.
- (10) Smith, S. C.; Gilbert, R. G. Angular momentum conservation in unimolecular and recombination reactions. *International Journal of Chemical Kinetics* **1988**, *20*, 307-329.
- (11) Truhlar, D. G.; Garrett, B. C. Variational Transition State Theory. *Ann. Rev. Phys. Chem.* **1984**, *35*, 159-189.
- (12) Yang, L.; Sonk, J. A.; Barker, J. R. HO + OCIO Reaction System: Featuring a Barrierless Entrance Channel with Two Transition States. *J. Phys. Chem. A* **2015**, *119*, 5723-5731; DOI: 10.1021/acs.jpca.5b03487.



## 11. TS and pTS: *J*-Resolved Steady-State Master Equation Solver

These computer codes were developed by Lam Nguyen and John Stanton.

**TS** is a serial code and **pTS** is a parallel version of the same code. The code features a *J*-resolved steady-state master equation that is solved by eigenvalue methods on large parallel computers. It utilizes the frozen-*J* approximation. The codes and User Manuals can be downloaded from the MultiWell web site. The codes must be compiled separately from the rest of the MultiWell Program Suite (see the User Manuals for instructions).

### Literature citation:

"TS is a chemical kinetic program that solves a two-dimensional master-equation for gas-phase reactions in parallel using the Steady-State approach. It is developed, implemented, and maintained by T. L. Nguyen and J. F. Stanton, version 01-03-2017."

### For assistance:

Users should submit questions to the "**Multiwell and Chemical Kinetics**" **question and answer forum**: all users are invited to join the forum, where questions can be asked and answered, and future upgrades will be announced. This forum is set up as a Google Group, which you can join at <https://groups.google.com/>. If for any reason, a user finds it difficult to use Google, please contact either Lam Nguyen or John Stanton:

[thanhlamnguyen08@gmail.com](mailto:thanhlamnguyen08@gmail.com)  
[jfstanton@gmail.com](mailto:jfstanton@gmail.com)

## Appendix A. Theoretical Basis

Much of this Appendix is based on an expanded and corrected version of the paper originally published in the International Journal of Chemical Kinetics: J.R. Barker, Multiple-well, multiple-reaction-path unimolecular reaction systems. I. MultiWell computer program suite. *Int. J. Chem. Kinetics*, **33**, 232-45 (2001). For a recent review of Monte Carlo stochastic methods for simulationg master equations, see Barker.<sup>6</sup>

### A.1. Introduction

Here, the theoretical basis for MultiWell is summarized. Inevitably, various approximations and assumptions must be adopted due to computational limitations and to the absence of physico-chemical knowledge. The numerical approximations are described so that program users can better assess MultiWell's limitations and strengths. The principal assumptions made in formulating the master equation are reviewed.

In the next section, the master equation is described formally. In subsequent sections, the stochastic methodology is described along with a brief discussion of some of the merits and limitations of the hybrid master equation approach relative to other methods. Methods for computing microcanonical unimolecular reaction rates and energy transfer step sizes are described, followed by a description of various initial conditions that can be selected as options. Finally, the calculation input and output are outlined.

### A.2. The Active Energy Master Equation

The current version of MultiWell is based on the one-dimensional master equation,<sup>26</sup> in which the active (randomizable) internal energy is modeled, but it is planned that future extensions will explicitly include angular momentum (the two-dimensional master equation<sup>17,22,25,27,29-32,35,36</sup>). The master equation provides the fundamental theoretical basis for modeling systems in which both energy transfer and chemical reaction can occur.<sup>4,11,12,14,28</sup> It is comprised of a set of coupled integro-differential equations that describe the rates of production and loss of chemical species at specified energies.

#### A.2.1 Internal Energy and Active Degrees of Freedom

Unless slow intramolecular vibrational energy redistribution (IVR) is specified, the internal energy  $E$  is always assumed to be fully randomized among the active degrees of freedom. The internal energy for a particular species (stable molecule or transition state) includes the energy (measured from the zero point energy; see Figure 0) that resides in the internal modes (vibrations, torsions, and internal rotations) and an active external rotation. Nonlinear polyatomic species have three external rotational degrees of freedom characterized by moments of inertia  $I_A$ ,  $I_B$ , and  $I_C$ . The usual pragmatic approach<sup>11,12</sup> is to assume the molecule can be approximated as a symmetric top with two of the moments of inertia equal to one another ( $I_B = I_C$ ), producing a degenerate two-dimensional external rotation. The third external rotor is associated with the symmetric top figure axis and is sometimes termed the K-rotor. The K-rotor is assumed to exchange energy freely with the other internal degrees of freedom, while the degenerate two-dimensional external rotation is assumed to be inactive.<sup>3,11,12,14,28</sup> See Appendix B.4 of this Manual for more discussion. (More sophisticated treatments of rotations can be utilized in the

present version of MultiWell by calculating specific rate constants ( $k(E)$ ) externally and then providing them in data files read by MultiWell.)

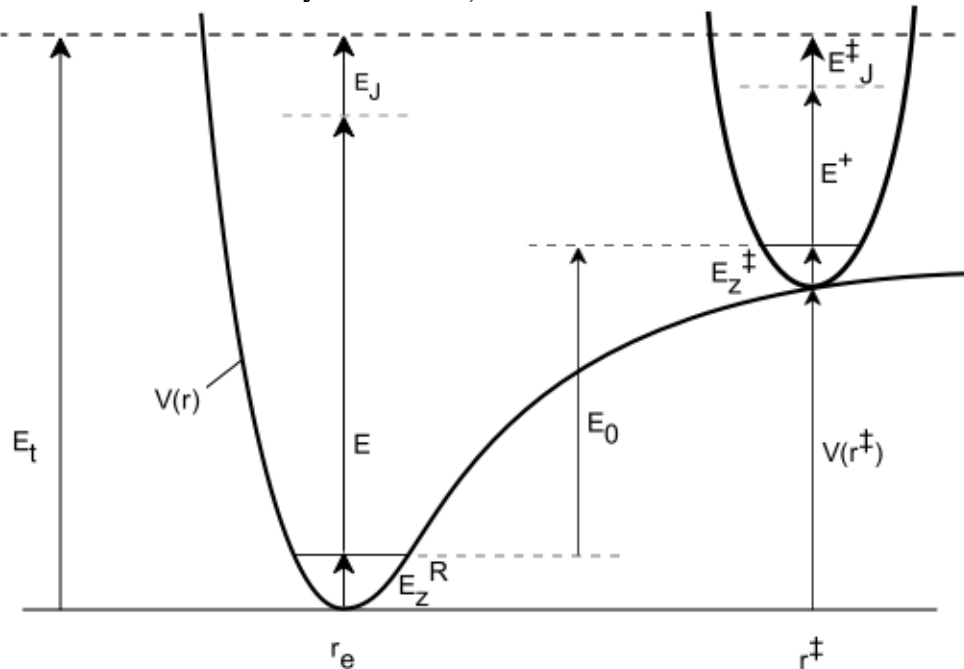


**Figure 0.** Energy schematic. The active energy  $E$  is measured from the zero point energy of the reactant well. The critical energy  $E_0$  is the zero point energy difference between the transition state and the reactant well.

### A.2.2 Sums and Densities of States

The MultiWell suite of computer codes includes **DenSum**, which utilizes the Stein-Rabinovitch<sup>34</sup> version of the Beyer-Swinehart algorithm<sup>9</sup> for exact counts of states for species comprised of separable degrees of freedom. The present version of **DenSum** can accommodate harmonic oscillators, Morse oscillators, and free rotors. The K-rotor is included with the internal degrees of freedom when calculating the sums and densities of states. There are two options for the treatment of rotations. The usual option is to use the convolution method developed by Astholz et al.,<sup>1</sup> which is computationally efficient and accurate for rotors with small rotational constants. The second method is to use exact counts of rotational states. The second method is preferred if the rotational constant is larger than  $\sim 1 \text{ cm}^{-1}$ . **DenSum** produces an output file that is subsequently used as an input file by **MultiWell**. The inactive two-dimensional external rotation is specified in the general MultiWell data file.

### Hindered Internal Rotations

In the MultiWell Program Suite, torsional modes are assumed to be separable from other motions (i.e. translations, vibrations, external rotations and other internal rotations) and are treated as one-dimensional quantum hindered internal rotations. The Schrödinger equation for such 1-D torsional motions is solved as described in the Technical Notes (see Appendix B).

The 1-D torsion coordinate is defined as  $\chi$ , the torsional dihedral angle ( $0 \leq \chi < 2\pi$ ). Users must supply the potential energy  $V(\chi)$  and the torsion rotational constant function  $B_{\text{hr}}(\chi)$  (or the corresponding moment of inertia function  $I(\chi)$ ). Potential energies  $V(\chi)$  and molecular geometries can be computed at discrete values of  $\chi$  by using any of the many available quantum chemistry codes, such as Gaussian,<sup>13</sup> Molpro,<sup>38</sup> or CFour.<sup>33</sup> The results for  $V(\chi)$  can be fitted to a suitable truncated Fourier series. **Program lamm**, a module in the MultiWell Program Suite, is intended to help users compute  $B_{\text{hr}}(\chi)$ , based on the output from quantum chemistry programs (see **Chapter 8** of this manual).

### A.2.3 Master Equation for the Vibrational Quasi-Continuum

Because of the difficulties encountered in solving the 2-D master equation, it is usually reduced to 1-D by making simplifying assumptions, and then solving numerically by one of the standard methods.<sup>4,5,20,21,24</sup> However, Marcus showed that the microcanonical RRKM specific rate constant depends on the active energy  $E$ , i.e. the energy not constrained by conservation of angular momentum. Thus angular momentum has an effect that must be taken into account for accurate results. The first approach to this problem also originated with Marcus,<sup>18</sup> who invoked the concept of adiabatic rotation to make "centrifugal corrections". Marcus' approach has been reviewed by Waage and Rabinovitch<sup>37</sup> and is found in standard monographs.<sup>12,14,16</sup> In this approach, the RRKM specific rate constant  $k(E_t, J)$ , which is written as depending on total energy  $E_t$  and the angular momentum quantum number  $J$  is reduced to an approximate  $k(E)$  (at a given temperature), where  $E$  is the active energy of the reactant: all explicit reference to angular momentum quantum number  $J$  has been removed from the 2DME, which has thus been reduced to a 1DME. This approach is outlined in the following.

At high vibrational energies, a quasicontinuum of vibrational states exists and intramolecular vibrational redistribution (IVR) is rapid. Experiments show that IVR is slow at low energy, exhibits multiple time scales, and becomes rapid at energies where the vibrational state density is of the order of  $10^2$ – $10^3$  states/cm<sup>-1</sup>.<sup>23</sup> At these state densities, some vibrational states overlap significantly within their natural widths as governed by infrared spontaneous emission rates. At state densities greater than  $\sim 10^7$  states/cm<sup>-1</sup>, most states are overlapped within their natural widths. The onset of "rapid" IVR is a convenient marker for the onset of the vibrational quasicontinuum. However, this criterion leaves some uncertainty because IVR exhibits multiple time constants and thus some modes remain isolated even at higher vibrational state densities.<sup>23</sup>

A shorter version of the following derivation of centrifugal corrections has been reported elsewhere.<sup>39</sup>

In the vibrational quasicontinuum, individual quantum states cannot be resolved and the master equation can be written as a function of either of two equivalent sets of independent variables:  $E_t, J$  or  $E, J$ . In terms of **active energy**  $E$  and angular momentum quantum number  $J$ , it takes the following form<sup>12,14,20,24</sup>:

$$\begin{aligned} \frac{dN(E', J', t)}{dt} = & F'(E', J', t) + \sum_J \int_0^\infty R(E', J'; E, J) N(E, J; t) dE \\ & - \sum_J \int_0^\infty R(E, J; E', J') N(E', J', t) dE - \sum_{i=1}^{\text{channels}} k_i(E', J') N(E', J', t) \end{aligned} \quad (2.3-1)$$

where the primed  $E'$  and  $J'$  refer to the current state and the unprimed quantities refer to a different state of the excited species, which is undergoing reaction. In Eq. 2.3-1,  $N(E',J',t)dE'$  is the concentration of a chemical species with active energy in the range  $E'$  to  $E'+dE'$ ;  $R(E,J;E',J')$  is the (pseudo-first-order) rate coefficient for collisional energy transfer from initial energy  $E'$  to energy  $E$  and quantum number  $J'$  to  $J$ ;  $F'(E',J',t)dE'$  is a source term (e.g. thermal, chemical, or photo activation, or isomerization); and  $k_i(E',J')$  is the unimolecular reaction rate constant for molecules at energy  $E'$  and rotational quantum number  $J'$  reacting *via* the  $i^{\text{th}}$  reaction channel.

To reduce the 2DME to a 1DME, we first assume that the rotational population distribution describing the adiabatic rotations is always Boltzmann:

$$P_e(J) = Q_J^{-1} g_J \exp(-E_J / k_B T) \quad (2.3-2a)$$

where  $g_J = 2J+1$  for a 2-D symmetric top (which is typically assumed; see Appendix B.4 of this Manual) and other forms for 1-D and spherical tops; the rotational energy  $E_J$  and the rotational partition function  $Q_J$  for the adiabatic rotor(s) are given by Eq. 2.3-2b and 2.3-2c, respectively:

$$E_J = BJ(J+1) \quad (2.3-2b)$$

$$Q_J = \sum_J g_J \exp(-E_J / k_B T) \quad (2.3-2c)$$

The constant  $B$  is the rotational constant. By using these expressions, the concentrations can be written as

$$N(E, J, t) = N(E, t) P_e(J) \quad (2.3-3)$$

In the same spirit, we assume the source function produces the same rotational distribution:

$$F'(E', J', t) = F(E', t) P_e(J') \quad (2.3-4)$$

Although recent trajectory calculations show that the assumption is probably not accurate,<sup>8)</sup> we follow Smith and Gilbert<sup>31</sup> and Miller et al.<sup>21</sup> in adopting the pragmatic assumption that the collision rates in Eq. 1 can be written in a separable form:

$$R(E, J; E', J') = R(E, E') P_e(J) \quad (2.3-5)$$

where  $R(E, E')$  has no dependence on angular momentum and can be expressed as the product of the total vibrationally inelastic collision frequency ( $\omega$ ) multiplied by the "collision step-size distribution",  $P(E, E')$ , which expresses the probability that a molecule initially in the energy range from  $E'$  to  $E'+dE'$  will undergo an inelastic transition to the energy range  $E$  to  $E+dE$ :

$$R(E, E') dE = \int_0^{\infty} R(E, E') dE' \left\{ \frac{R(E, E') dE}{\int_0^{\infty} R(E, E') dE'} \right\}, \quad (2.3-6a)$$

$$= \omega P(E, E') dE \quad (2.3-6b)$$

The first factor on the right hand side of Equation (2.3-6a), the integral over the rates of all inelastic transitions from initial energy  $E'$  can be identified with the frequency of inelastic

collisions,  $\omega$ , which may depend on the initial active energy  $E'$ . Usually, the collision frequency is calculated from the expression  $\omega = k_c[M]$ , where  $k_c$  is the bimolecular rate constant for inelastic collisions and  $[M]$  is bath gas concentration. The second factor (in curly brackets) on the right hand side of Equation (2.3-6a) is  $P(E,E')dE$ . It is important to emphasize that the factorization of  $R(E,E')$  in Equation (2.3-6) is merely for convenience and that  $k_c$  and  $P(E,E')$  never occur independently of one another. Furthermore,  $P(E,E')$  is only a proper probability density function when  $\omega$  is *exactly* equal to the inelastic collision rate constant. With this assumption,  $P(E,E')$  is normalized:

$$\int_0^{\infty} P(E,E')dE = 1 \quad (2.3-7)$$

Note that collision step-size distributions for activating and deactivating collisions are connected *via* detailed balance:

$$\frac{P(E,E')}{P(E',E)} = \frac{\rho(E)}{\rho(E')} \exp\left\{-\frac{E-E'}{k_B T_{trans}}\right\}, \quad (2.3-8)$$

where  $\rho(E)$  is the density of states at active energy  $E$ ,  $T_{trans}$  is the translational temperature, and  $k_B$  is the Boltzmann constant. The relationships among  $P(E,E')$ ,  $k_c$ , and the normalization integral are further discussed below.

Using these definitions, we obtain

$$R(E,J;E',J') = \omega P(E,E') P_e(J) \quad (2.3-9)$$

Smith and Gilbert showed that the master equation can be solved approximately when using this separable form. In MultiWell, this separable form is adopted pragmatically in order to obtain a semi-analytical solution to the master equation. (Miller and coworkers have further generalized the function postulated by Smith and Gilbert,<sup>31</sup> and the details may be found in their papers.<sup>20,21</sup>)

After combining Eq. 2.3-1-9, we obtain

$$\begin{aligned} \frac{dN(E',t)}{dt} P_e(J') &= F(E',t) P_e(J') + \sum_J P_e(J) \omega P_e(J') \int_0^{\infty} P(E';E) N(E,t) dE \\ &\quad - N(E',t) P_e(J') \sum_J P_e(J) \omega \int_0^{\infty} P(E;E') dE - N(E',t) P_e(J') \sum_{i=1}^{channels} k_i(E',J') \end{aligned} \quad (2.3-10)$$

In this expression, the sums over  $J$  are equal to unity because  $P_e(J)$  is normalized. Every term contains the factor  $P_e(J')$ . By summing every term in Eq. 2.3-6 over  $J'$  and noting that the sum equals unity in each term except the last, we obtain

$$\begin{aligned} \frac{dN(E',t)}{dt} &= F(E',t) + \omega \int_0^{\infty} [P(E';E) N(E,t) - P(E;E') N(E',t)] dE \\ &\quad - N(E',t) \sum_{i=1}^{channels} \langle k_i(E') \rangle_J \end{aligned} \quad (2.3-11a)$$

where  $\langle k_i(E') \rangle_J$  is the RRKM specific rate constant, averaged over the rotational energy distribution:

$$\langle k_i(E') \rangle_J = \sum_{J'=0}^{J'_{max}} P_e(J') k_i(E', J') \quad (2.3-11b)$$

The upper limit of the summation ( $J'_{max}$ ) in Eq. 2.3-11b corresponds to the largest angular momentum quantum number for which the well still exists. Eq. 2.3-11 summarizes the general form of the 1-D master equation treated by MultiWell.

The averaging of  $k_i(E', J')$  over the rotational energy distribution may be carried out as follows, using the variables defined in Fig. 2.3-1. The RRKM specific rate constant for a specific  $J'$  can be written<sup>18</sup>

$$k(E', J') = \frac{L^\ddagger G^\ddagger(E^+, J')}{h \rho(E', J')} \quad (2.3-12)$$

where  $L^\ddagger$  is the reaction path degeneracy,  $h$  is Planck's constant,  $G^\ddagger(E^+, J')$  is the sum of states of the transition state as a function of the active energy  $E^+$  in the transition state, and  $\rho(E', J')$  is the density of "vibrational" states of the reactant when the rotational quantum number is  $J'$ . The various energies are related as follows (see Fig. 2.3-1):

$$E' + E_J = E^+ + E_0 + E_J^+ \quad (2.3-13a)$$

or

$$E' = E^+ + E_0 + \Delta E_J \quad (2.3-13b)$$

where  $E_J$  and  $E_J^+$  are the energies of the adiabatic rotations in the reactant and in the transition state, respectively, and  $\Delta E_J = E_J^+ - E_J$ . The rotational energies are given by Eq. 2.3-2b and by the analogous equation:

$$E_J^+ = B^+ J(J+1) \quad (2.3-14)$$

Using these relationships,  $k_i(E', J')$  can be written

$$k(E', J') = \frac{L^\ddagger G^\ddagger(E' - E_0 - \Delta E_J)}{h \rho(E', J')} \quad (2.3-15)$$

From Eqs. 2.3-2b and 2.3-14 it is apparent that  $E_J = (B/B^+)E_J^+$ , and  $\Delta E_J$  can be written as a function of  $E_J^+$  alone:  $\Delta E_J = (1 - B/B^+)E_J^+$ .

For reactions involving bond fission, the rotational constant  $B^+$  for a rigid rotor transition state is smaller than that for the reactant and  $\Delta E_J < 0$ . As the angular momentum quantum number  $J'$  increases, the quantity  $(E_0 - \Delta E_J)$  approaches zero. In other words, the reactant well and the effective critical energy for reaction both vanish when  $J'$  is large enough:  $J'_{max}$  is the largest value of  $J'$  for which the well still exists. For  $J' > J'_{max}$ ,  $k(E', J')$  is not defined. When  $B^+ \leq B$  for rigid rotors,  $J'_{max} = \infty$ .

The rate constant must now be averaged over the rotational population distribution:

$$\langle k(E', J') \rangle_J = Q_J^{-1} \sum_{J'=0}^{J'_{max}} k(E', J') g_J \exp(-E_J / k_B T) \quad (2.3-16a)$$

From the definition of  $\Delta E_J$ , this expression can also be written

$$\langle k(E', J') \rangle_J = Q_J^{-1} \sum_{J'=0}^{J'_{\max}} k(E', J') g_J \exp\left[-(E_J^+ - \Delta E_J) / k_B T\right] \quad (2.3-16b)$$

Equations 2.3-16a and 2.3-12b are suitable for directly averaging over the rotational quantum number. Care must be taken however, because the rate constant is only defined at energies  $E' \geq (E_0 + \Delta E_J)$ . Because  $\Delta E_J \leq 0$ , the reaction threshold may be significantly lower in energy than  $E_0$ , the critical energy for  $J = 0$ .

The *ad hoc* approximate functions postulated by Smith and Gilbert<sup>31</sup> and by Miller and coworkers<sup>20,21</sup> are almost certainly not accurate.<sup>8</sup> Thus we feel that elaborate treatments cannot be justified and have instead adopted the following pragmatic approach.

The active degrees of freedom may include one or more external rotations, which, to a good approximation, may be treated as separable (see Appendix B.4). Typically, for a prolate symmetric top, the K-rotor is regarded as active. For a rigid rotor, the  $K$  quantum number is a "good" quantum number and is restricted to the range from  $-J$  to  $+J$ . However, a highly excited molecule is hardly rigid and  $K$  is not conserved, although it may exhibit a "propensity" to be conserved for some period of time. As a result, it is commonly assumed that the K-rotor of a non-rigid top can exchange energy freely with the internal degrees of freedom: i.e. the K-rotor is usually assumed to be an active degree of freedom.

It is common practice to allow  $K$  to vary freely, except for conservation of energy, and treat the K-rotor as just one more separable degree of freedom when computing densities of states.<sup>11,12,16,28</sup> In fact, treating the K-rotor in this way may be more accurate than restricting  $K$  to the range from  $-J$  to  $+J$ .<sup>2</sup> (This separable-rotors approximation<sup>10</sup> is discussed in Appendix B.4.) However, there always exist  $2J+1$  states with the same value of  $J'$ , even for a completely asymmetric top. Thus neglecting the restriction on  $K$  has the effect of increasing the density and sum of states slightly, but this error is insignificant except for molecules with small rotational constants at very low temperatures.

Here, it is pragmatically assumed that the K-rotor is active and the  $K$  quantum number has no restrictions other than conservation of energy. As a result, the approximate density of states of the reactant molecule has no explicit dependence on the  $J$  quantum number:  $\rho(E', J')$  is replaced by  $\rho(E')$  in Eq. 2.3-16 and the average specific rate constant can be written

$$\langle k(E', J') \rangle_J = \frac{I^\ddagger \langle G^\ddagger(E' - E_0 - \Delta E_J) \rangle_J}{h \rho(E')} \quad (2.3-17a)$$

where the averaged sum of states is given by

$$\langle G^\ddagger(E' - E_0 - \Delta E_J) \rangle_J = \frac{1}{Q_J} \sum_{J'=0}^{J'_{\max}} G^\ddagger(E' - E_0 - \Delta E_J) g_J \exp(-E_J / k_B T) \quad (2.3-17b)$$

where  $J'_{\max}$  is the largest value of  $J'$  for which  $k(E', J')$  is defined.

Another pragmatic approximation is useful. Marcus showed that by substituting an average value  $\langle \Delta E_J \rangle = (1 - B/B^+) \langle E_J^+ \rangle$  in place of  $\Delta E_J$  in Eq. 2.3-13, a useful approximate expression is obtained,<sup>18</sup> which does not retain any explicit dependence on the rotational state  $J'$ :

$$k_a(E') = \frac{I^\ddagger}{h} \frac{G^\ddagger(E' - E_0 - \langle \Delta E_J \rangle)}{\rho(E')} \quad (2.3-18)$$



where the subscript "a" was used by Marcus to denote the approximate form. For present purposes, it is convenient to use the same approximation in the exponential factor in Eq. 2.3-16b, giving

$$\langle k(E') \rangle_J = k_a(E') \exp(\langle \Delta E_J \rangle / k_B T) Q_J^{-1} \sum_{J'} g_{J'} \exp[-E_{J'}^+ / k_B T] \quad (2.3-19)$$

The remaining sum over  $J'$  in Eq. 2.3-19 can be recognized as  $Q_{J'}^+$ , the rotational partition function for the transition state. Marcus found  $\langle E_{J'}^+ \rangle = l k_B T / 2$  (where  $l$  is the number of adiabatic rotors), the average rotational energy in the transition state, by weighting the average according to the reactive flux<sup>18,19</sup> (also see the discussion in Robinson and Holbrook<sup>28</sup> and in Holbrook et al.<sup>16</sup>). Using this value of  $\langle \Delta E_J \rangle \approx (1 - B/B^+) l k_B T / 2 = (1 - I^+/I) l k_B T / 2$ , where  $I$  and  $I^+$  are the moments of inertia for the adiabatic rotor in the reactant and the transition state, respectively.<sup>18</sup> The final result can be written as

$$\langle k(E') \rangle_J = k_a(E') \frac{Q_J^+}{Q_J} \exp(\langle \Delta E_J \rangle / k_B T) \quad (2.3-20a)$$

or

$$\langle k(E') \rangle_J = k_a(E') \left( \frac{B}{B^+} \right)^{l/2} \exp\left( \frac{l}{2} \left[ 1 - \frac{B}{B^+} \right] \right) \quad (2.3-20b)$$

or

$$\langle k(E') \rangle_J = k_a(E') \left( \frac{I^+}{I} \right)^{l/2} \exp\left( \frac{l}{2} \left[ 1 - \frac{I^+}{I} \right] \right) \quad (2.3-20c)$$

where the ratio of the (classical) rotational partition functions has been replaced by the ratio of the rotational constants or moments of inertia, and  $l$  is the number of adiabatic rotors. Usually it is assumed that  $l = 2$ .

These simplified forms perform well in master equation simulations, although the energy transfer parameters may differ to some extent from other treatments. These possible differences are generally not considered further, because no current master equation treatment of energy transfer is known to be correct and because energy transfer parameters and collision step-size distributions generally are not known from other sources, but are simply used as empirical fitting parameters.

### High Pressure and Low Pressure Limits: $k_\infty$ and $k_0$

Prior to the release of Multiwell-2011.1, we became aware of a problem with the implementation of the centrifugal factors in MultiWell. David Golden pointed out that at very high temperatures, where it is possible to simulate both a recombination reaction and its reverse dissociation, the two rate constants were inconsistent with each other. This discrepancy was traced to the centrifugal corrections. This problem has been corrected, and a discussion of the current and prior versions of  $k_0$  and  $k_\infty$  can be found in Appendix B.10 of this User Manual.

The high pressure rate constant is the average rate constant at pressures high enough so that differences of the actual population distribution from the thermal Boltzmann distribution are negligible. The thermal Boltzmann energy distribution for reactant A is

$$B_A(E', T) = Q_A^{-1} \rho_A(E') \exp(-E' / k_B T) \quad (2.3-21a)$$

where the partition function  $Q_A$  is

$$Q_A = \int_0^{\infty} \rho_A(E') \exp(-E' / k_B T) dE' \quad (2.3-21b)$$

The average rate constant is therefore

$$k_{\infty}(T) = \frac{1}{Q_A} \int_0^{\infty} \langle k_a(E') \rangle_J \rho_A(E') \exp(-E' / k_B T) dE' \quad (2.3-22a)$$

or

$$k_{\infty}(T) = \frac{1}{Q_A} \frac{Q_J^{\dagger}}{Q_J} \int_0^{\infty} k_a(E') \rho_A(E') \exp\left[-\left(E' - \langle \Delta E_J \rangle\right) / k_B T\right] dE' \quad (2.3-22b)$$

By transforming the variable of integration from  $E'$  to  $E^+$  (i.e. by replacing  $\Delta E_J$  in Eq. 2.3-7b with the average value,  $\langle \Delta E_J \rangle$  and obtaining  $E^+ = E' - E_0 - \langle \Delta E_J \rangle$ ) and changing the limits of integration, the resulting expression for  $k_{\infty}$  is the same as canonical TST (Eq. 4.30 of Robinson and Holbrook,<sup>28</sup> and Eq. 3.30 in Holbrook et al.<sup>16</sup> at the high pressure limit).

### Comparison with Other Models

Equation 3.30 in Holbrook et al.<sup>16</sup> and Eq. 4.30 in Robinson and Holbrook<sup>28</sup> are based on the strong collision assumption, in which every collision results in producing a canonical active energy distribution. In this section, the strong-collision rate constant is derived using the rotationally averaged  $\langle k(E') \rangle_J$ . For convenience, concentration is written as the product of a normalized energy distribution,  $y(E', t)$ , and a time-dependent total concentration,  $N(t)$ :

$$N(E', t) = N(t) y(E', t) \quad (2.3-23)$$

where  $N(t)$  decays with time and the energy distribution  $y(E', t)$  is normalized at all times. With this substitution, the LHS of Eq. 2.3-5 becomes

$$\frac{dN(E', t)}{dt} = y(E', t) \frac{dN(t)}{dt} + N(t) \frac{dy}{dt} \quad (2.3-18)$$

In the absence of chemical reaction and input flux, and given enough time, the population distribution relaxes to steady state and  $dy/dt = 0$ . Furthermore, the unimolecular rate constant (for channel  $i$ ) is defined at steady state:  $k_{uni,i} = -N^{-1} dN/dt$ . Thus, after simplification the steady-state master equation can be written

$$\begin{aligned} -y(E') k_{uni,i} = & \frac{F(E', t)}{N(t)} + \int_0^{\infty} R(E'; E) y(E) dE \\ & - y(E') dE \left[ \int_0^{\infty} R(E; E') dE + \sum_{i=1}^{channels} \langle k_i(E') \rangle_J \right] \end{aligned} \quad (2.3-21)$$

When  $F(E', t) = 0$ , Eq. 2.3-21 can be solved for the steady-state population distribution  $y(E')$ :

$$y(E') = \frac{\int_0^{\infty} R(E'; E) y(E) dE}{\left[ \int_0^{\infty} R(E; E') dE + \sum_{i=1}^{\text{channels}} \langle k_i(E') \rangle_J \right] - k_{uni,i}} \quad (2.3-22)$$

To obtain  $k_{uni,i}$  with the strong-collider approximation, we use the following identity:

$$R(E; E') = k_c [M] \frac{\rho(E) \exp(-E/k_B T)}{Q_2(T)} \quad (2.3-23)$$

where the rate of energy transfer is expressed as the product of a collision rate constant  $k_c$  and collider bath concentration  $[M]$ , multiplying a thermal canonical energy distribution, which is normalized by the partition function. Note that according to the strong-collider assumption, the energy transfer rate has no dependence on the energy prior to collision. With this substitution, the integrals in eq. 2.3-22 can be evaluated readily:

$$\int_0^{\infty} R(E'; E) y(E) dE = k_c [M] \frac{\rho(E') \exp(-E'/k_B T)}{Q_2(T)} \int_0^{\infty} y(E) dE \quad (2.3-24a)$$

$$= k_c [M] \frac{\rho(E') \exp(-E'/k_B T)}{Q_2(T)} \quad (2.3-24b)$$

$$\int_0^{\infty} R(E; E') dE = \frac{k_c [M]}{Q_2(T)} \int_0^{\infty} \rho(E) \exp(-E/k_B T) dE = k_c [M] \quad (2.3-25)$$

Thus eq. 2.3-22 becomes

$$y(E') = \frac{k_c [M] \rho(E') \exp(-E'/k_B T)}{\left[ k_c [M] + \sum_{i=1}^{\text{channels}} \langle k_i(E') \rangle_J \right] - k_{uni,i}} \frac{1}{Q_2(T)} \quad (2.3-26)$$

Except at extremely low internal energies, the magnitude of  $k_{uni}$  is much smaller than the rotationally averaged  $\langle k(E') \rangle_J$  and hence can be neglected in the denominator. The reaction rate at active energy  $E'$  is given by the product of  $y(E')$  and  $\langle k(E') \rangle_J$ . After integrating over all internal energies greater than  $E_0' = E_0 + \langle \Delta E_J \rangle$ , the reaction critical energy, we obtain the strong-collider unimolecular rate constant for channel  $i$ :

$$k_{uni,i} = \int_{E_0 + \langle \Delta E_J \rangle}^{\infty} \frac{k_c [M] \langle k_i(E') \rangle_J}{\left[ k_c [M] + \sum_{i=1}^{\text{channels}} \langle k_i(E') \rangle_J \right]} \frac{\rho(E') \exp(-E'/k_B T)}{Q_2(T)} dE' \quad (2.3-27)$$

Low pressure limit:

$$k_{low,i} = \frac{k_c[M]}{Q_2(T)} \int_{E_0+\langle \Delta E_J \rangle}^{\infty} \rho(E') \exp(-E'/k_B T) dE' \quad (2.3-28)$$

High pressure limit:

$$k_{\infty,i} = \frac{1}{Q_2(T)} \int_{E_0+\langle \Delta E_J \rangle}^{\infty} \langle k_i(E') \rangle_J \rho(E') \exp(-E'/k_B T) dE' \quad (2.3-29)$$

### ***A.2.4 Multiple Species (Wells) and Multiple Reaction Channels***

Here we consider chemical species that can be identified with local minima (wells) on the potential energy hypersurface. These species are distinct from transition states, which are located at saddle points. In MultiWell, each well is assigned an arbitrary index for identification and reactions are conveniently labeled with two indices: one to designate the reactant and the other to designate the product. For simplicity in notation, one or more of these indices are omitted in some of the following discussion.

A master equation such as Equation (2.3-1) can be written for each well and the equations are coupled via the chemical reaction terms. Each reaction channel is associated either with another well, or with fragmentation products. Each isomerization is reversible and the transition state is the same for the corresponding forward and reverse reactions. In principle, the existence of isomers leads to splitting of vibrational levels, as in the inversion doubling of ammonia, but if tunneling is negligible, the wells can be considered independently.<sup>40</sup> Thus each well has its own vibrational assignment, molecular structure, and corresponding density of states.

Two technical problems arise when using an energy grained master equation<sup>11,12,14,16,28</sup> to simulate multiple-well systems. First, the number of coupled differential equations can grow prohibitively as the energy grain size ( $\Delta E_{\text{grain}}$ ) is reduced, making the numerical solution very difficult or impossible. Second, because each well has its own zero of energy and reaction threshold (critical) energies, it is difficult to match the energy grain boundaries. The reaction threshold energies for forward and reverse reactions are tied to one another. For accurate numerical results it is necessary to match the energy grains of the coupled wells. The matching of energy grains at one reaction threshold may lead to mis-matches at other thresholds and to artificially shifted energies of the wells, relative to one another. These energy shifts produce anomalous results for large grain sizes. This problem can be neglected if the energy grains are very small, but small energy grains lead to very large sets of coupled equations. In all cases, the calculations should be repeated with successively smaller energy grains until the results are independent of  $\Delta E_{\text{grain}}$ : convergence must be achieved.

When a continuum master equation is used, energy mis-matching and anomalous shifts never create problems. However, the sparse density of states regime at low energies within wells and for transition states near reaction thresholds is not well represented by a continuum model. This difficulty is minimized in MultiWell by using a hybrid master equation approach.

### ***A.2.5 Hybrid Master Equation Formulation***

Effectively, the hybrid master equation formulation uses a continuum master equation in the quasicontinuum at high vibrational energies, and an energy-grained master equation at low energies, where the state density is distinctly discontinuous. This is accomplished by using

Equation (2.3-1) for the continuum master equation throughout the entire energy range but discretizing the state density, population, and transition rates at low energy. At high energy, Multiwell employs interpolation to determine the density of states and specific rate constants ( $k(E)$ ). Values of  $\rho(E)$  and  $k(E)$  are stored in ordered arrays at specific values of  $E$  and intermediate values are determined by interpolation. At low energies, ordered arrays of  $\rho(E)$  and  $k(E)$  are stored at smaller energy spacing ( $\Delta E_{\text{grain}}$ ) and interpolation is not used: the array entries nearest in energy are utilized directly. The two ordered arrays used for each energy-dependent quantity ( $\rho(E)$ ,  $k(E)$ , etc.) are combined in "double arrays" which are discussed in the next section. At all energies, numerical integration is carried out with the trapezoidal rule, which introduces an energy grain in the low energy regime (where state densities are sparse), but gives good continuum results at high energy (where the state densities are smooth).

If a stochastic trial (see below) calls for a transition from the continuum space to an energy in the discrete space, the energy is aligned with the discrete energy grain. At low energy, many energy grains do not contain states ( $\rho(E) = 0$ ) and transitions are not allowed to those states in MultiWell. As a result, population only resides in energy grains that contain states and collisional transitions low on the energy ladder can only take place with relatively large energy changes, due to the sparse density of states.

### ***A.2.6 Energy Grain in the Hybrid Master Equation***

Through the use of double arrays, high energy resolution is achieved in densities and sums of states at low energy and near reaction thresholds. By default, the double arrays have 500 elements (the dimensions can be changed, if desired). The low energy portion of the array is specified according to  $\Delta E_{\text{grain}}$  and the number of array elements assigned to the low energy portion of the double array. The high energy portion is specified only according to the maximum energy. Thus the number of array elements used in the high energy portion and the energy grain in the high energy portion both depend on how many array elements remain after assigning the low energy portion. The same specifications are used for all double arrays, including arrays for densities of states ( $\rho(E)$ ), sums of states ( $G^\ddagger(E-E_0)$ ), specific rate constants ( $k(E-E_0)$ ), etc. The discretization of these quantities is the natural result of exact count algorithms.

An example of a double array for the density of states  $\rho(E)$  is shown in Figure 1 for benzene (vibrations<sup>15</sup> + K-rotor). In this example, the density of states was calculated using an energy grain of  $\Delta E_{\text{grain}} = 10 \text{ cm}^{-1}$  and exact counts up to an energy of  $85000 \text{ cm}^{-1}$ , although only energies up to  $10000 \text{ cm}^{-1}$  are shown in the figure. In this example, the low energy regime was defined as the first 250 elements of a double array and thus covered the range from 0 to  $2490 \text{ cm}^{-1}$ . The remaining 250 elements of the double array overlap the low energy portion and cover the range all the way from 0 to  $85000 \text{ cm}^{-1}$  (the high energy regime) with an energy grain of  $341.4 \text{ cm}^{-1}$ . In Figure 1,  $\rho(E)$  calculated with  $\Delta E_{\text{grain}} = 10 \text{ cm}^{-1}$  is shown as the thin solid line and the double array elements are shown as the solid dots. The upper energy boundary for low energy range was chosen to fall within the vibrational quasicontinuum, as evidenced by  $\rho(E) \geq 100 \text{ states/cm}^{-1}$  and by the relative smoothness of the plot of  $\rho(E)$ . When  $\rho(E)$  is sufficiently smooth, relatively little error is introduced by interpolating between the double array points.

In principle, convergence tests should be carried out for each simulation. Tests for convergence as  $\Delta E_{\text{grain}}$  is reduced reflect several simultaneous effects: the  $\rho(E)$  grain size is varied for every well, the  $G^\ddagger(E-E_0)$  grain size is varied for every reaction, and the energy range covered by the low energy portion of every double array is varied. Because several attributes are affected by  $\Delta E_{\text{grain}}$ , the variation of results with grain size cannot be interpreted precisely without

extensive tests. However, as long as the energy range covered by the low energy portion of the double arrays is sufficient, smaller grain sizes will produce more accurate results and the results are seen to converge at small  $\Delta E_{\text{grain}}$ , as illustrated in Figure 4 of Reference <sup>7</sup>.

Typical convergence tests<sup>7</sup> show that 250 bins with  $\Delta E_{\text{grain}} = 10 \text{ cm}^{-1}$  are usually suitable for the low energy portion of the double arrays. The upper energy bound for the high energy portion is typically  $85000 \text{ cm}^{-1}$  to  $100000 \text{ cm}^{-1}$ , depending on the temperature range and activation method being simulated. The small grain at every reaction threshold gives accurate results for the unimolecular reaction rates. The small grain at low energy within each well gives a good representation of the sparse density of states regime in every well. To achieve comparable numerical results by the matrix solution<sup>14</sup> of an energy-grained master equation for just a single well would require finding the eigenvalues of a matrix with  $8500 \times 8500$  elements...a difficult task. The hybrid master equation approach has a distinct advantage in this regard.

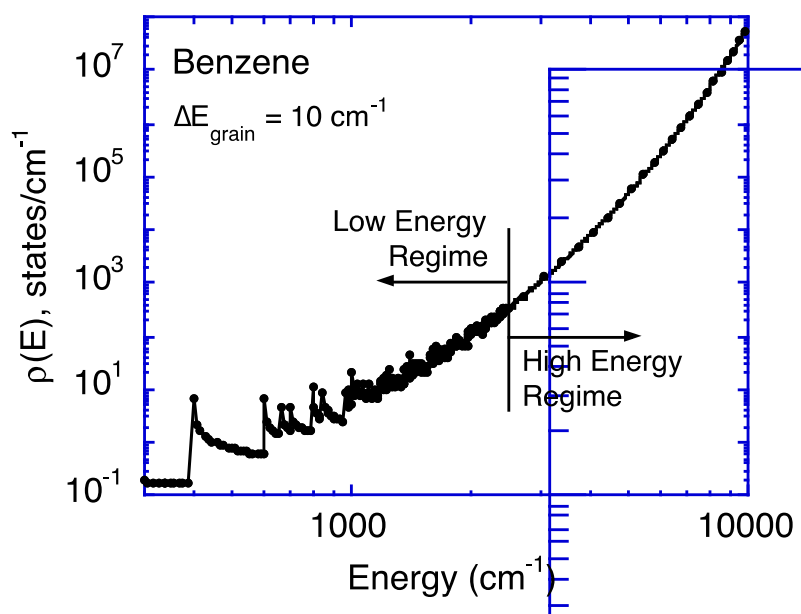


**Figure 1.** Density of states for benzene (including vibrations and one active external rotation). Solid line: density of states from exact count ( $\Delta E_{\text{grain}} = 10 \text{ cm}^{-1}$ ); solid dots: elements of double array (see text for details).

## References

- (1) Astholz, D. C.; Troe, J.; Wieters, W. Unimolecular processes in vibrationally highly excited cycloheptatrienes. I. Thermal isomerization in shock waves. *J. Chem. Phys.* **1979**, *70*, 5107-5116.
- (2) Aubanel, E. E.; Wardlaw, D. M.; Zhu, L.; Hase, W. L. Role of angular momentum in statistical unimolecular rate theory. *Int. Rev. Phys. Chem.* **1991**, *10*, 249-286.
- (3) Baer, T.; Hase, W. L. *Unimolecular Reaction Dynamics. Theory and Experiments*; Oxford University Press: New York, 1996.

- (4) Barker, J. R. Monte-Carlo Calculations on Unimolecular Reactions, Energy-Transfer, and IR-Multiphoton Decomposition. *Chem. Phys.* **1983**, *77*, 301-318.
- (5) Barker, J. R. Multiple-well, multiple-path unimolecular reaction systems. I. MultiWell computer program suite. *Int. J. Chem. Kinet.* **2001**, *33*, 232-245; <https://doi.org/10.1002/kin.1017>.
- (6) Barker, J. R. Monte Carlo stochastic simulation of the master equation for unimolecular reaction systems. In *Unimolecular Kinetics. Parts 2 and 3: Collisional Energy Transfer and The Master Equation*; Robertson, S. H., Ed.; Elsevier, 2019; Vol. 43; pp 409-463.
- (7) Barker, J. R.; Ortiz, N. F. Multiple-Well, multiple-path unimolecular reaction systems. II. 2-methylhexyl free radicals. *Int. J. Chem. Kinet.* **2001**, *33*, 246-261; DOI: 10.1002/kin.1018.
- (8) Barker, J. R.; Weston, R. E., Jr. Collisional Energy Transfer Probability Densities P(E,J;E',J') for Monatomics Colliding with Large Molecules. *J. Phys. Chem. A* **2010**, *114*, 10619-10633; 10.1021/jp106443d.
- (9) Beyer, T.; Swinehart, D. F. Number of multiply-restricted partitions. *Comm. Assoc. Comput. Machines* **1973**, *16*, 379.
- (10) Current, J. H.; Rabinovitch, B. S. Decomposition of Chemically Activated Ethyl-d<sub>3</sub> Radicals. Primary Intramolecular Kinetic Isotope Effect in a Nonequilibrium System. *J. Chem. Phys.* **1963**, *38*, 783-795.
- (11) Forst, W. *Theory of Unimolecular Reactions*; Academic Press: New York, 1973.
- (12) Forst, W. *Unimolecular Reactions. A Concise Introduction*; Cambridge University Press: Cambridge, 2003.
- (13) Frisch, M. J.; Trucks, G. W.; Schlegel, H. B.; Scuseria, G. E.; Robb, M. A.; Cheeseman, J. R.; Scalmani, G.; Barone, V.; Mennucci, B.; Petersson, G. A.; Nakatsuji, H.; Caricato, M.; Li, X.; Hratchian, H. P.; Izmaylov, A. F.; Bloino, J.; Zheng, G.; Sonnenberg, J. L.; Hada, M.; Ehara, M.; Toyota, K.; Fukuda, R.; Hasegawa, J.; Ishida, M.; Nakajima, T.; Honda, Y.; Kitao, O.; Nakai, H.; Vreven, T.; J. A. Montgomery, J.; Peralta, J. E.; Ogliaro, F.; Bearpark, M.; Heyd, J. J.; Brothers, E.; Kudin, K. N.; Staroverov, V. N.; Kobayashi, R.; Normand, J.; Raghavachari, K.; Rendell, A.; Burant, J. C.; Iyengar, S. S.; Tomasi, J.; Cossi, M.; Rega, N.; Millam, J. M.; Klene, M.; Knox, J. E.; Cross, J. B.; Bakken, V.; Adamo, C.; Jaramillo, J.; Gomperts, R.; Stratmann, R. E.; Yazyev, O.; Austin, A. J.; Cammi, R.; Pomelli, C.; Ochterski, J. W.; Martin, R. L.; Morokuma, K.; Zakrzewski, V. G.; Voth, G. A.; Salvador, P.; Dannenberg, J. J.; Dapprich, S.; Daniels, A. D.; Farkas, O.; Foresman, J. B.; Ortiz, J. V.; Cioslowski, J.; Fox, D. J. Gaussian 09, Revision A.1; Revision A.1 ed.; Gaussian, Inc.: Wallingford CT, 2009.
- (14) Gilbert, R. G.; Smith, S. C. *Theory of Unimolecular and Recombination Reactions*; Blackwell Scientific Publications: Oxford, 1990.
- (15) Goodman, L.; Ozkabak, A. G.; Thakur, S. N. A benchmark vibrational potential surface: ground state benzene. *J. Phys. Chem.* **1991**, *95*, 9044.
- (16) Holbrook, K. A.; Pilling, M. J.; Robertson, S. H. *Unimolecular Reactions*, 2 ed.; Wiley: Chichester, 1996.
- (17) Jeffrey, S. J.; Gates, K. E.; Smith, S. C. Full iterative solution of the two-dimensional master equation for thermal unimolecular reactions. *J. Phys. Chem.* **1996**, *100*, 7090-7096.
- (18) Marcus, R. A. Dissociation and isomerization of vibrationally excited species. III. *J. Chem. Phys.* **1965**, *43*, 2658-2661.

- (19) Marcus, R. A. Erratum: Dissociation and Isomerization of Vibrationally Excited Species [J. Chem. Phys. 43,2658 (1965)]. *J. Chem. Phys.* **1970**, *52*, 1018.
- (20) Miller, J. A.; Klippenstein, S. J. Master Equation Methods in Gas Phase Chemical Kinetics. *J. Phys. Chem. A* **2006**, *110*, 10528-10544.
- (21) Miller, J. A.; Klippenstein, S. J.; Raffy, C. Solution of some one- and two-dimensional master equation models for thermal dissociation: The dissociation of methane in the low pressure limit. *JPCA* **2002**, *106*, 4904-4913.
- (22) Penner, A. P.; Forst, W. Transfer of vibrational-rotational energy in thermal reactions: application to polyatomics. *Chemical Physics* **1976**, *13*, 51-64.
- (23) Perry, D. S. Time scales and mechanisms of intramolecular energy redistribution. In *Highly Excited States: Relaxation, Reaction, and Structure*; Mullin, A., Schatz, G. C., Eds.; American Chemical Society: Washington DC, 1997; Vol. 678; pp 70-80.
- (24) Pilling, M. J.; Robertson, S. H. Master equation models for chemical reactions of importance in combustion. *Annual Review of Physical Chemistry* **2003**, *54*, 245-275.
- (25) Press, W. H.; Teukolsky, S. A.; Vetterling, W. T.; Flannery, B. P. *Numerical Recipes in FORTRAN. The Art of Scientific Computing*, 2 ed.; Cambridge University Press: Cambridge, 1992.
- (26) Robertson, S. H. Foundations of the master equation. In *Unimolecular Kinetics: Parts 2 and 3: Collisional Energy Transfer and the Master Equation*; Robertson, S. H., Ed.; Elsevier, 2019; Vol. 43; pp 299-361.
- (27) Robertson, S. H.; Shushin, A. I.; Wardlaw, D. M. Reduction of the two dimensional master equation to a Smolouchowsky type differential equation with application to  $\text{CH}_4 \rightarrow \text{CH}_3 + \text{H}$ . *J. Chem. Phys.* **1993**, *98*, 8673-8679.
- (28) Robinson, P. J.; Holbrook, K. A. *Unimolecular Reactions*; Wiley-Interscience: London; New York, 1972.
- (29) Smith, S. C.; Frankcombe, T. J. Numerical Methods. In *Unimolecular Kinetics: Parts 2 and 3: Collisional Energy Transfer and the Master Equation*; Robertson, S. H., Ed.; Elsevier, 2019; Vol. 43; pp 363-408.
- (30) Smith, S. C.; Gilbert, R. G. Angular momentum conservation in multichannel unimolecular reactions. *International Journal of Chemical Kinetics* **1988**, *20*, 979-990.
- (31) Smith, S. C.; Gilbert, R. G. Angular momentum conservation in unimolecular and recombination reactions. *International Journal of Chemical Kinetics* **1988**, *20*, 307-329.
- (32) Smith, S. C.; McEwan, M. J.; Gilbert, R. G. The pressure dependence of ion-molecule association rate coefficients. *Journal of Chemical Physics* **1989**, *90*, 1630-1640.
- (33) Stanton, J. F.; Gauss, J.; Harding, M. E.; Szalay, P. G.; Auer, w. c. f. A. A.; Bartlett, R. J.; Benedikt, U.; Berger, C.; Bernholdt, D. E.; Bomble, Y. J.; Christiansen, O.; Heckert, M.; Heun, O.; Huber, C.; Jagan, T.-C.; Jonsson, D.; Jusélius, J.; Klein, K.; Lauderdale, W. J.; Matthews, D. A.; Metzroth, T.; O'Neill, D. P.; Price, D. R.; Prochnow, E.; Ruud, K.; Schiffmann, F.; Stopkowicz, S.; Vázquez, J.; Wang, F.; Watts, J. D. and the integral packages MOLECULE (J. Almlöf and P.R. Taylor); PROPS (P.R. Taylor); ABACUS (T. Helgaker, H.J. Aa. Jensen, P. Jørgensen, and J. Olsen); and ECP routines by A. V. Mitin and C. van Wüllen. CFOUR, a quantum chemical program package ([www.cfour.de/](http://www.cfour.de/)), 2009.
- (34) Stein, S. E.; Rabinovitch, B. S. Accurate evaluation of internal energy level sums and densities including anharmonic oscillators and hindered rotors. *J. Chem. Phys.* **1973**, *58*, 2438-2445.



- (35) Troe, J. Theory of thermal unimolecular reactions at low pressures. I. Solution of the Master Equation. *Journal of Chemical Physics* **1977**, *66*, 4745-4757.
- (36) Venkatesh, P. K.; Dean, A. M.; Cohen, M. H.; Carr, R. W. Master equation analysis of intermolecular energy transfer in multiple-well, multiple-channel unimolecular reactions. I. Basic Theory. *Journal of Chemical Physics* **1997**, *107*, 8904-8916.
- (37) Waage, E. V.; Rabinovitch, B. S. Centrifugal effects in reaction rate theory. *Chemical Reviews* **1970**, *70*, 377-387.
- (38) Werner, H.-J.; Knowles, P. J.; Lindh, R.; Manby, F. R.; Schütz, M.; Celani, P.; Korona, T.; Rauhut, G.; Amos, R. D.; Bernhardsson, A.; Berning, A.; Cooper, D. L.; Deegan, M. J. O.; Dobbyn, A. J.; Eckert, F.; Hampel, C.; Hetzer, G.; Lloyd, A. W.; McNicholas, S. J.; W. Meyer, W.; Mura, M. E.; Nicklass, A.; Palmieri, P.; Pitzer, R.; Schumann, U.; Stoll, H.; Stone, A. J.; Tarroni, R.; Thorsteinsson, T. MOLPRO version 2006.1 (a package of *ab initio* programs); version 2006.1 ed.; see <http://www.molpro.net>, 2006.
- (39) Weston, R. E., Jr.; Nguyen, T. L.; Stanton, J. F.; Barker, J. R. HO + CO Reaction Rates and H/D Kinetic Isotope Effects: Master Equation Models with *ab Initio* SCTST Rate Constants. *J. Phys. Chem. A* **2013**, *117*, 821-835; <http://dx.doi.org/10.1021/jp311928w>.
- (40) Wilson, E. B., Jr.; Decius, J. C.; Cross, P. C. *Molecular Vibrations. The Theory of Infrared and Raman Vibrational Spectra*; McGraw-Hill Book Company, Inc.: New York, 1955.

### A.3. Stochastic Method

#### A.3.1 Gillespie's (Exact) Stochastic Simulation Algorithm

Gillespie showed that a stochastic method gives the exact solution to a set of ordinary differential equations in the limit of an infinite number of stochastic trials.<sup>2,4</sup> The algorithm has been described in the context of chemical kinetics.<sup>1,3,5</sup> If a Markovian system is in a given state and can make transitions to other states via a set of transition rate coefficients, then for a given step in a stochastic simulation, Gillespie's algorithm gives a prescription for a) finding the duration of the time step and b) selecting the transition from among the choices. This algorithm is repeated step-by-step as long as desired and as long as transitions are possible.

Gillespie's method can be applied to both linear and non-linear systems.<sup>3</sup> Equation (2.3-1) is linear in  $y(E,t)$ , which leads to a particularly convenient result which is described below. If Equation (1) contained non-linear terms to describe energy pooling, for example, the terms would contain factors such as the product  $y(E,t) \times y(E',t)$ . To solve this system numerically requires using an energy-grained master equation with a swarm of stochastic trials and storing an evolving vector of populations as a function of energy. Here, the number of stochastic trials can be identified with a number of pseudo molecules that initially are placed in a set of energy grains. At each time step, a pseudo molecule is moved from one energy grain to another as described by Gillespie and the swarm of pseudo molecules maps out the evolving energy distribution. This approach has been used by Vereecken et al.<sup>10,11</sup> to simulate unimolecular and recombination reactions and it can in principle be extended to non-linear systems. The difficulties in this approach are associated with the energy-grained master equation (see above) and with the requirement for storage of the entire vector of  $y(E,t)$  at every time step. Given the current availability of inexpensive computer memory, the latter is not a serious limitation for single-well reaction systems. When several wells are involved, the bookkeeping is cumbersome.

Moreover, the memory requirements of this technique can become prohibitive in the future if the one-dimensional master equation is to be extended to two dimensions by explicitly including angular momentum. MultiWell is designed so that the future extension to two-dimensions will be feasible.

For linear master equations, a different strategy<sup>1</sup> is possible using Gillespie's algorithm. Instead of using a swarm of stochastic molecules and storage of  $y(E,t)$  at every step, stochastic trials are run one at a time and snapshots of  $E$  and other variables are stored at convenient time intervals. The vector  $y(E,t)$  does not need to be stored. A "snapshot" simply records the energy and other properties of a single stochastic molecule as it progresses through a stochastic trial. The snapshot has no effect on the physics of the trial. Since the system is linear, the averaged result of an ensemble of stochastic trials gives the same result as a swarm of stochastic molecules. By retaining only the averaged results of the snapshots, the memory storage requirements are greatly reduced.

For a linear master equation, the loss terms can be expressed as first order in  $y(E,t)$  with first order rate coefficients  $A_j$  for  $k$  paths. These rate coefficients can be identified with the unimolecular rate constants and the collision frequency in Equation (2.3-1). According to Gillespie's algorithm, the duration of the next time step is chosen by using the uniform random deviate (i.e. random number)  $r_1$  :

$$\tau = \frac{-\ln(r_1)}{A_T} \quad (3.1-1a)$$

where

$$A_T = \sum_{j=1}^k A_j \quad (3.1-1b)$$

The transition is selected from among the  $k$  paths by using a second random number  $r_2$ :

$$\sum_{j=1}^{n-1} A_j < r_2 A_T \leq \sum_{j=n}^k A_j \quad (3.1-2)$$

Here, the transition takes place via path  $n$  at time  $t+\tau$ .

According to Gillespie's algorithm, the time intervals between stochastic steps are chosen randomly by Equation (3.1-1a). Thus the progress of the stochastic simulation is monitored via snapshots, as mentioned above. If collisional activation or deactivation is the result of a transition, then the next stochastic step is calculated using rate coefficients appropriate to the new energy. If isomerization to another well is the result of a transition, then the next stochastic step is calculated using the first order rate coefficients appropriate to the new well, based on  $E$  measured from the zero point energy of the new well. The snapshots from many stochastic trials are averaged. The results include the time-dependent average fractional populations of the isomers, the average internal energy of each isomer, and fractional yields of the fragmentation products, etc.

The computer time required for any given stochastic simulation depends on  $N_{\text{trials}}$ , the simulated time duration, and on the properties of the system that affect  $A_T$  in Equation (3.1-1b). For example, one of the  $A_j$  terms is the collision frequency, which is proportional to pressure. If the collision frequency is the dominant term in Equation (3.1-1b), then the average stochastic time-step is inversely proportional to pressure and the number of time steps (and the

corresponding computer execution time) for the given simulated time duration is proportional to pressure. Of course, collision frequency is not always the dominant term in Equation (3.1-1b), but the same qualitative considerations can help in estimating required computer time.

Note that the effectiveness of Equation (3.1-2) is limited by the properties of the random number generator. The characteristics of various random number generators are discussed elsewhere,<sup>6-8</sup> where many potential pitfalls are described. It is important to use random number generators that have been thoroughly tested. Even assuming the random number generator produces a sequence that has no serial correlations, the number of random numbers in a sequence is limited and this imposes a limitation on the relative magnitudes of the  $A_m$  terms that can be selected according to Equation (3.1-2). For a 32-bit computer, a typical random number sequence contains  $2^{31}-1 \approx 2.1 \times 10^9$  equally-spaced numbers. Thus if the ratio of minimum to maximum values of the rate constants is less than  $\sim 0.5 \times 10^{-9}$ , then the path with the smaller rate can *never* be selected. Thus the random number generator places a rigorous upper bound on the dynamic range of rates that can be selected. A more serious limitation, however, is that an extraordinarily large number of stochastic trials is required in order to sample rare events with useful precision, as discussed in the next section.

### A.3.2 Stochastic Uncertainties

The precision of the results obtained using stochastic methods depends on the number of stochastic trials. In the systems simulated by MultiWell, several species coexist and their relative populations sum to unity:

$$1 = f_1 + f_2 + \dots = \sum_{i=1}^{\text{species}} f_i \quad (3.2-1)$$

The standard deviation in the instantaneous relative population of the  $i^{\text{th}}$  species is the square root of the variance calculated according to the multinomial distribution<sup>9</sup>:

$$\sigma_i = \sqrt{\frac{1}{N_{\text{trials}}} f_i (1 - f_i)} \quad (3.2-2)$$

where  $f_i$  is the fractional population of the  $i^{\text{th}}$  species and  $N_{\text{trials}}$  is the number of stochastic trials. Note that the standard deviation is reduced as the number of trials increases. Also note that the product  $f_i(1-f_i)$  appears in Equation (3.2-2). Thus, the standard deviation is the same when, for example,  $f_i=0.01$  and when  $f_i=0.99$ . These standard deviations are calculated and reported by MultiWell in its general output.

A large number of stochastic trials is needed when rare events must be simulated with high precision. Suppose that  $f_i = 0.01$  and the desired precision corresponds to a relative statistical error of 1% (i.e.  $\sigma_i/f_i = 0.01$ ). From Equation (8), one finds the required number of stochastic trials:  $N_{\text{trials}} \approx 10^6$ . For a relative error of 10%, only about  $10^4$  trials are needed. Thus, the required number of stochastic trials places a practical limit on the precision attainable for minor pathways.

## References

- (1) Barker, J. R. Monte-Carlo Calculations on Unimolecular Reactions, Energy-Transfer, and IR-Multiphoton Decomposition. *Chem. Phys.* **1983**, *77*, 301-318.
- (2) Gillespie, D. T. A general method for numerically simulating the stochastic time evolution of coupled chemical reactions. *J. Comp. Phys.* **1976**, *22*, 403-434.
- (3) Gillespie, D. T. Exact stochastic simulation of coupled chemical reactions. *J. Phys. Chem.* **1977**, *81*, 2340-2361.
- (4) Gillespie, D. T. Monte Carlo simulation of random walks with residence time dependent transition probability rates. *J. Comp. Phys.* **1978**, *28*, 395-407.
- (5) Gillespie, D. T. A rigorous derivation of the chemical master equation. *Physica A: Statistical and Theoretical Physics (Amsterdam)* **1992**, *188*, 404-425.
- (6) Knuth, D. E. *Seminumerical Algorithms*, 2 ed.; Addison-Wesley: Reading, MA, 1981; Vol. 2.
- (7) Press, W. H.; Teukolsky, S. A. [Random number generators]. *Computers in Physics* **1992**, *6*, 522-524.
- (8) Press, W. H.; Teukolsky, S. A.; Vetterling, W. T.; Flannery, B. P. *Numerical Recipes in FORTRAN. The Art of Scientific Computing*, 2 ed.; Cambridge University Press: Cambridge, 1992.
- (9) Tsokos, C. P. *Probability Distributions: An Introduction to Probability Theory with Applications*; Wadsworth Publishing Company Inc.: Belmont CA, 1972.
- (10) Venkatesh, P. K.; Dean, A. M.; Cohen, M. H.; Carr, R. W. Master equation analysis of intermolecular energy transfer in multiple-well, multiple-channel unimolecular reactions. I. Basic Theory. *Journal of Chemical Physics* **1997**, *107*, 8904-8916.
- (11) Vereecken, L.; Huyberechts, G.; Peeters, J. Stochastic simulation of chemically activated unimolecular reactions. *J. Chem. Phys.* **1997**, *106*, 6564-6573; <https://doi.org/10.1063/1.473656>.

## A.4. Processes

### A.4.1 Unimolecular Reactions

The energy-dependent specific unimolecular rate constant  $k(E)$  is given by the RRKM statistical theory<sup>12,15,16,20,30</sup>:

$$k(E) = \frac{\left[ \frac{m^\ddagger \sigma_{\text{ext}}^\ddagger}{m \sigma_{\text{ext}}^\ddagger} \right] \frac{g_e^\ddagger}{g_e} \frac{1}{h} G^\ddagger(E - E_0)}{\rho(E)} \quad (4.1-1)$$

where  $m^\ddagger$  and  $m$  are the number of optical isomers,<sup>16</sup>  $\sigma_{\text{ext}}^\ddagger$  and  $\sigma_{\text{ext}}$  are the external rotation symmetry numbers, and  $g_e^\ddagger$  and  $g_e$  are the electronic state degeneracies of the transition state and reactant, respectively;  $h$  is Planck's constant,  $G^\ddagger(E - E_0)$  is the sum of states of the transition state,  $E_0$  is the reaction threshold energy, and  $\rho(E)$  is the density of states of the reactant molecule. The

internal energy  $E$  is measured relative to the zero point energy of the reactant molecule and the reaction threshold energy (critical energy) is the difference between the zero point energies of reactant and transition state. Equation (4.1-1) was written by assuming that the rotational external symmetry numbers were not used in calculating the sums and densities of states.<sup>16</sup> It is, however, assumed that internal rotor symmetry numbers are used explicitly in the sum and density calculations and hence do not appear in Equation (4.1-1). Note that the quantity set off in square brackets is the *reaction path degeneracy*.<sup>16</sup>

At low energies, where densities of states may be very sparse,  $\rho(E)$  may be very small or zero in a given energy grain (lower energy portion of the double array). In MultiWell, this is treated as if there are no reactant states in the energy grain:  $k(E)$  is set equal to zero in that grain. During evolution of the population distribution, population never resides in energy grains that do not contain reactant states.

### Tight Transition States

For a tight transition state,  $G^\ddagger(E-E_0)$  can be calculated from a vibrational-rotational assignment and the reaction threshold energy can be corrected approximately for angular momentum effects by using a pseudo-diatomic model.<sup>13,15,16</sup> All polyatomics are treated by DenSum and MultiWell as SYMMETRIC TOPS with moments of inertia  $I_A, I_B = I_C$  and corresponding rotational constants  $A = \hbar^2/2I_A$  and  $B = \hbar^2/2I_B$ . The rotational energy of a symmetric top is given by

$$E_r(J,K) = J(J+1)B + (A-B)K^2$$

where quantum numbers  $J$  and  $K$  refer to the **two-dimensional 2-D adiabatic rotor** (i.e. the one that conserves angular momentum  $\mathbf{J}$ ) and to **one-dimensional rotation** about the top axis (projection of  $\mathbf{J}$  on the top axis), respectively (see Appendix B.4). For a given value of  $J$ , quantum number  $K$  can take values from  $-J$  to  $+J$ , inclusive; all such states are doubly degenerate except for  $K=0$ , which is singly degenerate. *In the present version of DenSum, the K-rotor is normally designated as a simple 1-D rotation (either quantized or classical).* The moment of inertia for the K-rotor  $I_K$  is given by

$$I_K = [I_A^{-1} - I_B^{-1}]^{-1}$$

In many applications,  $I_K \approx I_A$ .

Because the K-rotor is normally designated as a simple rotation in MultiWell simulations, the range of  $K$  is normally **not** restricted to  $\pm J$ . When  $I_A < I_B$  (prolate top), then  $I_K > 0$ . When  $I_A > I_B$  (oblate top), then  $I_K < 0$ . If the  $K$  quantum number is not constrained to  $K \leq |J|$ , then  $E_r(J,K)$  can be  $< 0$ . The unrestricted range of  $K$  is not serious a approximation for prolate tops, since the rotational energy is  $> 0$  for all values of  $J$  and  $K$ . For oblate tops, however,  $E_r(J,K)$  can be  $< 0$  when  $K \gg J$ . Thus the approximate treatment of the K-rotor may fail seriously for oblate tops. The **kro** degree of freedom type (see DenSum) employs the correct treatment for a user-specified value of  $J$ .

Thus the three external rotations of a non-linear molecule consist of a 1-dimensional rotor (the 1-D "**K-rotor**") and a 2-dimensional top (the **2-D adiabatic rotor**). The **K-ROTOR** properties are listed in **densum.dat** and included in density and sums of states calculations. Pragmatically,  $I_B$  is usually not equal to  $I_C$ , since most chemical species are not true symmetric tops. For *almost* symmetric tops (where  $I_B \approx I_C$ ), one can use either of two reasonable approximations for  $I_{2D}$  (see Appendix B.4):

$$I_{2D} \approx [I_B I_C]^{1/2} \text{ [Ref. }^{13,15}] \text{ or } I_{2D} \approx [I_B^{-1} + I_C^{-1}]^{-1} \text{ [Ref. }^{32}]$$

The **2-D ADIABATIC ROTOR** moment of inertia is listed in **multiwell.dat** on Line 8 (for wells) or Line 14 (for transition states). The moment of inertia  $I_K$  of the K-rotor is given by

$$I_K = [I_A^{-1} - I_{2D}^{-1}]^{-1}$$

This is sometimes approximated as  $I_K \approx I_A$ . The K-rotor is normally listed as a 1-D rotation in the DenSum data file.

When  $k(E)$  is calculated according to RRKM Theory, **centrifugal corrections** (recommended Keyword 'CENT2') are applied by averaging  $k(E, J)$  over a thermal distribution of  $J$ . Here,  $k(E, J)$  is given by Eq. 4.1-1, but with the density of states in the denominator written as in Section 4.10.1 in Robinson and Holbrook<sup>30</sup> (or Section 3.10 of Holbrook et al.<sup>20</sup>). Essentially,  $k(E, J)$  can be written

$$k(E, J) = \left[ \frac{m^\ddagger \sigma_{ext}^\ddagger}{m \sigma_{ext}^\ddagger} \right] \frac{g_e^\ddagger}{g_e} \frac{1}{h} \frac{G^\ddagger(E^+)}{\rho(E^+ + E_0 + \Delta E_r(J))} \quad (4.1-2a)$$

where  $E^+$  is the active energy that is assumed to randomize rapidly and  $\Delta E_{rot}(J)$  is the difference in the adiabatic rotational energy between transition state and reactant molecule:

$$\Delta E_{rot}(J) = \{B_\ddagger - B_e\} J(J+1) \quad (4.1-2b)$$

Here,  $B_\ddagger$  and  $B_e$  are the rotational constants (for the adiabatic 2-D rotations) of the transition state and the equilibrium reactant molecule, respectively. Since  $B_e$  is usually significantly larger than  $B_\ddagger$ ,  $\Delta E_{rot}(J)$  is usually negative. The rotational averaging is carried out as usual:

$$k(E) = \frac{1}{Q_{2D}} \sum_{J=0}^{\infty} k(E, J) \cdot (2J+1) \cdot \exp\left[\frac{-B_e \cdot J \cdot (J+1)}{k_B T}\right] \quad (4.1-2c)$$

This model amounts to assigning a fixed transition state, since  $B_\ddagger$  does not change with rotational state (or inter-fragment distance), and thus is a relatively poor approximation for loose transition states. The limitations of this approach are overcome to a large extent if a semi-empirical approach like the Hindered Gorin Model (see below) is applied, where  $B_\ddagger$  is assumed to vary with temperature.

### Loose Transition States

For loose transition states, more elaborate techniques are needed for calculating  $k(E)$  accurately. Such techniques include Variational Transition State Theory,<sup>1,16</sup> Adiabatic Channel Model,<sup>29</sup> and Flexible Transition State Theory.<sup>33</sup> Computer codes have been published for some of these theories.<sup>9,21</sup> These methods can be used in the current version of MultiWell by calculating  $k(E)$  externally and supplying the  $k(E)$  values an appropriately formatted external data file. MultiWell will accept double arrays (from external files) that specify  $G_{TS}(E-E_0)$  (which can be calculated conveniently using codes like DenSum, part of the MultiWell suite), or that specify  $k(E-E_0)$ . Since a double array is used, the effective energy grain can be very small near the reaction threshold, where high energy resolution is important.

The choice of approach depends on several factors, including personal preferences, computational costs, required accuracy, and whether experimental data are available. MultiWell

can in principle be used for any method that one wishes to use, but the most sophisticated methods require considerable work outside the MultiWell package; the simpler methods can be implemented with built-in options. Even when computer resources are not a limitation, the limitations of current electronic structure theories are significant, possibly leading one to choose one of the simpler methods.

In the following, we list several methods, starting with the simplest, and describe strengths and weaknesses. These methods require either some experimental data, or an empirical estimation method (e.g. thermochemical kinetics<sup>5</sup>), or perhaps both. They are based on fitting canonical (thermal) rate constants and then using the appropriate parameters in microcanonical master equation simulations.

### Inverse Laplace Transform Method

With this method, experimental Arrhenius parameters must be known or estimated for the high-pressure limit of the thermal decomposition reaction. If the Arrhenius parameters are known for the recombination reaction, the equilibrium constant  $K_{eq}$  can be used to determine the corresponding parameters for the unimolecular decomposition reaction. Since rate constants for recombination reactions are usually only weakly dependent on temperature, the activation energy for the recombination may be assumed to equal zero. In most cases, it is a good approximation to assume that  $E_\infty$ , the Arrhenius activation energy at the high pressure limit, is equal to the critical energy for reaction ( $E_0$ ). MultiWell input for ILT calls for only two parameters:  $E_0$  and the corresponding Arrhenius A-factor.

A selectable option in MultiWell is to calculate  $k(E)$  using the Inverse Laplace Transform method described by Forst:<sup>13-15</sup>

$$k(E) = \left[ \frac{m^\ddagger \sigma_{est}}{m \sigma_{est}^\ddagger} \frac{g_e^\ddagger}{g_e} \right] A_\infty \frac{\rho(E - E_\infty)}{\rho(E)} \quad (4.1-3)$$

where  $A_\infty$  and  $E_\infty$  are the Arrhenius parameters for the corresponding high pressure limiting thermal rate constant. Note that the reaction path degeneracy (the quantity in square brackets) can be absorbed into  $A_\infty$  if desired. For added accuracy near the reaction threshold,  $E_\infty$  may be replaced in Equation (4.1-3) by  $E_0$ , the threshold energy. This substitution may improve the threshold behavior, but it introduces a small error in the calculated high pressure limit activation energy.

Required info:

- Experimental (or estimated) Arrhenius parameters
- Reaction enthalpy and  $K_{eq}$  are needed to obtain the rate constant for the reverse reaction.

Strengths:

- Quickest and easiest method (a built-in option in MultiWell)
- Does not require TST parameters for the transition state.

Drawbacks:

- Over wide temperature ranges, the thermal rate constants may not obey the strict Arrhenius form. Errors from this source, however, are usually relatively small.

- This method for computing  $k(E)$  is not as accurate as transition state theory (i.e. RRKM theory).
- The ILT does not allow the use of centrifugal correction factors, which are needed to account for conservation of angular momentum. Neglect of angular momentum can affect the magnitude and temperature-dependence of the energy transfer parameters needed to describe pressure fall-off.

### Hindered Gorin Model

When the rate constant is known from experiments, it is often convenient to use a "restricted" or "hindered" Gorin Model with a "hindrance parameter" selected to reproduce a known rate constant for a recombination reaction.<sup>5,16,31</sup> The same transition state is appropriate for the corresponding unimolecular decomposition reaction. The basic idea is that the TST internal degrees of freedom consist of vibrations (the unperturbed vibrational frequencies of the reactants) plus internal rotations (the relative rotations of the two reactants with rotational constants modified by an empirical multiplicative constant) plus external rotations (two adiabatic rotations and the K-rotor). The empirical factor is adjusted in order to fit the experimental canonical recombination rate constant.

According to the Gorin model,<sup>18</sup> the two molecular fragments rotate independently of one another while separated at the distance corresponding to the centrifugal maximum ( $r_{max}$ ) of the effective potential of the bond being broken. In the present work, the rotations of both fragments and the over-all transition state are treated approximately as symmetric tops (see Appendix B.4). The over-all transition state has a 2-D external adiabatic rotation with moment of inertia given by  $I_{2D}^{\ddagger} = \mu r_{max}^2$ , where  $\mu$  is the reduced mass of the two fragments, and a 1-D external rotation (the "K-rotor") with moment of inertia  $I_k$ . The K-rotor is not adiabatic and is assumed, according to the usual approximation,<sup>16</sup> to mix energy freely with the active vibrations. The internal rotations of fragments A and B are characterized by 2-D rotations with moments of inertia  $I_a$  and  $I_b$ , respectively, and an internal rotation with reduced moment of inertia  $I_r$ . The moments of inertia  $I_r$  and  $I_k$  are obtained by combining the K-rotors of the individual fragments, as described by Gilbert and Smith.<sup>16</sup>

In the restricted, or Hindered Gorin Model,<sup>5,16,31</sup> it is assumed that the two fragments interfere sterically with each another and thus cannot rotate freely. The effect is to reduce the available phase space and hence reduce the sum of states. Operationally, a "hindrance" parameter  $\eta$  is defined,<sup>31</sup> which can vary from zero (free rotation) to unity (completely hindered). The 2-D moments of inertia  $I_a$  and  $I_b$  are multiplied by the factor  $(1-\eta)^{1/2}$  to obtain the effective 2-D moments of inertia used for calculating the sum of states. Examples of the Hindered Gorin Model used with MultiWell can be found elsewhere.<sup>2,17</sup>

THERMO (in the MultiWell Program Suite) has built-in capability for using the Hindered Gorin Model for fitting thermal recombination rate constants.

Required info:

- Experimental (or estimated) recombination rate constant
- Reaction enthalpy and  $K_{eq}$  are needed to obtain the rate constant for the reverse reaction.
- Vibrational frequencies and rotational constants of the recombination reactants.



- An assumed function for  $V(r)$  along the reaction coordinate (usually a Morse or Varshni potential) described by the center-of-mass distance between the two reactants.

Strengths:

- Relatively easy method.
- Generates TST parameters that fit the experimental canonical recombination rate constant at a given temperature.
- TST (i.e. RRKM) is a proven method; centrifugal corrections are employed.

Drawbacks:

- Experimental or estimated rate constants are required at every temperature.
- Fitting of the rate constants must be carried out at each temperature.
- TST parameters are different at each temperature.
- Separable harmonic oscillator and rigid rotor approximations may not be sufficiently accurate. Using separable hindered internal rotations is significantly more accurate, but more expensive.

### Semi-empirical Canonical Variational Transition State Theory

We are currently using Semi-empirical Canonical Variational Transition State Theory (VTST) for applications where electronic structure methods are not reliable, but can still supply useful information. The basic idea is to use methods like Density Functional Theory (DFT; e.g. B3LYP) and large basis sets to carry out constrained optimizations at fixed distances along a reaction path in order to obtain the rotational constants and the vibrational frequencies orthogonal to the path, but then use empirical expressions for  $V(r)$ , the potential energy along the path. For example, we have used  $V(r) = -Cr^{-n}$ , where  $C$  is a constant and  $n = 6$ .

The vibrational frequencies, rotational constants, and  $V(r)$  vary with position along the path. At each of the fixed points along the path, one can use those quantities as input to THERMO (in the MultiWell Program Suite) for computing a trial rate constant for the thermal reaction. The minimum trial rate constant corresponds to the VTST rate constant. The minimum rate constant is best obtained by interpolation between the fixed points, but for points separated by 0.1 Å or less it is almost as good to use the lowest trial rate constant, without interpolation. We find that by varying the constant  $C$ , it is possible to fit the experimental recombination rate constant at a given temperature (e.g. 298 K). According to our limited experience with this method, the value of the constant  $C$  fitted at a single temperature is in reasonable agreement with the temperature dependence of the recombination reaction, when known.

For a master equation simulation at temperature  $T$ , one uses the transition state parameters (vibrational frequencies, rotational constants, and  $V(r)$ ) corresponding to the variational transition state at  $T$ .

Required info:

- Experimental (or estimated) recombination rate constant
- Reaction enthalpy and  $K_{eq}$  are needed to obtain the rate constant for the reverse reaction.
- Constrained geometry optimizations at fixed distances along the reaction path; and corresponding vibrational frequencies and rotational constants.

- An assumed function for  $V(r)$  along the reaction coordinate (e.g.  $V(r) = -C/r^{-n}$  with  $n=6$ ).

Strengths:

- Uses theoretically calculated geometries and vibrational frequencies (which are more trustworthy than total energies).
- Generates TST parameters that fit the experimental canonical recombination rate constant at a given temperature.
- Temperature dependence of the rate constant can be estimated from fitting to the rate constant at a single temperature.
- TST (i.e. RRKM) is a proven method; centrifugal corrections are employed.

Drawbacks:

- Experimental or estimated rate constants are required at every temperature.
- Even for "economical" methods, the constrained optimizations and vibrational analysis can be expensive.
- For best accuracy, fitting of the rate constants must be carried out at each temperature. (However, fitting at a single temperature provides at least a rough estimate of the temperature dependence and may be adequate.)
- TST parameters are different at each temperature.
- Separable harmonic oscillator and rigid rotor approximations may not be sufficiently accurate. Using separable hindered internal rotations is significantly more accurate, but more expensive.

### High and Low Pressure Limits

Regardless of the method for calculating  $k(E)$ , the unimolecular rate constant at the high pressure limit  $k_{\infty}(T_{trans})$  is calculated in MultiWell by using  $\rho(E)$  and  $k(E)$ . The strong-collider rate constant at the low pressure limit is proportional to bath gas concentration:  $k_0^{SC}(T_{trans})[M]$ . The proportionality constant  $k_0^{SC}(T_{trans})$  is calculated by using  $\rho(E)$  and  $k_c$ , the bimolecular rate constant for collisions (see Appendix A.4.3):

$$k_{\infty}(T_{trans}) = \frac{1}{Q(T_{trans})} \int_{E_0}^{\infty} k(E) \rho(E) \exp(-E / k_B T_{trans}) dE \quad (4.1-4a)$$

$$k_0^{SC}(T_{trans}) = \frac{k_{coll}}{Q(T_{trans})} \int_{E_0}^{\infty} \rho(E) \exp(-E / k_B T_{trans}) dE \quad (4.1-4b)$$

In these expressions,  $Q(T_{trans})$  is the partition function of the reactant internal degrees of freedom (the degrees of freedom used to calculate  $\rho(E)$  and  $k(E)$ ) at translational temperature  $T_{trans}$ :

$$Q(T_{trans}) = \int_0^{\infty} \rho(E) \exp(-E / k_B T_{trans}) dE \quad (4.1-5)$$

The numerical integrations are carried out using the trapezoidal rule, because  $\rho(E)$  fluctuates wildly at low energies. Test show that the numerical integration produces values for  $k_{\infty}(T_{\text{trans}})$  that are accurate within a fraction of 1% for usual values of  $\Delta E_{\text{grain}}$ .<sup>3</sup> The activation energy is obtained by calculating  $k_{\infty}(T_{\text{trans}})$  at two closely-spaced temperatures:

$$E_{\infty} = -R \frac{\ln \left[ \frac{k_{\infty}(T_2)}{k_{\infty}(T_1)} \right]}{\left[ T_2^{-1} - T_1^{-1} \right]} \quad (4.1-6)$$

From the activation energy and the rate constant at one temperature, the A-factor ( $A_{\infty}$ ) can be calculated. Values for  $k_{\infty}(T_{\text{trans}})$ ,  $E_{\infty}$ , and  $A_{\infty}$  calculated in this way are reported (for each reaction) in the general output file. Note that the numerical values for the high pressure rate constant  $k_{\infty}(T_{\text{trans}})$  (also,  $E_{\infty}$  and  $A_{\infty}$ ) should be the same, regardless of whether centrifugal corrections are used or not (Keywords 'CENT2' or 'NOCENT'), but  $k_0^{\text{SC}}(T_{\text{trans}})$  depends on the particular choice. The value for  $k_{\infty}(T_{\text{trans}})$  is formally identical to that given by canonical transition state theory.

### Effects of Slow IVR

RRKM theory is based on the premise that energy is completely randomized on a time scale that is fast compared to chemical reaction. For most experiments, this condition appears to be met, but some examples of "intrinsic non-RRKM" behavior are known. For these reactions, the slow transfer of internal energy to the reaction coordinate from the other degrees of freedom limits the rate constant, which falls below the RRKM statistical limit. Several theories for the effects of slow IVR have been proposed,<sup>6-8,20,27,28</sup> but perhaps the most successful of these is the local random matrix model of Wolynes and coworkers.<sup>19,22-25</sup>

According to most of the IVR models,<sup>22,27</sup> the effects of slow IVR can be accounted for with an IVR transmission coefficient:

$$\kappa_{IVR}(U, [M]) = \frac{k_{IVR}^q(U) + k_{IVR}^c[M]}{k_{IVR}^q(U) + k_{IVR}^c[M] + \nu_{IVR}} \quad (4.1-7)$$

where  $U$  is the total vibrational energy and  $k_{IVR}^q(U)$  is the collision-free IVR rate constant, which must be calculated by one of the theories mentioned above. In particular, the Wolynes-Leitner<sup>22</sup> has been used with MultiWell.<sup>4,34</sup> For convenience in MultiWell, the total vibrational energy is measured from the reaction critical energy ( $U = E - E_{0r}$ ), and  $k_{IVR}^q(U)$  is expressed as a polynomial:

$$k_{IVR}^q(U) = C_{IVR,1} + C_{IVR,2}U + C_{IVR,3}U^2 \quad (4.1-8)$$

Parameter  $\nu_{IVR}$  is a characteristic frequency for IVR (identified by Leitner and Wolynes<sup>22</sup> as the imaginary frequency for an isomerization reaction) and parameter  $k_{IVR}^c$  is the bimolecular collision rate constant (expressed in units of  $\text{cm}^3 \text{s}^{-1}$ ) for collision-induced IVR. A threshold for IVR must also be specified:  $t_{IVR}$ , which in MultiWell is measured from the reaction critical energy. It can be used in cases where there is a sudden on-set of  $k_{IVR}(U)$  at the threshold, followed by a quadratic increase with energy. The specific unimolecular rate constant as modified by IVR is finally given by the product of the transmission coefficient  $\kappa_{IVR}(E, [M])$  and

the specific rate constant  $k_{RRKM}(E)$  calculated using RRKM theory, where  $E$  is the total vibrational energy measured from the zero point energy of the reactant, as usual:

$$k(E, [M]) = \kappa_{IVR}(E, [M]) \cdot k_{RRKM}(E) \quad (4.1-9)$$

The resulting specific (energy dependent) unimolecular rate constant depends on pressure, as indicated.

Using the Leitner-Wolynes model for IVR, simulations of data for trans-stilbene isomerization are in very good agreement with a large body of experimental data.<sup>22,34</sup> They indicate that collision-induced IVR occurs with a rate constant ( $k^{cIVR}$ ) similar in magnitude to the total collision rate constant  $k_q$  calculated using the method developed by Durant and Kaufman<sup>10</sup> (see the next section).

### Tunneling: Unsymmetrical Eckart Barrier

[NOTE: for a far more sophisticated treatment of tunneling, see Semi-Classical Transition State Theory (SCTST) in Chapter 7 and Appendix B.9.]

(This section on Eckart Tunneling contributed by Philip J. Stimac.)

Quantum mechanical tunneling corrections to the microcanonical rate constants  $k(E)$  have been implemented in MultiWell using a one dimensional unsymmetrical Eckart barrier.<sup>11</sup> The modification of  $k(E)$  within MultiWell is accomplished by evaluating the sum of states of the transition state according to Eq. 9 of the paper by Miller<sup>26</sup>:

$$G(E) = \int_{-V_0}^{E-V_0} P(E_l) \rho(E-E_l) dE_l \quad (4.1-10)$$

where  $V_0$  is the classical barrier height (in the direction of the forward reaction);  $E_l$  is the energy in the reaction coordinate, relative to the top of the energy barrier;  $E$  is the total energy;  $\rho(E-E_l)$  is the density of states at energy  $(E-E_l)$ ;  $P(E_l)$  is the tunneling probability:

$$P(E_l) = \frac{\sinh(a)\sinh(b)}{\sinh^2\left[\frac{(a+b)}{2}\right] + \cosh^2\left[\frac{c}{2}\right]} \quad (4.1-11a)$$

$$a = \frac{4\pi}{h\nu_i} \frac{\sqrt{E_l + V_0}}{\left(V_0^{-1/2} + V_1^{-1/2}\right)} \quad (4.1-11b)$$

$$b = \frac{4\pi}{h\nu_i} \frac{\sqrt{E_l + V_1}}{\left(V_0^{-1/2} + V_1^{-1/2}\right)} \quad (4.1-11c)$$

$$c = 2\pi \sqrt{\frac{V_0 V_1}{(h\nu_i)^2} - \frac{1}{16}} \quad (4.1-11d)$$

In these equations,  $\nu_i$  and  $V_1$  are the imaginary frequency (related to the curvature of the saddle point on the potential energy surface at the transition state) and the classical barrier height relative to the products, respectively. The tunneling corrections to the sum of states of the transition state were applied using Eqs. (4.1-10) and (4.1-11) after transforming the integral in Eq. (4.1-10) to the expression

$$G(E) = \int_0^E P(E - V_0 - E^\ddagger) \rho(E^\ddagger) dE^\ddagger. \quad (4.1-12)$$

$E^\ddagger$  is the energy in the vibrational modes orthogonal to the reaction coordinate and the quantity  $(E - V_0 - E^\ddagger)$  is the energy in the reaction coordinate. The primary difference between Equation (4.1-12) and Equation (4.1-10) is that the zero of energy is chosen to be at the minimum of the reactant in Equation (4.1-12), whereas the zero of energy is chosen to be at the transition state in Equation (4.1-10). Numerical tests showed that Equation (4.1-12) reproduces Fig. 2 of Miller.<sup>26</sup>

Equation (4.1-12) is evaluated in the subroutine Eckart within MultiWell. The integral is only evaluated at the grain energies. Evaluation of Equation (4.1-12) begins with all the energy in the reaction coordinate. This means that the tunneling probability is at a maximum while the density of states of the transition state is at a minimum. The integration continues until the tunneling probability  $P(E - V_0 - E^\ddagger)$  become less than some cutoff value ‘tunthresh’, which is specified in the include file declare1.inc. The default value in declare1.inc is tunthresh=1.0E-12.

The  $k(E)$  calculated using the modified sums of states of the transition state reflect the tunneling effects. These tunneling corrected  $k(E)$  are also used to calculate the high-pressure rate constant  $k_\infty$ , and are used to initialize the chemical activation distribution if both the CHEMACT and TUN keywords are selected. Please note that the TUN keyword cannot be used with the ILT or RKE keywords.

## References

- (1) Baer, T.; Hase, W. L. *Unimolecular Reaction Dynamics. Theory and Experiments*; Oxford University Press: New York, 1996.
- (2) Barker, J. R.; Lohr, L. L.; Shroll, R. M.; Reading, S. Modeling the Organic Nitrate Yields in the Reaction of Alkyl Peroxy Radicals with Nitric Oxide. II. Reaction Simulations. *J. Phys. Chem. A* **2003**, *107*, 7434-7444.
- (3) Barker, J. R.; Ortiz, N. F. Multiple-Well, multiple-path unimolecular reaction systems. II. 2-methylhexyl free radicals. *Int. J. Chem. Kinet.* **2001**, *33*, 246-261; DOI: 10.1002/kin.1018.
- (4) Barker, J. R.; Ortiz, N. F.; Preses, J. M.; Lohr, L. L.; Maranzana, A.; Stimac, P. J. MultiWell-1.5.1 Software (Development version) Ann Arbor, Michigan, USA, 2005.
- (5) Benson, S. W. *Thermochemical Kinetics*, 2nd ed.; Wiley: New York, 1976.
- (6) Bolton, K.; Nordholm, S. Beats in internal vibrational energy redistribution in trans-stilbene - A study of the quantum and classical correspondence. *Chemical Physics* **1996**, *207*, 63-76.
- (7) Bolton, K.; Nordholm, S. A classical molecular dynamics study of the intramolecular energy transfer of model trans-stilbene. *Chemical Physics* **1996**, *203*, 101-126.
- (8) Bolton, K.; Nordholm, S. Classical trajectory study of collision induced intramolecular energy transfer in trans-stilbene. *Chemical Physics* **1996**, *206*, 103-128.
- (9) Chuang, Y.-Y.; Corchado, J. C.; Fast, P. L.; Villà, J.; Hu, W.-P.; Liu, Y.-P.; Lynch, G. C.; Nguyen, K. A.; Jackels, C. F.; Gu, M. Z.; Rossi, I.; Coitiño, E. L.; Clayton, S.; Melissas, V. S.; Steckler, R.; Garrett, B. C.; Isaacson, A. D.; Truhlar, D. G. POLYRATE-version 8.1; University of Minnesota, Minneapolis, MN, 1999.
- (10) Durant, J. L.; Kaufman, F. Calculation and use of total collision rates in thermal systems. *CPL* **1987**, *142*, 246-251.
- (11) Eckart, C. The Penetration of a Potential Barrier by Electrons. *Phys. Rev.* **1930**, *35*, 1303-1309.
- (12) Forst, W. Unimolecular rate theory test in thermal reactions. *J. Phys. Chem.* **1972**, *76*, 342-348; <https://doi.org/10.1021/j100647a012>.
- (13) Forst, W. *Theory of Unimolecular Reactions*; Academic Press: New York, 1973.
- (14) Forst, W. Temperature-dependent A factor in thermal unimolecular reactions. *J. Phys. Chem.* **1983**, *83*, 100-108.
- (15) Forst, W. *Unimolecular Reactions. A Concise Introduction*; Cambridge University Press: Cambridge, 2003.
- (16) Gilbert, R. G.; Smith, S. C. *Theory of Unimolecular and Recombination Reactions*; Blackwell Scientific Publications: Oxford, 1990.
- (17) Golden, D. M.; Barker, J. R.; Lohr, L. L. Master Equation Models for the Pressure- and Temperature-Dependent Reactions  $\text{HO} + \text{NO}_2 \rightarrow \text{HONO}_2$  and  $\text{HO} + \text{NO}_2 \rightarrow \text{HOONO}$ . *JPCA* **2003**, *107*, 11057-11071.
- (18) Gorin, E. Photolysis of acetaldehyde in the presence of iodine. *Acta Physicochim., URSS* **1938**, *9*, 681.
- (19) Gruebele, M.; Wolynes, P. G. Vibrational energy flow and chemical reactions. *Accounts of Chemical Research* **2004**, *37*, 261-267.

- (20) Holbrook, K. A.; Pilling, M. J.; Robertson, S. H. *Unimolecular Reactions*, 2 ed.; Wiley: Chichester, 1996.
- (21) Klippenstein, S. J.; Wagner, A. F.; Robertson, S. H.; Dunbar, R.; Wardlaw, D. M. VariFlex Software; 1.0 ed.; Argonne National Laboratory, 1999.
- (22) Leitner, D. M.; Levine, B.; Quenneville, J.; Martinez, T. J.; Wolynes, P. G. Quantum energy flow and trans-stilbene photoisomerization: an example of a non-RRKM reaction. *Journal of Physical Chemistry A* **2003**, *107*, 10706-10716.
- (23) Leitner, D. M.; Wolynes, P. G. Many-dimensional quantum energy flow at low energy. *Phys. Rev. Lett.* **1996**, *76*, 216-219.
- (24) Leitner, D. M.; Wolynes, P. G. Models of intramolecular energy redistribution spanning deterministic and statistical approaches: Comparison with experiment - Comment. *ACH Models Chem.* **1997**, *134*, 658-659.
- (25) Leitner, D. M.; Wolynes, P. G. Quantum energy flow during molecular isomerization. *Chemical Physics Letters* **1997**, *280*, 411-418.
- (26) Miller, W. H. Tunneling Corrections to Unimolecular Rate Constants, with Application to Formaldehyde. *JACS* **1979**, *101*, 6810-6814.
- (27) Nordholm, S.; Back, A. On the role of nonergodicity and slow IVR in unimolecular reaction rate theory - A review and a view. *Physical Chemistry Chemical Physics* **2001**, *3*, 2289-2295.
- (28) Oref, I.; Rabinovitch, B. S. Do Highly Excited Polyatomic Molecules Behave Ergodically? *Accounts of Chemical Research* **1979**, *12*, 166-175.
- (29) Quack, M.; Troe, J. Specific rate constants of unimolecular processes. II. Adiabatic channel model. *Ber. Bunsen-Ges. Phys. Chem.* **1974**, *78*, 240-252.
- (30) Robinson, P. J.; Holbrook, K. A. *Unimolecular Reactions*; Wiley-Interscience: London; New York, 1972.
- (31) Smith, G. P.; Golden, D. M. Application of RRKM Theory to Reactions  $\text{OH} + \text{NO}_2 + \text{N}_2 = \text{HONO}_2 + \text{N}_2$  (1) and  $\text{ClO} + \text{NO}_2 + \text{N}_2 = \text{ClONO}_2 + \text{N}_2$  (2) - Modified Gorin Model Transition-State. *IJCK* **1978**, *10*, 489.
- (32) Townes, C. H.; Schlawow, A. L. *Microwave Spectroscopy*; McGraw-Hill: New York, 1955.
- (33) Wardlaw, D. W.; Marcus, R. A. RRKM reaction rate theory for transition states of any looseness. *J. Chem. Phys.* **1984**, *110*, 230-234.
- (34) Weston, R. E., Jr.; Barker, J. R. On modeling the pressure-dependent photoisomerization of trans-stilbene by including slow intramolecular vibrational redistribution. *J. Phys. Chem. A* **2006**, *110*, 7888-7897; DOI: 10.1021/jp061630b.

### A.4.2 Pseudo-First-Order Bimolecular Reactions

In many practical systems, unimolecular and recombination reactions may be in competition with bimolecular reactions involving the same vibrationally excited species.<sup>11</sup> For example, a vibrationally excited species ( $A^*$ ) produced by an exothermic reaction may both undergo isomerization and react in a bimolecular reaction with another species (B), prior to collisional deactivation. If B is present in great excess, the pseudo-first-order approximation is applicable and one can define a pseudo-first order rate coefficient:  $k^l = k_{bim}[B]$ , where  $k_{bim}$  is the bimolecular rate coefficient and  $[B]$  is the concentration of the reaction partner B, which is present in great excess.

Prior to incorporation of this feature, Moriarity and Frenklach<sup>10</sup> used MultiWell for assessing several complicated reaction paths that may lead to aromatic ring formation in combustion systems. They found that certain vibrationally excited intermediates persist for relatively long periods and therefore *bimolecular* reactions between energized adducts and gaseous partners may need to be included in future calculations.

The procedure for implementation of a pseudo-first-order competitive reaction in MultiWell depends on whether it is assumed that  $k_{bim}$  is independent of the energy distribution of  $A^*$ . In that case, option BIMOLRXN is available on Line 14opt of the multiwell input data file for bimolecular reactions between a Well and the bath gas. *Centrifugal corrections should not be employed for this reaction and the reaction should be treated as non-reversible.*

In the more general case, the bimolecular rate constant depends on the vibrational energy distribution of species  $A^*$ , thus requiring that an energy dependent expression for  $k_{bim}(E)$  be used. In principle, this energy-dependent rate constant can be calculated from classical trajectories, quantum scattering, or other dynamical theories. However, since MultiWell is for the most part based on statistical theory, it is also appropriate to use microcanonical transition state theory.<sup>9,13</sup> All of the tools necessary for such calculations are available in the MultiWell Software Suite.

### Theory

*The discussion in this section was adapted from our recent paper on reactions of acetyl radical with  $O_2$ .<sup>8</sup> (Recently, Green and Robertson confirmed this approach and extended it more generally.<sup>6</sup>)*

Bimolecular reactions can be treated by using the bimolecular pseudo-first-order microcanonical approach. The microcanonical bimolecular rate constant is given by

$$k_{bim}(E^+) = \left[ \frac{m_{AB}^\ddagger \sigma_A \sigma_B}{m_A m_B \sigma_{AB}^\ddagger} \right] \frac{g_{e(AB)}^\ddagger}{g_{e(A)} g_{e(B)}} \frac{1}{h} \frac{G_{AB}^\ddagger(E^+ - E_0)}{\rho_{AB}(E^+)} \quad (4.2-1)$$

$$\rho_{AB}(E^+) = \int_0^{E^+} \rho_A(E^+ - x) \rho_B(x) dx \quad (4.2-2)$$

where  $E^+$  is the total rovibrational energy,  $\rho_{AB}(E^+)$  is density of states of the A+B supermolecule, i.e.  $\rho_{AB}(E^+)$  is the convolved density of states of the two reactants A and B, including all degrees



of freedom except for the three coordinates of the supermolecule center of mass. The factor  $G_{AB}^\ddagger(E^+ - E_0)$  is the sum of states of the transition state. The other symbols ( $m$ ,  $g_e$ , and  $\sigma$ ) have the same meaning as in Eq. 4.1-1. Here, however, the 2D-rotors are assumed to be active and hence are included with the K-rotor in calculating  $\rho_{AB}(E^+)$  and  $G_{AB}^\ddagger(E^+ - E_0)$ . The canonical bimolecular rate constant can be calculated by averaging over the canonical energy distribution of the A+B supermolecule:

$$\langle k_{bim}(T) \rangle = \frac{\int_{E_0}^{\infty} k_{bim}(E^+) \rho_{AB}(E^+) e^{-E^+/RT} dE^+}{Q_{tot}(T)} \quad (4.2-3)$$

where  $Q_{tot}(T)$  is the total partition function of the supermolecule at temperature  $T$ :

$$Q_{tot}(T) = \int_0^{\infty} \rho_{AB}(E^+) e^{-E^+/RT} dE^+ \quad (4.2-4)$$

We assume that reaction occurs when two conditions are met:  $E^+$  is greater than the reaction threshold energy and the relative translational energy is greater than zero. For present purposes, we assume that the degrees of freedom of the supermolecule are partitioned into two groups. The degrees of freedom (DOF) in Group 1 are associated with the vibrations and K-rotor of excited species  $A^*$  (i.e. the active DOF of species A) and all of the remaining DOF are collected in Group 2. We also assume that the energy distribution of the Group 2 modes is thermal, while the energy of the Group 1 DOF is held fixed (adiabatic). The total energy can be expressed as  $E^+ = E_1 + E_2$ . Note that other groupings can be postulated, depending on the system to be simulated, and centrifugal corrections may be included in future work.

From the partitioning of the DOF, a semi-microcanonical bimolecular rate constant that depends on  $E_1$  and  $T$  is obtained by averaging over the canonical  $E_2$  energy distribution:

$$\langle k_{bim}(E_1, T) \rangle_2 = \frac{\int_{E_{low}}^{\infty} k_{bim}(E_1 + E_2) \rho_2(E_2) \exp\left(\frac{-E_2}{kT}\right) dE_2}{Q_2(T)} \quad (4.2-5)$$

where  $E_{low}$  is the lower limit to the integral,  $\rho_2(E_2)$  is the density of states for the Group 2 DOF of the supermolecule and  $Q_2(T)$  is the corresponding partition function:

$$Q_2(T) = \int_0^{\infty} \rho_2(E_2) \exp\left(\frac{-E_2}{kT}\right) dE_2 \quad (4.2-6)$$

In the absence of quantum mechanical tunneling,  $E_{low} = 0$ . The canonical bimolecular rate constant can be obtained from  $\langle k_{bim}(E_v, T) \rangle_2$  by averaging over  $E_1$ :

$$\langle k_{bim}(T) \rangle = \frac{\int_0^{\infty} \langle k_{bim}(E_1, T) \rangle_2 \rho_1(E_1) \exp\left(\frac{-E_1}{kT}\right) dE_1}{Q_1(T)} \quad (4.2-7)$$

where  $\rho_1(E_1)$  and  $Q_1(T)$  are the density of states and the corresponding partition function, respectively, of the Group 1 DOF:

$$Q_1(T) = \int_0^{\infty} \rho_1(E_1) \exp\left(\frac{-E_1}{kT}\right) dE_1 \quad (4.2-8)$$

Numerical integrations of Eq. 4.2-3 and of 4.2-7, carried out by the trapezoidal rule, give results at 300 K for the  $\mathbf{A2} + \text{O}_2$  reaction that agree to within  $\sim 1\%$  when the energy grain is  $\leq 5 \text{ cm}^{-1}$ .<sup>8</sup>

The semi-microcanonical pseudo-first order rate constant (units of  $\text{s}^{-1}$ ), which depends only on the active energy of reactant  $\mathbf{A}^*$ , is obtained by multiplying  $\langle k_{\text{bim}}(E_1, T) \rangle_2$  by  $[\mathbf{B}]$ , the concentration of the reactant that is present in great excess:

$$k^I(E, T) = \langle k_{\text{bim}}(E_1, T) \rangle_2 [\mathbf{B}] \quad (4.2-9)$$

The rate constants  $\langle k_{\text{bim}}(E_1, T) \rangle_2$ ,  $k_{\text{bim}}(E_1 + E_2)$ , and  $\langle k_{\text{bim}}(T) \rangle$  are compared in Figure 4.2.<sup>8</sup>

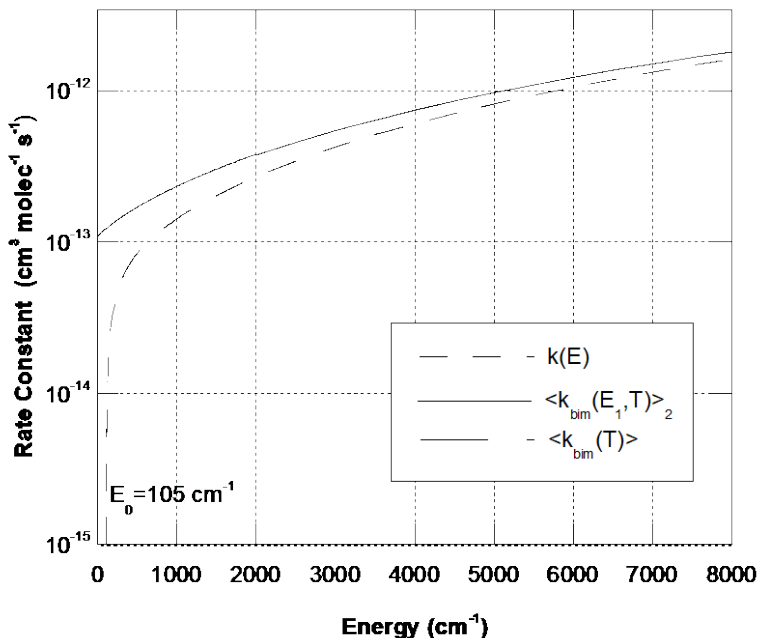


**FIGURE 4.2:** A comparison of  $k(E)$ ,  $\langle k_{\text{bim}}(E_1, T) \rangle_2$ , and  $\langle k_{\text{bim}}(T) \rangle$  at  $T=298 \text{ K}$  for the reaction  $\mathbf{A2}' + \text{O}_2 \rightarrow \mathbf{B1}$  [see reference<sup>8</sup> for details].

In order to treat competition between unimolecular and bimolecular pathways,  $k^I(E, T)$  is calculated and stored in an external data file, which is used as input to the MultiWell master equation computer program. Group 1 consists of the active DOF in species A. Thus  $k^I(E, T)$  can be used directly in the master equation simulations as if it were an ordinary microcanonical rate constant for a unimolecular reaction. Care must be taken, however, to treat it as an irreversible reaction in MultiWell, since the detailed balance relations<sup>3</sup> have been coded only for unimolecular reactions. To include the reverse reaction would require using a theory for partitioning energy between unimolecular reaction products<sup>2,14</sup> in order to obtain the energy distribution in A (i.e. dissociation of the reaction product to regenerate  $\mathbf{A} + \mathbf{B}$ ). Since such a treatment has not been implemented in MultiWell, one should treat the bimolecular reaction as irreversible. Treating such bimolecular reactions as irreversible may be a good approximation at ambient temperature, but a poor approximation at combustion temperatures.

In master equation simulations, unimolecular reaction, bimolecular reaction, and collisional deactivation of  $\mathbf{A}^*$  take place concurrently. Furthermore, the concentration of species B determines both the rate of collisional deactivation and the rate of the pseudo-first-order bimolecular reaction. Consequently, the importance of the microcanonical method is expected to

be significant only at low pressures. After A\* is thermalized by collisions, the microcanonical treatment coincides with the canonical approach.

### DenSum Calculation

Using DenSum, it is easy to calculate the sum and density of states for the bimolecular reaction. For the transition state, all vibrations, torsions, and external rotations should be included in calculating the sum of states. The same is true in calculating the combined density of states of A+B. In addition, the 3-dimensional relative translation between A and B must also be included. *Once again, centrifugal corrections should not be employed for this reaction and the reaction should be treated as non-reversible in MultiWell.*

DenSum first uses the analytic convolution of classical translational states with the classical rotor states. The analytic expression for convolved classical trans-rot states is obtained as follows. First, note that the classical partition function is the Laplace transform of the classical density of states:<sup>4,5</sup>  $Q(\beta) = \mathcal{L}[\rho(E)]$ , where  $\beta$  is the Laplace transform parameter and can be identified as  $\beta = (k_B T)^{-1}$ . The corresponding sum of states is  $G(E) = \mathcal{L}^{-1}[Q(\beta)/\beta]$ , where the right hand side is the inverse Laplace transform. Now consider a microcanonical system with total energy  $E$  partitioned into two parts, the total sum of states is given by the convolution integral:<sup>5</sup>

$$G_{12}(E) = \int_0^E G_1(x) \rho_2(E-x) dx \quad (4.2-10)$$

where  $G_1(x)$  is the sum of states for the first group of degrees of freedom, which contain energy  $x$ , and  $\rho_2(E-x)$  is the density of states for the second group, which contain the remaining energy. This convolution can also be expressed as an inverse Laplace transform:<sup>5</sup>

$$G_{12}(E) = \mathcal{L}^{-1} \left\{ \frac{Q_1(\beta) Q_2(\beta)}{\beta} \right\} \quad (4.2-11)$$

where  $Q_i(\beta)$  is the partition function of the  $i^{\text{th}}$  group of modes. For  $p$  independent classical rotations, the partition function can be written<sup>5,7</sup>

$$Q_{rot}(T) = \prod_{i=1}^p \left\{ \left( \frac{8\pi^2 I_i k_B T}{h^2} \right)^{d_i/2} \Gamma\left(\frac{d_i}{2}\right) \right\} = a_r (k_B T)^{r/2} \quad (4.2-12a)$$

$$r = \sum_{i=1}^p d_i \quad (4.2-12b)$$

where  $d_i$  is the dimensionality of the  $i^{\text{th}}$  rotation,  $I_i$  is its moment of inertia, and the other symbols take their usual definitions.

For 3-D relative translation, the partition function can be written<sup>5</sup>

$$Q_{trans}(T) = \left\{ \frac{2\pi\mu}{h^2} \right\}^{3/2} V (k_B T)^{3/2} = a_t (k_B T)^{3/2} \quad (4.2-13)$$

where  $\mu$  is the reduced mass and  $V$  is the volume. Therefore the total sum of states for combined translation and rotation is obtained using Equation (4.2-11):

$$G_r(E) = a_r a_i \mathcal{L}^{-1}(p^{-1-(r+3)/2}) = \frac{2a_r a_i E^{(r+3)/2}}{(r+3)\Gamma\left(\frac{(r+3)}{2}\right)} \quad (4.2-14)$$

When no rotations are present, the sum of states is just the sum of translational states:<sup>5,13</sup>

$$G_t(E) = \frac{4\pi(2\mu E)^{3/2}}{3h^3} V \quad (4.2-15)$$

These expressions are used by DenSum to calculate the number of states in each energy bin when initializing the sums of states array, according to the Astholz et al.<sup>1</sup> modification of the Stein-Rabinovitch state-counting method.<sup>12</sup>

## References

- (1) Astholz, D. C.; Troe, J.; Wieters, W. Unimolecular processes in vibrationally highly excited cycloheptatrienes. I. Thermal isomerization in shock waves. *J. Chem. Phys.* **1979**, *70*, 5107-5116.
- (2) Baer, T.; Hase, W. L. *Unimolecular Reaction Dynamics. Theory and Experiments*; Oxford University Press: New York, 1996.
- (3) Barker, J. R. Multiple-well, multiple-path unimolecular reaction systems. I. MultiWell computer program suite. *Int. J. Chem. Kinet.* **2001**, *33*, 232-245; <https://doi.org/10.1002/kin.1017>.
- (4) Forst, W. *Theory of Unimolecular Reactions*; Academic Press: New York, 1973.
- (5) Forst, W. *Unimolecular Reactions. A Concise Introduction*; Cambridge University Press: Cambridge, 2003.
- (6) Green, N. J. B.; Robertson, S. H. General master equation formulation of a reversible dissociation/association reaction. *Chem. Phys. Letters* **2014**, *605*, 44-46; 10.1016/j.cplett.2014.05.012.
- (7) Holbrook, K. A.; Pilling, M. J.; Robertson, S. H. *Unimolecular Reactions*, 2 ed.; Wiley: Chichester, 1996.
- (8) Maranzana, A.; Barker, J. R.; Tonachini, G. Master Equation Simulations of Competing Unimolecular and Bimolecular Reactions: Application to OH Production in the Reaction of Acetyl Radical with O<sub>2</sub>. *Phys. Chem. Chem. Phys.* **2007**, *9*, 4129 - 4141; DOI:10.1039/b705116f.
- (9) Marcus, R. A. Chemical-Reaction Cross Sections, Quasiequilibrium, and Generalized Activated Complexes. *J. Chem. Phys.* **1966**, *45*, 2138.
- (10) Moriarty, N. W.; Frenklach, M. Ab Initio Study of Naphthalene Formation by Addition of Vinylacetylene to Phenyl. *Proc. Combust. Inst.* **2000**, *28*, 2563-2568.
- (11) Olzmann, M. On the role of bimolecular reactions in chemical activation systems. *Phys. Chem. Chem. Phys.* **2002**, *4*, 3614-3618; <https://doi.org/10.1039/B203244A>.
- (12) Stein, S. E.; Rabinovitch, B. S. Accurate evaluation of internal energy level sums and densities including anharmonic oscillators and hindered rotors. *J. Chem. Phys.* **1973**, *58*, 2438-2445.
- (13) Steinfeld, J. I.; Francisco, J. S.; Hase, W. L. *Chemical Kinetics and Dynamics*, 2 ed.; Prentice-Hall, 1998.
- (14) Wittig, C.; Nadler, I.; Reisler, H.; Noble, M.; Catanzarite, J.; Radhakrishnan, G. Nascent product excitations in unimolecular reactions: The separate statistical ensembles method. *J. Chem. Phys.* **1985**, *83*, 5581-5588.

### A.4.3 Collisions

#### Frequency of Inelastic Collisions

It is conventionally assumed that the inelastic collision frequency is the same as that experienced by molecules subject to a Lennard-Jones intermolecular potential. For the Lennard-Jones potential,  $k_c$  takes the following form:<sup>18</sup>

$$k_c = \pi\sigma^2 \langle v \rangle \Omega^{(2,2)*} \quad (4.3-1)$$

where  $\langle v \rangle$  is the average speed at the translational temperature,  $\sigma$  is the Lennard-Jones diameter, and  $\Omega^{(2,2)*}$  is the collision integral,<sup>9</sup> which depends on the Lennard-Jones parameters. Since only the product  $k_c P(E, E')$  appears in the master equation, if  $k_c$  is underestimated, then normalization of the step-size distribution is not appropriate. If, on the other hand,  $k_c$  is overestimated, then  $P(E, E')$  must include elastic collisions.<sup>13</sup> The inclusion of elastic collisions in the master equation causes no problems in principle, except to reduce the efficiency of certain numerical solutions. However, the fundamental question remains: is the frequency of inelastic collisions the same as the Lennard-Jones collision frequency?

Lawrance and Knight<sup>12</sup> used single vibrational level fluorescence and found that the observed total cross sections for inelastic collisions are in quantitative agreement with the Lennard-Jones collision frequency for a moderately high density of vibrational states. Classical trajectory calculations support this assumption,<sup>17,21</sup> but the argument is somewhat circular in this case since the assumed potential energy functions are often constructed from pair-wise Lennard-Jones potentials. Recently, Xue et al.<sup>19</sup> used quantum beat spectroscopy to investigate a single vibrational level of SO<sub>2</sub> at high vibrational energy, and found cross sections substantially greater than predicted by the Lennard-Jones interaction potential. However, in the sparse density of states regime at low vibrational energies it is well known that the inelastic collision cross section is small<sup>20</sup> and thus the total inelastic collision rate constant is probably smaller than  $k_{LJ}$ .

A rigorous upper limit to  $k_c$  is provided by the total collision rate constant  $k_q$ , which is based on the total quantum cross section. Because of concern about the proper choice of  $k_c$  and normalization of the step size distribution (see below), MultiWell provides an option for utilizing the total collision rate constant, which can be estimated from Lennard-Jones parameters by using the method of Durant and Kaufman.<sup>4</sup>

In a new development,<sup>2</sup> it is now assumed in MultiWell that the rate constant for *inelastic* collisions depends on the internal energy, reflecting the reduced rate constant for inelastic collisions, which is expected at lower energies where the density of states is sparse. This new development is described in the following section. (This new approach optionally can be overridden by a keyword in the `multiwell` input file.)

#### Normalization

The rate coefficient  $R(x, y)$  is conventionally written as the product of the total vibrationally inelastic collision frequency  $k_c(y)[M]$  multiplied by the "collision step-size distribution",  $P(x, y)$ , which expresses the probability density that a molecule initially with initial energy  $y$  will undergo an inelastic transition to the energy range  $x$  to  $x+dx$ :

$$R(x,y)dx = \int_0^{\infty} R(x,y)dx \left\{ R(x,y)dx / \int_0^{\infty} R(x,y)dx \right\}, \quad (4.3-2a)$$

$$= k_c(y)P(x,y)dx \quad (4.3-2b)$$

The first factor on the right hand side of Equation (4.3-2a), the integral over the rates of all inelastic transitions from initial energy  $y$ , is the frequency of inelastic collisions,  $k_c(y)[M]$  and the second factor (in curly brackets) is  $P(x,y)dx$ . Note that  $P(x,y)$  is normalized:

$$\int_0^{\infty} P(x,y)dx = 1 \quad (4.3-3)$$

It is important to emphasize that the factorization of  $R(x,y)$  in Equation (4.3-2) is merely for convenience and that  $k_c(y)[M]$  and  $P(x,y)$  never occur independently of one another. Furthermore,  $P(x,y)$  only has an unambiguous physical interpretation when  $k_c(y)[M]$  is *exactly* equal to the total inelastic collision rate constant. Since the exact inelastic collision frequency is not known, the inevitable errors in  $k_c(y)$  are compensated in part by errors in  $P(x,y)$ , when experimental data are fitted to this prescription. Thus it is important to use  $k_c(y)$  and  $P(x,y)$  in a matched pair whenever possible.<sup>5,8,10</sup>

By considering detailed balance at equilibrium in the absence of reactions, the relationship between  $R(x,y)$  and  $R(y,x)$  can be found. Detailed balance requires that in every increment of energy, the rates of forward and reverse processes must balance. The Detailed Balance relationship between the probability densities for up- and down-collisions is given by

$$\frac{P(x,y)}{P(y,x)} = \frac{k_c(x)}{k_c(y)} \frac{\rho(x)}{\rho(y)} \exp[-(x-y)/k_B T] \quad (4.3-4)$$

The total probability density for an energy changing collision is normalized (see Eq. 4.3-3) and can be written as the sum of two integrals corresponding to down- and up-collisions:

$$1 = \int_0^y P(x,y)dx + \int_y^{\infty} P(x,y)dx \quad (4.3-5)$$

In order to construct a normalized collision step size distribution (the probability density), it is common practice to specify a (dimensionless) non-normalized function  $f(x,y)$ , which is assumed to be proportional to  $P(x,y)$ :

$$P(x,y) = \frac{f(x,y)}{N(y)} \quad (4.3-6)$$

where  $N(y)$  is a normalization constant. With this definition, the normalization equation becomes

$$1 = \int_0^y \frac{f(x,y)}{N(y)} dx + \int_y^{\infty} \frac{f(x,y)}{N(y)} dx \quad (4.3-7)$$

After rearranging this expression, we obtain a formal expression for the normalization constant  $N(y)$ , expressed as a sum of integrals:

$$N(y) = \int_0^y f(x,y) dx + \int_y^{\infty} f(x,y) dx \quad (4.3-8a)$$

$$= N_d(y) + N_u(y) \quad (4.3-8b)$$

where subscripts  $d$  and  $u$  denote down-steps ( $x < y$ ) and up-steps ( $x > y$ ), respectively.

For convenience, the un-normalized function  $f(x,y)$  is usually specified for down-steps, but one could choose to specify a function for up-steps instead. We will follow convention and specify the function for down-steps,  $f(x,y) = f_d(x,y)$  with  $x < y$ . Thus  $N_d(y)$  is easily evaluated:

$$N_d(y) = \int_0^y f_d(x,y) dx \quad (4.3-9)$$

and  $N_u(y)$  can be expressed in terms of  $f_d(x,y)$  by the detailed balance relationship:

$$N_u(y) = \int_y^{\infty} f_d(y,x) \frac{N(y) k_c(x) \rho(x)}{N(x) k_c(y) \rho(y)} \exp[-(x-y)/k_B T] dx \quad (4.3-10)$$

If we had assumed that  $f(x,y)$  was specified for up-steps, an analogous procedure would be followed.

Since  $N(x)$  appears in the integral expression for  $N_u(y)$ , the solution of Eq. 4.3-10 is not completely straightforward. Normalization constant  $N(y)$  can be found by using trial values for  $N(x)$  and employing an iterative solution<sup>1</sup> of Eq. 4.3-10, or by rearranging the equation as follows:

$$N(y) = \frac{\int_0^y f_d(x,y) dx}{1 - \int_y^{\infty} \frac{f_d(y,x) k_c(x) \rho(x)}{N(x) k_c(y) \rho(y)} \exp[-(x-y)/k_B T] dx} \quad (4.3-11)$$

Eq. 4.3-11 can be solved with the finite difference algorithm described by Gilbert and coworkers<sup>7,8</sup>. Both of these approaches to finding  $N(y)$  are based on specifying  $f_d(x,y)$  and requiring that  $N(y)$  first be estimated at very high energies, well above the energies of interest, where  $N_d(y)$  and  $N_u(y)$  tend to become independent of energy (at least when the average energy transferred per collision is independent of energy).

As discussed in the previous section,  $k_c(y)$  is expected to depend on the initial energy,  $y$ , but it is common practice to assume that the inelastic collision rate constants are independent of internal energy<sup>1,6,7,10</sup>. This constant is conventionally identified with  $k_{LJ}$ , the bimolecular rate constant for collisions between particles governed by a Lennard-Jones intermolecular potential.<sup>6,8,10</sup> An accurate empirical expression for the collision integral has been reported by Neufeld et al.<sup>14</sup>, which has been cited by, for example, Gilbert and Smith.<sup>8</sup>

Experience has shown that the assumption the  $k_c$  is independent of energy leads to problems with normalization.<sup>2</sup> Iterative normalization<sup>1</sup> converges reasonably rapidly at high energies, but problems emerge at low energies, where the density of states is sparse and has large relative fluctuations. The problems are most severe when an energy grain that contains just a few states is bracketed on both sides by energy grains containing much higher densities of states. For these cases, the normalization factors for some of the energy grains tend to diverge, instead of



converging during the iterative calculation. Because of this problem, it was necessary to limit the number of iterations to e.g. 2-5, so that normalization at high energy converges sufficiently, while normalization at low energy does not diverge too much. This strategy, although not completely satisfactory, is reasonably effective in producing steady-state energy distributions that simulate the equilibrium Boltzmann distribution.

Related problems arise at low energies when using the finite difference algorithm of Gilbert and coworkers.<sup>7,8</sup> The Gilbert algorithm is quite general, but in practice the pragmatic assumption is made that the collision frequency is independent of excitation energy. These problems result in normalization constants that are negative and therefore un-physical in some energy grains.

*Starting with MultiWell v.2009.0, we have incorporated a new treatment of collisions that solves the problems outlined above.<sup>2</sup>*

In principle it should be possible to express  $k_c(y)$  as a function of  $N(y)$ , but the specific functional dependence is not known. In the absence of specific knowledge about  $k_c(y)$ , we make the simplest possible assumption: that  $k_c(y)$  is directly proportional to  $N(y)$ .<sup>2</sup> With this assumption, the following ratio, which appears in Eq. 4.3-10, equals unity

$$\frac{N(y) k_c(x)}{N(x) k_c(y)} = 1 \quad (4.3-12)$$

The assumption that  $k_c(y)$  is directly proportional to  $N(y)$  requires that the collision frequency for a molecule with excitation energy  $y$  be calculated using  $k_c(y) = C \cdot N(y)$  (see Eq. 4.3-12), where the proportionality constant  $C$  must be established by some other means. Since the Lennard-Jones rate constant  $k_{LJ}$  conventionally has been used for calculating the low pressure limit of unimolecular and recombination reactions, we have adopted the following form for the total energy-dependent rate constant for the inelastic collision frequency:

$$\frac{N(y) k_c(x)}{N(x) k_c(y)} = 1 \quad (4.3-13)$$

where  $E_{ref}$  is a reference energy.

In reaction studies, the rate of energy transfer is most important at energies near the reaction critical energy. Thus we identify  $E_{ref}$  with the critical energy of the lowest reaction threshold energy (when multiple reaction channels are involved) that is higher in energy than the energy boundary (parameter Emax1) between the lower and upper portions of the double array in MultiWell. If no reaction threshold energies are below Emax1, we arbitrarily specify  $E_{ref}$  as equal to Emax1. At Emax1,  $N(y)$  is a relatively smooth function and the density of states is typically  $>10$ -100 states/cm<sup>-1</sup>. Except at low energies, the numerical results obtained using this new approach are nearly the same as those obtained using the old conventional approach.<sup>2</sup>

For convenience in the Monte Carlo selection of step sizes, both the normalization factor  $N(E')$  and the probability of an activating collision  $P(E,E') = [N_a(E')/N(E')]$  are stored in double arrays for each well. At low state densities,  $P(E,E')$  exhibits random fluctuations and some energy grains may contain no states, while the function is quite smooth at high energies. Since it is desirable to be able to use arbitrary functions for the collision step size distribution, it is not feasible to employ analytic expressions for the integrals in the normalization equation, which would allow much shorter computer execution times. In fact, several approximate analytical expressions were tested, but none was sufficiently accurate in the sparse density of states regime. For this reason, normalization is carried out numerically using the open-ended trapezoidal rule,

which is a particularly robust algorithm.<sup>16</sup> For low energies, the energy step size is set equal to that used in the lower energy portion of the double arrays ( $\Delta E_{\text{grain}}$ ). At higher energies, the energy step size is set equal to a fraction (typically 0.2) of the magnitude of a characteristic energy transfer step:

$$\delta E_d = \left| \frac{d(\ln f_d(E, E'))}{dE} \right|^{-1}, \quad \text{for } E' > E, \quad (4.3-14a)$$

$$\delta E_a = \left| \frac{d(\ln f_a(E', E))}{dE} \right|^{-1}, \quad \text{for } E' < E, \quad (4.3-14b)$$

where  $f_a(E, E')$  and  $f_d(E, E')$  were defined above. For the exponential model,  $\delta E_d$  is equal to  $\alpha(E)$ , which varies with internal energy. In general, both the characteristic energy length and the integration step size vary with energy.

### Collision Step-Size Distribution

Many step-size distribution models have been used in energy transfer studies and there is still considerable uncertainty about the appropriate collision model and functional form of  $P(E, E')$ .<sup>3,15,18</sup> Note that  $P_d(E, E')$  for de-activating collisions is expressed in terms of an un-normalized function  $f_d(E, E')$  and normalization factor  $N(E)$ :

$$P_d(E, E') = \frac{1}{N(E')} f_d(E, E') \quad \text{for } E' > E, \quad (4.3-15)$$

To offer a wide selection, MultiWell includes a number of different optional functional forms for  $f_d(E, E')$ , including biexponential, Gaussian, Weibull distribution, etc. The best information currently available suggests that a generalized exponential function is most appropriate for deactivation steps:<sup>11</sup>

$$f_d(E, E') = \exp \left\{ - \left| \frac{E' - E}{\alpha(E')} \right|^\gamma \right\}, \quad \text{for } E' > E, \quad (4.3-15)$$

where  $\alpha(E)$  is a linear function of vibrational energy, and  $\gamma$  is a parameter that ranges from  $\sim 0.5$  to  $\sim 1.5$ . The corresponding expression for activation collisions is obtained from detailed balance. When the parameter  $\gamma$  is less than unity, the wings of the step-size distribution have enhanced relative probabilities that qualitatively resemble the bi-exponential distribution. When  $\gamma=1$ , Equation (4.3-15) gives the venerable exponential model.

### Monte Carlo Selection of Step-Size

Two random numbers are used for selecting the collision step size. The first random number selects activating, or deactivating collisions by comparison to the up-transition probability  $P_{up}(E)$ :

$$P_{up}(E) = N_a(E) / N(E) \quad \text{up-transition probability} \quad (4.3-16)$$

$$0 \leq r_3 < P_{up}(E), \quad \text{activating} \quad (4.3-16a)$$

$$P_w(E) \leq r_3 < 1, \quad \text{de-activating} \quad (4.3-16b)$$

To select the step-size, the second random number is used with the cumulative distribution for  $P(E, E')$  to find the final energy  $E$ , given initial energy  $E'$ .<sup>1</sup>

$$r_4 = \frac{1}{N_a(E')} \int_{E'}^E f_a(x, E') dx, \quad \text{activating} \quad (4.3-17a)$$

$$r_4 = \frac{1}{N_a(E')} \int_{E'}^E f_d(x, E') dx, \quad \text{de-activating} \quad (4.3-17b)$$

The integrals are evaluated by the trapezoidal rule, just as described in the preceding section, until the equalities in Equation (4.3-17) are satisfied. In the high energy regime, this is accomplished by integrating step-by-step until an integration step gives a value for the right hand side of Equation (4.3-17) that is larger than  $r_4$ . Linear interpolation is then used to find the value of final energy  $E$  that satisfies the equality. In the low energy regime, the integration is carried out step-by-step to find the energy step which gives the best agreement between the LHS and right hand side of Equation (4.3-17). Note that the normalization integrals in the low energy regime are stored in the lower energy portion of the double arrays. In the high energy regime, the normalization integrals are found by interpolation of values stored the high energy portion of the double arrays.

Occasionally, the normalization integrals are overestimated due to imperfect interpolation and thus the equalities in Equation (4.3-17) cannot be satisfied. In such a case, the integral is evaluated step-by-step until the additional partial sum is less than a selected relative error (typically  $10^{-6}$ ). This procedure yields an explicitly calculated value for the normalization integral. The interpolated normalization integral is then replaced with this new value and the energy step selection process is repeated. This procedure is somewhat cumbersome and computationally intensive, but it was found to produce more accurate thermal distribution functions.

## References

- (1) Barker, J. R. Monte-Carlo Calculations on Unimolecular Reactions, Energy-Transfer, and IR-Multiphoton Decomposition. *Chem. Phys.* **1983**, *77*, 301-318.
- (2) Barker, J. R. Energy Transfer in Master Equation Simulations: A New Approach. *Int. J. Chem. Kinet.* **2009**, *41*, 748-763.
- (3) Barker, J. R.; Yoder, L. M.; King, K. D. Feature Article: Vibrational Energy Transfer Modeling of Non-Equilibrium Polyatomic Reaction Systems. *J. Phys. Chem. A* **2001**, *105*, 796-809.
- (4) Durant, J. L.; Kaufman, F. Calculation and use of total collision rates in thermal systems. *CPL* **1987**, *142*, 246-251.
- (5) Forst, W. *Theory of Unimolecular Reactions*; Academic Press: New York, 1973.
- (6) Forst, W. *Unimolecular Reactions. A Concise Introduction*; Cambridge University Press: Cambridge, 2003.

- (7) Gilbert, R. G.; King, K. D. Gas/Gas and Gas/Wall Average Energy Transfer from Very Low-Pressure Pyrolysis. *Chemical Physics* **1980**, *49*, 367-375.
- (8) Gilbert, R. G.; Smith, S. C. *Theory of Unimolecular and Recombination Reactions*; Blackwell Scientific Publications: Oxford, 1990.
- (9) Hirschfelder, J. O.; Curtiss, C. F.; Bird, R. B. *Molecular Theory of Gases and Liquids*; Wiley: New York, 1964.
- (10) Holbrook, K. A.; Pilling, M. J.; Robertson, S. H. *Unimolecular Reactions*, 2 ed.; Wiley: Chichester, 1996.
- (11) Hold, U.; Lenzer, T.; Luther, K.; Reihs, K.; Symonds, A. C. Collisional energy transfer probabilities of highly excited molecules from kinetically controlled selective ionization (KCSI). I. The KCSI technique: Experimental approach for the determination of P(E,E) in the quasicontinuous energy range. *Journal of Chemical Physics* **2000**, *112*, 4076-4089.
- (12) Lawrance, W. D.; Knight, A. E. W. Collisional deactivation of a selected energy level in S<sub>0</sub> p-difluorobenzene embedded in a dense vibrational field: Absolute rate constants for a variety of collision partners. *J. Chem. Phys.* **1983**, *79*, 6030-6042.
- (13) Lendvay, G.; Schatz, G. C. Choice of gas kinetic rate coefficients in the vibrational relaxation of highly excited polyatomic molecules. *J. Phys. Chem.* **1992**, *96*, 3752-3756.
- (14) Neufeld, P. D.; Janzen, A. R.; Aziz, R. A. Empirical Equations to Calculate 16 of the Transport Collision Integrals  $\Omega(l, s)^*$  for the Lennard - Jones (12-6) Potential. *J. Chem. Phys.* **1972**, *57*, 1100.
- (15) Oref, I.; Tardy, D. C. Energy transfer in highly excited large polyatomic molecules. *Chem. Rev.* **1990**, *90*, 1407-1445.
- (16) Press, W. H.; Teukolsky, S. A.; Vetterling, W. T.; Flannery, B. P. *Numerical Recipes in FORTRAN. The Art of Scientific Computing*, 2 ed.; Cambridge University Press: Cambridge, 1992.
- (17) Stace, A. J.; Murrell, J. N. A classical trajectory study of collisional energy transfer in thermal unimolecular reactions. *J. Chem. Phys.* **1978**, *68*, 3028-3039.
- (18) Tardy, D. C.; Rabinovitch, B. S. Intermolecular vibrational energy transfer in thermal unimolecular systems. *Chem. Rev.* **1977**, *77*, 369-408.
- (19) Xue, B.; Han, J.; Dai, H.-L. Collision Relaxation Cross Section for Highly Vibrationally Excited Molecules. *Physical Review Letters* **2000**, *84*, 2606-2609.
- (20) Yardley, J. T. *Introduction to Molecular Energy Transfer*; Academic Press: New York, 1980.
- (21) Yoder, L. M.; Barker, J. R. Quasiclassical Trajectory Simulations of Pyrazine-Argon and Methylpyrazine-Argon van der Waals Cluster Predissociation and Collisional Energy Transfer. *JPCA* **2000**, *104*, 10184-10193.

#### **A.4.4 Other Processes**

Additional processes can be incorporated into MultiWell calculations by using the capability of reading rate constants from external data files.

Several processes have been neglected in the present version of MultiWell. For example, spontaneous infrared emission<sup>3</sup> by the vibrationally excited species, which is particularly important at low pressure,<sup>2</sup> has not been included. Similarly, stimulated emission, which is important in laser-induced chemical reactions,<sup>1,4</sup> has also been neglected. Future versions of MultiWell may include these processes, especially if the kinetics community expresses an interest in them.

#### **References**

- (1) Barker, J. R. Infrared Multi-Photon Decomposition - a Comparison of Approximate Models and Exact-Solutions of the Energy-Grained Master Equation. *Journal of Chemical Physics* **1980**, *72*, 3686-3694.
- (2) Barker, J. R. Radiative Recombination in the Electronic Ground State. *J. Phys. Chem.* **1992**, *96*, 7361-7367; DOI: 10.1021/j100197a042.
- (3) Durana, J. F.; McDonald, J. D. *Journal of Chemical Physics* **1977**, *64*, 2518.
- (4) Golden, D. M.; Rossi, M. J.; Baldwin, A. C.; Barker, J. R. Infrared multiphoton decomposition: photochemistry and photophysics. *Accounts of Chemical Research* **1981**, *14*, 56-62.

## A.5. Initial Conditions

At the start of each stochastic trial, initial conditions must be specified. MultiWell selects the initial energy *via* Monte Carlo selection techniques that are based on the cumulative distribution function corresponding to a selected physical process. It is assumed that the reactant is at infinite dilution in a heat bath and thus there are no temperature changes due to reaction exothermicity or energy transfer. For most laboratory experiments, this is an acceptable approximation.

### A.5.1 Monte Carlo Selection of Initial Energies

Monte Carlo selection of the initial internal energy is carried out by equating random number  $r_5$  to the cumulative distribution function  $Y_0(E)$  corresponding to a given initial energy density distribution  $y_0(E)$ :

$$r_5 = Y_0(E) = \int_0^E y_0(E') dE' \quad (5.1-1)$$

where  $E'$  is the integration variable. In MultiWell,  $Y_0(E)$  is found by rectangular rule in the lower portion of the double array and by trapezoidal integration in the upper portion; the values are stored as a function of initial energy in a linear array.  $Jsize$  (which user-selected) array elements are used to cover the relevant energy range. For a thermal distribution (see below), the relevant energy range is assumed to be  $\sim 20k_B T$ . The Monte Carlo selection is carried out by interpolating in the stored array to find the value of  $E$  at which  $Y_0(E) = r_5$ . Interpolation in this fashion is much more computationally efficient than calculating the integral in Equation (5.1-1) for each stochastic trial.

### A.5.2 Optional Initial Energy Density Distributions

The initial energy density distributions that are included as options in MultiWell are described here. In addition to these choices, there is also a provision for providing a user-defined double array of  $Y_0(E)$  values and for a delta function (which does not require Monte Carlo selection). Examples of user-defined functions include prior distributions<sup>10-12</sup> and energy distributions that are the result of bond fission.<sup>9</sup>

### Thermal Activation

In an ordinary thermal unimolecular reaction system that takes place at infinite dilution, the translational and vibrational temperatures are equal and do not change during reaction ( $T_{trans} = T_{vib}$ ). For shock wave simulations, it is assumed that  $T_{trans}$  changed instantaneously when the shock occurred and therefore is elevated at  $t=0$ , but  $T_{vib}$  remains at the temperature that described the thermal system prior to the shock. Subsequent vibrational energy transfer collisions cause the internal energy to increase. The only difference between shock tube and isothermal simulations is that in the former, the two temperatures are unequal. In both cases, the initial internal energy distribution function is a Boltzmann distribution characterized by  $T_{vib}$ . The probability of the initial energy  $E$  falling in the range between  $E$  and  $E+dE$  is given by the probability density function

$$y_0^{(therm)}(E) dE = \frac{\rho(E) e^{-\frac{E}{k_B T_{vb}}} dE}{\int_0^{\infty} \rho(E') e^{-\frac{E'}{k_B T_{vb}}} dE'} \quad (5.2-1)$$

### Single Photon Photo-Activation

The energy distribution produced by absorption of a single photon is assumed to be described by the thermal population at the ambient vibrational temperature added to the energy of the photon ( $h\nu$ ). Hence, the probability density function for photo-activation is given by Equation (5.2-1) and the selected thermal energy is then increased by  $h\nu$ .

### Chemical Activation and Recombination Reactions

Chemical activation is the process by which a single vibrationally excited species  $C(E)$  is produced from the bimolecular reaction of two precursor species (A and B):



where  $E$  is the vibrational energy. The excited molecule  $C(E)$  can then react by passing back out of the entrance channel, or proceeding forward through the product channel, as shown in Fig. 5.1. The energy distribution of  $C(E)$  before it has a chance to react or be collisionally stabilized is the known as the chemical activation distribution function. It is appropriate for any recombination reaction that takes place under thermal conditions.

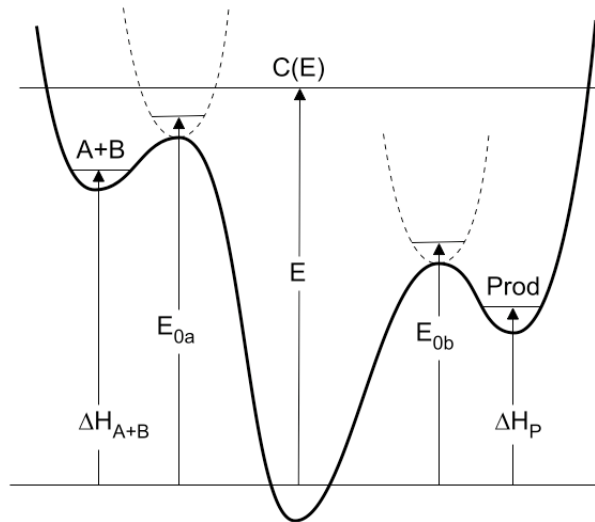


Figure 5.1. Energy diagram for chemical activation.

The chemical activation distribution function is obtained from the reverse reaction by using detailed balance.<sup>3-6,8</sup> The reverse reaction is the unimolecular decomposition reaction with rate constant  $k_a(E)$  that produces the product set  $A+B$ . The index  $a$  specifies the particular unimolecular reaction channel  $C(E) \rightarrow A + B$ . The resulting probability density function is a thermal distribution weighted by  $k_a(E)$ . The probability density function and corresponding Monte Carlo selection expression are as follows:

$$y_0^{(ca,i)}(E)dE = \frac{k_a(E)\rho(E)e^{-\frac{E}{k_B T_{\text{vib}}}} dE}{\int_{E_{0a}}^{\infty} k_a(E')\rho(E')e^{-\frac{E'}{k_B T_{\text{vib}}}} dE'}, \quad \text{for } E \geq E_{0a} \quad (5.2-3)$$

$$r_5 = \int_{E_{0a}}^{E'} y_0^{(ca,i)}(E)dE \quad (5.2-4)$$

where the lower limits of the above equations are equal to  $E_{0a}$ , the unimolecular reaction threshold energy. The density of states  $\rho(E)$  is for the molecule C. The trapezoidal rule is used in the selection procedure, as described above for thermal activation.

A recombination reaction produces a recombination product, which is a chemically activated species. The chemically activated recombination product  $C(E)$  can react *via* the reverse of Reaction (5.2-2), and possibly by other unimolecular pathways, in competition with collisional energy transfer. Several quantities may be of interest, including branching ratios, net rates of reaction to produce specific final products, etc. In all cases, the first step is to simulate the reactions of the chemically activated recombination product  $C(E)$  under the desired conditions of temperature and pressure. The results of the simulation can be used in various ways to find the quantities of interest.<sup>1</sup>

The total rate constant for the recombination reaction at the high pressure limit is obtained from detailed balance by using the equilibrium constant  $K(T_{\text{trans}})$  at translational temperature  $T_{\text{trans}}$ :

$$k_{\text{rec},\infty} = k_{\text{uni},\infty} / K(T_{\text{trans}}) \quad (5.2-5)$$

where  $k_{\text{rec},\infty}$  and  $k_{\text{uni},\infty}$  are the high pressure limiting recombination and unimolecular decomposition rate constants, respectively; the latter of these is calculated and reported in the MultiWell standard output. The equilibrium constant  $K(T_{\text{trans}})$  is calculated using the program Thermo (part of the MultiWell computer program suite), which employs standard statistical mechanics formulas<sup>2,7</sup> for the partition functions of the reactants A and B.

To calculate the over-all rate constant for producing the  $i^{\text{th}}$  product, the relative population (fraction)  $f_i$  of that species at the end of the simulation is multiplied by  $k_{\text{rec},\infty}$ :

$$k = f_i k_{\text{rec},\infty} = f_i k_{\text{uni},\infty} / K(T_{\text{trans}}) \quad (4.2-6)$$

This procedure is appropriate whether or not there is an intrinsic energy barrier for the recombination reaction.



## References

- (1) Barker, J. R.; Ortiz, N. F. Multiple-Well, multiple-path unimolecular reaction systems. II. 2-methylhexyl free radicals. *Int. J. Chem. Kinet.* **2001**, *33*, 246–261; DOI: 10.1002/kin.1018.
- (2) Davidson, N. *Statistical Mechanics*; McGraw-Hill Book Company, Inc.: New York, 1962.
- (3) Forst, W. *Theory of Unimolecular Reactions*; Academic Press: New York, 1973.
- (4) Forst, W. *Unimolecular Reactions. A Concise Introduction*; Cambridge University Press: Cambridge, 2003.
- (5) Gilbert, R. G.; Smith, S. C. *Theory of Unimolecular and Recombination Reactions*; Blackwell Scientific Publications: Oxford, 1990.
- (6) Holbrook, K. A.; Pilling, M. J.; Robertson, S. H. *Unimolecular Reactions*, 2 ed.; Wiley: Chichester, 1996.
- (7) Mayer, J. E.; Mayer, M. G. *Statistical Mechanics*; John Wiley & Sons, Inc.: New York, 1940.
- (8) Robinson, P. J.; Holbrook, K. A. *Unimolecular Reactions*; Wiley-Interscience: London; New York, 1972.
- (9) Tsang, W.; Bedanov, V.; Zachariah, M. R. Master equation analysis of thermal activation reactions: Energy-transfer constraints on falloff behavior in the decomposition of reactive intermediates with low thresholds. *J. Phys. Chem.* **1996**, *100*, 4011-4018.
- (10) Urbain, P.; Leyh, B.; Remacle, F.; Lorquet, A. J. Unimolecular reaction dynamics from kinetic energy release distributions. III. A comparative study of the halogenobenzene cations. *J. Chem. Phys.* **1999**, *110*, 2911.
- (11) Venkatesh, P. K.; Dean, A. M.; Cohen, M. H.; Carr, R. W. Master equation analysis of intermolecular energy transfer in multiple-well, multiple-channel unimolecular reactions. I. Basic Theory. *Journal of Chemical Physics* **1997**, *107*, 8904-8916.
- (12) Vereecken, L.; Huyberegts, G.; Peeters, J. Stochastic simulation of chemically activated unimolecular reactions. *J. Chem. Phys.* **1997**, *106*, 6564-6573; <https://doi.org/10.1063/1.473656>.

## A.6. Input

### A.6.1 Major Options

### A.6.2 Densities of States: $\rho(E)$

Densities of states for the wells are provided in an external file (in the form of a double array). DenSum is provided as a tool to calculate sums and densities of states according to the Whitten-Rabinovitch approximation,<sup>10,11</sup> or according to the Stein-Rabinovitch method<sup>7</sup> of exact counts. Molecular assignments for use in the current version of DenSum can be expressed in any combination of separable harmonic oscillators, Morse oscillators, and free rotors. For non-separable degrees of freedom, other approaches will be needed (see references<sup>3,8,9</sup>, for example).

The moments of inertia needed for calculating rotational constants are evaluated with the program MomInert. This code requires Cartesian coordinates for the molecular structure. Such structures can be calculated with good accuracy by using quantum chemistry programs.

### ***A.6.3 Specific Unimolecular Rate Constants: $k(E)$***

Specific rate constants are needed for each reaction. There are three ways to provide rate constants: a) they may be calculated internally via the Inverse Laplace Transform (ILT) method, b) the sums of states can be provided in an external file, and c) the  $k(E)$  values can be provided in an external file. Data provided in an external file is in the form of a double array with energy origin at the reaction threshold energy. The double array allows high energy resolution near the reaction threshold where it is most important. For most purposes, it is most efficient to use DenSum, which calculates sums of states ( $G^\ddagger(E-E_0)$ ) and generates an external file suitable for input into MultiWell. However, Densum is only suitable for fixed transition states with separable degrees of freedom and therefore other methods must be used to calculate  $G^\ddagger(E-E_0)$  or  $k(E-E_0)$  for non-separable and flexible transition states. If the reaction is a reversible isomerization reaction, MultiWell uses the same external data file to calculate  $k(E-E_0)$  for both forward and reverse reactions. By using the same external file for both forward and reverse reactions, the reversible isomerization rates are internally self-consistent.

### ***A.6.4 Properties of Wells and Transition States***

Energies (e.g.  $\Delta H_f^\circ$  at 0 K) are required for all wells and transition states, in order to establish the relative energies of isomers and reaction thresholds. Moments of inertia are needed for the inactive degenerate two-dimensional external rotation. Energy transfer parameters are needed for each well and MultiWell does not require that they be the same for all wells. One would expect the energy transfer parameters for a cyclic species to differ from those of a linear isomer. However, to the best of my knowledge the energy transfer parameters are not known for more than one isomer in any system. Until additional information becomes available, it is pragmatic to assume that all isomers have the same energy transfer parameters.

## **A.7. Output**

MultiWell generates several output files that summarize the input data and the calculation results.

### ***A.7.1 multiwell.out***

This general output file summarizes the input parameters, thermochemistry, high pressure limit rate constants for each reaction, time-dependent average fractional populations (with standard deviations from Equation (11)), and average vibrational energies. The time-dependent quantities are the instantaneous (snapshot) values averaged over  $N_{\text{trials}}$  stochastic trials: they are not averaged over the time interval, as was done in previous master equation codes from this laboratory.<sup>2,4,6</sup>

### A.7.2 *multiwell.rate*

This file stores the time-dependent output of average unimolecular "rate constants" or *flux coefficients*<sup>1,5,12</sup> (which vary with time in non-steady-state systems) for every reaction pathway:

$$\langle r_j(t) \rangle = \frac{1}{N_{\text{trials}}} \sum_{i=1}^{N_{\text{trials}}} k_j(E_i(t)) \quad (7.2-1)$$

where  $j$  designates the reaction channel. Many trials are needed to accumulate good statistics. To improve statistics, the binned results correspond to the number of visits to the bin (which can be many times larger than  $N_{\text{trials}}$ ) and thus are averaged over the time-duration of the bin. Note that this averaging method differs from the snapshot method described above, where the number of snapshots is equal to  $N_{\text{trials}}$ . In a steady-state thermal system with irreversible reactions,  $\langle r \rangle$  is independent of time and equal to the average unimolecular rate constant  $k_{\text{uni}}(T)$ , which obtains when the energy distribution is in a steady state. In non-steady-state systems,  $\langle r(t) \rangle$  varies with time and relaxes to a constant value as the system itself undergoes relaxation. As relaxation takes place, some reactions achieve steady-state, which is apparent as  $\langle r(t) \rangle$  approaches a constant value. Thus, this output file is useful for several purposes, including monitoring relaxation and the approach to steady state.

### A.7.3 *multiwell.flux*

This file stores the average time-dependent "reactive flux" through reaction channel  $j$ :

$$\langle F_j(t) \rangle = f_{\text{react}}(t) \langle r_j(t) \rangle \quad (7.3-1)$$

where  $f_{\text{react}}(t)$  is the time-dependent average fraction of the reactant species and  $\langle r_j(t) \rangle$  is the average flux coefficient described above by Eq. 7.2-1. When two reactions come into pseudo-equilibrium with one another, their reactive fluxes are equal to each other. Thus, this output file is useful for several purposes, including monitoring the evolution toward equilibrium and diagnosing pseudo-equilibrium conditions.

### A.7.4 *multiwell.dist*

This file stores time-dependent vibrational distributions within each well. Only the non-zero array elements are tabulated. Many trials are needed to accumulate good statistics and thus the binned results correspond to the number of visits to the bin (which can be many times larger than  $N_{\text{trials}}$ ) and are averaged over the time-bin. To limit the size of this file, each (default) time bin is set at ten times that of the time-bins used for the other time-dependent output.

### A.7.5 *multiwell.array*

This file tabulates all energy-dependent input data, including densities of states, specific rate constants for every reaction, collision up-transition probabilities and normalization factors, and initial energy distributions.

## A.8. Concluding Remarks

MultiWell calculates time-dependent concentrations, yields, vibrational distributions, and rate constants as functions of temperature and pressure for unimolecular reaction systems that

consist of multiple stable species and multiple reaction channels interconnecting them. Users may supply unimolecular reaction rates, sums of states and densities of states, or optionally use the Inverse Laplace Transform method. For weak collision effects, users can select different collision models for down-steps including exponential, biexponential, generalized exponential, etc., and user-defined functions.

The code is intended to be relatively easy to use. It is designed so that even the most complicated unimolecular reaction systems can be handled via the data file without restructuring or recompiling the code.

MultiWell is most suitable for time-dependent non-equilibrium systems. The real time needed for a calculation depends mostly upon the number of collisions during a simulated time period and on the number of stochastic trials needed to achieve the desired precision. For slow reaction rates and precise yields of minor reaction products, the code will require considerable computer time, but it will produce results. For long calculation runs, we often just let the simulation run overnight or over a weekend.

## References

- (1) Aguda, B. D.; Pritchard, H. Reversible and irreversible formulation of unimolecular reactions. *J. Chem. Phys.* **1992**, *96*, 5908-5914.
- (2) Barker, J. R. Monte-Carlo Calculations on Unimolecular Reactions, Energy-Transfer, and IR-Multiphoton Decomposition. *Chem. Phys.* **1983**, *77*, 301-318.
- (3) Barker, J. R. Sums of Quantum States for Non-Separable Degrees of Freedom: Multidimensional Monte Carlo Integration. *J. Phys. Chem.* **1987**, *91*, 3849-3854.
- (4) Barker, J. R.; King, K. D. Vibrational Energy Transfer in Shock-Heated Norbornene. *J. Chem. Phys.* **1995**, *103*, 4953-4966.
- (5) Miller, J. A.; Klippenstein, S. J. Master Equation Methods in Gas Phase Chemical Kinetics. *J. Phys. Chem. A* **2006**, *110*, 10528-10544.
- (6) Shi, J.; Barker, J. R. Incubation in Cyclohexene Decomposition at High Temperatures. *Int. J. Chem. Kinet.* **1990**, *22*, 187-206.
- (7) Stein, S. E.; Rabinovitch, B. S. Accurate evaluation of internal energy level sums and densities including anharmonic oscillators and hindered rotors. *J. Chem. Phys.* **1973**, *58*, 2438-2445.
- (8) Toselli, B. M.; Barker, J. R. Ro-vibrational State Densities Based on Spectroscopic Data for Non-separable Systems. *CPL* **1989**, *159*, 499-504.
- (9) Toselli, B. M.; Barker, J. R. Symmetry Specific Densities of Rovibrational Energy Levels for Nonseparable Systems. *J. Phys. Chem.* **1989**, *93*, 6578-6581.
- (10) Whitten, G. Z.; Rabinovitch, B. S. Accurate and Facile Approximation for Vibrational Energy - Level Sums. *J. Chem. Phys.* **1963**, *38*, 2466.
- (11) Whitten, G. Z.; Rabinovitch, B. S. Approximation for Rotation—Vibration Energy Level Sums. *J. Chem. Phys.* **1964**, *41*, 1883.
- (12) Widom, B. Molecular Transitions and Chemical Reaction Rates. *Science* **1965**, *148*, 1555-1560.



## Appendix B. Technical Notes

### B.1 Conversion Factors (Rotational Data)

Moment of Inertia (I):

$$\begin{aligned} I(\text{amu } \text{Å}^2) &= I(\text{g cm}^2) / 1.66054 \times 10^{-40} \\ I(\text{amu} * \text{Å}^2) &= 16.85763 / B(\text{cm}^{-1}) \\ I(\text{amu} * \text{Å}^2) &= 5.0538 \times 10^5 / B(\text{MHz}) \\ I(\text{amu} * \text{Å}^2) &= 5.0538 \times 10^2 / B(\text{GHz}) \end{aligned}$$

Rotational Constant

$$\begin{aligned} B(\text{cm}^{-1}) &= B(\text{Hz}) / 2.99793 \times 10^{10} \\ B(\text{cm}^{-1}) &= B(\text{MHz}) / 2.99793 \times 10^4 \\ B(\text{cm}^{-1}) &= B(\text{GHz}) / 2.99793 \times 10^1 \end{aligned}$$

### B.2 Anharmonic Vibrations

#### *Separable Anharmonic Vibrations*

As described by Herzberg,<sup>4</sup>  $\omega$  (=  $v/c$ , where  $v$  is the harmonic frequency and  $c$  is the speed of light) is used in the following expression for the vibrational energy, where  $s$  is the number of *separable* oscillators, the vibrational energy  $E_v$  is expressed in units of  $\text{cm}^{-1}$  (relative to the zero point energy  $E_z$ ), and the other symbols have their usual meanings:

$$E_{vib} = \sum_{i=1}^s \omega_i \left( v_i + \frac{1}{2} \right) + \sum_{i=1}^s X_{ii} \left( v_i + \frac{1}{2} \right)^2 \quad (1)$$

where the zero point energy is given by

$$E_z = \frac{1}{2} \sum_{i=1}^s \omega_i + \frac{1}{4} \sum_{i=1}^s X_{ii} \quad (2)$$

In **DenSum** and **Thermo**, vibrational anharmonicities can be entered directly for each independent vibration. The energy of each oscillator is computed as

$$E_{vib} = WE * (v+1/2) + ANH * (v+1/2) * (v+1/2), v=0,1,2,3,\dots$$

where parameter  $WE$  and  $ANH$  are the harmonic frequency and anharmonicity, respectively (both expressed in  $\text{cm}^{-1}$  units). For a Morse oscillator,  $ANH < 0$  for this convention. **DenSum** and **Thermo** assume *separable* degrees of freedom, where inter-mode couplings are neglected. Thus they can only consider the diagonal elements of the  $X_{ij}$  anharmonicity coefficient matrix. Thus parameter  $ANH$  is identified with the diagonal  $X_{ii}$  element.

Because Densum and Thermo are limited to separable modes, various choices can be made, depending on the information that is available. Sometimes the  $X_{ij}$  anharmonicity coefficients are available from experiments. They can also be computed as standard options by electronic structure codes, although they are expensive to calculate. They are computed from a perturbation theory treatment based on higher derivatives of the potential energy surface at the equilibrium geometry. Thus they are closely related to the computed harmonic frequencies, which are based on the 2nd derivatives of the same potential energy surface.

### Possible Choices (in decreasing order of preference)

1. For densities and sums of states, treat the vibrations as *non-separable* by using program **bdens** instead of **DenSum**. See the next section.
2. If the fundamental frequency for the 0-1 transition and the full (or diagonal)  $X_{ij}$  matrix are known, one should use the fundamental frequency as "FUN" and the  $X_{ii}$  diagonal term as ANH.
3. If the harmonic frequency and the full  $X_{ij}$  matrix are known, then one should first compute the fundamental frequency and then use Choice #1.
4. If the harmonic frequency and the diagonal terms of the  $X_{ij}$  matrix are known, then one should use the harmonic frequency as "HAR" and the  $X_{ii}$  diagonal term as ANH.
5. If the fundamental 0-1 transition frequency is known, but the  $X_{ij}$  matrix is not known, then one should use the fundamental frequency as "FUN" and ANH=0.0.
6. If the harmonic frequency is known and the  $X_{ij}$  matrix is not known, then one should use the harmonic frequency as "HAR" and ANH=0.0.
7. If nothing is known, then one must use estimation methods.<sup>2</sup>

### *Non-Separable Anharmonic Vibrations*

For asymmetric top molecules, the vibrational energy level relative to the zero point energy is given by the following perturbation theory expansion for the vibrational energy:<sup>30,31,43</sup>

$$\begin{aligned}
 E_v = -E_z + \sum_{i=1}^N \omega_i \left( \nu_i + \frac{1}{2} \right) + \sum_{i=1}^N \sum_{j=i}^N X_{ij} \left( \nu_i + \frac{1}{2} \right) \left( \nu_j + \frac{1}{2} \right) + \\
 \sum_{i=1}^N \sum_{j=i}^N \sum_{k=j}^N Y_{ijk} \left( \nu_i + \frac{1}{2} \right) \left( \nu_j + \frac{1}{2} \right) \left( \nu_k + \frac{1}{2} \right) + \\
 \sum_{i=1}^N \sum_{j=i}^N \sum_{k=j}^N \sum_{l=k}^N Z_{ijkl} \left( \nu_i + \frac{1}{2} \right) \left( \nu_j + \frac{1}{2} \right) \left( \nu_k + \frac{1}{2} \right) \left( \nu_l + \frac{1}{2} \right) + \dots
 \end{aligned} \tag{3}$$



where  $\omega_i$  is the harmonic oscillator frequency,  $X_{ij}$ ,  $Y_{ijk}$ , and  $Z_{ijkl}$  are the anharmonicity constants,  $\nu_i$  is the vibrational quantum number,  $N$  is the number of vibrational modes, and  $E_z$  is the zero-point vibrational energy, which is obtained by setting all  $\nu_i = 0$ :

$$E_z = \frac{1}{2} \sum_{i=1}^N \omega_i + \frac{1}{4} \sum_{i=1}^N \sum_{j=i}^N X_{ij} + \frac{1}{8} \sum_{i=1}^N \sum_{j=i}^N \sum_{k=j}^N Y_{ijk} + \frac{1}{16} \sum_{i=1}^N \sum_{j=i}^N \sum_{k=j}^N \sum_{l=k}^N Z_{ijkl} + \dots \quad (4)$$

The array of harmonic frequencies ( $\omega$ ) and the matrices composed of the anharmonicity constants ( $\mathbf{X}$ ,  $\mathbf{Y}$ ,  $\mathbf{Z}$ ) can be either obtained from experiment or computed directly from first principles, e.g. by quantum chemistry software packages equipped with VPT2. Note that the zero point energy computed using VPT2 includes an additional small term,  $G_0$ , which must be included for high accuracy work. This term does not affect spectroscopic transitions, but it should be included for kinetics and thermochemistry calculations.<sup>3,5</sup>

When all quantized vibrational energy levels are known, sums and densities of states can be counted exactly. From Eq. 3, all  $E_\nu$  can in principle be computed when all allowed values of  $\nu$  are known. Therefore, the problem reduces to finding all allowed values of  $\nu_i$  up to a given total internal energy. For a separable harmonic oscillator, all quantum numbers from  $\nu=0$  to  $\nu=\infty$  are allowed. A Morse oscillator, however, can dissociate and has only a finite number of vibrational states ranging from  $\nu=0$  to  $\nu=\nu_{max}$ . The allowed quantum numbers therefore range from  $\nu=0$  to  $\nu=\nu_{max}$ . For a *coupled* set of anharmonic vibrations, the maximum quantum number allowed for the  $k^{\text{th}}$  vibration,  $\nu_{D,k}$ , depends on the quantum numbers assigned for all other vibrations. When the state energies are described by a perturbation theory expansion containing only  $\mathbf{X}$  (i.e.  $\mathbf{Y}$  and  $\mathbf{Z} = 0$ ),  $\nu_{D,k}$  can be found analytically<sup>27</sup>:

$$\nu_{D,k} = \left[ -\frac{\omega_k + \sum_{j \neq i} X_{kj} \left( \nu_j + \frac{1}{2} \right)}{2X_{kk}} - \frac{1}{2} \right] \quad (5)$$

It must be remembered that  $\nu_{D,k}$  depends on all of the other quantum numbers. When  $X_{kk} < 0$ , then  $\nu_{D,k}$  is the quantum number for the highest bound level of the  $k^{\text{th}}$  vibration and the corresponding dissociation energy (relative to the zero point energy) of this vibrational mode is  $D_k$ :

$$D_k = -\frac{\left( \omega_k + \sum_{j \neq k} X_{jk} \left( \nu_j + \frac{1}{2} \right) \right)^2}{4X_{kk}} - \left( \frac{1}{2} \omega_k + \sum_{j \neq k} \frac{1}{4} X_{jk} \right) \quad (6)$$

This dissociation energy corresponds to the energy at which  $E_\nu$  reaches a maximum as  $\nu_k$  is increased, i.e.  $(\partial E_\nu / \partial \nu_k) = 0$  at  $\nu_k = \nu_{D,k}$ .

While computing the sums of states from  $E_\nu=0$  to a maximum value  $E_\nu=E_{tot}$ , the range of allowed quantum numbers is further restricted. Suppose one proceeds by first starting with all quantum numbers set to zero and then assigning quantum numbers one at a time. After assigning  $k-1$  quantum numbers and before assigning the  $k^{\text{th}}$ ,  $\nu_k=0$  and the remaining unassigned energy  $E_u$  is given by

$$E_u = E_{tot} - E_{\nu,k-1} \quad (7)$$

where  $E_{v,k-1}$  is the vibrational energy  $E_v$  computed using the  $k-1$  quantum numbers already assigned. The range of possible quantum numbers for the  $k^{\text{th}}$  oscillator is therefore  $v_k=0$  to  $v_{\text{max},k}$ , where  $v_{\text{max},k}$  depends on the amount of unassigned energy:

$$v_{\text{max},k} = v_{D,k} \quad \text{for } E_u \geq D_k \quad (8a)$$

$$v_{\text{max},k} = v_{D,k} \left[ 1 - \sqrt{1 - \frac{E_u}{D_k}} \right] \quad \text{for } E_u \leq D_k \quad (8b)$$

When the **Y** and/or **Z** higher-order anharmonicities are included in Eq. 3, analytical solution for  $v_{D,k}$  is not obtainable and iterative calculations are necessary. In the present work,  $v_{\text{max},k}$  is computed iteratively by increasing trial values of  $v_k$  by unit steps from 0 and monitoring  $E_v(v_k)$  while all other quantum numbers ( $v_i, i \neq k$ ) are held constant. The iterative procedure stops as soon as  $E_v(v_k)$  becomes smaller than  $E_v(v_{k-1})$ . This decrease corresponds to passing the maximum where  $(\partial E_v / \partial v_k) = 0$ . For a state to be "bound" with respect to the  $k^{\text{th}}$  degree of freedom, the derivative must be greater than zero for the trial value of  $v_k$ :  $(\partial E_v / \partial v_k) > 0$ . This process is repeated by increasing  $v_k$  until the  $(\partial E_v / \partial v_k) < 0$  for a trial value of  $v_k$ . The assignment of  $v_{D,k}$  is then based on the sign of the first derivative  $(\partial E_v / \partial v_k)$  at  $v_{k-1}$  (see Figure 1), which enables one to ensure that the state with  $v_{D,k}$  is lower in energy than the classical maximum  $E_v$ . When  $(\partial E_v / \partial v_k)$  is  $> 0$  at  $v_{k-1}$ , then  $v_{D,k} = v_{k-1}$ ; otherwise,  $v_{D,k}$  is set equal to  $v_{k-2}$ .

At energies above the dissociation limit, quasi-bound states exist, where the quantum number for every mode does not exceed the dissociation limit for that particular mode. Of course, if the energy is redistributed, dissociation can take place. For computing RRKM rate constants, quasi-bound states must be counted. Quasi-bound states are identified when the partial derivatives  $(\partial E_v / \partial v_i) > 0$  for all  $i$ . Therefore, after all quantum numbers <sup>1</sup> have been assigned, the partial derivatives  $[\partial E_v / \partial v_i]_{i=1,N}$  are computed and the assigned  $[v_i]_{i=1,N}$  is accepted if all elements are positive; otherwise the state is rejected.

## References

- (1) Allison, T. C.; Ramachandran, B.; Senekowitsch, J.; Truhlar, D. G.; Wyatt, R. E. Variational transition state theory calculations of thermal rate coefficients for the O(P-3)+HCl reaction. *Theochem-Journal of Molecular Structure* **1998**, *454*, 307-314.
- (2) Benson, S. W. *Thermochemical Kinetics*, 2nd ed.; Wiley: New York, 1976.
- (3) Cohen, M. J.; Handy, N. C.; Hernandez, R.; Miller, W. H. Cumulative reaction probabilities for H + H2 = H2 + H from a knowledge of the anharmonic force field. *Chem. Phys. Lett.* **1992**, *192*, 407-416.
- (4) Herzberg, G. *Molecular Spectra and Molecular Structure. II. Infrared and Raman Spectra*, 2 ed.; Van Nostrand Reinhold Co.: Cincinnati, 1945.
- (5) Truhlar, D. G.; Isaacson, A. D. Simple perturbation theory estimates of equilibrium constants from force fields. *J. Chem. Phys.* **1990**, *94*, 357-359.

### B.3 Vibrational Degeneracies

In **DenSum** and **Thermo**, vibrational degeneracies are treated as accidental. Identical results are obtained if each vibrational degree of freedom with degeneracy **NG** is entered in the data file **NG** times as a non-degenerate vibration.

For Harmonic oscillators, the state energies for accidental degeneracies are exactly the same as for true degeneracies that arise, for example, from symmetry considerations. For anharmonic vibrations, the state energies are no longer quite the same for accidental and for true degeneracies, but the differences are small and can be neglected for most kinetics purposes.

[G. Herzberg, "Infrared and Raman Spectra", D. van Nostrand Co., Inc., 1945, p. 210 ff]

### B.4 External molecular rotations

All non-linear polyatomics have principal moments of inertia  $I_A, I_B, I_C$  and corresponding rotational constants  $A = \hbar^2/2I_A$ , etc. When two of the rotational constants are equal to each other, the molecule is termed a *symmetric top*. Otherwise, it is an *asymmetric top*.

#### *Symmetric and Spherical Tops*

In Eq. (1a) for the rotational energy of a symmetric top (e.g. a prolate top with rotational constants  $A \neq B = C$ ):

$$E_r(J,K) = BJ(J+1) + (A-B)K^2 \quad (1a)$$

where quantum number  $J$  is for the total angular momentum and the quantum number  $K$  is for the projection of the total angular momentum on the symmetry axis of rotation. The first term in Eq. 1a is identified with a **two-dimensional (2D) rotor** that is often loosely assumed to be most responsible for conservation of angular momentum: a 2D adiabatic rotation referred to as the "*J-rotor*". In the same spirit, the second term in Eq. 1a is loosely identified with a **1D rotation** about the top axis: the "*K-rotor*". For a rigid symmetric top molecule, the  $K$  quantum number is constrained to take integer values from  $-J$  to  $+J$ . Thus each energy level with  $|K| \neq 0$  is doubly degenerate and those with  $K=0$  are singly degenerate. Because the rotational constants may also be related as  $A = B \neq C$  (e.g. an oblate top), it is convenient to identify the unique rotational constant as  $B_1$  and the twinned rotational constant at  $B_2$ :

$$E_r(J,K) = B_2J(J+1) + (B_1 - B_2)K^2 \quad (1b)$$

Note that it is also required that  $E_r(J,K)$  must be  $\geq 0$  (this becomes an issue for oblate symmetric tops, as discussed below). Spherical tops are symmetric tops with  $B_1 = B_2$ .

#### *Separable Rotors Approximation for Symmetric and Spherical Tops*

In a symmetric top, the  $J$ -rotor and the  $K$ -rotor are coupled, due to the constraint on the  $K$  quantum number:  $-J \leq K \leq +J$ . A spherical top is just a symmetric top with all of the rotational constants equal to each other. It is often more convenient to ignore the constraint and treat the two rotors as separable. In fact, centrifugal corrections (an option in MultiWell) *require* that the rotors are treated as separable, without the constraint on  $K$ . Treating the two external rotors as a

separable 2D rotor with rotational constant  $B_2$  and a separable 1D rotor (the K-rotor) with rotational constant  $B_1$  allows one to treat the K-rotor as "active" by including it with the vibrations and internal rotations when computing the sums and densities of states (see the following sub-section). However, there always exist  $2J+1$  rotational states with the same value of  $J$ , even for a completely asymmetric top. Thus neglecting the restriction on  $K$  has the effect of increasing the density and sum of states. Fortunately, this error is insignificant except for molecules with small rotational constants at very low temperatures.

Current and Rabinovitch examined the separable-rotors approximation and showed that it is reasonably accurate, especially when the following definitions are adopted:  $B_2 = (BC)^{1/2}$ ,  $B_1 = A$ , and the rotational energy is given by:<sup>1,2</sup>

$$E_r(J,K) \approx B_2 J(J+1) + B_1 K^2 \quad (3)$$

without any constraint on the value of  $K$ , except for energy conservation. The accuracy obtained using this approximation is illustrated in Table 9.4. In the second column are canonical rate constants for  $\text{OH} + \text{CO} \rightarrow \text{trans-HOCO}$  computed using SCTST (Semi-classical Transition State Theory; see Appendix B.9 of this Manual), including the proper constraint on the  $K$  quantum number.<sup>4</sup> In the third and fourth columns, the external rotors of the transition state were treated with the separable rotors approximation and two choices for  $B_1$ . It is clear that the separable rotors approximation is quite accurate, especially for the choices  $B_2 = (BC)^{1/2}$  and  $B_2 = A$ .

**Table 10.4. Bimolecular rate constants <sup>a</sup> for  $\text{OH} + \text{CO} \rightarrow \text{trans-HOCO}$  computed using three different treatments of the external rotors <sup>b</sup>**

T(K)	Properly Constrained	Separable Rotors Approximation	
	$-J \leq K \leq +J$	$B_K = A$	$B_K = A - B_{2D}$
200	4.517	4.496	4.642
300	8.201	8.191	8.453
500	17.25	17.29	17.84
1000	50.95	51.28	52.91
2000	146.0	147.6	152.3

<sup>a</sup> Units of  $10^{-13} \text{ cm}^3 \text{ molecule}^{-1} \text{ s}^{-1}$ .

<sup>b</sup> Rotational constants  $A$ ,  $B$ , and  $C$  ( $\text{cm}^{-1}$ ): 3.6640, 0.2264, 0.2132;  $B_{2D} = 0.2197 \text{ cm}^{-1}$ .

### Asymmetric Tops

The rotational states of **asymmetric tops** cannot be calculated from a simple algebraic formula, but partition functions and densities of states can be obtained conveniently to very good accuracy by averaging the two rotational constants that are most similar to each other and treating the asymmetric top as *approximately* symmetric. This is called the **quasi-symmetric top approximation**. For this purpose, the effective rotational constant  $B_2$  for the  $J$ -Rotor is set equal to the geometric mean of the two rotational constants that are most similar. For example, when  $B \approx C$  and neither one is equal to  $A$ , the constant  $B_2 = (BC)^{1/2}$ . This is the same choice utilized in the **separable rotors approximation**, which is quite accurate (see preceding paragraphs).

The difference between these two approximations is that in the *quasi-symmetric top approximation* the  $K$  quantum number is restricted to the range  $-J \leq K \leq +J$  and the rotational energy is constrained to non-negative energies ( $E_r(J,K) \leq 0$ ), while in the *separable rotors approximation* the first of these constraints is abandoned. Both of these approximations are very

accurate for thermodynamics applications under most conditions. However, the separable rotors approximation is utilized for making the centrifugal corrections to rate constants as described by Marcus.<sup>3</sup> This type of centrifugal correction is a user-selected option in the MULTIWELL master equation code, as described elsewhere in this User Manual.

Note that treating the rotations in an asymmetric top as three separable 1D rotors is **NEVER** correct, because the three external rotations are not independent of each other: they are constrained by the total angular momentum. Thus treating the three rotors as independent 1D rotations always leads to **incorrect** results. One should always use either the separable rotors approximation or the quasi-symmetric top approximation for practical calculations.

### **Active Energy and the K-rotor**

In a free molecule, only the total angular momentum is conserved. Thus the  $J$  quantum number is assumed to be adiabatic (conserved), but the  $K$  quantum number can vary within its constraints, as do the vibrational quantum numbers, subject to conservation of energy in the "active" degrees of freedom. The "active energy" is the energy associated with the vibrational quantum numbers and  $K$ , collectively. Thus it is said that the energy in the active degrees of freedom randomizes, or the  $K$ -rotor energy "mixes" with the vibrational energy.

For a **prolate symmetric top** (e.g. a cigar shape),  $A > B$  and therefore  $B_l > 0$ . For prolate symmetric tops, the rigorous constraint  $-J \leq K \leq +J$  is often relaxed in the interest of more convenient computation of densities of states. This popular approximation is reasonably accurate except at the lowest total energies and is simple to implement because the rotational energy  $E_r(J, K) \geq 0$  for all values of  $J$  and  $K$ .

For an **oblate symmetric top** (e.g. disk-shaped),  $A < B$  and hence  $(A-B) < 0$ ; this can give  $E_r(J, K) < 0$  when the unconstrained  $K \gg J$ . Thus the approximate treatment of the  $K$ -rotor may fail seriously for oblate tops, since the term  $(A-B)K^2$  in Eq. 1b is  $< 0$ . The **Separable Rotors Approximation** avoids this issue, since the term  $B_l K^2$  term in Eq. 3 is always  $> 0$ .

To utilize the **Separable Rotors Approximation in DenSum, Thermo, bdens, and sctst**, the  $K$ -rotor is declared as a simple 1D free rotation (type "rot" or "qro") and included with the vibrational degrees of freedom when computing the density of states as a function of active energy. Centrifugal corrections based on the  $B_2 J(J+1)$  term in Eq. 3 are applied separately in the MultiWell master equation code: the **2D ADIABATIC ROTOR** moment of inertia is listed in data file **multiwell.dat** on Line 8 (for wells) or Line 14 (for transition states).

(The *kro* degree of freedom type employs the correct constraints on  $K$  for a single user-specified value of  $J$ . Because it considers only a single value of  $J$ , it is not used for general applications.)

If all degrees of freedom including the external rotations are assumed to be active (i.e. "mixed" with the vibrations), no centrifugal corrections are to be applied in the multiwell master equation code (use the **NOCENT** key word) and the "top" type of degree of freedom for symmetrical tops can be utilized in densum, bdens, and sctst when calculating sums and densities of states.

## References

- (1) Current, J. H.; Rabinovitch, B. S. Decomposition of Chemically Activated Ethyl-d<sub>3</sub> Radicals. Primary Intramolecular Kinetic Isotope Effect in a Nonequilibrium System. *J. Chem. Phys.* **1963**, *38*, 783-795.
- (2) Holbrook, K. A.; Pilling, M. J.; Robertson, S. H. *Unimolecular Reactions*, 2 ed.; Wiley: Chichester, 1996.
- (3) Marcus, R. A. Dissociation and isomerization of vibrationally excited species. III. *J. Chem. Phys.* **1965**, *43*, 2658-2661.
- (4) Nguyen, T. L.; Xue, B.; Weston, R. E., Jr.; Barker, J. R.; Stanton, J. F. Reaction of HO with CO: Tunneling is Indeed Important *J. Phys. Chem. Letters* **2012**, *3*, 1549–1553; dx.doi.org/10.1021/jz300443a.

## B.5 Symmetry numbers, internal rotation, and optical isomers (mirror images)

### External Symmetry Numbers

External symmetry numbers are based on the geometry of the chemical species).<sup>4</sup> For use in DenSum, MultiWell, and Thermo, **we recommend the Gilbert and Smith<sup>5</sup> convention for symmetry numbers**: The external symmetry number should not contain any contribution from internal rotors and the external symmetry numbers are *not* used in the calculation of sums and densities of states. INTERNAL ROTOR symmetry numbers are explicitly included in the data lines for the specific internal rotors (DenSum and Thermo data files).

According to the Gilbert and Smith convention, the external symmetry number for Ethane is  $3 \times 2 = 6$ . The symmetry numbers for the external K-rotor and adiabatic 2-D-rotor are set equal to unity in both DenSum and Thermo. (Note that the codes are flexible enough so that other self-consistent conventions may be used instead.)

### Hindered Internal Rotation

Internal rotors are characterized by both the symmetry of the potential energy (i.e. the foldedness, or number of minima (and maxima) per  $2\pi$  rotation), and the symmetry of the mass distribution (or substituents) around the rotor. A potential energy surface computed using the Born-Oppenheimer approximation is independent of the masses of the nuclei. The potential energy surface for ethane internal rotation, for example, is 3-fold symmetric, but isotopic substitution can give either unsymmetrical or symmetrical mass distributions. If both the PES and the mass distribution have identical symmetries, then that is also the symmetry number of the internal rotor. It is also the number of "indistinguishable minima"; the symmetry number compensates for over-counting the number of indistinguishable minima when computing the partition function.<sup>3</sup>

$$q_{hr} = \frac{1}{\sigma_{hr}} \sum_{i=1}^{\infty} \exp\left(\frac{-E_i}{k_B T}\right)$$

where  $\sigma_{hr}$  is the symmetry number for the hindered rotor and  $E_i$  is the  $i^{\text{th}}$  energy eigenvalue.

MultiWell has provision in Thermo and DenSum for both symmetrical and unsymmetrical hindered internal rotations. For user convenience, the parameters for **symmetrical hindered internal rotations** may be entered in any one of three ways, designated by degree of freedom types "hra", "hrb", and "hrc". These types assume that the reduced internal moment of inertia is constant (independent of dihedral angle) and the potential energy of the internal rotation is given by a simple cosine function:

$$V(\chi) = \frac{U}{2} [1 - \cos(\sigma_{hr} \chi)]$$

where  $U$  is the height of the hindrance barrier, and  $\chi$  is the dihedral angle (for more complex symmetrical potentials, use type "hrd", which is discussed below). If  $U = 0$ , then the internal rotation should be modeled using a 1-D free rotor (types "rot" or "qro") with the symmetry number for the internal rotation.

Types "hra", "hrb", and "hrc" offer three convenient methods for entering the identical information. The information is identical because the harmonic frequency, hindrance barrier height, and the reduced moment of inertia for a symmetrical 1-D hindered internal rotation are related by the single equation:

$$v_t = \frac{\sigma_{hr}}{2\pi} \left( \frac{U}{2I_r} \right)^{1/2}$$

where  $v_t$  is the harmonic torsion frequency,  $U$  is the height of the hindrance barrier, and  $I_r$  is the reduced moment of inertia. With any two of these quantities, the third is defined. Note that this equation is only valid for  $\sigma_{hr} > 1$ .

**Unsymmetrical hindered internal rotations** ( $\sigma_{hr}=1$ ) are entered in Thermo and DenSum by designating degree of freedom type "hrd", which is a **general treatment** of one-dimensional hindered internal rotation. This general treatment can be used to describe internal rotation with just one well, or with two or more distinguishable wells. It can also be used for symmetrical potentials with more complicated potential energy functions. To calculate the internal rotor eigenvalues requires the potential energy function and the reduced moment of inertia (or rotational constant) as a function of dihedral angle. For an example, see the data for ClOOCl in the thermodynamics data base (directory [multiwell/thermo-database/](#)).

For convenience, three forms of the torsional potential energy are accepted by DenSum and Thermo (all coefficients in units of  $\text{cm}^{-1}$ ) for using the General hindered internal rotation treatment:

$$\text{Type Vhrd1} \quad V(\chi) = \sum_{n=1}^N \frac{V_n}{2} [1 - \cos(n\sigma_v(\chi + \phi_v))] ]$$

Type **Vhrd2** 
$$V(\chi) = V_0 + \sum_{n=1}^N V_n \cos(n\sigma_v(\chi + \phi_v))$$

Type **Vhrd3** 
$$V(\chi) = V_0 + \sum_{n=1}^N V_n^c \cos(n\sigma_v(\chi + \phi_v)) + \sum_{n=1}^N V_n^s \sin(n\sigma_v(\chi + \phi_v))$$

where  $\chi$  is the dihedral angle (radians). The parameters  $\sigma_v$  (symmetry number for the potential energy: SYMMV) and  $\phi_v$  (phase angle for the potential: PHASEV (radians)) are merely for convenience in curve-fitting.

Also for convenience, either the rotational constant or the moment of inertia, which are functions of the dihedral angle, can be entered (all coefficients in units of  $\text{cm}^{-1}$ ).

Type **Bhrd1** (all coefficients in units of  $\text{cm}^{-1}$ )

$$B(\chi) = B_0 + \sum_{n=1}^N B_n \cos(n\sigma_B(\chi + \phi_B))$$

Type **Ihrd1** (all coefficients in units of  $\text{amu}\cdot\text{\AA}^2$ )

$$I(\chi) = I_0 + \sum_{n=1}^N I_n \cos(n\sigma_I(\chi + \phi_I))$$

where  $\chi$  is the dihedral angle (radians),  $\sigma_B$  and  $\sigma_I$  are symmetry numbers (SYMMM) and  $\phi_B$  and  $\phi_I$  are phase angles (PHASEM). *It is VERY IMPORTANT that the angles are defined in the same way both for the potential and for the mass factor.*

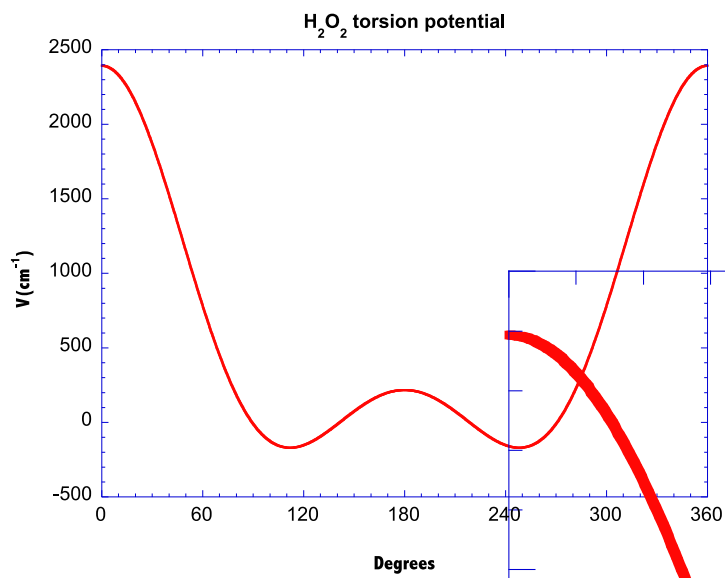
**"hrd" Also Used for Symmetrical Internal Rotors.** This degree of freedom type can also be used for symmetrical hindered internal rotations. The rotor symmetry number (NG) must be given, as well as coefficients for  $V(\chi)$ , which must have the same symmetry as the rotor symmetry number (the parameter SYMMV may equal unity or a convenient multiple of NG; it is only required that  $V(\chi)$  have the correct symmetry). For an example, see the data for HONO<sub>2</sub> in the thermodynamics data base (directory multiwell/thermo-database/).

### Optical Isomers

The classic example of a chemical species that has "optical isomers" (chiral stereoisomers or mirror images) is methane substituted with four unique atoms or isotopes. There is no internal rotation in this classic example, but internal rotation can also produce optical isomers. For example, hydrogen peroxide has right-handed and left-handed forms, which are identical in all respects except for their handedness; they are mirror images of each other. The "gauche" structures of hydrocarbons may also be optical isomers. Consider the case of ethane substituted with one deuterium on each carbon: CH<sub>2</sub>D-CH<sub>2</sub>D. This molecule has three unique staggered conformers characterized by the D-C-C-D dihedral angle  $\chi$ : right-handed gauche with  $\chi = +60^\circ$ , left-handed gauche with  $\chi = -60^\circ$ , and a conformer with C<sub>s</sub> symmetry at  $\chi = 180^\circ$ . Usually (and maybe always), an internal rotation that connects optical isomers involves an unsymmetrical rotor and therefore **care must be taken to treat the optical isomers and unsymmetrical hindered internal rotation in a mutually consistent fashion.**

Consider, for example, hydrogen peroxide (H<sub>2</sub>O<sub>2</sub>), which has an internal rotation around the O-O bond and two non-planar equilibrium structures,<sup>1</sup> as shown below.





This  $V(\chi)$  has symmetry number  $\sigma_v = 1$ . Over one full rotation, it has two wells of equal depth, but the two maxima are of unequal height. Furthermore, the two wells are distinguishable because their geometries cannot be superimposed by simple rigid external rotations: they are optical isomers (mirror images of each other). Essentially, this is a double-well potential.

There are several ways of modeling this double-well potential. The simplest, but least accurate way is to treat this double-well potential as to describe one well as a single harmonic oscillator with harmonic frequency evaluated at the minimum and then multiply the sum of states, density of states, or partition function by  $\times 2$ , since there are twice as many states in a double-well potential. In other words, the number of optical isomers (parameter  $m$ ) is equal to the number of wells and the exact partition function for this 1-D unsymmetrical hindered internal rotation is being approximated as follows:

$$q_{hr} = \sum_{i=1}^{\infty} \exp\left(\frac{-E_i}{k_B T}\right) \approx m \cdot q_{HO} \quad \text{and} \quad \rho_{hr}(E) \approx m \cdot \rho_{HO}(E)$$

where the harmonic oscillator partition function  $q_{HO}$  (and density of states  $\rho_{HO}(E)$ ) is calculated using the harmonic frequency evaluated at the bottom of the well. Clearly, this approximation is only acceptable when the lowest torsion barrier is  $\gg k_B T$ .

A second approximate method for treating these optical isomers is to treat the hindered internal rotation as *symmetric* with  $\sigma_{hr} = m$  and an assumed hindrance barrier height or reduced moment of inertia  $I_r$ . Reasonable estimates for  $I_r$  at the equilibrium structure can be obtained,<sup>2,6</sup> but this approximation cannot provide accurate results over the entire range of temperatures, since it is not possible to approximate both barriers (and the angle-dependent reduced moment of inertia) simultaneously. According to this method, the exact partition function is approximated as follows:

$$q_{hr} = \sum_{i=1}^{\infty} \exp\left(\frac{-E_i}{k_B T}\right) \approx m \cdot q_{shr} = m \cdot \left[ \frac{1}{m} \sum_{i=1}^{\infty} \exp\left(\frac{-E_{s,i}}{k_B T}\right) \right] = \sum_{i=1}^{\infty} \exp\left(\frac{-E_{s,i}}{k_B T}\right)$$

$$\rho_{hr}(E) \approx m \cdot \rho_{shr}(E)$$

where the "shr" subscript designates the symmetric hindered rotor,  $E_i$  are the exact eigenfunctions for the unsymmetrical internal rotation, and  $E_{s,i}$  are the eigenfunctions for the symmetric rotor. Although not accurate over the entire temperature range, this approximation performs slightly better than the harmonic oscillator approach at low to intermediate temperatures.

In both of the above approximations,  $m$  (the number of optical isomers) is used as a multiplier and must be entered in the MultiWell and Thermo input files.

The most accurate approach is to calculate the eigenvalues for the double-well potential and use them directly in calculating the partition function for the hindered internal rotor. This is done by specifying the "hrd" type of degree of freedom, entering the coefficients for the angle-dependent potential energy function and angle-dependent reduced moment of inertia<sup>6</sup> (or rotational constant). For this calculation,  $m$  must be set equal to  $m = 1$ , since the resulting partition function (and density of states) already has the requisite number of levels and should *not* be multiplied by an additional factor. For example, see the data for HOOH in the thermodynamics data base (directory multiwell/thermo-database/).

Of course, not all optical isomers are associated with hindered internal rotation. Those optical isomers that are *not* associated with a hindered rotation should still be included in  $m$  and entered in the data files.

Note that the **external symmetry number** is **not** affected by the hindered rotor treatment and is the same for any treatment of internal rotation, including a harmonic oscillator approximation. When CH<sub>2</sub>D-CH<sub>2</sub>D, HOOH, or any other unsymmetrical internal rotations are treated using the "hrd" degree of freedom type (general hindered internal rotation), then users should set the **internal rotor symmetry** to NG=1 and the number of **optical isomers** to  $m=1$ , but the **external molecular symmetry number** should simply describe the over-all molecular symmetry, which is not affected by the internal rotor treatment. Determining the external symmetry number is usually easiest for the global minimum energy conformation.

## Examples

	$\sigma_V$ : Potential Symmetry	$\sigma_M$ : Mass Symmetry	$\sigma_{hr}$ : Rotor Symmetry	$m$ : Optical Isomers	External Symmetry
CH <sub>3</sub> -CD <sub>3</sub>	3	3	3	1	3
CH <sub>3</sub> -CD <sub>2</sub> H	3	3	3	1	1
CH <sub>3</sub> -CDH <sub>2</sub>	3	3	3	1	1
CH <sub>3</sub> -CH <sub>3</sub>	3	3	3	1	6
CH <sub>2</sub> D-CH <sub>2</sub> D	3	1	1	2	2
CH <sub>2</sub> D-CD <sub>2</sub> H	3	1	1	2	1
CD <sub>3</sub> -CD <sub>3</sub>	3	3	3	1	6
HOOH	1	1	1	2	2
CHFCIBr	—	—	—	2	1

## References

- (1) Dorofeeva, O. V.; Iorish, V. S.; Novikov, V. P.; Neuman, D. B. NIST-JANAF Thermochemical Tables. II Three Molecules Related to Atmospheric Chemistry: HNO<sub>3</sub>, H<sub>2</sub>SO<sub>4</sub>, H<sub>2</sub>O<sub>2</sub>. *J. Phys. Chem. Ref. Data* **2003**, *32*, 879-901.
- (2) East, A. L. L.; Radom, L. Ab initio statistical thermodynamical models for the computation of third-law entropies. *J. Chem. Phys.* **1997**, *106*, 6655-6673.
- (3) Ellingson, B. A.; Lynch, V. A.; Mielke, S. L.; Truhlar, D. G. Statistical thermodynamics of bond torsional modes: Tests of separable, almost-separable, and improved Pitzer-Gwinn approximations. *Journal of Chemical Physics* **2006**, *125*.
- (4) Fernández-Ramos, A.; Ellingson, B. A.; Meana-Pañeda, R.; Marques, J. M. C.; Truhlar, D. G. Symmetry numbers and chemical reaction rates. *Theor. Chem. Account.* **2007**, *118*, 813–826; DOI 10.1007/s00214-007-0328-0.
- (5) Gilbert, R. G.; Smith, S. C. *Theory of Unimolecular and Recombination Reactions*; Blackwell Scientific Publications: Oxford, 1990.
- (6) Wong, B. M.; Thom, R. L.; Field, R. W. Accurate Inertias for Large-Amplitude Motions: Improvements on Prevailing Approximations. *J. Phys. Chem. A* **2006**, *110*, 7406-7413.

## B.6 A Handy List of Lennard-Jones Parameters

Combining rules for Lennard-Jones parameters for A + B collisions:

$$\sigma_{AB} = \frac{1}{2}(\sigma_A + \sigma_B) \quad (\epsilon/k_B)_{AB} = [(\epsilon/k_B)_A (\epsilon/k_B)_B]^{1/2}$$

Species	$\sigma / \text{\AA}$	$\epsilon/k_B / \text{K}$	Ref
He	2.5238	9.8725	23
Ne	2.6016	75.748	23
Ar	3.3237	143.78	23
Kr	3.5160	207.44	23
Xe	3.903	262.68	23
H <sub>2</sub>	2.7828	63.997	23
D <sub>2</sub>	2.73	69	9
CO	3.70	105	9
N <sub>2</sub>	3.7047	84.942	23
NO	3.49	117	9
O <sub>2</sub>	3.3920	121.74	23
CO <sub>2</sub>	3.94	201	9
N <sub>2</sub> O	3.78	249	9
NO <sub>2</sub>	4.68	146	22
"	3.46	357	17
H <sub>2</sub> O	2.71	506	9
N <sub>2</sub> O <sub>5</sub>	4.93	380	11
NH <sub>3</sub>	2.90	558	1
CH <sub>4</sub>	3.79	153	9
C <sub>2</sub> H <sub>2</sub>	4.13	224	9
C <sub>2</sub> H <sub>4</sub>	4.23	217	9
C <sub>2</sub> H <sub>6</sub>	4.39	234	9
C <sub>3</sub> H <sub>6</sub>	4.78	271	9
c-C <sub>3</sub> H <sub>6</sub>	4.63	299	9
C <sub>3</sub> H <sub>8</sub>	4.94	275	9
1-C <sub>4</sub> H <sub>8</sub>	5.28	302	9
cis-2-C <sub>4</sub> H <sub>8</sub>	5.27	312	9
n-C <sub>4</sub> H <sub>10</sub>	5.40	307	9
i-C <sub>4</sub> H <sub>10</sub>	5.39	298	9
n-C <sub>5</sub> H <sub>12</sub>	5.85	327	9
neo-C <sub>5</sub> H <sub>12</sub>	5.76	312	9
C <sub>6</sub> H <sub>6</sub>	5.46	401	9
n-C <sub>6</sub> H <sub>14</sub>	6.25	343	9
c-C <sub>6</sub> H <sub>12</sub>	5.78	394	9
C <sub>7</sub> H <sub>8</sub>	5.92	410	9
C <sub>7</sub> H <sub>16</sub>	6.65	351	9
C <sub>8</sub> H <sub>18</sub>	7.02	359	9
C <sub>9</sub> H <sub>20</sub>	7.34	362	9
C <sub>10</sub> H <sub>22</sub>	7.72	363	9
C <sub>11</sub> H <sub>24</sub>	8.02	362	9
CF <sub>4</sub>	4.40	166	9
C <sub>2</sub> F <sub>6</sub>	5.19	201	9

Species	$\sigma / \text{\AA}$	$\epsilon/k_B / \text{K}$	Ref
C <sub>3</sub> F <sub>8</sub>	5.75	228	9
c-C <sub>4</sub> F <sub>8</sub>	5.93	252	9
C <sub>4</sub> F <sub>10</sub>	6.30	247	9
C <sub>5</sub> F <sub>12</sub>	6.81	261	9
C <sub>6</sub> F <sub>14</sub>	7.17	265	9
C <sub>7</sub> F <sub>16</sub>	7.78	265	9
C <sub>8</sub> F <sub>18</sub>	7.91	268	9
CF <sub>3</sub> Br	4.92	249	9
CF <sub>3</sub> Cl	4.79	217	9
CF <sub>2</sub> CCl <sub>2</sub>	5.08	276	9
CHClF <sub>2</sub>	4.30	331	9
CHCl <sub>2</sub> F	4.57	405	9
CHCl <sub>3</sub>	5.18	378	9
CHF <sub>3</sub>	4.04	268	9
CH <sub>2</sub> Cl <sub>2</sub>	4.54	458	9
CH <sub>3</sub> Br	4.31	416	9
CH <sub>3</sub> Cl	4.07	373	9
1,1-C <sub>2</sub> H <sub>4</sub> Cl <sub>2</sub>	4.85	469	9
1,2-C <sub>2</sub> H <sub>4</sub> Cl <sub>2</sub>	4.78	503	9
i-C <sub>3</sub> H <sub>7</sub> Cl	4.81	435	9
t-C <sub>4</sub> H <sub>8</sub> Cl	5.23	455	9
CS <sub>2</sub>	4.58	415	16
SO <sub>2</sub>	4.11	336	22
SF <sub>6</sub>	5.20	212	9
C <sub>4</sub> H <sub>4</sub> N <sub>2</sub> (Pyrazine)	5.35	307	2
C <sub>2</sub> H <sub>4</sub> O (ethene oxide)	4.08	421	9
SiH <sub>4</sub>	4.08	208	5,21
SiH <sub>3</sub>	3.94	170	5
SiH <sub>2</sub>	3.80	133	5
SiH	3.66	95.8	5
Si	2.91	3036	21, 5
Si <sub>2</sub> H <sub>6</sub>	4.83	301	5
Si <sub>2</sub> H <sub>5</sub>	4.72	306.9	5
H <sub>3</sub> SiSiH	4.60	312.6	5
H <sub>2</sub> SiSiH <sub>2</sub>	4.60	312.6	5
Si <sub>2</sub> H <sub>3</sub>	4.49	318	5
Si <sub>2</sub> H <sub>2</sub>	4.36	323.8	5
Si <sub>2</sub>	3.28	3036	5,21
Si <sub>3</sub> H <sub>8</sub>	5.56	331	5
Si <sub>3</sub>	3.55	3036	5

## References

### B.7 Elements and Isotopes in MomInert and Thermo

The following atomic symbols (atom types) are recognized. Note that isotopic species have the atomic mass associated with the name, except for Deuterium (D) and Tritium (T), which are given their common symbols. Most atomic masses were taken from the "Table of the relative atomic masses of the elements, 1981" [Pure Appl. Chem. **55**, 1101 (1983)], which is cited by JANAF/NIST.<sup>3</sup> Isotopic masses were taken from N. E. Holden, "Table of the Isotopes (Revised 1998)".<sup>10</sup>

Species	Atomic Mass	Species	Atomic Mass
H	1.00794	P	30.97376
H1	1.007825	S	32.06
D	2.014102	S32	31.9720707
T	3.016049	S33	32.97145876
He	4.00260	S34	33.9678668
Li	6.941	Cl	35.453
Li6	6.0151228	Cl35	34.96885271
Li7	7.0160046	Cl37	36.9659
Be	9.012182	Ar	39.948
B	10.81	K	39.0983
B10	10.0129	V	50.9415
B11	11.0093	Zn	65.38
C	12.011	Zn64	63.929
C12	12.0	Zn66	65.926
C13	13.003355	Zn68	67.925
C14	14.003242	Se	78.96
C16	16.0147	Se78	77.917
N	14.00674	Se80	79.917
N14	14.003074	Br	79.904
N15	15.00010897	Br79	78.918338
O	15.9994	Br81	80.916291
O16	15.994915	Kr	83.80
O17	16.9991315	Rb	85.4678
O18	17.999160	Sn	118.69
F	18.998403	I	126.9045
Ne	20.179	Te	127.60
Na	22.98977	Xe	131.29
Mg	24.305	Hg	200.59
Mg24	23.985	U	238.0289
Mg25	24.985	U235	235.04393
Mg26	25.983	U238	238.050788
Si	28.0855		
Si29	28.98		
Si30	29.97		

## B.8 Eigenstates for large amplitude motions

Energy eigenstates for large amplitude motions are needed for computing densities of states and partition functions. In the MultiWell Program Suite, the eigenstates are computed by solving the Schrödinger equation, as described here.

### Theory

The Schrödinger equation for one-dimensional large-amplitude vibration separable from all other motions in the molecule is written as follows<sup>7,8,13,14</sup>

$$\left[ -\frac{\hbar^2}{2} \frac{\partial}{\partial q} \frac{1}{I_{eff}} \frac{\partial}{\partial q} + V(q) \right] \psi(q) = E\psi(q) \quad (1)$$

where  $q$  is the vibrational coordinate,  $\hbar$  is Planck's constant,  $E$  and  $\psi$  are energy eigenvalue and eigenvector, respectively.  $V(q)$  is the vibrational potential energy function, and  $I_{eff}$  is the effective mass, which is in general a function of coordinate  $q$ , but which, depending on  $V(q)$ , is sometimes constant.  $I_{eff}$  can be derived from the ro-vibrational  $G$  matrix, which is defined as:<sup>7,8,15,18,19</sup>

$$G = \begin{pmatrix} I & X \\ X^T & Y \end{pmatrix}^{-1} \quad (2)$$

where the  $I$  matrix is the  $3 \times 3$  moment of inertia tensor, the  $Y$  matrix ( $N_{vib} \times N_{vib}$ ) is the pure vibration contribution, and the  $X$  matrix ( $3 \times N_{vib}$ ) corresponds to the vibration-rotation interaction (Coriolis) terms. Here,  $N_{vib}$  is the number of vibration modes, which equals unity for a 1-D separable degree of freedom. All elements of  $I$ ,  $X$ , and  $Y$  can be computed from the molecular structure as:

$$I_{kk} = \sum_{\alpha=1}^{N_{atom}} m_{\alpha} \left[ \left( \vec{r}_{\alpha} \cdot \vec{r}_{\alpha} \right) - \left( r_{\alpha k} \right)^2 \right]; \quad k = x, y, \text{ or } z \quad (3a)$$

$$I_{kk'} = \sum_{\alpha=1}^{N_{atom}} m_{\alpha} r_{\alpha k} r_{\alpha k'}; \quad k \neq k' \quad (3b)$$

$$X_{ij} = \sum_{\alpha=1}^{N_{atom}} m_{\alpha} \left[ \vec{r}_{\alpha} \times \frac{\partial \vec{r}_{\alpha}}{\partial q_j} \right]_i \quad (4)$$

$$Y_{ij} = \sum_{\alpha=1}^{N_{atom}} m_{\alpha} \left( \frac{\partial \vec{r}_{\alpha}}{\partial q_i} \right) \cdot \left( \frac{\partial \vec{r}_{\alpha}}{\partial q_j} \right) \quad (5)$$

where the  $\alpha$  index runs on the number of atoms ( $N_{atom}$ ) in the molecule.

For one-dimensional large-amplitude **vibrations**, the ro-vibrational  $G$  matrix is expressed as:

$$G = \begin{pmatrix} I_{xx} & -I_{xy} & -I_{xz} & X_{11} \\ -I_{yx} & I_{yy} & -I_{yz} & X_{12} \\ -I_{zx} & -I_{zy} & I_{zz} & X_{13} \\ X_{11} & X_{12} & X_{13} & Y_{11} \end{pmatrix}^{-1} \quad (6)$$

By inverting the right hand side of eq. (6), one obtains:

$$G = \begin{pmatrix} g_{11} & g_{12} & g_{13} & g_{14} \\ g_{21} & g_{22} & g_{23} & g_{24} \\ g_{31} & g_{32} & g_{33} & g_{34} \\ g_{41} & g_{42} & g_{43} & g_{44} \end{pmatrix} \quad (7)$$

Finally,  $I_{eff}$  is obtained as:  $I_{eff} = g_{44}^{-1}$ .

Note that in this work, central finite differences are used to compute the derivatives in Eqs. (4) and (5). Thus the steps between adjacent positions (e.g. dihedral angles) must be small enough so that the derivatives are sufficiently accurate. Acceptable step-sizes must be found by trial and error.

### ***Hindered internal rotations***

For hindered internal rotations, the large-amplitude motions are torsional changes in dihedral angles. The Schrödinger equation (1) for a 1-D torsion can be rewritten as follows<sup>14</sup>:

$$\left[ -\frac{\hbar^2}{2} \frac{\partial}{\partial \chi} \frac{1}{I_{eff}(\chi)} \frac{\partial}{\partial \chi} + V(\chi) \right] \psi(\chi) = E\psi(\chi). \quad (8a)$$

By defining the rotational constant  $B_{hr} = \frac{\hbar^2}{2I_{eff}}$ , we obtain:

$$\left[ -\frac{\partial}{\partial \chi} B_{hr}(\chi) \frac{\partial}{\partial \chi} + V(\chi) \right] \psi(\chi) = E\psi(\chi) \quad (8b)$$

where  $\chi$  is the torsional (dihedral) angle ( $0 \leq \chi < 2\pi$ ),  $V(\chi)$  is the torsional potential energy function, and  $I_{eff}$  is the effective reduced moment of inertia. Both  $I_{eff}$  and  $B_{hr}$  are in general functions of dihedral angle, but are constants for a rigid rotor. When  $B_{hr}$  is assumed to be a constant, which is realistic only for symmetrical rotors, equation (8b) simplifies:

$$\left[ -B_{hr} \frac{\partial^2}{\partial \chi^2} + V(\chi) \right] \psi(\chi) = E\psi(\chi) \quad (9)$$

Solutions of equation (9) are not given here, but are well known.<sup>4,12,14</sup>

For the purpose of calculating densities of states and computing partition functions in the MultiWell Suite, Eq. (8b) is diagonalized to obtain energy eigenvalues, whether or not  $B_{hr}$  is assumed to be constant. The solutions are obtained by using the method described by Meyer.<sup>14</sup> The Hamiltonian matrix of Eq. (8b) is given by:

$$\mathbf{H} = -\mathbf{D}B_{hr}\mathbf{D} + \mathbf{V} = \mathbf{D}^T B_{hr} \mathbf{D} + \mathbf{V} \quad (10)$$

where  $\mathbf{D}$  is the matrix of the first-order derivative ( $\partial/\partial\chi$ ) operator of the internal rotation angle,  $\mathbf{D}^T$  is the transpose of  $\mathbf{D}$  (i.e.  $D^T(i,j) = D(j,i)$ ),  $\mathbf{V}(i,i)$  is the diagonal matrix of the potential energy operator, and  $B_{hr}(i,i)$  is the diagonal matrix element of the rotational constant; the indices are for equally spaced torsion angle grid points. For  $2N + 1$  grid points, the elements of  $\mathbf{D}$  are:

$$D(i,i) = 0 \quad (11a)$$

$$D(i,j) = (-1)^{i-j} \left\{ 2 \sin \left[ (i-j) \pi / (2N-1) \right] \right\}^{-1} \quad \text{for } i \neq j \quad (11b)$$

To construct the symmetric matrix  $\mathbf{H}$ , one requires both  $V(\chi)$  and  $B_{hr}(\chi)$ . Several common representations of  $V(\chi)$  and  $B(\chi)$  (or the corresponding moment of inertia function  $I(\chi)$ ) can be understood by MultiWell, as explained elsewhere in this manual. The matrix  $\mathbf{H}$  is diagonalized in order to obtain a vector of energy eigenvalues, which are convoluted with states from the other degrees of freedom to compute ro-vibrational densities of states or partition functions.

Users must supply the functions  $V(\chi)$  and  $B_{hr}(\chi)$  (or moment of inertia function  $I(\chi)$ ). Potential energies  $V(\chi)$  and molecular geometries can be computed at discrete values of  $\chi$  by obtained by using any of the many available quantum chemistry codes, such as Gaussian,<sup>6</sup> C-Four,<sup>20</sup> and Molpro.<sup>24</sup> The results for  $V(\chi)$  can be fitted to a suitable truncated Fourier series, and one may use codes like the I\_Eckart program<sup>25</sup> (written for use with MatLab) or LAMM program given in the MultiWell Suite to compute  $B_{hr}(\chi)$  or  $I_{hr}(\chi)$ .



## References

- (1) Barker, J. R.; Toselli, B. M. Infrared Emission Studies of the Vibrational Deactivation of Benzene Derivatives. *Int. Rev. Phys. Chem.* **1993**, *12*, 305-338.
- (2) Bevilacqua, T. J.; Weisman, R. B. Collisional vibrational relaxation of a triplet state: Energy dependent energy loss from T1 pyrazine. *J. Chem. Phys.* **1993**, *98*, 6316.
- (3) Chase, M. W., Jr. NIST-JANAF Thermochemical Tables. Fourth Edition. *J. Phys. Chem. Ref. Data* **1998**, *Monograph No. 9*, 1-1951.
- (4) Colbert, D. T.; Miller, W. H. *J. Chem. Phys.* **1992**, *96*, 1982-1991.
- (5) Coltrin, M. E.; Kee, R. J.; Miller, J. A. *Electrochem. Soc.* **1986**, *133*, 1206-1213.
- (6) Frisch, M. J.; Trucks, G. W.; Schlegel, H. B.; Scuseria, G. E.; Robb, M. A.; Cheeseman, J. R.; Scalmani, G.; Barone, V.; Mennucci, B.; Petersson, G. A.; Nakatsuji, H.; Caricato, M.; Li, X.; Hratchian, H. P.; Izmaylov, A. F.; Bloino, J.; Zheng, G.; Sonnenberg, J. L.; Hada, M.; Ehara, M.; Toyota, K.; Fukuda, R.; Hasegawa, J.; Ishida, M.; Nakajima, T.; Honda, Y.; Kitao, O.; Nakai, H.; Vreven, T.; J. A. Montgomery, J.; Peralta, J. E.; Ogliaro, F.; Bearpark, M.; Heyd, J. J.; Brothers, E.; Kudin, K. N.; Staroverov, V. N.; Kobayashi, R.; Normand, J.; Raghavachari, K.; Rendell, A.; Burant, J. C.; Iyengar, S. S.; Tomasi, J.; Cossi, M.; Rega, N.; Millam, J. M.; Klene, M.; Knox, J. E.; Cross, J. B.; Bakken, V.; Adamo, C.; Jaramillo, J.; Gomperts, R.; Stratmann, R. E.; Yazyev, O.; Austin, A. J.; Cammi, R.; Pomelli, C.; Ochterski, J. W.; Martin, R. L.; Morokuma, K.; Zakrzewski, V. G.; Voth, G. A.; Salvador, P.; Dannenberg, J. J.; Dapprich, S.; Daniels, A. D.; Farkas, O.; Foresman, J. B.; Ortiz, J. V.; Cioslowski, J.; Fox, D. J. Gaussian 09, Revision A.1; Revision A.1 ed.; Gaussian, Inc.: Wallingford CT, 2009.
- (7) Harthcock, M. A.; Laane, J. Calculation of kinetic energy terms for the vibrational Hamiltonian: Application to large-amplitude vibrations using one-, two-, and three-dimensional models. *J. Mol. Spectros.* **1982**, *91*, 300-324.
- (8) Harthcock, M. A.; Laane, J. Calculation of two-dimensional vibrational potential energy surfaces utilizing prediagonalized basis sets and Van Vleck perturbation methods. *J. Phys. Chem.* **1985**, *89*, 4231-4240.
- (9) Hippler, H.; Troe, J.; Wendelken, H. J. Collisional deactivation of vibrationally highly excited polyatomic molecules II. Direct observations for excited toluene. *J. Chem. Phys.* **1983**, *78*, 6709-6717.
- (10) Lide, D. R. *CRC Handbook of Chemistry and Physics*, 81 ed.; CRC Press: Boca Raton, 2000.
- (11) Makko, M. W.; Troe, J. *Int. J. Chem. Kinet.* **1982**, *14*, 399-416.
- (12) Marston, C. C.; Balint-Kurti, G. G. *J. Chem. Phys.* **1989**, *91*, 3571-3576.
- (13) Meyer, A.; Schroeder, J.; Troe, J. Photoisomerization of trans-stilbene in moderately compressed gases: Pressure-dependent effective barriers. *J. Phys. Chem. A* **1999**, *103*, 10528-10539.
- (14) Meyer, R. Trigonometric Interpolation Method for One-Dimensional Quantum-Mechanical Problems. *J. Chem. Phys.* **1970**, *52*, 2053-2059.
- (15) Meyer, R.; Günthard, H. H. General Internal Motion of Molecules, Classical and Quantum-Mechanical Hamiltonian. *J. Chem. Phys.* **1968**, *49*, 1510-1520.

- (16) Mourits, F. M.; Rummens, F. H. A. A critical evaluation of Lennard-Jones and Stockmayer potential parameters and of some correlation methods. *Can. J. Chem.* **1977**, *55*, 3007.
- (17) Patrick, R.; Golden, D. M. *Int. J. Chem. Kinet.* **1983**, *15*, 1189-1227.
- (18) Pickett, H. M. Vibration—Rotation Interactions and the Choice of Rotating Axes for Polyatomic Molecules. *J. Chem. Phys.* **1972**, *56*, 1715-1723.
- (19) Podolsky, B. Quantum-Mechanically Correct Form of Hamiltonian Function for Conservative Systems. *Phys. Rev. E* **1928**, *32*, 812-816.
- (20) Stanton, J. F.; Gauss, J.; Harding, M. E.; Szalay, P. G.; Auer, w. c. f. A. A.; Bartlett, R. J.; Benedikt, U.; Berger, C.; Bernholdt, D. E.; Bomble, Y. J.; Christiansen, O.; Heckert, M.; Heun, O.; Huber, C.; Jagan, T.-C.; Jonsson, D.; Jusélius, J.; Klein, K.; Lauderdale, W. J.; Matthews, D. A.; Metzroth, T.; O'Neill, D. P.; Price, D. R.; Prochnow, E.; Ruud, K.; Schiffmann, F.; Stopkowicz, S.; Vázquez, J.; Wang, F.; Watts, J. D. and the integral packages MOLECULE (J. Almlöf and P.R. Taylor); PROPS (P.R. Taylor); ABACUS (T. Helgaker, H.J. Aa. Jensen, P. Jørgensen, and J. Olsen); and ECP routines by A. V. Mitin and C. van Wüllen. CFOUR, a quantum chemical program package ([www.cfour.de/](http://www.cfour.de/)), 2009.
- (21) Svehla, R. A. NASA-TR 132, NASA 1962,
- (22) Troe, J. Theory of thermal unimolecular reactions at low pressures. II. Strong collision rate constants. Applications. *Journal of Chemical Physics* **1977**, *66*, 4758-4775.
- (23) Weaver, A. B.; Alexeenko, A. A. Revised Variable Soft Sphere and Lennard-Jones Model Parameters for Eight Common Gases up to 2200 K. *J. Phys. Chem. Ref. Data* **2015**, *44*, 023103; <http://dx.doi.org/10.1063/1.4921245>.
- (24) Werner, H.-J.; Knowles, P. J.; Lindh, R.; Manby, F. R.; Schütz, M.; Celani, P.; Korona, T.; Rauhut, G.; Amos, R. D.; Bernhardsson, A.; Berning, A.; Cooper, D. L.; Deegan, M. J. O.; Dobbyn, A. J.; Eckert, F.; Hampel, C.; Hetzer, G.; Lloyd, A. W.; McNicholas, S. J.; W. Meyer, W.; Mura, M. E.; Nicklass, A.; Palmieri, P.; Pitzer, R.; Schumann, U.; Stoll, H.; Stone, A. J.; Tarroni, R.; Thorsteinsson, T. MOLPRO version 2006.1 (a package of *ab initio* programs); version 2006.1 ed.; see <http://www.molpro.net>., 2006.
- (25) Wong, B. M.; Thom, R. L.; Field, R. W. Accurate Inertias for Large-Amplitude Motions: Improvements on Prevailing Approximations. *J. Phys. Chem. A* **2006**, *110*, 7406-7413.

## B.9 Semi-Classical Transition State Theory (SCTST)

Much of this section was adapted from Ref. <sup>15</sup>.

Program `parstst` (or older program `sctst`) uses a new algorithm<sup>15</sup> developed for computing rate constants with semi-classical transition state theory (SCTST), which was formulated by Miller and coworkers.<sup>8-11</sup> SCTST incorporates non-separable coupling among all degrees of freedom and multi-dimensional quantum mechanical tunneling along the curved reaction path. The algorithm, which is practical for reactants containing dozens of atoms, predicts both microcanonical and canonical rate constants. In addition, the quantum chemistry code CFOUR has been extended to efficiently compute fully coupled vibrational anharmonicities for transition states at the CCSD(T) level of theory.

Semi-classical transition state theory (SCTST), has been described by W. H. Miller and coworkers.<sup>8-11</sup> In combination with second-order vibrational perturbation theory (VPT2),<sup>12</sup> the

SCTST accounts explicitly for non-separable coupling among all degrees of freedom (including the reaction coordinate) in the transition state region and multidimensional semi-classical tunneling.<sup>8,11</sup> Miller, Handy and coworkers have shown that the SCTST thermal rate constants are in close agreement with those of full quantum dynamic calculations and experiments.<sup>5,6,11</sup> However, the SCTST method has been limited to small reaction systems having only 3-4 atoms because of the large number of quantum states that must be computed for larger systems.<sup>5,6,11</sup>

The new computer code `parstst` (or older program `sctst`) makes it practical to apply the theory to polyatomic reactions. The new algorithm is based on an extension of methods for computing sums and densities of states for fully-coupled anharmonic vibrations, which were described recently.<sup>13</sup> In addition, an extension of the CFOUR electronic structure code<sup>17</sup> is described for computing the anharmonicity constants of transition states at the CCSD(T) level of theory. This new extension has enabled rate constant predictions based on a high level of theory.<sup>15</sup>

## Theory

According to the SCTST of W. H. Miller and coworkers,<sup>11</sup> the microcanonical and canonical rate constants are written:

$$k(E) = \frac{1}{h} \frac{G^\ddagger(E)}{\rho(E)} \quad (1)$$

$$k(T) = \frac{1}{h} \frac{\int_{-\infty}^{\infty} G^\ddagger(E) \exp(-E/k_B T) dE}{Q_{re}(T)} \quad (2a)$$

where  $h$  is Planck's constant,  $k_B$  is Boltzmann's constant,  $T$  is the temperature,  $\rho(E)$  is the density of states of the reactant,  $Q_{re}$  is the total partition function of the reactant(s), and  $G^\ddagger(E)$  is the cumulative reaction probability (CRP).<sup>9</sup> The center of mass translations are rigorously separable. At temperatures that are not too high, it is a good approximation to treat the overall rotations as separable from the vibrations (including internal rotations), so that Eq. (2a) can be written:

$$k(T) = \frac{1}{h} \frac{Q_t^\ddagger Q_r^\ddagger}{Q_t Q_r} \frac{\int_{-\infty}^{\infty} G_v^\ddagger(E_v) \exp(-E_v/k_B T) dE_v}{Q_v(T)} \quad (2b)$$

in which vibrational energy  $E_v$  is the variable of integration and the vibrational CRP is given by:

$$G_v^\ddagger(E_v) = \sum_{n_1=0}^{F-1} \sum_{n_2=0}^{F-1} \dots \sum_{n_{F-2}=0}^{F-1} \sum_{n_{F-1}=0}^{F-1} P_n(E_v) \quad (3)$$

In Eq. 3,  $F-1$  is the total number of vibrational degrees of freedom orthogonal to the reaction path. The semi-classical tunneling probability  $P_n$  is given by<sup>11</sup>

$$P_n(E) = \frac{1}{1 + \exp[2\theta(n, E)]} \quad (4)$$

where

$$\theta(n, E) = \frac{-\pi\Delta E}{\Omega_F} \frac{2}{1 + \sqrt{1 - 4x_{FF}\Delta E / \Omega_F^2}} \quad (5)$$

$$\Delta E = E - \Delta V_o - G_o - \sum_{k=1}^{F-1} \omega_k \left( n_k + \frac{1}{2} \right) - \sum_{i=1}^{F-1} \sum_{j=i}^{F-1} x_{ij} \left( n_i + \frac{1}{2} \right) \left( n_j + \frac{1}{2} \right) \quad (6a)$$

$$\Omega_F = \bar{\omega}_F - \sum_{k=1}^{F-1} \bar{x}_{kF} \left( n_k + \frac{1}{2} \right) \quad \text{with } \bar{\omega}_F = -i\omega_F \text{ and } \bar{x}_{kF} = ix_{kF} \quad (7)$$

In these expressions,  $\omega_k$  is the harmonic vibrational frequency,  $\omega_F$  is the imaginary frequency of the reaction barrier,  $x_{ij}$  are the anharmonicity constants that describe coupling among the orthogonal degrees of freedom,  $x_{kF}$  are the (pure imaginary) coupling terms between the reaction coordinate and the orthogonal degrees of freedom, and  $x_{FF}$  is the real-valued anharmonicity constant for the reaction path, and  $\Delta V_o$  is the classical barrier height. [Note that the definition of  $\Delta E$  used here and in a review article<sup>14</sup> has the opposite sign from the definition given in the original papers; this also affects the Eq. 5.] Note that  $\Omega_F$  is the amplitude of the effective imaginary frequency, which is affected by coupling to all of the other vibrations (Eq. 7) and must always satisfy  $\Omega_F > 0$  for acceptable states; unacceptable states are discarded. The term  $G_o$  is a constant, which is irrelevant in spectroscopic measurements (where only energy differences are important), but which must be included for thermochemistry and kinetics.<sup>5,18</sup>

For convenience, the reaction barrier height is often expressed as the difference between the zero point energy of the transition state and that of the reactant(s) (i.e. the vibrationally adiabatic ground-state potential energy difference  $\Delta V_a^{G^\ddagger}$ ), giving the following expressions:

$$k(T) = \frac{1}{h} \frac{Q^\ddagger Q_r^\ddagger}{Q_r Q_t} \frac{\int_{-\infty}^{\infty} G_v^\ddagger(E_v) \exp(-E_v / k_B T) dE_v}{Q_v(T)} \quad (2c)$$

$$\Delta E = \Delta V_a^{G^\ddagger} - E + E_v^\ddagger \quad (6b)$$

$$E_v^\ddagger = \sum_{k=1}^{F-1} \omega_k \left( n_k + \frac{1}{2} \right) + \sum_{i=1}^{F-1} \sum_{j=i}^{F-1} x_{ij} \left( n_i + \frac{1}{2} \right) \left( n_j + \frac{1}{2} \right) - \frac{1}{2} \sum_{k=1}^{F-1} \omega_k - \frac{1}{4} \sum_{i=1}^{F-1} \sum_{j=i}^{F-1} x_{ij} \quad (8)$$

and  $G_o$  is incorporated into the zero-point vibrational energy of the orthogonal modes:

$$E_{zpe} = G_o + \frac{1}{2} \sum_{k=1}^{F-1} \omega_k + \frac{1}{4} \sum_{i=1}^{F-1} \sum_{j=i}^{F-1} x_{ij} \quad (9)$$

There are three known scenarios where SCTST/VPT2 is not sufficient.<sup>14,19</sup> Two of these scenarios start to be come important only at extremely high and extremely low energies and temperatures. The third scenario becomes significant only at very high energies. None of these scenarios significantly affects rate constants at the temperatures that are important for most atmospheric and combustion applications.

Because the VPT2 approach is used, the SCTST/VPT2 model is subject to failures. In Eq. (5), SCTST/VPT2 will fail catastrophically when the term  $1 - 4x_{FF}\Delta E / \Omega_F^2$  becomes negative, or  $\Omega_F^2 < 4x_{FF}\Delta E$ . In such a case, the quadratic equation that governs the barrier penetration integral has no physically meaningful solutions. Two possible scenarios lead to this failure: (i)

First, when  $x_{FF} < 0$  (as is usually the case in calculations on real systems), it can happen when  $\Delta E$  is less than  $\Omega_F^2/4x_{FF}$  and becomes negative ( $\Delta E < \Omega_F^2/4x_{FF} < 0$ ). This case, which corresponds to  $\Delta E$  values being “*too negative*”, occurs in the deep-tunneling regime below the TS, and Wagner<sup>19</sup> has given an extensive analysis of the problem, along with a suggested solution. When this occurs in our implementation,  $P_n(E)$  is set to zero; (ii) Second, when  $x_{FF} > 0$  (which is very uncommon), leading to  $\Delta E > \Omega_F^2/4x_{FF} > 0$ . This case, which corresponds to  $\Delta E$  values being “*too positive*”, can be seen in the high-energy regime above the TS. Our practical workaround to this case is to set  $P_n(E)$  to unity.

The SCTST/VPT2 approach can also experience a third type of failure. When the energy is high enough, the quantum numbers of the orthogonal degrees of freedom may be quite large. If, in addition, the off-diagonal anharmonicities (i.e., the  $x_{kF}$  terms) that couple the reaction coordinate to the orthogonal modes are negative,  $\Omega_F$  may be reduced to zero, or even to negative values (see Eq. 7). Since  $\Omega_F$  is the effective magnitude of the imaginary frequency, a reduced value of  $\Omega_F$  suggests that the barrier thickness has increased and the probability of tunneling has therefore decreased. When  $\Omega_F = 0$ , the barrier is essentially infinite and there is no tunneling. The “negative omega” scenario (for  $\Omega_F \leq 0$ ) is considered to be unphysical: SCTST/VPT2 breaks down because there is no effective maximum. Possibly a higher order of vibrational perturbation theory can remedy this failure in future, but for present purposes a practical workaround is needed for the “negative omega” scenario. Our practical approach is to regard the barrier as infinitely thick if  $\Omega_F \leq 0$  and we thus assume in that case that the system behaves classically: the tunneling probability  $P_n = 0$  when  $\Delta E \leq 0$ , and  $P_n = 1$  when  $\Delta E > 0$ .

In the next section, the new algorithm for computing the CRP is presented. For canonical (thermal) systems, Hernandez and Miller have described an efficient method for computing the rate constants directly from SCTST without the necessity for computing the CRP.<sup>8</sup> A small modification of the new algorithm presented below can be used for this purpose, but will not be described here because we are primarily interested in computing  $k(E)$ , the microcanonical rate constant, which requires the use of the CRP. However, with the CRP in hand, thermal rate constants can easily be obtained by averaging  $k(E)$  over the thermal energy distribution function. With minor extensions, the methods described here are also appropriate for computing  $k(E,J)$ , the microcanonical rate constant for a specified total angular momentum quantum number  $J$ .

## ***New Algorithm***

In Eqs. (1) and (2c), the CRP is obtained by summing over all states of the transition state. When the state energies can be estimated from harmonic frequencies and anharmonicity constants, the summations in Eq. 3 can be evaluated exactly. In this “exact count” method, a realization of the vector  $[n_k]$  of the vibrational quantum numbers is first determined for every quantum state of the transition state and the CRP is obtained *via* nested DO-loops using Eqs. (3)-(8). Such calculations are quite fast for systems with 3-4 atoms, but they become impossibly slow for systems containing more atoms. The same obstacle is encountered when computing densities of states for coupled vibrational states.<sup>13</sup>

Recently, three practical methods for computing vibrational sums and densities of states were compared.<sup>13</sup> These included the brute force direct method, an “efficient” Monte Carlo method,<sup>1</sup> and an extended version of the algorithm published by Basire et al.,<sup>4</sup> which is based on the Wang-Landau algorithm.<sup>20</sup> The extended algorithm is particularly useful for large molecular systems. As explained elsewhere,<sup>13</sup> all three of the algorithms are based on a perturbation theory expansion of the state energies expressed as functions of the vibrational quantum numbers.

(These algorithms are implemented in programs `paradensum`, `parsctst` (or older program `sctst`), and `bdens`.) A logical extension of these algorithms allows computation of the CRP.

According to SCTST, only  $\Omega_F$  in Eq. (7) and  $E_{v^\ddagger}$  in Eq. (8) depend on the vector  $[n_k]$  of vibrational quantum numbers; all of the other quantities are constants. In the implementation of the Wang-Landau algorithm,<sup>13</sup> the energy axis is divided into many small grains (i.e. energy bins, e.g. with  $\delta E=10 \text{ cm}^{-1}$ ). The algorithm is a random walk procedure in which each step is accepted or rejected, based on certain criteria. For each step that is accepted, a vector of quantum numbers has been generated, which is accepted as long as each quantum number is not greater than the highest bound state in each degree of freedom. This condition is evaluated by computing partial derivatives of the state energy with respect to the quantum numbers, as described by Nguyen and Barker<sup>13</sup>. Acceptable states include the metastable states, which have total energies above the dissociation energy (or reaction energy barrier), but do not have enough energy localized in the reaction coordinate to react. These are the vibrational states of the transition state.

The density of states algorithm is carried out iteratively. During each iteration, each energy bin that contains a vibrational state is sampled a large number of times. The relative density of states estimate is up-dated on the fly and, after a series of iterations, it converges to the exact relative density of states. After the relative density of states is normalized, the algorithm terminates (see Ref. <sup>13</sup> for a detailed description). The CRP can be calculated by using the vibrational density of states  $\rho_{v^\ddagger}(E)$  (which may have been computed previously)<sup>13</sup> and by carrying out a single iterative cycle with the same stepping algorithm used for the density of states calculation. On every accepted step into an energy bin,  $\Omega_F$  and  $E_{v^\ddagger}$  are computed using the vector of quantum numbers  $[n_k]$ . From these quantities, average values and the corresponding average probability are obtained by using Eqs. 4-7 for the  $i^{\text{th}}$  energy bin at energy  $E_i$ :  $\langle \Omega_F \rangle_i = \Omega_{Fi}/H_i$ ,  $\langle E_{v^\ddagger} \rangle_i = E_{v^\ddagger i}/H_i$ , and average probability  $\langle P(E_i) \rangle$ , where  $H_i$  is the number of samples in the  $i^{\text{th}}$  bin. The averages become essentially independent of the number of samples for a sufficiently large number (typically  $10^4/\text{bin}$ ). The algorithm accumulates samples in all of the energy bins where acceptable states exist. If no acceptable states exist in a bin, then  $\langle P(E_i) \rangle = 0$  in that bin. Finally, the CRP is obtained by using the average probability multiplied by the number of states in each energy bin (i.e.  $\rho(E_i)\delta E$ ):

$$G_v^\ddagger(E_v) = \delta E \sum_{E_i}^{\rho_{v^\ddagger} \delta E} \rho(E_i) \langle P(E_i) \rangle \quad (10)$$

## Implementations

In the published `bdens` computer program for computing sums and densities of states,<sup>2</sup> the number of samples in each energy bin is conveniently selected by specifying a key word: *FAIR*, *GOOD*, *BETTER*, *BEST*, or *EXTRA* specifies  $10^2$ ,  $10^3$ ,  $10^4$ ,  $10^5$ , or  $10^6$ , samples per bin, respectively. These key words are also used for specifying the number of samples used to compute the average quantities defined above for the SCTST.

The accuracy of this new random walk algorithm was tested by comparing results obtained using the new algorithm with those obtained from the exact count method (i.e. the nested DO-loops method) for the OH + H<sub>2</sub> reaction. For this reaction, the agreement between the two approaches is excellent, as shown in Figure 1, when  $\geq 10^4$  samples/bin are used for computing the averages. The differences between the "exact" CRP (obtained using explicit nested DO-loops) and the ones based on the new algorithm are less than 5% even at the highest

energy (50000 cm<sup>-1</sup>), resulting in differences of <0.5% between the vibrational partition functions at 2500 K for the transition state.

Program `parsctst` (Section 8.4; or older program `sctst`, Section 8.3) generates a supplementary data file named `<name>.qcrp`, which is required when using program `Thermo` to compute thermal rate constants using the SCTST. This data file contains the partition function corresponding to the CRP.

$$Q_v^\ddagger(T) = \int_0^{\infty} \rho_v^\ddagger(E_v) \exp(-E_v / k_B T) dE_v = (k_B T)^{-1} \int_0^{\infty} G_v^\ddagger(E_v) \exp(-E_v / k_B T) dE_v \quad (11)$$

where  $\rho_v^\ddagger(E_v)$  is the derivative of  $G_v^\ddagger(E_v)$  with respect to  $E_v$ . The integral on the right hand side of Eq. 11 is needed for Eq. 2c. The expression for  $Q_v^\ddagger(T)$  is more convenient for use with program `Thermo`.

### ***VPT2/CCSD(T) for Transition States***

All of the harmonic vibrational frequencies and  $x_{ij}$  anharmonicity coefficients can be obtained for stable species from first principles by using second order vibrational perturbation theory (VPT2), which has been implemented for stable molecules in quantum chemical software packages such as GAUSSIAN<sup>7</sup> and CFOUR<sup>17</sup>. The anharmonicity coefficients are obtained from the full cubic force field together with the semi-diagonal quartic force field, which can be computed by finite differences from the analytic first and second derivatives<sup>3,17</sup>. For highly accurate methods such as CCSD(T), analytic second derivatives are only available in CFOUR<sup>17</sup>. For this work, VPT2 computation of the anharmonicities was implemented for transition states at the CCSD(T) level of theory in CFOUR. Whenever Fermi resonances are detected, deperturbation was applied using a criterion of 100 cm<sup>-1</sup> for the frequency difference. The combination of the new algorithm for the SCTST and implementation of VPT2 for transition states constitutes an effective tool for computing the CRP and/or thermal rate constants from first principles with high accuracy.

### ***Reaction Critical Energy***

In the absence of quantum mechanical tunneling, the critical energy  $E_0$  for a unimolecular reaction (or a bimolecular reaction according to microcanonical TST) is the difference between the enthalpies at 0 K of the transition state and the reactant(s):

$$E_0 = \Delta_f H_{TS}(0) - \Delta_f H_{\text{react}}(0) \quad (12)$$

This definition of the reaction critical energy is **not** appropriate when quantum mechanical tunneling occurs, because tunneling takes place at lower energies. Tunneling occurs whenever the energy is below the top of the barrier (i.e.  $E < E_0$ , where  $E_0$  is defined as above) but above that of the zero point energy of the product. Thus when tunneling is included the appropriate value to be utilized for " $E_0$ " depends on whether the reaction is endothermic or exothermic (including zero point energy corrections), regardless of the reaction barrier height.

In the MultiWell master equation code, the critical energy is defined as in Eq. 12 even when tunneling through an Eckart barrier is invoked (keyword 'tun' on Line 14 in the `multiwell.dat` data file), because the reactant and product enthalpies are employed automatically to account for tunneling below the top of the barrier. When using an external file containing the CRP generated by Program `sctst`, this step is NOT automated and the user must enter the value for critical energy obtained from the following:

Endothermic reactions:  $E_0 = \Delta_f H_{\text{prod}}(0) - \Delta_f H_{\text{reac}}(0)$  (13a)

Exothermic reactions:  $E_0 = 0$  (13b)

(Note: the keyword 'tun' only applies to tunneling through an Eckart barrier and must **NOT** be employed when using the CRP, since tunneling is already included in the CRP.)



## References

### B.10 Legacy and Current Versions of $k_0$ and $k_\infty$ in MultiWell

Early in 2011 it was discovered that the centrifugal corrections had not been implemented correctly. This affected the "informational" values of  $k_0$  and  $k_\infty$  tabulated in the MultiWell output files. This section summarizes the actual implementations. See Appendix Section 2.3 of this User Manual for a summary of the theory.

#### Legacy Basis

Legacy expressions for  $k_{uni}$ ,  $k_\infty$  and  $k_0$  were based on Robinson & Holbrook Eq. 4.30.<sup>16</sup> In the following,  $\omega = k_2[M]$  (in the notation of Robinson & Holbrook).

$$k_{uni} = \frac{Q_1^+}{Q_1 Q_2} \exp(-E_0 / kT) \omega \int_0^\infty \frac{\rho(E^+ + E_0 + \langle \Delta E_J \rangle) k_a(E^+ + E_0 + \langle \Delta E_J \rangle) e^{-E^+ / kT} dE^+}{\omega + k_a(E^+ + E_0 + \langle \Delta E_J \rangle)}$$

where

$$k_a(E^+ + E_0 + \langle \Delta E_J \rangle) = \frac{L^\ddagger}{h} \frac{G(E^+)}{\rho(E^+ + E_0 + \langle \Delta E_J \rangle)}$$

$$\langle \Delta E_J \rangle = \left(1 - \frac{I^\ddagger}{I}\right) kT$$

$G(E^+)$  is the sum of states starting from the ZPE of the TS;  $L^\ddagger$  is the reaction path degeneracy.

The limits:

$$k_\infty = \frac{Q_1^+}{Q_1 Q_2} \exp(-E_0 / kT) \int_0^\infty \rho(E^+ + E_0 + \langle \Delta E_J \rangle) k_a(E^+ + E_0 + \langle \Delta E_J \rangle) e^{-E^+ / kT} dE^+$$

$$k_0 = \frac{Q_1^+}{Q_1 Q_2} \exp(-E_0 / kT) k_{LJ} \int_0^\infty \rho(E^+ + E_0 + \langle \Delta E_J \rangle) e^{-E^+ / kT} dE^+$$

**As actually implemented in the Codes:**

#### Multiwell-2011

CENT

$$k_\infty = \frac{I^\ddagger}{I} \frac{1}{Q_2} \exp(-E_0 / kT) \int_0^\infty \rho(E^+ + E_0 + \langle \Delta E_J \rangle) k_a(E^+ + E_0 + \langle \Delta E_J \rangle) e^{-E^+ / kT} dE^+$$

$$k_0 = \frac{I^+}{I} \frac{1}{Q_2} \exp(-E_0 / kT) k_{LJ} \int_0^\infty \rho(E^+ + E_0 + \langle \Delta E_J \rangle) e^{-E^+ / kT} dE^+$$

NOCENT

$$k_\infty = \frac{I^+}{I} \frac{1}{Q_2} \exp(-E_0 / kT) \int_0^\infty \rho(E^+ + E_0) k_a(E^+ + E_0) e^{-E^+ / kT} dE^+$$

$$k_0 = \frac{I^+}{I} \frac{1}{Q_2} \exp(-E_0 / kT) k_{LJ} \int_0^\infty \rho(E^+ + E_0) e^{-E^+ / kT} dE^+$$

For this case,  $E' = E_0 + E^+$ . Therefore:

$$k_\infty = \frac{I^+}{I} \frac{1}{Q_2} \int_{E_0}^\infty \rho(E') k(E') e^{-E' / kT} dE'$$

$$k_0 = \frac{I^+}{I} \frac{1}{Q_2} k_{LJ} \int_{E_0}^\infty \rho(E') e^{-E' / kT} dE'$$

### **Multiwell-2011.1 and later versions**

'NOCENT' for no centrifugal correction

'CENT1' for quasi-diatomic centrifugal correction with 1 adiabatic external rotation  
(for special cases)

'CENT2' **(This is the usual choice for most reactants)** for quasi-diatomic centrifugal correction with 2 adiabatic external rotations

'CENTX' for **legacy centrifugal correction** with 2 adiabatic external rotations (**not recommended**)

[Note: the calculated  $k_\infty$  is numerically the same for all options.]

NOCENT

(These expressions differ from v.2011 by elimination of the factor  $I^+/I$ .)

$$k_\infty = \frac{1}{Q_2} \int_{E_0}^\infty \rho(E') k(E') e^{-E' / kT} dE'$$

$$k_0 = \frac{1}{Q_2} k_{LJ} \int_{E_0}^\infty \rho(E') e^{-E' / kT} dE'$$

CENT1, CENT2, and CENT3

Note: variable of integration; may be  $E^+$  or  $E'$ .

$$k'_a(E') = \frac{I^+}{I} \exp(\langle \Delta E_J \rangle / kT) k_a(E')$$

$$k_\infty = \frac{1}{Q_2} \int_{E_0 + \langle \Delta E_J \rangle}^{\infty} \rho(E') k'_a(E') e^{-E'/kT} dE'$$

$$k_0 = \frac{1}{Q_2} k_{LJ} \int_{E_0 + \langle \Delta E_J \rangle}^{\infty} \rho(E') e^{-E'/kT} dE'$$

### CENTX

Here,  $x = E^+$ .

$$k_\infty = \frac{I^+}{I} \frac{1}{Q_2} \int_0^{\infty} \rho(x + E_0 + \langle \Delta E_J \rangle) k_a(x + E_0 + \langle \Delta E_J \rangle) e^{-(x+E_0)/kT} dx$$

$$k_0 = \frac{I^+}{I} \frac{1}{Q_2} k_{LJ} \int_0^{\infty} \rho(x + E_0 + \langle \Delta E_J \rangle) e^{-(x+E_0)/kT} dx$$

### References

- (1) Barker, J. R. Sums of Quantum States for Non-Separable Degrees of Freedom: Multidimensional Monte Carlo Integration. *J. Phys. Chem.* **1987**, *91*, 3849-3854.
- (2) Barker, J. R.; Ortiz, N. F.; Preses, J. M.; Lohr, L. L.; Maranzana, A.; Stimac, P. J.; Nguyen, T. L.; Kumar, T. J. D. MultiWell-2010.1 Software Ann Arbor, Michigan, USA, 2010.
- (3) Barone, V. Anharmonic vibrational properties by a fully automated second-order perturbative approach. *J. Chem. Phys.* **2005**, *122*, 014108.
- (4) Basire, M.; Parneix, P.; Calvo, F. Quantum anharmonic densities of states using the Wang-Landau method. *J. Chem. Phys.* **2008**, *129*, 081101.
- (5) Cohen, M. J.; Handy, N. C.; Hernandez, R.; Miller, W. H. Cumulative reaction probabilities for  $H + H_2 = H_2 + H$  from a knowledge of the anharmonic force field. *Chem. Phys. Lett.* **1992**, *192*, 407-416.
- (6) Cohen, M. J.; Willetts, A.; Handy, N. C. Cumulative reaction probabilities for  $OH + H_2 = H_2O + H$  and  $ClH + Cl = Cl + HCl$  from a knowledge of the anharmonic force field. *J. Chem. Phys.* **1993**, *99*, 5885-5897.
- (7) Frisch, M. J.; Trucks, G. W.; Schlegel, H. B.; Scuseria, G. E.; Robb, M. A.; Cheeseman, J. R.; Scalmani, G.; Barone, V.; Mennucci, B.; Petersson, G. A.; Nakatsuji, H.; Caricato, M.; Li, X.; Hratchian, H. P.; Izmaylov, A. F.; Bloino, J.; Zheng, G.; Sonnenberg, J. L.; Hada, M.; Ehara, M.; Toyota, K.; Fukuda, R.; Hasegawa, J.; Ishida, M.; Nakajima, T.;

- Honda, Y.; Kitao, O.; Nakai, H.; Vreven, T.; J. A. Montgomery, J.; Peralta, J. E.; Ogliaro, F.; Bearpark, M.; Heyd, J. J.; Brothers, E.; Kudin, K. N.; Staroverov, V. N.; Kobayashi, R.; Normand, J.; Raghavachari, K.; Rendell, A.; Burant, J. C.; Iyengar, S. S.; Tomasi, J.; Cossi, M.; Rega, N.; Millam, J. M.; Klene, M.; Knox, J. E.; Cross, J. B.; Bakken, V.; Adamo, C.; Jaramillo, J.; Gomperts, R.; Stratmann, R. E.; Yazyev, O.; Austin, A. J.; Cammi, R.; Pomelli, C.; Ochterski, J. W.; Martin, R. L.; Morokuma, K.; Zakrzewski, V. G.; Voth, G. A.; Salvador, P.; Dannenberg, J. J.; Dapprich, S.; Daniels, A. D.; Farkas, O.; Foresman, J. B.; Ortiz, J. V.; Cioslowski, J.; Fox, D. J. Gaussian 09, Revision A.1; Revision A.1 ed.; Gaussian, Inc.: Wallingford CT, 2009.
- (8) Hernandez, R.; Miller, W. H. Semiclassical transition state theory. *Chem. Phys. Lett.* **1993**, *214*, 129-136.
  - (9) Miller, W. H. Semiclassical limit of quantum mechanical transition state theory for nonseparable systems. *J. Chem. Phys.* **1975**, *62*, 1899-1906.
  - (10) Miller, W. H. Semi-Classical Theory for Non-separable Systems: Construction of "Good" Action-Angle Variables for Reaction Rate Constants. *Faraday Discuss. Chem. Soc.* **1977**, *62*, 40-46.
  - (11) Miller, W. H.; Hernandez, R.; Handy, N. C.; Jayatilaka, D.; Willetts, A. Ab initio Calculation of Anharmonic Constants for a Transition-State, with Application to Semiclassical Transition-State Tunneling Probabilities. *Chemical Physics Letters* **1990**, *172*, 62-68; Doi 10.1016/0009-2614(90)87217-F.
  - (12) Mills, I. M. Vibration-Rotation Structure in Asymmetric- and Symmetric-Top Molecules. In *Molecular Spectroscopy: Modern Research*; Rao, K. N., Mathews, C. W., Eds.; Academic Press: New York, 1972; Vol. 1; pp 115-140.
  - (13) Nguyen, T. L.; Barker, J. R. Sums and Densities of Fully-Coupled Anharmonic Vibrational States: A Comparison of Three Practical Methods. *J. Phys. Chem. A* **2010**, *114*, 3718-3730.
  - (14) Nguyen, T. L.; Barker, J. R.; Stanton, J. F. Atmospheric Reaction Rate Constants and Kinetic Isotope Effects Computed Using the HEAT Protocol and Semi-Classical Transition State Theory. In *Advances in Atmospheric Chemistry*; Barker, J. R., Steiner, A. L., Wallington, T. J., Eds.; World Scientific: Singapore, 2017; Vol. 1; pp 403-492.
  - (15) Nguyen, T. L.; Stanton, J. F.; Barker, J. R. A Practical Implementation of Semi-Classical Transition State Theory for Polyatomics. *Chem. Phys. Letters* **2010**, *499*, 9-15.
  - (16) Robinson, P. J.; Holbrook, K. A. *Unimolecular Reactions*; Wiley-Interscience: London; New York, 1972.
  - (17) Stanton, J. F.; Gauss, J.; Harding, M. E.; Szalay, P. G.; Auer, w. c. f. A. A.; Bartlett, R. J.; Benedikt, U.; Berger, C.; Bernholdt, D. E.; Bomble, Y. J.; Christiansen, O.; Heckert, M.; Heun, O.; Huber, C.; Jagan, T.-C.; Jonsson, D.; Jusélius, J.; Klein, K.; Lauderdale, W. J.; Matthews, D. A.; Metzroth, T.; O'Neill, D. P.; Price, D. R.; Prochnow, E.; Ruud, K.; Schiffmann, F.; Stopkowicz, S.; Vázquez, J.; Wang, F.; Watts, J. D. and the integral packages MOLECULE (J. Almlöf and P.R. Taylor); PROPS (P.R. Taylor); ABACUS (T. Helgaker, H.J. Aa. Jensen, P. Jørgensen, and J. Olsen); and ECP routines by A. V. Mitin and C. van Wüllen. CFOUR, a quantum chemical program package ([www.cfour.de/](http://www.cfour.de/)), 2009.
  - (18) Truhlar, D. G.; Isaacson, A. D. Simple perturbation theory estimates of equilibrium constants from force fields. *J. Chem. Phys.* **1990**, *94*, 357-359.

- (19) Wagner, A. F. Improved Multidimensional Semiclassical Tunneling Theory. *J. Phys. Chem. A* **2013**, *117*, 13089–13100; dx.doi.org/10.1021/jp409720s.
- (20) Wang, F.; Landau, D. P. Efficient, Multiple-Range Random Walk Algorithm to Calculate the Density of States. *Phys. Rev. Letters* **2001**, *86*, 2050-2053.

## Appendix C. How to ...

This section outlines how to carry out various tasks needed by many users. It is under development and more sections will be added in future releases of this User Manual.

### C.1 How to set up the double arrays in MultiWell

The double arrays consist of two arrays in one. The lower energy portion ranges in energy from  $E = 0$  up to  $E_{\max 1}$ ; the upper energy portion ranges in energy from  $E = 0$  up to  $E_{\max 2}$ . The total size of the double array is  $I_{\text{size}}$  and the number of "energy grains" (i.e. energy bins) in the lower and upper parts of the double array are  $I_{\max 1}$  and  $I_{\max 2}$ , respectively, and the respective energy grain sizes are  $E_{\text{grain}1}$  and  $E_{\text{grain}2}$ . The relationships among these quantities are as follows:

$$E_{\max 1} = (I_{\max 1} - 1) * E_{\text{grain}1}$$

$$E_{\max 2} = (I_{\max 2} - 1) * E_{\text{grain}2}$$

$$I_{\text{size}} = I_{\max 1} + I_{\max 2}$$

To set up double arrays, users must specify  $E_{\text{grain}1}$ ,  $I_{\max 1}$ ,  $E_{\max 2}$ , and  $I_{\text{size}}$ ; the remaining parameters are determined by the program from the relationships given above. The following guidelines are useful for deciding on the values for the parameters.

#### $E_{\text{grain}1}$

- Should be small enough so that further reductions in its size do not significantly affect the numerical results (i.e. it should achieve numerical convergence).
- Should be  $\sim 10\%$  of  $k_B T$ , or less (for good accuracy in computing  $k_\infty$ ).
- Should not be too small, since that adds a computational burden.
- Typical choices: 5 or 10  $\text{cm}^{-1}$  (usually 10  $\text{cm}^{-1}$ ).

#### $I_{\max 1}$

- Should be large enough so that the density of states in adjacent energy grains near  $E_{\max 1}$  differ by less than 5%. DenSum will give a warning if the grain-to-grain fluctuations are too large.
- Typically,  $I_{\max}$  should be large enough so that  $E_{\max 1}$  is greater than the highest vibrational wavenumber (typically greater than  $\sim 3000 \text{ cm}^{-1}$ ).
- Typical choice: 400 (for  $E_{\text{grain}1} = 10 \text{ cm}^{-1}$ ).

#### $E_{\max 2}$

- Should be high enough so that none of the stochastic trials attempt to reach a higher energy. If that occurs, MultiWell execution will halt and a Fatal Error will be reported.
- Typical choices: 50000  $\text{cm}^{-1}$  for  $T \leq 300 \text{ K}$ ; 85000  $\text{cm}^{-1}$  for  $T \leq 3000 \text{ K}$ .

#### $I_{\text{size}}$

- Should be chosen large enough so that  $E_{\text{grain}2} \leq k_B T / 2$  (for good convergence on the numerical computation of  $k_\infty$ ).
- Typical choices: 1000 for simulations at 300 K, 1500 for very high temperatures.

## C.2 How to test the double-array parameters in MultiWell

In principle, it is wise to test your choices of parameters to determine whether the calculations are reaching numerical convergence. In other words, one should determine whether the choices of Egrain1 and Egrain2 are small enough and that Emax1 and Emax2 are high enough.

The tests are carried out on a small subset of representative simulations with pressures and temperatures at the middle and at the extremes of their ranges, for a total of nine simulations. For narrow pressure ranges and temperature ranges, only one representative set of conditions may be necessary. Thus the amount of testing depends on the system and on experience with similar simulations.

Numerical convergence has been achieved when the grain sizes are small enough and the maximum energies are high enough so that further grain size reductions and/or further maximum energy increases do not result in significant differences in the calculations.

The most important measure of convergence is to ascertain whether the fractional yields computed for the same simulated time duration are independent of the grain size.

Two additional key quantities affected by grain size and maximum energy are  $k_{inf}$  and  $k_{osc}$  (i.e. the high pressure limit  $k_{\infty}$  and the low pressure limit  $k_0$ ), which are printed by MultiWell for information purposes in the table summarizing transition state and reaction properties (preceding the table summarizing the stochastic simulations). These rate constants are not actually used by MultiWell in the simulations, but they are useful to users. The value for  $k_{\infty}$  should agree within a few percent with the corresponding canonical rate constant calculated by Thermo with the same input parameters.

## C.3 How estimate Lennard-Jones and energy transfer parameters

It is very difficult to compute proper energy transfer parameters. Instead, they are usually obtained by fitting experimental rate constant data. There are two parts to the problem: obtaining Lennard-Jones (LJ) parameters and estimating energy transfer parameter  $\alpha$  for the exponential-down model, which is recommended for most purposes.

The LJ parameters can be estimated by using the critical properties of the compound, which may in turn be estimated using various empirical correlations. However, it is almost always sufficiently accurate to estimate the parameters, based on analogy. A table of LJ parameters can be found in Appendix B.6 of this User Manual.

Experience shows that parameter  $\alpha$  in the exponential model (i.e. a single component of the bi-exponential model) usually is in the range from  $100 \text{ cm}^{-1}$  to  $1000 \text{ cm}^{-1}$ ;  $250 \text{ cm}^{-1}$  is a good first guess.

Experimental rate constant data can be fitted by varying the value of parameter  $\alpha$  until a good fit has been achieved. It is efficient to start by computing results for several values of  $\alpha$  that cover the whole range expected (typically 100, 250, 500, and  $1000 \text{ cm}^{-1}$ ). For most molecular species, the "true" value is probably somewhere in this range. By examining a plot of the data superimposed on a plot of this family of simulations, it will be possible to get a better estimate of the fitted value. The plot will also demonstrate the sensitivity of the simulations to the assumed value.

## C.4 How to obtain rate constants from MultiWell simulations

Master equation simulations are accurate at all time-scales over which statistical rate theory is valid, but "rate constants" are valid only *after* an initial energy relaxation has been completed. When simulating experiments (in which intermediates might *never* be thermalized), it is not necessary to define rate constants. In that case, the master equation results are employed directly. However, master equations are also used to compute rate constants for predictions and for comparisons with experimental values.

MultiWell does not calculate conventional reaction rate constants directly; the output must be analyzed further. The data from the simulation can be analyzed by using least squares fitting and other techniques, just as is done in analyzing experiments.<sup>1,6,8,11,13,15,16</sup> In the following, several pragmatic approaches are described.

### *Single-well Unimolecular Reactions*

Single-well reaction systems may have multiple channels and all of the reaction channels are **irreversible** unimolecular reactions in multiwell simulations. To find  $k_{\text{uni}}$  in the pressure fall-off regime, you need to carry out simulations at the temperature and pressure of interest. Then, you can find  $k_{\text{uni}}$  in one of two ways (outlined below), both of which depend on the population distribution reaching STEADY STATE. The population distribution will approach steady-state after an initial transient period if the reaction rates are slower than the energy relaxation rates. As the population distributions approach steady state, the average vibrational energy of the system (E<sub>vib</sub> in output file multiwell.out) and the reaction flux coefficients (in output file multiwell.rates) will asymptotically approach constant values. Due to the stochastic simulation noise that accompanies stochastic simulations, these values will usually display fluctuations.

Here are the two methods for finding unimolecular rate constants:

a) Reaction Flux Coefficients: the output file 'multiwell.rate' gives reaction flux coefficients for all the reactions, based on the instantaneous population distributions and on  $k(E)$  for each reaction. When the population distribution in the well is AT STEADY STATE, the flux coefficient for each irreversible channel is equal to  $k_{\text{uni}}$  for that channel; the total  $k_{\text{uni}}$  is equal to the sum of the channel-specific rate constants. To use this feature, however, requires many, many stochastic trials in a single simulation in order to reduce the stochastic sampling noise. This technique **should not be used for multi-well reaction systems**, because the reactions are reversible and the unimolecular rate constants therefore depend algebraically on more than one reaction flux coefficient.

b) Curve fitting: the decay of population in a SINGLE-WELL reaction is exponential with total rate constant  $k_{\text{uni}}$ , which may be obtained from a semi-log plot: natural logarithm of population ("fraction") vs. time; the slope of the plot is equal to  $-k_{\text{uni}}$ . For multi-channel reactions, the branching ratios of the individual channels can be obtained from the relative rates of producing products or relative product yields ("fractions"), evaluated for the period over which the population is in steady-state.

It is important to note that if the analysis requires time periods longer than needed for more than a few thousand collisions, the simulations become very time-consuming. MultiWell is not designed for computing slow, steady-state unimolecular reactions. The factors affecting computation time are discussed in the following sub-section.



## Execution Speed for Unimolecular Reactions

The time needed to perform a stochastic simulation and obtain a unimolecular rate constant depends on several factors, including clock speed of the computer, the level of statistical error that can be tolerated, the physical conditions being simulated (e.g., pressure and temperature), and the complexity of multiple-well, multiple-channel reaction systems. Reactions with slow rate constants cannot be simulated as readily as those with fast ones, because some of these factors are limited by computer characteristics, numeric of random number generators, computer codes, and human time constraints. Obviously, there are several possible trade-offs among these factors.

To illustrate how these factors can affect the difficulty of extracting a rate constant, we will consider a very simple single-well, single-channel problem. We want to find the *slowest* reaction rate that can be simulated in a practical calculation using one computer processing unit (i.e., a cpu, or core). (Note that simulations of chemical activation are much more efficient; see later in this chapter.)

For *slow* reactions, the initial energy relaxation can be neglected. The stochastic simulation produces a time-history of  $y$  vs.  $t$ , where  $y$  is the time-dependent relative concentration of the reactant (relative to its initial concentration) and  $t$  is duration of simulated time. Thus at  $t = 0$ ,  $y = 1$ . The first order rate constant,  $k$ , can be obtained from a least-squares fit of  $\ln(y)$  vs.  $t$ , but for slow reactions we will consider the following approximation, which is appropriate for  $kt \ll 1$ :

$$y = \exp(-kt) \approx 1 - kt \quad (1)$$

This approximate form is useful for  $1 \geq y \gtrsim 0.5$ .

To obtain the rate constant, the simulated time duration,  $t$ , must be long enough so that  $y$  is significantly larger than the stochastic sampling noise. Because of stochastic sampling noise (see Sec. A.3.2 in this User Manual), the standard deviation of the relative concentration is given by<sup>4</sup>

$$\sigma_y = \left[ \frac{y(1-y)}{N_t} \right]^{1/2} \quad (2)$$

where  $N_t$  is the number of stochastic trials. When  $y \approx 1$ , this expression reduces to

$$\sigma_y \approx \left[ \frac{(1-y)}{N_t} \right]^{1/2} = \left[ \frac{kt}{N_t} \right]^{1/2} \quad (3)$$

From propagation of errors, the corresponding standard deviation of  $k$  is given by

$$\sigma_k = t^{-1} \sigma_y \quad (4)$$

It is convenient to define the relative stochastic error  $R_k$  in the rate constant:

$$R_k = \frac{\sigma_k}{k} = \frac{\sigma_y}{kt} = \left[ \frac{1}{ktN_t} \right]^{1/2} \quad (5)$$

It is clear from these expressions that the relative error is large when the simulated time duration is too short and/or when the number of stochastic trials is too small. In principle, the number of stochastic trials can be increased, but a practical limit of  $\sim 2 \times 10^7$  stochastic trials is imposed by the random number generator that is currently in use (each stochastic trial requires *at least* 3 random numbers (if no collisions are involved) and *at least* 5 random numbers when collisions are dominant).

In collisional systems (except at very low pressures), the cpu time is often proportional to the total number of collisions that must be simulated. The total number of collisions,  $Z$ , depends on the collision frequency ( $\omega$ ), the simulated time duration ( $t$ ), and the number of stochastic trials ( $N_t$ ):

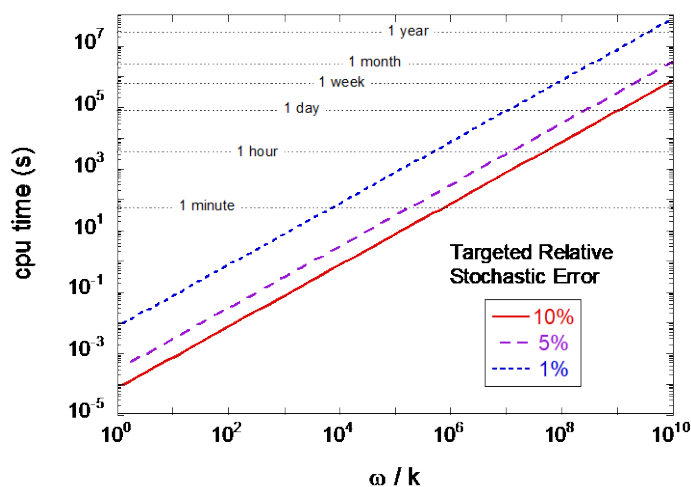
$$Z = \omega t N_t \quad (6)$$

From Eqs. 1, 5, and 6, we find that  $Z$  depends only on the dimensionless ratio of the collision frequency divided by the unimolecular rate constant, and the reciprocal of the relative error, squared:

$$Z = \frac{1}{R_k^2} \frac{\omega}{k} \quad (7)$$

Because computation time is approximately proportional to  $Z$ , Eq. 7 can be used to estimate the amount of cpu time needed to obtain a unimolecular rate constant with a specified "target" relative error  $R_k$ . In recent tests using a desktop iMac computer (2.7 GHz), MultiWell simulated  $\sim 5 \times 10^9$  collisions in one hour of cpu time. Also, at 1 bar and room temperature,  $\omega$  is of the order of  $\sim 10^{10} \text{ s}^{-1}$ . This value is useful for estimates at other temperatures, because  $\omega$  is only weakly dependent on temperature and on the identity of colliders.

Because of limitations associated with the random number generator utilized in MultiWell,  $N_t$  can be no greater than  $\sim 2 \times 10^7$ , as mentioned above. There are also limits to how long users are willing to wait while a simulation is being performed. The figure provides an order-of-magnitude estimate of the cpu time needed to achieve a given "target" relative error as a function of the  $\omega/k$  ratio.



Computer execution time as a function of collision frequency, rate constant, and targeted level of stochastic error.

From the figure, it is clear that "slow reactions" (i.e., slow compared to collision frequency) require long simulation times in order to achieve small relative stochastic errors. Obviously, very long simulations can be performed. In our research, we sometimes run simulations that require ~24 hrs of wall-clock time, but rarely longer than that. Stochastic simulations are best suited to cases where the pressure (and thus the collision frequency  $\omega$ ) is small and the rate constant is large. At very low pressures, the cpu times reach a small but finite lower limit (due to computational overhead) that is not described by Eq. 7.

### ***Multiple-Well Unimolecular Reactions***

A least squares analysis of the simulation results is useful and accurate for reaction systems that include reversible isomerization reactions. Such systems may also include irreversible reactions (e.g. fragmentation reactions). For very complicated reaction systems that include reversible isomerization reactions, the most convenient method for extracting rate constants is currently the Barts-Widom approach,<sup>7</sup> which has been implemented in several eigenvalue codes.<sup>9,12,14</sup> Because the Barts-Widom method relies on linear algebra techniques, it is not available for stochastic simulations, which are accompanied by stochastic sampling noise. However, for systems that are not too complicated, least squares analysis of stochastic simulations can be used to obtain similar results.<sup>15</sup>

The basic approach is to carry out simulations at various temperatures and pressures. Just as when analyzing experimental data, the time-dependent output (fractions vs. time) can be fitted by using a postulated mechanism with unknown rate constants (the fitting parameters). For a postulated mechanism similar to the "phenomenological rate constants" described by Barts-Widom, the postulated mechanism should neglect energy transfer processes and include only chemical transformations. For phenomena involving vibrational relaxation (e.g. incubation times following a shock wave), the chemical mechanism can be augmented by including vibrationally excited species and their activation/deactivation steps. The analysis will require a computer code that can carry out a least squares analysis using an embedded numerical integration of the coupled rate equations as a function of time (e.g. the Kintecus package by James Ianni: [www.kintecus.com](http://www.kintecus.com)). For simple cases, analytical expressions for concentration vs. time can be fitted using standard least-squares packages.

### ***Recombination and Chemical Activation Rate Constants***

#### **General Discussion of Chemical Activation**

As explained elsewhere,<sup>2,4</sup> the stochastic simulations of chemical activation are carried out for a large ensemble of chemical activation events, taken one at a time, in order to determine the probabilities of all possible outcomes of the chemical activation process. Chemical activation (which includes recombination reactions) is the result of a bimolecular association reaction that produces an internally excited species; in the following, we refer to this as a "capture event". The excited species produced in the capture event subsequently may re-dissociate back along the entrance channel, react further via other reaction channels, or be stabilized by collisions (and by other means<sup>3</sup>). The average chemical activation rate constant for producing products other than the initial reactants is a bimolecular rate constant:

$$k_i(T, [M]) = k_{cap,j}(T) f_i(T, [M]) \quad (1)$$

where  $k_{cap,j}(T)$  is the bimolecular rate constant for the initial capture event which takes place via the  $j^{\text{th}}$  reaction channel and  $f_i(T, [M])$  is the probability of reacting via the  $i^{\text{th}}$  ( $\neq j$ ) reaction channel, and  $[M]$  is the concentration of a collider gas. Because of back-reaction *via* entrance reaction channel  $j$ , the net reaction rate constant for the recombination reaction is given by:

$$k_j(T, [M]) = k_{cap,j}(T) \{1 - f_i(T, [M])\} \quad (2)$$

Since collisional stabilization depends on pressure  $[M]$  and the sum of the probabilities is equal to unity, the bimolecular rate constants for all of these processes depend on pressure.

In the bulk, the capture events that lead to chemical activation occur randomly, whilst obeying a second order rate law. The random initiation of these events is not convenient for stochastic simulations, which could be carried out far more conveniently if all of the reactive events were initiated at the same instant. Fortunately, since each capture event is completely independent of the others, it does not matter at what time it is initiated. Thus a stochastic algorithm exploiting this property can be used for computing the probabilities.<sup>2,4</sup>

Using the ideas described in the previous paragraph, a time-dependent stochastic simulation is carried out by assuming that all of the capture events producing nascent excited species occur at  $t = 0$  and the nascent species has an initial internal energy  $E$  (or  $E, J$ ) selected from the chemical activation distribution, which is the appropriate energy probability density function for this process.

From statistical rate theory, the chemical activation distribution depends on temperature and on  $k(E)$ , the microcanonical rate constant describing the re-dissociation of the nascent complex.<sup>10</sup> The thermal average of  $k(E)$  is equal to the high pressure limit of the canonical unimolecular rate constant for re-dissociation,  $k_{uni,\infty}(T)$  which, in turn is related via the equilibrium constant  $K_{rec}(T)$  to the canonical bimolecular rate constant for the association (recombination) reaction at the high pressure limit. Since the capture rate constant can be identified with the rate constant for the association reaction at the high pressure limit, we obtain

$$k_{cap,j}(T) = k_{rec,\infty,j}(T) = K_{rec,j} k_{uni,\infty,j}(T) \quad (3)$$

By carrying out this algorithm for many capture events and keeping tallies of the outcomes, one can determine the average probabilities for use in the equations given above. The statistical uncertainties in the probabilities decrease as the number of simulations increases.

Figures 1 and 2 show results from a set of simulations of the reaction  $C_2H_5 + O_2$ , carried out as described above.<sup>5</sup>



In these reactions, the asterisk (\*) denotes vibrational excitation and M is an inert bath gas. Figure 1 shows the fraction of the  $C_2H_5O_2$  initially formed that still survives at later times. At  $t = 0$ , none of the excited  $C_2H_5O_2^*$  formed in the association reaction has reacted and its energy is distributed in the chemical activation distribution. Very quickly, the excited  $C_2H_5O_2^*$  begins to

react by re-dissociating (Reaction -1) or by reacting via Reaction 2. The excited  $C_2H_5O_2^*$  also undergoes non-reactive energy transfer collisions, which alter the energy distribution, resulting in changes in the average vibrational energy ( $E_{vib}$ ) of the surviving  $C_2H_5O_2$ . The chemical consequences of the chemical activation process are manifest over an extended period of time. During the first few nanoseconds, the most highly excited  $C_2H_5O_2$  molecules react away at rates controlled by the sum of the  $k(E)$ s for the two reaction channels. The total rate of loss of  $C_2H_5O_2$  during this period is much greater than would be predicted by the sum of the corresponding high pressure limits for the two channels, because the latter canonical rate constants are *averages of the sum of the  $k(E)$ s over a thermal distribution*, while the former are *averages of the sum of the  $k(E)$ s over an energized non-thermal distribution*.

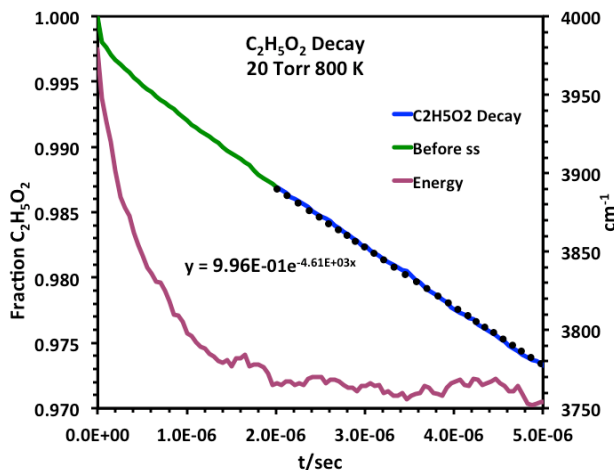


Figure 1: Surviving  $C_2H_5O_2$  and its average vibrational energy (red line). The green and blue lines show the fraction of  $C_2H_5O_2$  during the initial relaxation and afterwards, respectively. The broken line shows the least squares fit of the thermalized portion.<sup>5</sup>

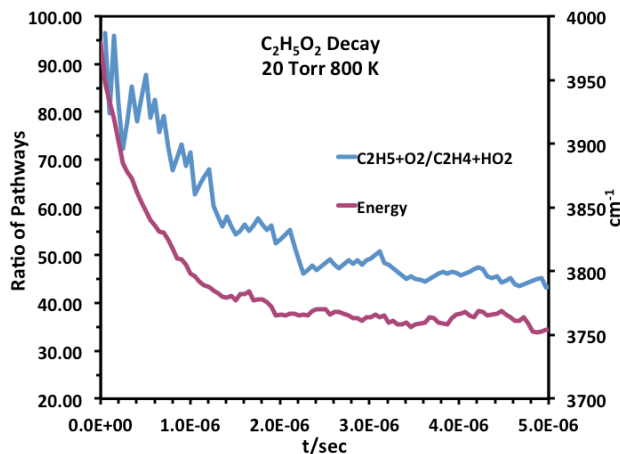


Figure 2: Product channel branching ratio and  $E_{vib}$  as functions of time for the same calculation illustrated in Figure 1.<sup>5</sup>

After the first few nanoseconds, the most highly excited  $C_2H_5O_2^*$  molecules have already reacted away and surviving molecules react away more slowly. During the period up to  $\sim 2 \mu s$ , the  $C_2H_5O_2$  decay is almost, but not quite, first order, suggesting that the chemical activation event has concluded. A more sensitive diagnostic,  $E_{vib}$  for the surviving  $C_2H_5O_2$  molecules, shows that the energy distribution is still evolving and the chemical activation process is still underway up to  $\sim 2 \mu s$ . Figure 2 shows that the branching ratio between the two dissociation pathways changes by about a factor of two during this period. This change is due to the changes in the energy distribution function that are taking place during this *initial energy relaxation period*.

From simulations such as these, it is convenient to define the bimolecular chemical activation rate constants in terms of the probabilities evaluated at the end of the initial relaxation period. Subsequent reaction of the thermalized species takes place at a rate controlled by the thermal reaction. Thus a single simulation can be used to obtain both the chemical activation rate constant and the thermal rate constant.

When the time scales of energy relaxation and the subsequent reactions of the thermalized intermediate in a single channel reaction (e.g.  $C_2H_5O_2$ ) are widely separated, it is easy to identify the end of the initial relaxation as the time when  $E_{vib}$  and the reaction flux coefficients become constant.<sup>5</sup> For multi-channel reactions, the end of the initial relaxation is less distinct even under favorable circumstances, since isomerization reactions can affect both  $E_{vib}$  and the reaction flux coefficients.<sup>6,15</sup> Under most conditions, the initial relaxation seldom requires more than a few hundred collisions (when using typical Lennard-Jones and energy transfer parameters).

### At the High Pressure Limit

The best way to compute the infinite pressure limit rate constants for recombination and unimolecular reaction is to use THERMO, which has the capability to compute canonical transition state theory rate constants (CTST), which uses the standard separable approximation (and can include quantum tunneling through an unsymmetrical Eckart barrier), and semi-classical transition state theory (SCTST), which includes full inter-mode coupling and multidimensional quantum tunneling. You will need to supply vibration/rotational constants and relative energies for the reactant(s) and transition state.

Note that  $k_{rec}(T, [M])$  and  $k_{uni}(T, [M])$ , the recombination and unimolecular rate constants at concentration  $[M]$  (which is proportional to pressure) and temperature  $T$ , are related according to equilibrium constant:



$$K_{eq} = \frac{k_{rec}(T, [M])}{k_{uni}(T, [M])}$$

This relation ship applies at all values of  $[M]$ .

### In the Pressure Fall-Off

To compute fall-off rate constants as a function of pressure, two or three steps are required. The choice of procedure must account for the fact that both forward and reverse

reactions are taking place simultaneously, along with collisional activation and deactivation. In most cases, the time constant for collisional activation/deactivation (typically corresponding to 50 to 1000 collisions) is much shorter than the characteristic time constant for unimolecular reaction, and a rate constant can be defined formally, but in some cases the reaction rates cannot be disentangled from the collisional thermalization process. Multiwell can simulate the whole range of behaviors. The following describes strategies for the normal case when rate constants can be defined.

In MultiWell, the chemical identity of each chemical species (MOL) is independent of its internal energy. Thus, molecules are assumed to have unique chemical identities even when they have energies in excess of reaction barriers and while they are undergoing activation and deactivation.

Recombination and unimolecular dissociation reactions are closely related:



Where the forward reaction is recombination and the reverse is unimolecular decomposition. The relationship between the rate constants and the equilibrium constant, which can be calculated by THERMO, will be used later

$$K_{eq} = k_{rec} / k_{uni}$$

In the case of a simple *recombination reaction* (which is one variety of a *chemical activation reaction*) one can use MULTIWELL to simulate the reaction over a time interval, typically a few hundred or a few thousand collisions. As written, the reaction has one Well ("C") and one set of terminal products ("A+B") corresponding to a single reaction channel. It is important to note that if the unimolecular decay requires more than a few thousand collisions, the simulations become very time-consuming. MultiWell is not designed for computing slow, steady-state unimolecular reactions.

Steps in the procedure:

1) Using vibrational and rotational constants for "C" and for the transition state (TS), compute sums and densities of states using DENSUM and place the "\_\_\_\_.dens" files in directory DensData for use by MULTIWELL.

2) Use MULTIWELL in one of two ways, Method A or Method B, depending on the reaction system and conditions. Both methods rely on **separation of time scales**: the steady-state reaction must be considerably slower than collisional thermalization and associated relaxation of the non-steady-state energy distribution. If one runs a longer simulation, one will often find that product C hasn't really become constant, but is decaying with a slower time constant. If this decay is slow enough, it can be neglected when assessing the much faster chemical activation process.

The reliance on separation of time scales is typically a good method as long as the time scales for the recombination and unimolecular decomposition differ by an order of magnitude or more. When that condition is not satisfied, as is often true at high temperatures, a better course of action is to determine the steady-state  $k_{uni}(T,[M])$  by Method B and use the relationship between the rate constants and the equilibrium constant to obtain  $k_{rec}(T,[M])$ . But if the time scales are too similar, and a steady-state energy distribution is not established, a rate constant cannot be defined

and it will not be possible to separate the reaction rate from the effects of collisional thermalization.

**Method A:** When the unimolecular decomposition reaction rate is much slower than collisional "thermalization", initiate the simulations using the chemical activation energy distribution (key word CHEMACT) for Well "C". Run the simulations for a simulated time duration  $t_{\max}$  corresponding to a number of collisions sufficient for thermalizing all of the surviving population of excited "C" (typically 50 to 1000 collisions). Over the course of time, the population of C is affected simultaneously by both collisional deactivation and bond fission back to the initial reactants. Thus the energy of C decreases monotonically until it reaches steady state. At the same time, the yield of C (its "fraction") asymptotically decreases toward a constant value. When the energy of C is low enough, the subsequent very slow steady-state unimolecular bond fission can be neglected. MULTIWELL will report  $f(C, t_{\max})$ , the fraction of initial "C" that survives to the end of the simulation (conveniently reported in output file `multiwell.sum`). If  $t_{\max}$  is large enough and bond fission is slow, the numerical value of  $f(C, t_{\max})$  will remain constant even if  $t_{\max}$  is increased. The recombination and unimolecular reaction rate constants at that pressure and temperature are given by:

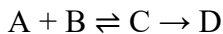
$$k_{rec}(T, [M]) = k_{rec,\infty}(T) \cdot f(C, t_{\max})$$

When the reaction is just one of several in a multi-channel reaction system, it is necessary to use the following method.

**Method B:** At high T, when  $k_{uni}(T, [M])$  is fast (i.e. when the time scale for reaction is shorter than the time corresponding to roughly  $10^4$  collisions), it is more effective to simulate the unimolecular decomposition reaction. This is accomplished by initiating the reaction of "C" with the thermal energy distribution (key word THERMAL). Multiwell will report  $f(C, t)$  the fraction of C that survives to time t in output file `multiwell.out`. The fraction  $f(C, t)$  is proportional to the concentration of species "C" as a function of time. Initially,  $f(C, t)$  decays very rapidly as the initial population distribution evolves and converges to the steady-state distribution, which is called the "fall-off" distribution for a simple unimolecular reaction. Once the steady-state distribution has been established,  $f(C, t)$  decays exponentially and a plot of  $\ln[f(C, t)]$  v.s t will give a straight line with slope =  $-k_{uni}(T, [M])$ .

Thus this method requires plotting the results vs. time and extracting the rate constant. This is easily done using spreadsheets, or data plotting applications.

For *chemical activation* reactions, the procedures are similar to those for recombination reactions.



In a chemical activation reaction, the excited intermediate C initially has enough energy to react and produce product D. The yield ("fraction") of D depends on the competition between collisional deactivation and unimolecular reactions involving the intermediate C. The effective chemical activation rate constant describing the production of D is obtained from the yield of D, which is reported by MULTIWELL as the fraction  $f(D, t)$  at the end of the simulation:

$$k_{A+B \rightarrow D}(T, [M]) = k_{rec,\infty}(T) \cdot f(D, \infty)$$



where  $k_{\text{rec},\infty}(T)$  is the high pressure limit for A + B recombination.

With all of these methods, one must bear in mind that the presence of competing reactions (e.g. reverse reaction and other reaction channels) may strongly influence the steady-state energy distribution, which ultimately controls the reaction rates and derived rate constants. The separation of time scales is often, but not always, sufficient to simplify the analysis. But sometimes it is only possible to determine individual rate constants by analyzing the simulation output just like analyzing experimental kinetics data.

Sometimes, steady state is never established and rate constants cannot be rigorously defined. Even under non-steady-state conditions, however, the Multiwell simulations can be used to accurately model the time-dependent fractions and the final product yields.

## References

- (1) Andraos, J. A Streamlined Approach to Solving Simple and Complex Kinetic Systems Analytically. *J. Chem. Educ.* **1999**, *76*, 1578-1583; DOI: 10.1021/ed076p1578.
- (2) Barker, J. R. Monte-Carlo Calculations on Unimolecular Reactions, Energy-Transfer, and IR-Multiphoton Decomposition. *Chem. Phys.* **1983**, *77*, 301-318.
- (3) Barker, J. R. Radiative Recombination in the Electronic Ground State. *J. Phys. Chem.* **1992**, *96*, 7361-7367; DOI: 10.1021/j100197a042.
- (4) Barker, J. R. Multiple-well, multiple-path unimolecular reaction systems. I. MultiWell computer program suite. *Int. J. Chem. Kinet.* **2001**, *33*, 232-245; <https://doi.org/10.1002/kin.1017>.
- (5) Barker, J. R.; Frenklach, M.; Golden, D. M. When Rate Constants Are Not Enough. *J. Phys. Chem. A* **2015**, *119*, 7451-7461; DOI: 10.1021/acs.jpca.5b00640
- (6) Barker, J. R.; Frenklach, M.; Golden, D. M. Reply to “Comment on ‘When Rate Constants Are Not Enough’”. *J. Phys. Chem. A* **2016**, *120*, 313-317; DOI: 10.1021/acs.jpca.5b06652.
- (7) Bartis, J. T.; Widom, B. Stochastic models of the interconversion of three or more chemical species. *J. Chem. Phys.* **1974**, *60*, 3474-3482; doi: 10.1063/1.1681562.
- (8) Boyd, S.; Vandenberghe, L. *Convex Optimization*; Cambridge University Press: Cambridge, UK, 2004.
- (9) Duong, M. V.; Nguyen, H. T.; Truong, N.; Le, T. N. M.; Huynh, L. K. Multi-Species Multi-Channel (MSMC): An Ab Initio-based Parallel Thermodynamic and Kinetic Code for Complex Chemical Systems. *International Journal of Chemical Kinetics* **2015**, *47*, 564-575; doi: 10.1002/kin.20930.
- (10) Forst, W. *Unimolecular Reactions. A Concise Introduction*; Cambridge University Press: Cambridge, 2003.
- (11) Frenklach, M.; Packard, A.; Feeley, R. Optimization of Reaction Models with Solution Mapping. In *Modeling of Chemical Reactions*; Carr, R. W., Ed.; Elsevier: Amsterdam, 2007; Vol. 42; pp 243-291.
- (12) Glowacki, D. R.; Liang, C. H.; Morley, C.; Pilling, M. J.; Robertson, S. H. MESMER: An Open-Source Master Equation Solver for Multi-Energy Well Reactions. *J. Phys. Chem. A* **2012**, *116*, 9545-9560; 10.1021/jp3051033.
- (13) Lewis, E. S.; Johnson, M. D. The Reactions of p-Phenylene-bis-diazonium Ion with Water. *J. Am. Chem. Soc.* **1960**, *82*, 5399-5407; DOI: 10.1021/ja01505a027.
- (14) Miller, J. A.; Klippenstein, S. J. Master Equation Methods in Gas Phase Chemical Kinetics. *J. Phys. Chem. A* **2006**, *110*, 10528-10544.
- (15) Miller, J. A.; Klippenstein, S. J.; Robertson, S. H.; Pilling, M. J.; Shannon, R.; Zádor, J.; Jasper, A. W.; Goldsmith, C. F.; Burke, M. P. Comment on “When Rate Constants Are Not Enough”. *J. Phys. Chem. A* **2016**, *120*, 306-312; DOI: 10.1021/acs.jpca.5b06025.
- (16) Mucientes, A. E.; Peña, M. A. d. l. Kinetic Analysis of Parallel-Consecutive First-Order Reactions with a Reversible Step: Concentration-Time Integrals Method. *J. Chem. Educ.* **2009**, *86*, 390-392; DOI: 10.1021/ed086p390.

## C.5 How to tell if the simulated time is long enough

### *Experiments*

When simulating actual experiments, the simulated time should match the experiment times. Bear in mind, however, that Multiwell is not intended for simulating slow steady state reactions. Because it simulates every individual collision, it is most suitable for simulated times corresponding to a few thousand collisions, or less. This is quite sufficient for many kinds of experiments with short timescales.

For longer simulations, it is better to use Multiwell to determine individual rate constants and then use those rate constants in an elementary reaction mechanism, which can be solved using a suitable stiff differential equation code. One such code is KINTECUS, which was designed for chemical kinetics and is free of charge for users at academic institutions (available from [www.kintecus.com](http://www.kintecus.com)).

### *Unimolecular Reactions*

In general, the initial energy distribution assumed in the simulation must relax to the steady-state distribution. The relaxation time, which depends on the initial energy distribution, is minimized when the assumed initial energy distribution is most similar to the steady-state distribution. For example, if the pressure is high enough so that the reaction is near the high pressure limit, the relaxation time will be minimal if the initial energy distribution is assumed to be thermal (THERMAL). Generally, the initial transient (when the initial distribution is relaxing to the steady-state distribution) is quite manageable when using an initial energy distribution with average energy close to the reaction critical energy. The final steady state distribution does not depend on the particular choice of the initial distribution, whether it is a delta function (DELTA), thermal distribution (THERMAL), or chemical activation distribution (CHEMACT).

The simulation must be run for a simulated time that is sufficient for steady state to be achieved and for the rate constant to be determined. If the rate constant is to be determined by plotting  $\ln(\text{fraction})$  vs. time (see Section C.4), then plot initially will be non-linear during the transient period when steady state is being established, and subsequently will become linear with slope equal to the desired rate constant. The simulation must be long enough to enable determination of the slope of the straight line portion.

### *Chemical Activation or Recombination Reactions*

When simulating chemical activation or recombination reactions, one should run the simulations long enough to satisfy two criteria:

a) The average energy of a product molecule (C) is well below any of its reaction thresholds (also remember that the distribution of internal energy extends well above the average)

b) The yield of C becomes independent of time (when time-scale separation is sufficient). It is best to carry out some preliminary calculations (using a smaller number of trials) to determine the time duration (or number of collisions) that will be needed for the excited species

to be deactivated sufficiently. At low temperatures, this may require only a few dozen collisions, but at high temperatures it may require several hundred.



## C.6 How to deal with Barrierless Reactions

Treating barrier-less reactions with "loose transition states" is more complicated than reactions that have intrinsic energy barriers. There are several choices of methods. Generally, there is a trade-off between ease of use and predictive accuracy. If the method is not being used to *predict* rate constants, but is instead being used to *fit* experimental rate constants, then the simpler methods are usually sufficient. For all of the methods, vibrational and rotational constants are usually obtained from quantum chemistry calculations.

In order, starting with the best (and most difficult) method:

1. Microcanonical variational transition state theory (mVTST): In the MultiWell Software Suite, this method has been implemented in program **ktools**, which computes canonical (thermal) VTST rate constants (cVTST rate constants) as well as microcanonical sums and densities of states, which are appropriate for master equation simulations.
2. Canonical transition state theory (CTST), which uses molecular constants to compute partition functions: CTST is implemented in **thermo**, which can be used with molecular constants along a reaction path to find the canonical variational transition state and a corresponding cVTST rate constant. The molecular data required for this calculation are exactly the same as those used by **ktools**, but the **ktools** calculations are preferred, because they are significantly more accurate.
3. Hindered Gorin model: see Index of this User Manual.
4. Inverse Laplace transform method: a built-in option in **MULTIWELL** (key word **ILT**). This method is often investigated first, because it is the easiest and least expensive, but also the least accurate.

Methods #1 to #4 can be employed relatively easily in Multiwell. Method #1 is preferred. Typically, #3 and #4 are used empirically by fitting a known (or estimated) thermal rate constant at a given temperature.

Several applications of methods #2, #3, and #4 are described in recent articles.<sup>1-4</sup>

## References

- (1) Ali, M. A.; Barker, J. R. Comparison of Three Isoelectronic Multiple-Well Reaction Systems: OH + CH<sub>2</sub>O, OH + CH<sub>2</sub>CH<sub>2</sub>, and OH + CH<sub>2</sub>NH. *J. Phys. Chem. A* **2015**, *119*, 7578–7592; DOI: 10.1021/acs.jpca.5b00910.
- (2) Ali, M. A.; Sonk, J. A.; Barker, J. R. Predicted Chemical Activation Rate Constants for HO<sub>2</sub> + CH<sub>2</sub>NH: The Dominant Role of a Hydrogen-Bonded Pre-reactive Complex. *J. Phys. Chem. A* **2016**, *120*, 7060–7070; DOI: 10.1021/acs.jpca.6b06531.
- (3) Golden, D. M.; Barker, J. R. Pressure- and Temperature-Dependent Combustion Reactions. *Combust. Flame* **2011**, *158*, 602–617.
- (4) Yang, L.; Sonk, J. A.; Barker, J. R. HO + OCIO Reaction System: Featuring a Barrierless Entrance Channel with Two Transition States. *J. Phys. Chem. A* **2015**, *119*, 5723–5731; DOI: 10.1021/acs.jpca.5b03487.

## C.7 Some Questions and Answers

(Most of the answers were written by JRB; Some questions and answers are rather old!)

**1. QUESTION: Every molecule has a 2 dimensional external inactive rotor and an external active rotor (the K-rotor). I can see where the external inactive rotor goes but I'm not sure about the external active rotor.**

ANSWER: The parameters "MolMom" on line #8 and "RR" on line #15 of the data file are moments of inertia for the 2-dimensional external (inactive) rotors for the reactant and the transition state, respectively. The external active rotor is included with the other degrees of freedom in the density and sum of states calculation. Therefore it is included in the data file for SumDen. For example, O<sub>3</sub> (ozone) has 3 vibrations and 3 rotations. The SumDen data file should include 4 degrees of freedom: 3 vibrations + 1 rotor (the active external rotation, which I usually label the "K-rotor"). The moment of inertia for the remaining 2-D external (inactive) rotor appears on line #15.

**2. QUESTION: If there is an internal active rotor, do I remove the vibration associated with it from the Densum input?**

ANSWER: An internal degree of freedom is either a rotor, or a vibration...not both. Thus, if you have a vibrational assignment (from Gaussian, say), you may wish to replace a low frequency vibrational mode with a free rotor mode. Then you remove the vibration and insert the rotor in its place, so that the number of internal degrees of freedom is preserved.

**3. QUESTION: In all your examples you use an energy spacing of 10 cm<sup>-1</sup> and when I use 1 cm<sup>-1</sup> the code freezes. Do you recommend using 1 cm<sup>-1</sup> and if so should I increase the size of the array, which is currently 14000?**

ANSWER: We usually recommend 10 cm<sup>-1</sup>, because we have found that for most systems it gives excellent numerical convergence at room temperature and above, and because few thermochemical values are known to better accuracy. In previous work, 25 cm<sup>-1</sup> spacing also worked very well. If you want to use a smaller grain size, then the arrays should be increased in size. In principle, one should always test to make sure that the grain size is small enough so that it does not affect the results significantly.

**4. QUESTION: In using DenSum, when should one use quantum state counting for rotors ("qro") and when should one use classical state densities ("rot")?**

ANSWER: As a rough rule of thumb, if the rotational constant is greater than  $B = 1 \text{ cm}^{-1}$ , use "qro"; if it is less than  $0.1 \text{ cm}^{-1}$ , use "rot"; in between, you can try it both ways and then decide if the difference will affect your calculations. If you use "qro" for a case where the rotational constant is extremely small, there may be computational problems... this limit has not been tested thoroughly ... and it would be better to use "rot".

**5. QUESTION: What will happen if the density of states function is not a smooth, continuous function at energies corresponding to the upper half of the double array?**

ANSWER: Subroutine COLSTEP assumes that the density of states is smooth in the upper portion of the double array. In general, you should plot the density of states vs. E to confirm that the energy dividing the two portions of the double array is high enough so that the density of states does not fluctuate more than, say, 5%. If the fluctuations are larger, they will cause problems in selecting the step sizes, resulting in anomalously large probabilities of large activating steps.

**6. QUESTION: Why does my compiler have trouble reading the example data files that contain names (CHARACTER CONSTANTS)?**

ANSWER: If your compiler does not accept the CHARACTER CONSTANTS in the example data files, enclose the CHARACTER CONSTANTS in apostrophes (') and try again. "Free format" (list directed input) is used by the MultiWell suite. Different compilers may choose to use different delimiters to separate the input fields in free format. Most compilers use commas and spaces, but some also will recognize tabs, returns, linefeeds, and other characters. Most compilers will recognize CHARACTER CONSTANTS (e.g. file names and chemical species names) when they are contained in apostrophes (e.g. 'xyz'). Other compilers will also accept quotes (e.g. "xyz"), or text without any special enclosing delimiters (e.g. xyz).

**7. QUESTION: How can the 2-D hindered rotations in loose transition states be handled using DenSum?**

ANSWER: There are at least three different ways 2D-hindered rotors for loose transition states can be handled by DenSum. The first is by using the restricted Gorin prescription of Smith and Golden<sup>6</sup> (see Benson's discussion<sup>1</sup> of the Hindered Gorin Model), which is based on a modified version of the Gorin Model.<sup>2</sup> The second is to replace the restricted rotor formulation with one based on particle-in-a-box. The third is to use two 1-D hindered rotors (implemented in DenSum) instead of one 2-D hindered rotor (2-D hindered rotors are not implemented in DenSum).

Smith and Golden<sup>6</sup> use a "hindrance parameter" to modify the moment of inertia of a 2-D free rotor: the Hindered Gorin Model. They find the value of the hindrance empirically by varying it until they achieve a fit with experimental rate constant data. In my opinion, a potential drawback of the Smith and Golden approach is that the rotor model has no zero point energy, and restricting the range of rotational motion results in a model that is more like a particle-in-a-box, which has a finite zero point energy. It is for this reason that I added the particle-in-a-box degree of freedom type to DenSum. The zero point energy is important because of the role it plays in isotopic reactions. To use particle-in-a-box energy levels (instead of free rotor levels), one can empirically vary the "frequency" parameter until agreement with experiment is achieved, just as done by Smith and Golden.

The third alternative is to use two 1-D hindered rotors for each 2-D internal rotation. Here, the moment of inertia can be used directly in DenSum and the hindrance potential is then varied until agreement with the rate constant data is achieved. I've done a few brief tests of this



approach and it seems to work well. The use of an actual hindered rotor is attractive to me, because it seems more physically realistic (one of these days we'll investigate this using quantum chemical calculations). The drawback is that state degeneracies may not be calculated correctly.

I don't know if there is a significant difference among rate constants calculated using the methods described above. Each of the methods is probably quite adequate in fitting almost any experimental data (a detailed comparison of the methods would be quite interesting). However, making predictions for temperatures where no experimental data are available requires formulation of an ad hoc model for hindrance as a function of temperature. Jordan, Smith, and Gilbert<sup>3</sup> have formulated such a model (based on free rotors) and have tested it for a few cases; it is possible that their method could be used with Densum. The Marcus and Wardlaw approach<sup>7,8</sup> is more predictive, but only if an accurate multi-dimensional potential energy surface is available. Miller and Klippenstein<sup>5</sup> have used VariFlex software,<sup>4</sup> which implements an extended version of the Marcus-Wardlaw approach.

#### **8. QUESTION: Why is the output "noisy" and what is the meaning of the columns labeled "+/-error"?**

ANSWER: Multiwell works by carrying out stochastic trials, each of which is a random walk governed by the physics of the reaction system. In each trial, one or more wells may be "visited" during the random walk and the random walker will be found in a well or reaction product at the end of the trial. Multiwell carries out stochastic trials one at a time and sums up the results. But it is convenient to discuss the summed result as if a whole "swarm" of random walkers was released at the same time... an equivalent procedure. During a set of trials, each of the time steps records a "snapshot" of the number of walkers in each well or product set at the instant of the time step. The fractions are based on these snapshots.

For a set of, say,  $N=100$  stochastic trials, there are 100 random walkers. If only one random walker out of the whole set is in a well at the time of a snapshot, then the corresponding fraction is 0.01. If 37 are in the well, then the fraction is 0.37. The smallest possible non-zero fraction (greater than zero) is equal to  $1/N$ . Furthermore, for a finite number of stochastic trials, a statistical error is associated with each fraction. The estimated statistical error (specifically, 1 standard deviation) is reported by multiwell in the columns labeled "+/-Error". As the number of stochastic trials is increased, the smallest non-zero fraction decreases and the statistical error decreases. Thus changing the number of trials will produce small changes in the fractions... changes that should be consistent with the actual statistical fluctuations. (The theory behind the estimated statistical errors is presented in Appendix A.3.2 of the User Manual.)

When carrying out longer trials, the last "snapshot" occurs at a later time and the fraction recorded by the final snapshot (reported in output file multiwell.sum) may vary with time. Even if equilibrium has been achieved and no further time variation is expected, the stochastic "noise" (i.e. statistical errors) associated with the finite number of stochastic trials may be observed, but it should be consistent with the estimated statistical errors.

It is not possible to completely eliminate the stochastic noise for a finite number of trials. You should decide what level of noise is tolerable... i.e. what statistical precision is needed... and set the number of trials accordingly. A very large number (millions) of stochastic trials may be needed to obtain high precision results for a reaction product that is produced with a very small fractional yield. The required computer time is proportional both to the number of trials and to

the length of simulated time (see Appendix A.3.2). As a result, certain simulations are simply not feasible, or they may be feasible if creative alternative approaches are devised.

## References

- (1) Benson, S. W. *Thermochemical Kinetics*, 2nd ed.; Wiley: New York, 1976.
- (2) Gorin, E. Photolysis of acetaldehyde in the presence of iodine. *Acta Physicochim., URSS* **1938**, *9*, 681.
- (3) Jordan, M. J. T.; Smith, S. C.; Gilbert, R. G. Variational transition state theory: a simple model for dissociation and recombination reactions of small species. *Journal of Physical Chemistry* **1991**, *95*, 8685-8694.
- (4) Klippenstein, S. J.; Wagner, A. F.; Robertson, S. H.; Dunbar, R.; Wardlaw, D. M. VariFlex Software; 1.0 ed.; Argonne National Laboratory, 1999.
- (5) Miller, J. A.; Klippenstein, S. J. Theoretical Considerations in the  $\text{NH}_2 + \text{NO}$  Reaction. *J. Phys. Chem. A* **2000**, *104*, 2061-2069.
- (6) Smith, G. P.; Golden, D. M. Application of RRKM Theory to Reactions  $\text{OH} + \text{NO}_2 + \text{N}_2 = \text{HONO}_2 + \text{N}_2$  (1) and  $\text{ClO} + \text{NO}_2 + \text{N}_2 = \text{ClONO}_2 + \text{N}_2$  (2) - Modified Gorin Model Transition-State. *IJCK* **1978**, *10*, 489.
- (7) Wardlaw, D. M.; Marcus, R. A. Unimolecular Reaction-Rate Theory for Transition-States of Any Looseness. 3. Application to Methyl Radical Recombination. *Journal of Physical Chemistry* **1986**, *90*, 5383-5393.
- (8) Wardlaw, D. W.; Marcus, R. A. RRKM reaction rate theory for transition states of any looseness. *J. Chem. Phys.* **1984**, *110*, 230-234.

## Index

- <name>.dens, 92
- <name>.qcrp, 92
- 2 dimensional rotor, 233
- 2-D adiabatic rotor, 151
- 2-D hindered rotations, 234
- 2-dimensional external rotation, 30
- 3-D relative translation, 165
- Accuracy
  - Thermo, 65
- active energy, 23, 191
- active rotor, 233
- adensum, 80
- Adiabatic Channel Model, 152
- adiabatic rotor, 189
- A-factor, 32
- angular momentum, 151
- ANH, 185
- Anharmonic oscillator, 47
- anharmonicity coefficients, 91, 186
- anharmonicity constants, 187
- ansum, 80
- asymmetric top, 190
- atom type, 62
- atom types, 199
- atomic mass, 199
- ATYPE, 62
- average vibrational energy, 223
- averaged results, 148
- barrier-less reactions, 232
- batch option, 58
- bdens, 11, 12, 47, 80
  - program, 64
- bdens, 208
- BEST, 208
- BETTER, 208
- Beyer-Swinehart algorithm, 56
- Biexponential Model, 37
- bimolecular, 162
- bimolecular microcanonical transition state theory, 35
- bimolecular reactions
  - competing with unimolecular, 162
- BIMOLRXN option, 162
- B<sub>J</sub>, 49
- B<sub>K</sub>, 49
- canonical bimolecular rate constant, 163
- canonical rate constant
  - trial, 112
- canonical transition state theory, 6, 157
- Canonical transition state theory, 232
- Canonical Transition State Theory, 65
- capture rate constant, 222
- CENT1, 33, 212
- CENT2, 33, 157, 212
- centrifugal corrections, 134, 157, 191
- CENTX, 33, 212
- CFOUR, 205, 209
- checkpoint file, 92
- CHEMACT, 36
- chemical activation, 221
- Chemical activation, 36
- Chemical Activation, 177
- chiral stereoisomer, 194
- COLL, 36
- collision frequency, 136, 168, 171
- collision integral, 31, 168, 170
- collision models, 31, 36
- collision step-size distribution, 135, 168
- collision-induced IVR, 34, 157
- competition between unimolecular and bimolecular reactions, 164
- compiler options, 24
- computation time, 220
- computer time, 148, 235
- convergence tests, 144
- Conversion Factors, 185
- convolution, 165
- cpu time, 221
- critical energy, 23, 32, 151, 209
- CRP, 91, 208
- CTST, 232
- cumulative reaction probabilities, 7
- cumulative reaction probability, 33, 91
- cVTST, 232
- data files, 75
- defaults, 24
- definitions, 22
- degeneracies, 189
- degrees of freedom, 67
- DELTA, 36
- DensData, 36
- DensData, 39
- densities of states, 39, 143
- Density Functional Theory, 155
- density of states, 234
- densum, 9, 47
- DenSum, 133, 233
- densum.batch, 58
  - Batch file format, 58
- densum.lev, 56
- densum.out, 56
- detailed balance, 136, 169
- directory
  - DensData, 25, 36

dissociation energy, 187  
dividing surface, 112  
doloops, 80  
DO-loops, 208  
double array, 118  
Double array, 28, 143  
double-well potential, 195  
Eckart barrier, 6, 32, 71, 158  
Egrain1, 28, 43, 57  
Einit, 36  
Elements, 199  
E<sub>max</sub>2, 28, 43, 57  
energy grain, 143  
energy relaxation, 218  
Energy schematic, 23, 133  
energy transfer, 31  
energy transfer parameter, 217  
energy units, 29  
energy units for THERMO, 65  
enthalpy for formation, 65  
Enthalpy function  
  [H(T)-H(0)], 65  
enthalpy of formation, 30  
entropy, 65  
equilibrium constant, 64  
Equilibrium constant, 65  
Eunits, 29  
exact counts, 133  
Example multiwell Models, 14  
exponential Model, 37  
Exponential model, 36  
exponential-down model, 217  
EXTERNAL, 36  
external file, 33  
external symmetry number, 49  
EXTRA, 208  
FAIR, 208  
fall-off, 226  
FAST, 32  
filename  
  user-defined, 25, 61, 70  
FileName, 25, 26, 27  
fit, 66  
Fitting Experimental Rate Constants, 66  
Flexible Transition State Theory, 152  
flux coefficient, 26, 181  
FUN, 47, 56, 73, 186  
fundamental frequency, 47  
gauche structures, 194  
gauss2multi, 12, 75  
GAUSSIAN, 209  
Gaussian 03, 75  
Gaussian 98, 75  
getting started, 5  
Gillespie Exact Stochastic algorithm, 22  
Gillespie's Exact Stochastic Method, 147  
GOOD, 208  
gor, 66  
Gorin model, 154  
Gorin Model, 234  
grain size, 233  
HAR, 56, 57, 73, 84, 93  
harmonic frequency, 47, 185  
Harmonic oscillator, 47  
Heat Capacity, 65  
high pressure limit, 156  
high pressure rate constant, 157  
Hindered Gorin model, 232  
Hindered Gorin Model, 66, 152, 154, 234  
hindered internal rotation, 103, 133, 193  
Hindered internal rotation  
  General, 50, 53, 193  
  Optical isomers, 194  
  symmetrical, 50  
hindered rotor  
  symmetrical, 52  
hindrance parameter, 66, 234  
Hmol, 30  
HMol, 30  
hybrid master equation, 142  
hydrogen peroxide, 194  
IDUM, 28  
ILT, 33  
imaginary frequency, 33, 91, 159  
imax1, 28, 43  
lmax1, 57  
IMol, 30  
inelastic collision frequency, 169, 171  
inelastic collisions, 169  
initial conditions, 176  
initial energy relaxation, 218  
initial relaxation, 224  
initial well, 36  
INPUT ERRORS, 43  
internal rotation, 133  
  optical isomers, 194  
  unsymmetrical, 193  
internal rotor symmetry, 192  
internal rotors, 50  
Internal rotors, 192  
intrinsic upper limit, 121  
Inverse Laplace Transform (ILT) Method, 153  
Inverse Laplace transform method, 232  
lsize, 28, 43, 57  
isomerization, 142  
IVR, 134, 157  
IVR threshold energy, 34  
IVR transmission coefficient, 33, 157  
J-summed, 11  
  densities of states, 117  
  sums of states, 117  
J-summing, 117, 118

K quantum number restrictions, 49  
 k(E), 180  
**KEYWORD**, 32, 36  
 Klaus Luther's empirical function, 38  
 K-rotor, 52, 132, 133, 151, 189, 233  
 ktools, 11, 47, 110, 232  
 ktools.dat, 121  
 lamm, 12, 103, 134  
 Laplace transform, 165  
 large amplitude motions, 103  
 Lennard-Jones parameters, 31, 168, 217  
     Table, 198  
 linear master equation, 148  
**LOGT**, 36  
 loose transition state, 152, 232  
 loose transition states, 234  
 low pressure limit, 156  
 master equation, 132  
     J-resolved, 8, 131  
     steady-state, 8, 131  
 maximum number of collisions, 36  
 microcanonical, 162  
 microcanonical bimolecular rate constant, 162  
 microcanonical rate constant, 91  
 microcanonical transition state theory, 162  
 Miller, W. H., 204  
 Miller, W. H., 91  
 Miller, W. H., 205  
 mirror image, 194  
 molecular constants  
     sources, 74  
**Molele**, 30  
**Molinit**, 36  
**MolMom**, 30  
**MolName**, 30  
**Molopt**, 30  
**Molsym**, 30  
 moment of inertia, 30  
 Moment of Inertia, 185  
 moments of inertia, 61  
 mominert, 10, 12  
**MORERXN**, 35  
**MORSE**, 67  
 Morse oscillator, 47, 185  
*Morse Oscillator*, 67  
 Morse oscillator anharmonicity, 47  
 Morse Potential, 155  
 multinomial distribution, 149  
 multiple-transition state model, 114  
 multiple-well systems, 142  
**multiwell**, 13  
**MultiWell**, 22  
     Data files, external, 39, 42  
     Examples, 154, 176  
     Input File, 5, 179  
     Input file format, 28, 56  
     Output files, 56, 180  
     Symmetry Examples, 196  
**MultiWell** input options, 27  
 multiwell.array, 26, 181  
 multiwell.dist, 26, 181  
 multiwell.flux, 27, 181  
 multiwell.out, 26, 180  
 multiwell.rate, 26, 181  
 multiwell.sum, 26  
 mVTST, 232  
**NOCENT**, 33, 157, 212  
 noise, 219  
 non-RRKM, 157  
 non-separable degrees of freedom, 91  
 non-separable vibrations, 186  
**NOREV**, 32  
 normalization, 169, 170  
 normalization problems, 170  
 normalization, finite difference algorithm, 171  
**NOTUN**, 32  
**Np**, 29  
**NProds**, 30  
 number of trials, 36  
 numerical convergence, 217, 233  
**NWells**, 30  
 oblate symmetric top, 191  
 oblate top, 151  
**obs**, 47  
**OLDET**, 31  
 optical isomer, 194  
 optical isomers, 30, 32  
 Optical isomers  
      Hindered internal rotation, 194  
 output files, 26  
**paradensum**, 7, 11, 12, 47, 86, 87  
     program, 64  
 Particle in a Box, 49  
 particle-in-a-box, 52, 234  
 partition function, 91, 165  
 perturbation theory expansion, 186  
 Photo-Activation, 177  
 precision, 149  
 pressure units, 29  
 Product set, 30  
 Product sets, 30  
 Product sets, defined, 22  
 Program Execution, 25  
 prolate symmetric top, 191  
 prolate top, 151  
 pseudo-diatomic model, 151  
 pseudo-first-order, 162  
**Punits**, 29  
 qro, 233  
 quantum mechanical tunneling, 209  
 Quantum mechanical tunneling, 158  
 quasi-bound states, 188

quasicontinuum, 134  
 quasi-symmetric top approximation, 190  
 Questions and Answers, 233  
 radiationless transitions, 38  
 random number generator, 149  
 random walkers, 235  
 rate constant  
   canonical, 205  
   chemical activation, 227  
   microcanonical, 205  
   unimolecular, 225  
 Reactant Sets, 22  
 reaction flux coefficient, 26, 181  
 reaction flux coefficients, 224  
 reactive flux, 139, 181  
 recombination, 221  
 recombination reaction, 67  
 Recombination Reactions, 177  
 re-crossing, 112  
 reduced moment of inertia, 61, 104  
 relative translation, 51  
 restricted Gorin model, 154  
 REV, 32  
 RKE, 33  
 rot, 233  
 rotation, 52, 132  
   quantized, 52  
 Rotation, 48  
 rotational, 29  
 Rotational Constant, 185  
 rotational constants, 29  
 rotational degrees of freedom, 67  
 rotations of a linear molecule, 48  
 rotations of a non-linear molecule, 48  
 rotations of a spherical top molecule, 48, 49  
 Rotatunits, 29  
 RRKM theory, 150  
 Schrödinger equation, 103  
 sctst  
   program, 64  
 sctst, 12, 13, 47  
 SCTST, 64, 68, 91, 92, 190, 204, 208  
 SCTST, limitations, 206  
 sctst.out, 91, 92  
 selection of step sizes, 171  
 semi-classical transition state theory, 68, 91, 204  
 Semi-Classical Transition State Theory (SCTST), 7  
 Semi-empirical Canonical Variational Transition  
   State Theory, 155  
 semi-microcanonical bimolecular rate constant, 163  
 semi-microcanonical pseudo-first order rate constant,  
   164  
 separable rotors approximation, 190, 191  
 separable-rotors approximation, 138, 190  
 separation of time scales, 225  
 shock-tube simulations, 29  
 simulated time, 229  
 SLOW, 32, 33  
 Slow IVR, 157  
 sMORSE, 67  
 source code, 24  
 specific rate constants, 39, 143  
 spherical top, 48, 49, 189  
   separable rotors approximation, 189  
 standard state, 64  
 statistical errors, 235  
 statistical fluctuations, 235  
 steady-state distribution, 226  
 step-size distribution, 172  
*Stiff Morse Oscillator*, 67  
 Stochastic Method, 147  
 stochastic noise, 235  
 stochastic sampling noise, 219  
 stochastic trials, 235  
 SUM, 33  
 sums and densities of states, 207  
 sums of states, 39, 143  
 supplementary reactions, 35  
 symmetric top, 48, 52, 189  
   separable rotors approximation, 189  
 symmetric tops  
   *almost symmetric*, 151, 190  
 symmetry  
   internal rotation, 192  
   potential energy, 192  
 symmetry number, 30, 32  
   hindered internal rotation, 53  
 symmetry numbers, 151  
 Symmetry Numbers, external, 192  
 symmetry numbers, internal rotors, 192  
 Temp, 29  
 terminology, 22  
 THERMAL, 36  
 Thermal Activation, 176  
 thermo  
   program, 64  
 thermo, 9, 12, 47  
 THERMO, 155  
 thermodynamics database, 74  
 threshold energy, 151  
 tight transition state, 151  
 time, 36  
 TIME, 36  
 time step, 148  
 top, 52  
 torsion, 133  
 torsion rotational constant function, 134  
 torsions, 103  
 total collision rate constant, 31  
 total collision frequency, 34  
 total collision rate constant, 158, 168  
 transition state, 71

- loose, 152
- tight, 151
- Transition state parameter entry, 32
- transition state theory, 64, 91, 204
- transition states, 142
- Transition states, 22
- translation, 54
- Translation, 51
- translational states, 166
- translational temperature, 29
- trial transition states, 110
- trn, 54
- TS computer code, 131
- tun, 210
- TUN, 32, 33
- tunneling, 32, 71, 91, 158, 205
- tunneling corrections, 6
- tunneling probability, 158
- Tvib, 29
- Uncertainties, 149
- unified rate constant, 114
- Unimolecular Reactions, 150
- unsymmetrical hindered internal rotation, 50
- utilities, 75
- utilities for creating data files, 75
- variational transition state theory, 232
  - canonical, 110, 111
  - J-resolved, 110, 114
  - microcanonical, 110, 114
- Variational Transition State Theory, 152
- VariFlex software, 235
- VARSHNI*, 67
- Varshni Oscillator*, 67
- Viblo, 40
- vibration, 52
- vibrational
  - anharmonicity, 185
  - vibrational anharmonicity, 68, 204
  - vibrational energy, 185
    - perturbation theory expansion, 186
  - vibrational perturbation theory, 209
  - vibrational temperature, 29
- vibrations
  - non-separable, 186
  - separable, 185
- vimag(Mol,i), 33
- VPT2, 94, 209
- VPT4 correction, 94
- VPT4A, 94
- VPT4B, 94
- VPTx, 94
- Wang-Landau algorithm, 91
- Warnings, 43
- wells, 142
- Wells, 30
- Wells, defined, 22
- Whitten-Rabinovitch approximation, 56
- $X_{ij}$  anharmonicity coefficient matrix, 185